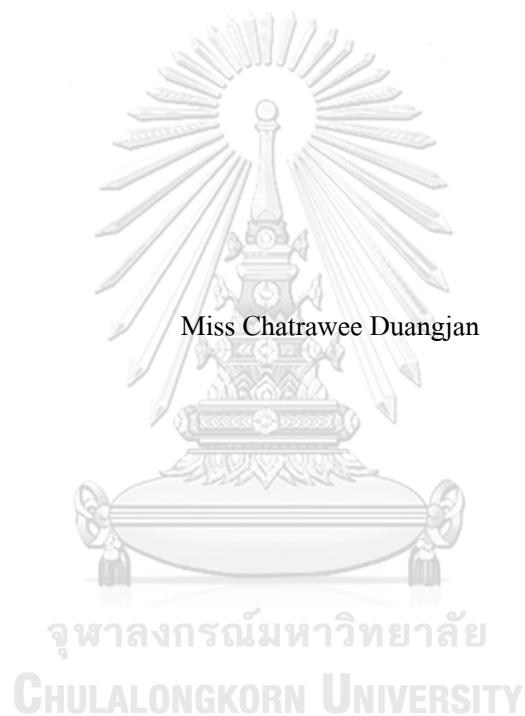


EFFECTS AND MECHANISMS OF *ANACARDIUM OCCIDENTALE* AND *GLOCHIDION ZEYLANICUM* LEAF EXTRACTS ON NEUROPROTECTIVE, NEURITOGENESIS, OXIDATIVE STRESS RESISTANCE AND ANTI-AGING PROPERTIES.



A Dissertation Submitted in Partial Fulfillment of the Requirements
for the Degree of Doctor of Philosophy in Clinical Biochemistry and Molecular Medicine
Department of Clinical Chemistry
Faculty of Allied Health Sciences
Chulalongkorn University
Academic Year 2019
Copyright of Chulalongkorn University

ผลและกลไกของสารสกัดใบมะม่วงหิมพานต์และใบมันปูต่อการป้องกันระบบประสาท
การกระตุ้นการเจริญของนิวโรท์ การต้านภาวะเครียดออกซิเดชัน และการต้านความชรา



วิทยานิพนธ์นี้เป็นส่วนหนึ่งของการศึกษาตามหลักสูตรปริญญาวิทยาศาสตรดุษฎีบัณฑิต

สาขาวิชาชีวเคมีคลินิกและอนุทางการแพทย์ ภาควิชาเคมีคลินิก

คณะสหเวชศาสตร์ จุฬาลงกรณ์มหาวิทยาลัย

ปีการศึกษา 2562

ลิขสิทธิ์ของจุฬาลงกรณ์มหาวิทยาลัย

Thesis Title	EFFECTS AND MECHANISMS OF <i>ANACARDIUM OCCIDENTALE</i> AND <i>GLOCHIDION ZEYLANICUM</i> LEAF EXTRACTS ON NEUROPROTECTIVE, NEURITOGENESIS, OXIDATIVE STRESS RESISTANCE AND ANTI-AGING PROPERTIES.
By	Miss Chatrawee Duangjan
Field of Study	Clinical Biochemistry and Molecular Medicine
Thesis Advisor	Assistant Professor Dr. TEWIN TENCOMNAO

Accepted by the Faculty of Allied Health Sciences, Chulalongkorn University in Partial Fulfillment of the Requirement for the Doctor of Philosophy

..... Dean of the Faculty of Allied Health Sciences
(Associate Professor Dr. PALANEE AMMARANOND)

DISSERTATION COMMITTEE

..... Chairman
(Assistant Professor Dr. VIROJ BOONYARATANAKORNKIT)

..... Thesis Advisor
(Assistant Professor Dr. TEWIN TENCOMNAO)

..... Examiner
(Associate Professor Dr. RACHANA SANTIYANONT)

..... Examiner
(Assistant Professor Dr. TEWARIT SARACHANA)

..... External Examiner
(Associate Professor Dr. WIPAWAN THANGNIPON)

CHULALONGKORN UNIVERSITY

นั้ตรระวี คววจันท์ : ผลและกลไกของสารสกัดใบมะม่วงหิมพานต์และใบมันปูต่อการป้องกันระบบประสาท การกระตุ้นการเจริญของนิวโร้ การต้านภาวะเครียดออกซิเดชัน และการต้านความชรา . (EFFECTS AND MECHANISMS OF ANACARDIUM OCCIDENTALE AND GLOCHIDION ZEYLANICUM LEAF EXTRACTS ON NEUROPROTECTIVE, NEURITOGENESIS, OXIDATIVE STRESS RESISTANCE AND ANTI-AGING PROPERTIES.) อ.ที่ปรึกษาหลัก : ผศ. ดร.เทวิน เทนคำเนาวิ

ความแก่ชราเป็นปัจจัยเสี่ยงสำหรับโรคทางระบบประสาทและอาจส่งผลเสียต่อคุณภาพชีวิต โรคที่เกี่ยวกับระบบประสาทมีการเชื่อมโยงกับการตายของเซลล์ประสาทและการเสื่อมของเซลล์ประสาท อันเนื่องมาจากภาวะเครียดจากออกซิเดชัน (Oxidative stress) ปัจจุบันผู้คนต้องการมีชีวิตที่ยืนยาว และมี สุขภาพที่ดี โภชนาการที่ดีต่อสุขภาพจึงได้รับความสนใจมากขึ้น งานวิจัยจำนวนมากรายงานความสัมพันธ์ เชิงบวกระหว่างสารต้านอนุมูลอิสระในอาหาร และการป้องกัน การรักษาโรคทางระบบประสาท รวมทั้ง การมีอายุยืนยาว ผลิตภัณฑ์ธรรมชาติจากพืชและสมุนไพรที่มีคุณสมบัติต้านอนุมูลอิสระอาจสามารถช่วย ต่อต้านโรคอันเนื่องมาจากความชรา รวมทั้ง สามารถ ช่วย ส่ง เสริม การ มี อายุ ยืน ยาว ไปได้ สารสกัดจาก ใบ มะ ม่วง หิมพานต์และใบมันปูมีความน่าสนใจอย่างมากอันเนื่องมาจากฤทธิ์ต้านอนุมูลอิสระ อย่างไรก็ตามปัจจุบัน ยังขาดงานวิจัยรับรองเกี่ยวกับผลของสารสกัดจากใบมะม่วงหิมพานต์และใบมันปูต่อการป้องกันระบบประสาท การกระตุ้นการเจริญของนิวโร้ การ ต่อ ด้าน ภาวะ เครียด ที่ เกิด จาก ออกซิเดชัน และการ ส่ง เสริม การ มี อายุ ยืน ยาว ดังนั้นในงานวิจัยฉบับนี้มีวัตถุประสงค์เพื่อทดสอบผลของสารสกัดจากใบมะม่วงหิมพานต์และใบมันปูต่อการ ป้องกันระบบประสาทและการกระตุ้นการเจริญของนิวโร้ ในเซลล์ประสาทเพาะเลี้ยง (HT22 และ Neuro-2a) อีกทั้งเพื่อทดสอบการต่อต้านภาวะเครียดที่เกิดจากออกซิเดชัน และการ ส่ง เสริม การ มี อายุ ยืน ยาว ใน หนอน *C.elegans* ผลการทดลองในเซลล์ประสาทเพาะเลี้ยง พบว่า สารสกัดจาก ใบ มะ ม่วง หิมพานต์ และ ใบ มัน ปู สามารถป้องกันการตายของเซลล์ประสาทเพาะเลี้ยงที่ถูกกระตุ้นโดยสารกลูตาเมต และไฮโดรเจนเปอร์ออกไซด์ โดยใช้กลไกในการยับยั้งการสะสมอนุมูลอิสระ และการเพิ่มเอนไซม์ต้านอนุมูลอิสระผ่านทางวิถี SIRT1-Nrf2 นอกจากนี้สารสกัดจากใบมะม่วงหิมพานต์และใบมันปู ยังสามารถกระตุ้นการเจริญ ของนิวโร้ ผ่านทางโปรตีน Ten-4 ผลการทดลองในหนอน *C.elegans* พบว่าสารสกัดจากใบมะม่วงหิมพานต์และใบมันปูสามารถป้องกัน การตายของหนอนที่ถูกกระตุ้นให้เกิดความเครียดจากสาร Jugrone โดยใช้กลไกในการเพิ่มการแสดงออกของยีน ต้านอนุมูลอิสระผ่านทางวิถี DAF-16/FoxO และวิถี SKN-1/Nrf2 นอกจากนี้สารสกัดจากใบมะม่วงหิมพานต์ และใบมันปูยังสามารถต้านความชรา และส่งเสริมการมีอายุยืนยาวในหนอน *C.elegans* จากผลการศึกษาี้แสดงให้เห็นถึงข้อมูลทางวิทยาศาสตร์เกี่ยวกับองค์ประกอบทางพฤกษเคมี ในสารสกัดใบมะม่วงหิมพานต์ (*A. occidentale*) และใบมันปู (*G. zeylanicum*) รวมทั้งฤทธิ์ในการป้องกันระบบประสาท การกระตุ้นการเจริญ ของนิวโร้ การต้านอนุมูลอิสระ และการต้านความชรา ทั้งในเซลล์ ประสาทเพาะเลี้ยง (*In vitro*) และหนอน *C. elegans* (*In vivo*) การวิจัยนี้สามารถเพิ่มมูลค่าใ้ใบมะม่วงหิมพานต์และใบมันปู อีกทั้งยังสามารถนำไปประยุกต์เพื่อการพัฒนาการรักษาและป้องกันโรคทางระบบประสาทอันเนื่องมาจากความชราได้ในอนาคต

สาขาวิชา ชีวเคมีคลินิกและอนุทางการแพทย์

ปีการศึกษา 2562

ลายมือชื่อ นิสิต

ลายมือชื่อ อ.ที่ปรึกษาหลัก

5776951437 : MAJOR CLINICAL BIOCHEMISTRY AND MOLECULAR MEDICINE

KEYWORD: Anacardium occidentale, Glochidion zeylanicum, Neuroprotective, Neuritogenesis, Antioxidant, Antiaging, HT22 cells, Neuro-2a cells, Caenorhabditis elegans, Glutamate, H₂O₂, Teneurin-4, SIRT1-Nrf2 signaling pathway, DAF-16/FoxO signaling pathway, SKN-1/Nrf-2 signaling pathway

Chatrawee Duangjan : EFFECTS AND MECHANISMS OF *ANACARDIUM OCCIDENTALE* AND *GLOCHIDION ZEYLANICUM* LEAF EXTRACTS ON NEUROPROTECTIVE, NEURITOGENESIS, OXIDATIVE STRESS RESISTANCE AND ANTI-AGING PROPERTIES.. Advisor: Asst. Prof. Dr. TEWIN TENCOMNAO

Aging is the primary risk factor for most neurodegenerative diseases and can negatively affect the quality of life. Neurodegenerative diseases are linked to neuronal cell death and neurite outgrowth impairment that are often caused by oxidative stress. As people want to live longer and healthier, healthy nutrition has been increasingly received much attention in recent years. Several studies reported a positive correlation between antioxidants in foods and longevity. Natural products from food supplements and medicinal plants with antioxidant properties could be promising candidates for fighting against various aging-related diseases and promoting longevity. Leaf extracts from *A. occidentale* (AO) and *G. zeylanicum* (GZ) have been of great interest due to their pronounced antioxidant effects. However, the anti-oxidant and anti-aging effects of AO and GZ leaf extracts still have not been reported. The current study aims to document beneficial effects of leaf extracts from AO and GZ extracts with neuroprotective, neuritogenesis, oxidative stress resistance properties and lifespan extension in the cultured neuronal (HT22 and Neuro-2a) cells and the *C. elegans* model. In cultured neuronal cell models, the AO and GZ extracts have a protective effect against glutamate/H₂O₂-mediated oxidative stress-induced cell death via inhibition of ROS accumulation, up-regulation of endogenous antioxidant enzymes, and the increase of the SIRT1-Nrf2 signaling pathway. The AO and GZ extracts increase neurite outgrowth mediated Ten-4 transmembrane protein. In *C. elegans* models, the AO and GZ extracts mediated the survival rate of nematodes under oxidative stress by stimulation stress-response genes (SOD-3 and GST-4), attenuating intracellular reactive oxygen species (ROS) accumulation via DAF-16/FoxO and SKN-1/Nrf-2 signaling pathway. The AO and GZ extracts exhibited anti-aging activities and enhanced longevity by improving pharyngeal pumping function, attenuation of pigment accumulation (lipofuscin) and a lifespan extension in wild-type worm. Collectively, this study is the first report about the phytochemical composition of *A. occidentale* and *G. zeylanicum* along with neuroprotective, neuritogenesis, antioxidant and anti-aging effects in cultured neuronal cells (*In vitro*) and *C. elegans* models (*In vivo*). Our novel findings could initiate further applications of AO and GZ leaf extracts as natural products beneficial to humans for developing new treatment and protection aging-related diseases in the future.



Field of Study: Clinical Biochemistry and Molecular Medicine Student's Signature

Academic Year: 2019 Advisor's Signature

ACKNOWLEDGEMENTS

Firstly, I would like to express my sincere gratitude to my advisor Asst. Prof. Dr. Tewin Tencomnao for the continuous support of my Ph.D. study and related research. The door to Dr. Tewin office was always open whenever I ran into a trouble spot or had a question about my research or writing. He consistently allowed me to do every kind of research and always supported every research financial. He made me believed that everything can possible under the supervision of him.

My sincere thanks also go to Prof. Dr. Michael Wink at Heidelberg University who provided me an opportunity to do short term research fellowship, and who supported the laboratory and research facilities in *C. elegans* field. His patience, motivation, immense knowledge, guidance helped me in all the time of research and writing of all of my research. Without his support, it would not be possible to conduct this research.

I would also like to acknowledge a scholarship from “72nd Birthday Anniversary of His Majesty the King’s for Doctoral Scholarship”, “The 90th Anniversary Chulalongkorn University Fund (Ratchadaphiseksomphot Endowment Fund)” funding code GCUGR1125603032D No.29 for research expense and also “The Overseas Research Experience Scholarship for Graduate Students” from Graduate School, Chulalongkorn University. This project was carried out at the Department of Clinical Chemistry, Faculty of Allied Health Sciences, Chulalongkorn University and Institute of Pharmacy and Molecular Biotechnology, Heidelberg University, and also thanks for supporting laboratory instruments.

I would like to extend thanks to all colleagues from the Department of Clinical Chemistry, Faculty of Allied Health Sciences, Chulalongkorn University who provided useful assistance, helpful suggestions, and for all the fun we had during the research. Also, I thank my friends especially Xiaojie Gu, from the Institute of Pharmacy and Molecular Biotechnology, Heidelberg University who provided instruction on *C. elegans* experiments, useful discussion, technical support and all the party that we had in Heidelberg University. In particular, I sincerely thank Mr. Panthakarn Rangsinth for his patience to answer the question, his support in the experiment, his guidance to correct English grammar and improve the manuscripts. I could not have imagined having a better friend and research partner for my Ph.D. life. Also, I am grateful to Mrs. Laong Kwunpet and Mrs. Korakod Choosri for helping and supplying the plant sample from Songkhla Province, Thailand.

Finally, I must express my very profound gratitude to my family and Shaoxiong Zhang for providing me with unfailing support and continuous encouragement throughout my years of study and through the process of researching and writing this thesis. This accomplishment would not have been possible without them. They always stand by my side and made my life worth living. Thank you from my heart.

Chatrawee Duangjan

TABLE OF CONTENTS

	Page
ABSTRACT (THAI)	iii
ABSTRACT (ENGLISH).....	iv
ACKNOWLEDGEMENTS.....	v
TABLE OF CONTENTS.....	vi
LIST OF TABLES	xi
LIST OF FIGURES	xii
LIST OF ABBRAVIATIONS	15
CHAPTER I INTRODUCTION.....	17
1.1 Background and rationale	17
1.2 Research questions.....	22
1.3 Research objectives	22
1.4 Research hypotheses	23
1.5 Conceptual framework.....	24
1.6 Experimental design	26
CHAPTER II LITERATURE REVIEW	28
2.1 Aging and neurodegeneration	28
2.2 Neurite outgrowth.....	30
2.3 Molecular and cellular theory of neurite outgrowth	32
2.3.1 MEK/ERK and PI3K/AKT signaling pathway	33
2.3.2 PKC pathway activation.....	33
2.3.3 Teneurin 4.....	34
2.4 Glutamate/H ₂ O ₂ and neurodegeneration	35
2.5 Oxidative stress and age-associated neurodegeneration.....	38
2.6 Antioxidant defense mechanism.....	39
2.6.1 Endogenous antioxidant	39
2.6.2 SIRT1/Nrf2 signaling pathway	40

2.7 The cultured neuronal cells model.....	41
2.7.1 The mouse hippocampal neuronal HT22 cells	41
2.7.2 The mouse neuroblastoma Neuro-2a cells	42
2.8 <i>Caenorhabditis elegans</i> ; a model for aging and age-related diseases	42
2.9 Oxidative resistance and longevity pathways in <i>C.elegans</i>	43
2.9.1 The insulin/IGF-1 signaling (IIS) pathway	43
2.9.2 DAF-16/FOXO signaling pathway	45
2.9.3 The SKN-1/Nrf-2 signaling pathway	47
2.10 Thai plant in this study	48
2.10.1 <i>Anacardium occidentale</i>	48
2.10.2 <i>Glochidion zeylanicum</i>	50
2.11 Herbal medicines in anti-aging and neurodegenerative diseases.....	51
2.11.1 Plant extracts and neuroregenerative properties.....	51
2.11.2 Plant extracts and anti-aging properties	53
CHAPTER III MATERIALS AND METHODS	55
3.1 Materials	55
3.1.1 Chemicals and reagents	55
3.1.2 Tools and devices	60
3.1.3 Plant materials	64
3.1.3.1 <i>Anacardium occidentale</i> L. (AO)	64
3.1.3.2 <i>Glochidion zeylanicum</i> (Gaertn) A. Juss (GZ).....	65
3.1.4 The cultured neuronal cell models	66
3.1.5 The <i>C. elegans</i> models	67
3.2 Methods	68
3.2.1 Plant extraction.....	68
3.2.2 Phytochemical analysis	69
3.2.2.1 Gas/Liquid Chromatography-Mass Spectrometry analysis.....	69
3.2.2.2 High Performance Liquid Chromatography (HPLC) analysis	70
3.2.3 Determination of antioxidant properties <i>In vitro</i>	71

3.2.3.1 Radical scavenging activity	71
3.2.3.2 Total phenolic content	71
3.2.3.3 Total flavonoid content	71
3.2.3.4 Cell-based antioxidant measurement.....	72
3.2.4 Cell culture and treatment condition	72
3.2.5 Determination of cell viability	72
3.2.6 RNA isolation and quantitative RT-PCR	73
3.2.7 Western blot analysis.....	74
3.2.8 Measurement of neurite outgrowth and neurite-bearing cells.....	75
3.2.9 Knockdown of Teneurin-4 expression	75
3.2.10 <i>C. elegans</i> culture and treatment condition	76
3.2.11 Determination of survival rate under juglone-induced oxidative stress.	78
3.2.12 Measurement of intracellular ROS in <i>C. elegans</i>	78
3.2.13 Quantification of HSP-16.2::GFP, GST-4::GFP and SOD-3::GFP expression.....	78
3.2.14 Determination of subcellular localization of DAF-16 and SKN-1.....	79
3.2.15 Measurement of brood size assay.....	79
3.2.16 Measurement of body length and body surface area	79
3.2.17 Quantification of lipofuscin.....	80
3.2.18 Measurement of pharyngeal pumping rate	80
3.2.19 Measurement of lifespan	81
3.2.20 Statistical analysis	81
CHAPTER IV RESULTS.....	82
4.1 Phytochemical constituents of AO and GZ extracts	82
4.2 Antioxidant properties of AO and GZ extracts.....	89
4.2.1 The antioxidant properties (<i>In vitro</i>)	89
4.2.2 The antioxidant properties in cells	92
4.2.3 The antioxidant properties (<i>In vivo</i>)	95
4.3 Neuroprotective effects of AO and GZ extracts	97

4.3.1 Protective effects against H ₂ O ₂ -induced toxicity	99
4.3.2 Protective effects against glutamate-induced toxicity	104
4.4 Oxidative stress resistance properties of AO and GZ extracts	108
4.5 Anti-aging properties of AO and GZ extracts	111
4.5.1 The autofluorescent pigment lipofuscin	111
4.5.2 The pharyngeal pumping rate	112
4.5.3 Dietary restriction (DR) effects	116
4.5.4 Lifespan	117
4.6 The underlying mechanisms of AO and GZ extracts (<i>In vivo</i>).....	121
4.6.1. Antioxidant gene expression	121
4.6.2 SIRT1 and Nrf2 signaling pathway	123
4.7 The underlying mechanisms of AO and GZ extracts (<i>In vivo</i>).....	129
4.7.1 <i>HSP-16.2</i> gene expression.....	129
4.7.2 <i>SOD-3</i> gene expression	129
4.7.3 <i>GST-4</i> gene expression	130
4.7.4 DAF-16/FoxO transcription factor	133
4.7.5 SKN-1/Nrf-2 transcription	134
4.7.6 Lifespan	139
4.8 Neurite outgrowth properties and underlying mechanisms of AO and GZ extracts.....	140
4.8.1 Neurite outgrowth.....	140
4.8.2 Neurite outgrowth mechanisms (Teneurin 4).....	143
CHAPTER V DISCUSSION	147
CHAPTER VI CONCLUSION	157
6.1 Conclusion	157
6.2 Benefits of the study	159
6.3 Limitations of the study	159
REFERENCES	160
APPENDIX.....	173

VITA.....180



จุฬาลงกรณ์มหาวิทยาลัย
CHULALONGKORN UNIVERSITY

LIST OF TABLES

	Page
Table 1. List of the gene-specific sequences of primers in this study.	74
Table 2. Proposed phytochemical constituents in the AOH extract using GC-MS	86
Table 3. Proposed phytochemical constituents in the GZH extract using GLC-MS ..	87
Table 4. Proposed phytochemical constituents in the AOM extract using LC-MS....	87
Table 5. Proposed phytochemical constituents in the GZH extract using LC-MS.....	88
Table 6. Individual phytochemical constituents in the AO extract using HPLC.....	88
Table 7. Individual phytochemical constituents in the GZ extract using HPLC	88
Table 8. The antioxidant properties of AO extracts (<i>In vitro</i>)	91
Table 9. The antioxidant properties of GZ extracts (<i>In vitro.</i>).....	92
Table 10. Results and statistical analyses of the AO extracts treated <i>C. elegans</i> in lifespan assay	119
Table 11. Results and statistical analyses of GZ extracts treated <i>C. elegans</i> in lifespan assay.....	120

LIST OF FIGURES

	Page
Figure 1. Various mechanisms involved in aging process.....	30
Figure 2. The process of neuron development.....	31
Figure 3. NGF and neurite outgrowth signaling pathways.....	35
Figure 4. The glutamate synapse and excitotoxicity mediated cell death.....	37
Figure 5. Generation of ROS.....	40
Figure 6. The mechanisms of SIRT1-Nrf2 signaling pathway on oxidative stress resistance properties. (Image from [95]).....	41
Figure 7. Schematic of <i>C. elegans</i> IIS.....	45
Figure 8. DAF-16 interacts with specific proteins under different stimuli.....	46
Figure 9. The SKN-1/Nrf2 signaling pathway on stress resistance properties in <i>C. elegans</i> and mammals.....	48
Figure 10. <i>Anacardium occidentale</i> L.....	49
Figure 11. <i>Glochidion zeylanicum</i> (Gaertn) A. Juss.....	50
Figure 12. Chemical structures of polyphenols with neurotrophic activity.....	53
Figure 13. <i>Anacardium occidentale</i> L. Leave.....	64
Figure 14. <i>Glochidion zeylanicum</i> (Gaertn) A. Juss. Leave.....	65
Figure 15. The morphology of cultured neuronal.....	66
Figure 16. <i>C. elegans</i> wild-type (N2).....	67
Figure 17. Plant extraction.....	68
Figure 18. Knockdown efficiency of Ten-4 by siRNA.....	76
Figure 19. The toxicity tests.....	77
Figure 20. Phytochemical constituents of AO extracts.....	84
Figure 21. Phytochemical constituents of GZ extracts.....	85
Figure 22. The structure of major compounds found in AO and GZ extracts.....	86
Figure 23. The <i>In vitro</i> antioxidant properties of AO extracts.....	90
Figure 24. The <i>In vitro</i> antioxidant properties of GZ extracts.....	91

Figure 25. The antioxidant properties of AO extracts in cells.....	93
Figure 26. The antioxidant properties of GZ extracts in cells.	94
Figure 27. Effect of AO extracts on intracellular ROS in wild-type worms.	95
Figure 28. Effect of GZ extracts on intracellular ROS in wild-type worms.....	96
Figure 29. Cytotoxicity of the extracts in cultured neuronal cells.....	98
Figure 30. The optimum condition of H ₂ O ₂ , glutamate and quercetin	101
Figure 31. Protective effects of AO extracts against H ₂ O ₂ -induced toxicity.....	102
Figure 32. Protective effects of GZ extracts against H ₂ O ₂ -induced toxicity	103
Figure 33. Protective effects of AO extracts against glutamate-induced toxicity	106
Figure 34. Protective effects of GZ extracts against glutamate-induced toxicity.....	107
Figure 35. Effect of AO and GZ extracts on the survival rate of wild-type worms .	109
Figure 36. Pro-oxidant effect of AO and GZ extracts	110
Figure 37. Effect of AO and GZ extracts on age-related markers (lipofuscin).	111
Figure 38. Effect of AO extracts on age-related markers (pharyngeal pumping). ...	114
Figure 39. Effect of GZ extracts on age-related markers (pharyngeal pumping).....	115
Figure 40. Dietary restriction (DR) effects of AO extracts.	116
Figure 41. Dietary restriction (DR) effects of GZ extracts.....	117
Figure 42. Effect of AO and GZ extracts on the lifespan of wild-type worms.....	118
Figure 43. The effect of AO extracts on antioxidant gene expression.....	122
Figure 44. The effect of GZ extracts on antioxidant gene expression	123
Figure 45. Effect of AO extracts on SIRT1 signaling pathway.....	125
Figure 46. Effect of GZ extracts on SIRT1 signaling pathway.	126
Figure 47. Effect of AO extracts on Nrf2 signaling pathway.	127
Figure 48. Effect of GZ extracts on Nrf2 signaling pathway.	128
Figure 49. Effect of AO extracts on the stress resistance genes in <i>C. elegans</i>	131
Figure 50. Effect of GZ extracts on stress resistance genes in <i>C. elegans</i>	132
Figure 51. Effect of AO extracts on nuclear localization of DAF-16 and SKN-1....	135
Figure 52. Effect of GZ extracts on nuclear localization of DAF-16 and SKN-1....	136
Figure 53. Effect of AO extracts on oxidative stress resistance properties	137

Figure 54. Effect of GZ extracts on oxidative stress resistance properties.....	138
Figure 55. Effect of AO and GZ extracts on the lifespan of mev-1 mutant worms..	139
Figure 56. Effect of RA on neurite outgrowth.....	141
Figure 57. Effect of AO extracts on neurite outgrowth.	141
Figure 58. Effect of GZ extracts on neurite outgrowth.....	142
Figure 59. Effect of AO extracts on Ten-4-mediated neurite outgrowth.....	144
Figure 60. Effect of GZ extracts on Ten-4-mediated neurite outgrowth.	145
Figure 61. Effect of siTen-4-mediated neurite outgrowth.	146
Figure 62. Effects and underlying mechanisms of <i>Anacardium occidentale</i> and <i>Glochidion zeylanicum</i> leaf extracts on neuroprotective, neuritogenesis, oxidative stress resistance and anti-aging properties <i>in vitro</i> and <i>in vivo</i> models.	158



LIST OF ABBRAVIATIONS

ABTS: ABTS, 2,2-Azino-bis(3-ethylbenzothiazoline-6-sulfonic acid)

AD: Alzheimer's disease

AO: *Anacardium occidentale L.*

AOD: AO dichloromethane extract

AOH: AO hexane extract

AOM: AO methanol extract

AREs: Antioxidant response elements (AREs)

CAT: Catalase

C. elegans: *Caenorhabditis elegans*

DAF-16/FoxO: Forkhead box protein O

DMEM: Dulbecco's Modified Eagle's Medium

DMSO: Dimethyl sulfoxide

DNA: Deoxyribonucleic acid

DPPH: Diammonium salt, 2,2-Diphenyl-1-picrylhydrazyl

EAAT3: Excitatory amino acid transporter 3

EGCG: Epigallocatechin gallate

FBS: Fetal bovine serum

GAE: Gallic acid equivalents

GAP-43: Growth associated protein 43

GCLM: Glutamate cysteine ligase complex modifier subunit

GC-MS: Gas Chromatography-Mass Spectrometry

GPx: Glutathione peroxidase

GR: Glutathione reductase

GSH: Glutathione

GST-4: Glutathione S-transferase 4

GZ: *Glochidion zeylanicum* (Gaertn.) A. Juss.

GZD: GZ dichloromethane extract

GZH: GZ hexane extract

GZM: GZ methanol extract

HamF12: Ham's Nutrient Mixture F12

H₂DCF-DA: 2,7-Dichlorofluorescein diacetate
HD: Huntington's disease
H₂O₂: Hydrogen peroxide
HPLC: High-Performance Liquid Chromatography;
HSP-16.2: Heat shock protein-16.2
Juglone: (5-Hydroxy-1,4-naphthoquinone)
LC-MS: Liquid Chromatography-Mass Spectrometry
LDH: Lactate dehydrogenase
MTT: 3-(4,5-Dimethylthiazol-2-yl)-2,5-diphenyltetrazolium bromide
NaOH: Sodium hydroxide
NaOCl: Sodium hypochlorite
Nrf2: Nuclear factor (erythroid-derived 2)-like 2 (Nrf2)
NQO1: NAD(P)H, quinone oxidoreductase 1
PBS: Phosphate buffer saline
PCR: Polymerase chain reaction
PD: Parkinson's disease
QE: Quercetin equivalents
RNA: Ribonucleic acid
RNS: Reactive nitrogen species
ROS: Reactive oxygen species
SIRT1: Sirtuin 1
SKN-1/Nrf-2: Nuclear factor erythroid 2-related factor 2
SOD: Superoxide dismutase
SOD-3: Superoxide dismutase-3
Ten-4: Teneurin-4
VCEAC: Vitamin C equivalent antioxidant capacity

CHAPTER I

INTRODUCTION

1.1 Background and rationale

Neurodegenerative diseases are referred to hereditary and sporadic conditions which are characterized by losing of structure or function of neurons as well as neuronal cell death. These disorders are associated with atrophy of the affected central or peripheral structures of the nervous system such as Alzheimer's (AD), Parkinson's (PD), and Huntington's disease (HD). All of the neurodegenerative disease, Alzheimer disease (AD) is the most prevalent which is characterized by progressive memory decline and movement dysfunction including impairment in decision making, orientation to physical surroundings, judgments, and language so it has effect with quality of life severely and cause concern to themselves and families [1]. Epidemiological surveys have shown that AD affects about 2% of the population over 65 years of age and 50–60% of individuals aged more than 85 years old may develop to AD. [2] Several patients suffering from AD in worldwide are expected to increase from 30.8 million in 2010 to more than 106.2 million in 2050. The current therapies for AD mainly rely on drug treatment such as rivastigmine, galantamine, and donepezil which have mild benefit in improving cognitive and behavioral symptoms effects on cognitive function.[3] However, the drug cannot prevent or delay neurodegeneration and other neurodegenerative diseases are also only few effective therapy. The new research and discovery of new drugs or natural compounds for AD and neurodegenerative disease prevention and treatment are expressly required. Neurogenesis describes the process of growth, survival, proliferation, differentiation and regeneration of neurons [4]. Impairment of neurogenesis affects neuronal differentiation and neuronal cell loss in various neurodegenerative disorders [4]. During neuronal differentiation, neurite outgrowth is an essential step for functional networks (connectome) of neurons. Regulation of neurite outgrowth can promote neuronal regeneration from nerve injury or neurological disorders, which plays an important role in development of therapies for neurodegenerative diseases [5]. Neurite outgrowth is an important step in the differentiation of neurons. *In vivo*, cerebellar

neurons were completely developed for since few weeks after the birth. However, *In vitro* neuronal cell model, neuron can cause differentiation of axon and dendrites as well as today need represent an experimental model of postnatal development and axon regeneration [6]. Established cell lines derived from nervous system tissue are going to be powerful tools for explanation cellular and molecular mechanisms of nervous system development and function. Several study also have been used to understand nervous system development by study characteristic of neuronal morphology with the ability of extending neurite, Thus neurite outgrowth in cultured neurons is considered to be one of the indicators of neuroregenerative potential [7]. Teneurin-4 (Ten-4), a transmembrane protein, is highly expressed in the central nervous system and plays a role in neurogenesis. Ten-4 expression mediates neurite outgrowth of the Neuro-2a cells [8]. Glutamate, the main excitatory neurotransmitter in the brain, has been recognized as one initiating factor for several neurodegenerative disorders [9, 10]. High levels of glutamate activate structural degradation, ROS/RNS production, mitochondrial and DNA damage, which further lead to neurotoxicity and neuronal cell damage [9, 11]. Glutamate oxidative stress and neurotoxicity play a major role in a variety of neurodegenerative diseases, especially Alzheimer's disease (AD) [9, 12].

Long life and healthy aging depend on many fold interactions among biological and environmental factors. Aging is an inevitably natural process accompanied by accumulation of damaged macromolecules such as nucleic acids, lipids and proteins. Consequently, physiological characters changed such as increased oxidative stress and increased inflammation can negatively affect the quality of life [13]. Although the mechanisms of the aging process are not completely understood, increasing evidence suggests that aging is apparently associated with the bioactivity of reactive oxygen species (ROS). The protective effects of ROS are the strategy to delay aging and related degenerative diseases. Several lines of evidence previously reported that the reduction of ROS and low-grade inflammation can extend lifespan in a wide spectrum of model organisms [13, 14]. The free-living soil nematode *Caenorhabditis elegans* (*C. elegans*) has become a valuable model for studying genetic and pharmacological influences of ROS on health and longevity. *C. elegans*

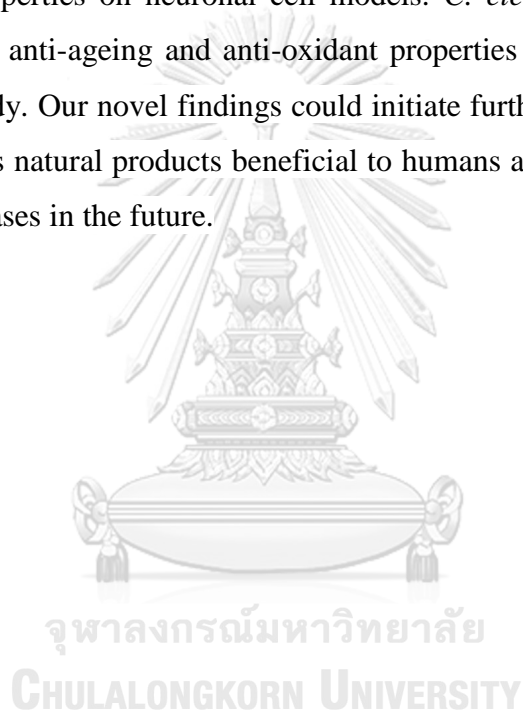
has a rapid reproduction rate, a short lifespan, and is easy to maintain [15]. Its genome has been completely sequenced, and various transgenic strains are available for experimental studies [16]. Importantly, *C. elegans* has conserved longevity and stress resistance genes that are homologous to human genes and thus can serve as a model for human aging processes [17]. Therefore, *C. elegans* has become a popular model organism to explore the potential anti-aging and stress resistance properties of natural compounds. The insulin/IGF-1 signaling (IIS) pathway is one of the most well-known pathways studied in *C. elegans*, which is involved in the regulation of nutrient level responses via the forkhead box O (FoxO) transcription factor and its downstream targets. The components of the IIS pathway are well-conserved, and are linked to longevity in *C. elegans* and humans as well [18]. In *C. elegans*, the FoxO transcription factor DAF-16 plays a role in metabolism, dauer formation, stress resistance and lifespan modulation [19, 20]. In addition, the transcriptional target genes of DAF-16, including superoxide dismutase-3 (SOD-3), catalase-1 (CTL-1), and small heat shock protein-16.2 (HSP-16.2), are key factors that contribute to mediating oxidative stress and heat shock stress response [21-23]. The SKN-1/Nrf-2 signaling pathway, with the transcription factor SKN-1, is localized in the intestine. It is regulated and influenced by growth, nutrients, and metabolic signals in *C. elegans*. SKN-1 is also involved in acute stress response functions by regulating its downstream targets such as glutathione S-transferase 4 (GST-4), which is a phase II detoxification enzyme. Importantly, SKN-1 plays a central role in many regulatory pathways and interventions that extend lifespan in *C. elegans* [24]. A previous report suggests that both DAF-16 and SKN-1 promote stress resistance and, consequently, lifespan extension [25]. SIRT1 regulates transcription factors, including nuclear factor-E2-related factor 2 (Nrf2) that is a major regulator in antioxidant defenses. Evidence suggests that SIRT1 and Nrf2 are also involved in the CNS redox balance of neurodegenerative disorders by promoting antioxidant responses [26]. In addition, enhancing SIRT1 and Nrf-2/HO-1 expression can protect neurons against oxidative injury in neuronal cells [27].

The Cashew tree *Anacardium occidentale* L. (AO), which is known as Mamuanghimmaphan in Thai, belongs to the family Anacardiaceae. It originates from

Brazil, but is presently cultivated in many tropical countries around the globe. A recent study reported that leaf extracts from *A. occidentale* are rich in beta-carotene, lutein, and polyphenols, which are known for high antioxidant activities [28]. *Glochidion zeylanicum* (Gaertn) A. Juss. (GZ), belongs to the family Phyllanthaceae, which is known as Man pu, Phung mu or Chumset in Thai, can be cultivated in many tropical countries. Glochidion species are used as food, and as local medicinal plants for the treatment of rheumatoid arthritis, influenza, dysentery, impaludism, and dyspepsia [29]. These plants are rich sources of flavanol glucosides, which have a powerful antioxidant [30], anti-inflammation [29], and antitumor potential [31].

As people want to live longer and healthier, a healthy nutrition has been increasingly received much attention in recent years. Several studies reported a positive correlation between antioxidants in foods, drinks and longevity. A number of natural products have been reported to extend lifespan in *C. elegans*, such as a variety of antioxidant compounds [32, 33] including epigallocatechingallate [34], quercetin [35] or anthocyanins [36]. Many polyphenolic compounds from natural herbal have been studied on neurite outgrowth promotion in neuronal cell lines. A number of studies have shown that different polyphenols including flavonoids such as genistein, quercetin, liquiritin from *Glycyrrhizae radix* plant, isorhamnetin (a flavonolaglycone from *Ginkgo biloba* plant), and acetylated flavonoid glycosides from *Scopariadulcis* together with the stilbenoid compound resveratrol (a polyphenol present in grapes and red wine) can significantly promote neurotrophin (nerve growth factor [NGF] and brain-derived neurotrophic factor [BDNF]) through neurite outgrowth in neuronal cells line [37]. Moreover, reduction of oxidative stress and induction of neuronal differentiation are key parameters for neuroprotective effects. Therefore, natural products from food supplements and medicinal plants with antioxidant and neuroprotective properties could provide an alternative approach to treat aging-related diseases and promote longevity. Leaf extracts from AO and GZ have been of great interests due to their pronounced antioxidant effects [28, 38, 39]. However, the effect of AO and GZ leaf extracts on neuroprotective and neuroregenerative properties as well as age-related diseases and lifespan extension

still unclear for underlying mechanism and there are no studies that have been explored in this topic. Therefore, the objectives of this study were aimed at investigating the modulatory roles and underlying mechanisms of AO and GZ leaf extracts on neuroprotective, neuritogenesis, oxidative stress resistance properties and lifespan extension in the cultured neuronal (HT22 and Neuro-2a) cells and the *C. elegans* model. The HT22 cells which sensitive with glutamate induced toxicity[10] and Neuro-2a cells which have been extensively used to study neuronal differentiation and neurite growth [40] were used to examine neuroprotective and neuritogenesis properties on neuronal cell models. *C. elegans* is a powerful model organism to study anti-ageing and anti-oxidant properties [41] were used as *in vivo* models in this study. Our novel findings could initiate further applications of AO and GZ leaf extracts as natural products beneficial to humans as therapeutic candidate for aging-related diseases in the future.



1.2 Research questions

1.2.1 Whether and how *A. occidentale* and *G. zeylanicum* extracts have neuroprotective effect in cultured neuronal cells?

1.2.2 Whether and how the AO and GZ extracts have neurite outgrowth activity in cultured neuronal cells?

1.2.3 What are the protective mechanisms of the AO and GZ extracts against glutamate/H₂O₂-induced oxidative toxicity?

1.2.4 What are the underlying mechanisms of the AO and GZ extracts on neurite outgrowth activity?

1.2.5 Whether and how the AO and GZ extracts have oxidative stress resistance properties in *C. elegans*?

1.2.6 What are the underlying mechanisms of the AO and GZ extracts on oxidative stress resistance properties?

1.2.7 Do the AO and GZ extracts have anti-aging properties in *C. elegans*?

1.3 Research objectives

1.3.1 To examine the protective effects and underlying mechanisms of the AO and GZ extracts against glutamate/H₂O₂-induced oxidative toxicity using cultured neuronal cell models (HT22 and Neuro-2a).

1.3.2 To examine the neurite outgrowth activity and underlying mechanisms of the AO and GZ extracts using the mouse neuroblastoma Neuro-2a cells.

1.3.3 To examine the oxidative stress resistance properties and underlying mechanisms of the AO and GZ extracts using *C. elegans* models.

1.3.4 To examine the anti-aging properties of the AO and GZ extracts using *C. elegans* models.

1.3.5 To characterize the phytochemical profiles of the promising extracts by GLC-MS, LC-MS and HPLC analysis.

1.4 Research hypotheses

1.4.1 The AO and GZ extracts can protect against glutamate/H₂O₂-induced oxidative toxicity in cultured neuronal cells.

1.4.2 The AO and GZ extracts have neuroprotective effects in cultured neuronal cells via inhibition of ROS accumulation, up-regulation of endogenous antioxidant enzymes, and the increase of the SIRT1-Nrf2 signaling pathway.

1.4.3 The AO and GZ extracts can increase neurite outgrowth in cultured neuronal cells.

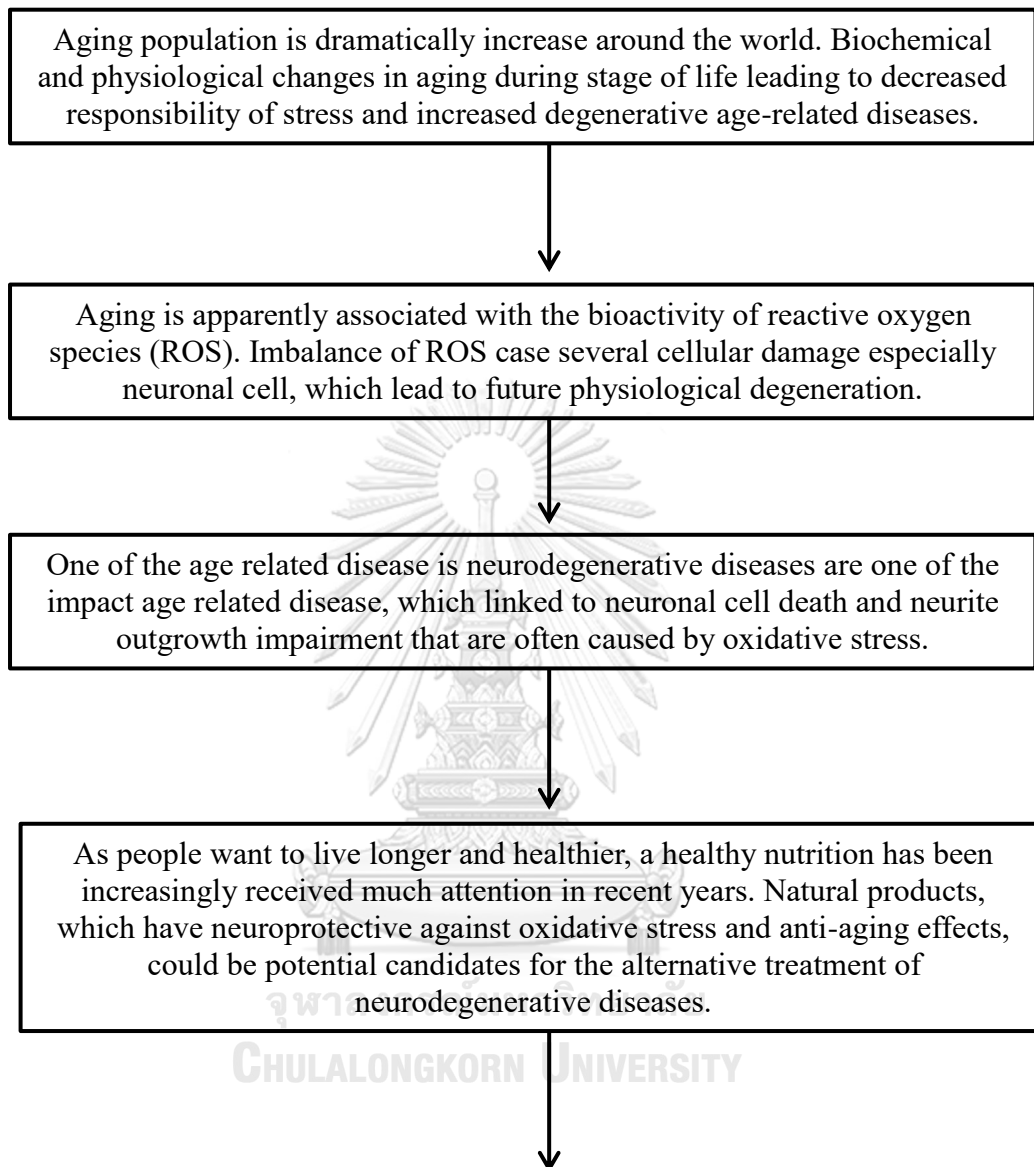
1.4.4 The AO and GZ extracts promote neurite outgrowth via the up-regulation of Ten-4 expression.

1.4.5 The AO and GZ extracts can protect against juglone-induced oxidative stress in *C. elegans*.

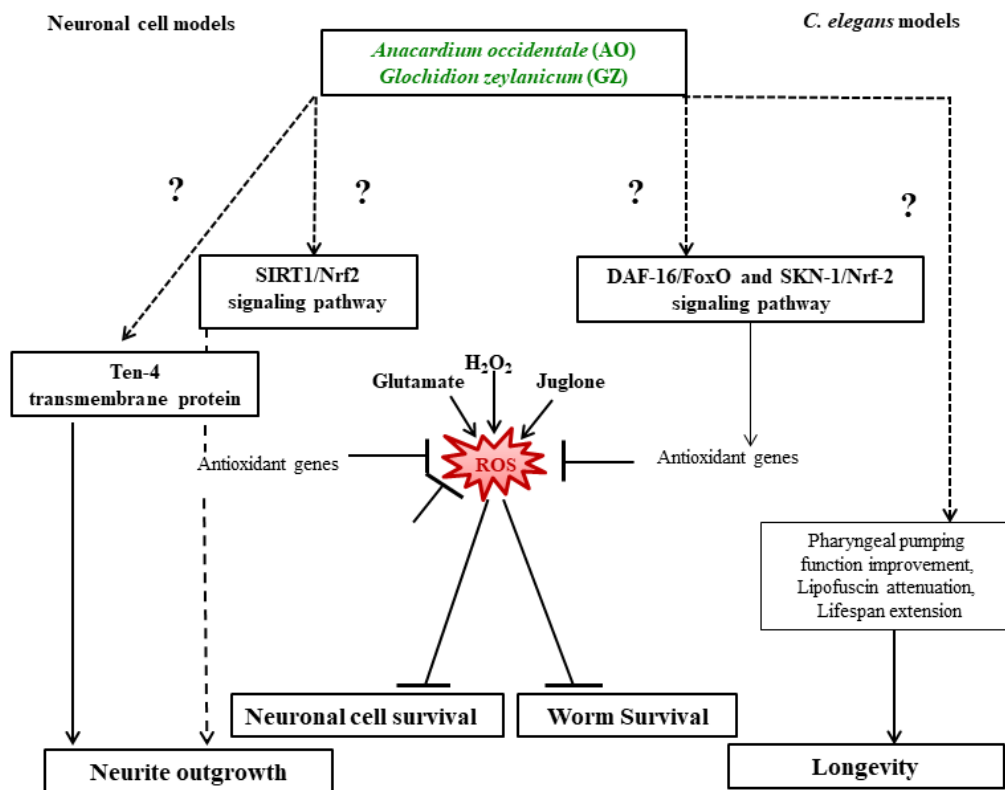
1.4.6 The AO and GZ extracts have oxidative stress resistance properties via DAF-16/FOXO and SKN-1/Nrf-2 signaling pathway.

1.4.7 The AO and GZ extracts have anti-aging activity via pharyngeal pumping improvement, auto fluorescent pigment attenuation and lifespan extension in *C. elegans*.

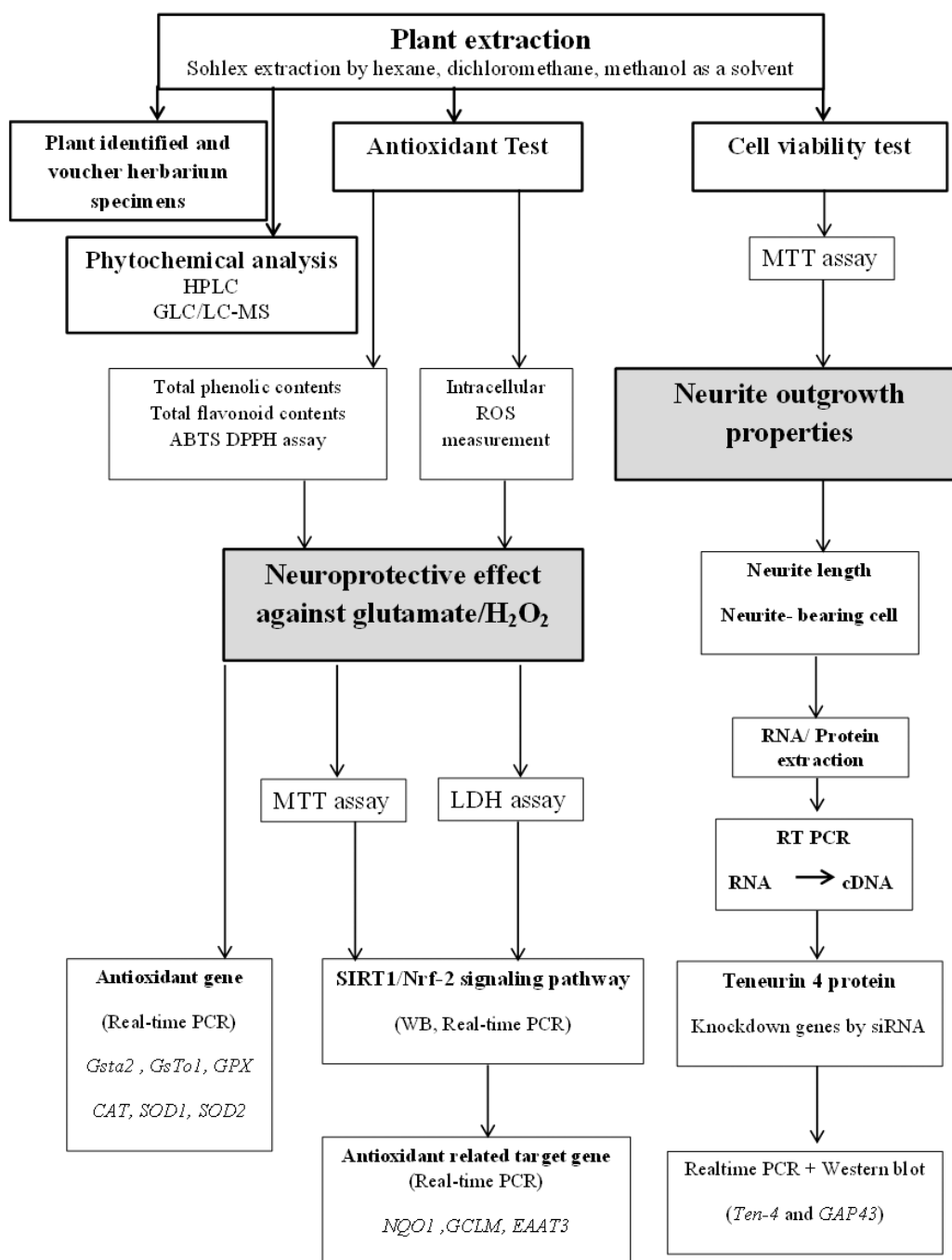
1.5 Conceptual framework

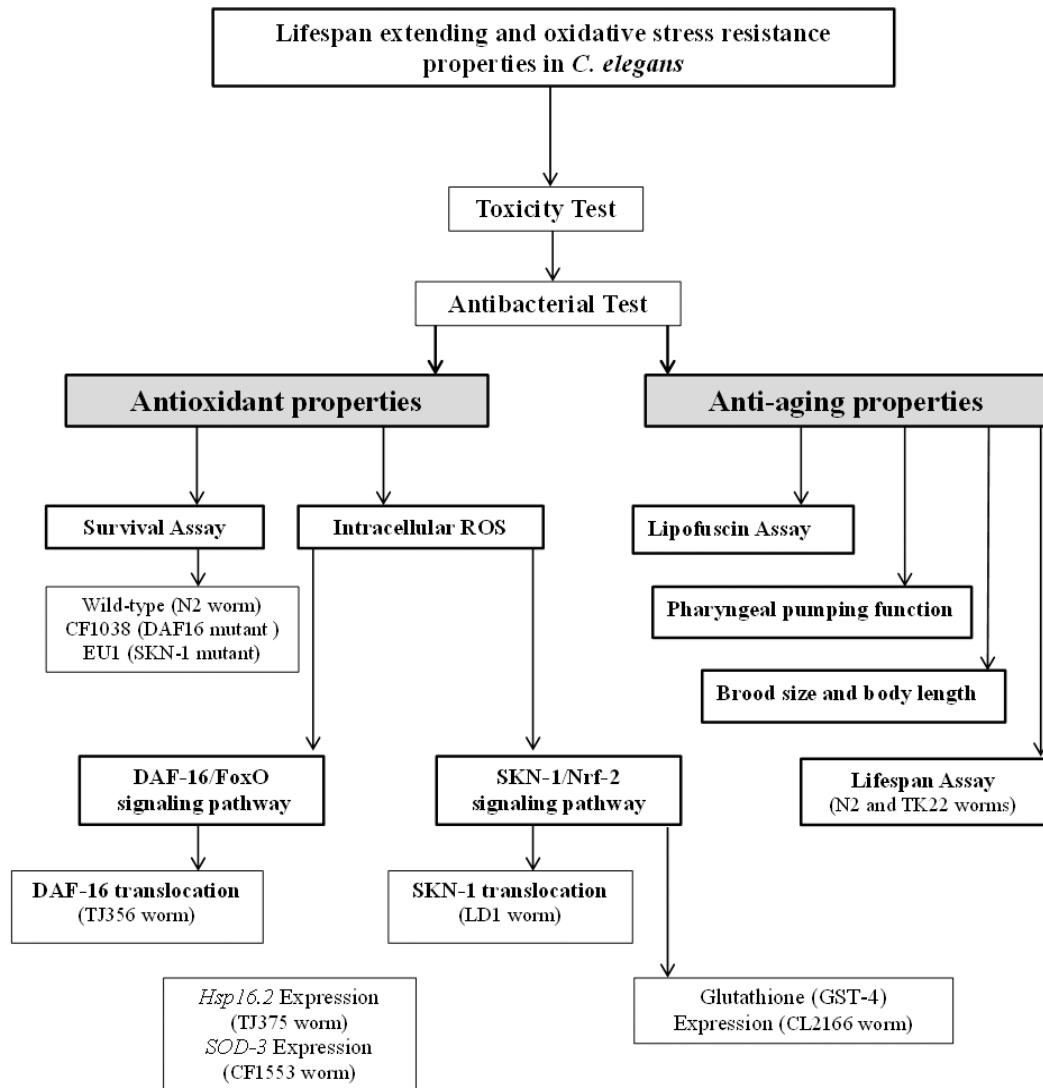


Could *A. occidentale* and *G. zeylanicum* leaf extracts have effects on neuroprotective against oxidative stress and anti-aging?



1.6 Experimental design





CHAPTER II

LITERATURE REVIEW

2.1 Aging and neurodegeneration

Neurodegeneration is the progressive loss of structure or function of neurons, including death of neurons during aging. Neurodegenerative disorders such as Alzheimer's, Parkinson's, and Huntington's diseases represent rapidly growing causes of disability and death, which have profound economic and social implications. All of the neurodegenerative diseases, Alzheimer disease (AD) is the most common characterized by a decline in memory and other cognitive functions of patients. Epidemiological surveys have shown that AD affects about 2% of the population over 65 years of age and 50–60% of individuals aged more 85 years old may develop AD [2]. Several patients suffering from AD worldwide are expected to increase from 30.8 million in 2010 to 106.2 million in 2050. The current therapies for AD mainly rely on cholinesterase inhibitors drug such as rivastigmine, galantamine, donepezil and memantine which have mild beneficial in improving cognitive and behavioral symptoms effects on cognitive function [3]. However, another neurodegenerative disease is also only few effective disease-modifying therapies. Thus, the new research and discovery of new drugs or lead compounds from natural source for AD and neurodegenerative disease are expressly required. The etiology of neurodegenerative diseases is still unclear. However, several study reported that neurodegenerative diseases associated with blood-brain barrier impairment, protein aggregation, toxin exposure, and mitochondrial dysfunction, which lead to oxidative stress and inflammation, and consequently neuronal toxicity and damaged [42].

Aging is an important risk factor for various diseases such as diabetes, cancer as well as several neurodegenerative diseases, including Alzheimer's, Huntington's, and Parkinson's diseases [43, 44]. Aging is an inevitable biological process. Biochemical and physiological changes in aging during stage of life leading to decreased responsibility of stress response and increased degenerative age-related diseases, finally decreasing the individual life span [45]. Although the determined mechanisms of aging process are not completely identified (Figure 1), increasing new

evidences suggest that aging is considerably associated with reactive oxygen species (ROS) [13]. ROS including superoxide radical, hydrogen peroxide and hydroxyl free radical, cause oxidative damage to DNA and other macromolecules in the cell [46]. Oxidative stress caused by ROS can lead to oxidation of biomolecules such as protein, DNA and bio-membranes which is assumed to be the major cause factor of aging. Mitochondrial metabolism is a hallmark of aging. Reduced respiratory capacity and increased oxidative stress associated with age, including muscle and several brain regions [47]. According to, The mitochondrial/free radical theory of aging explain by that mitochondrial energy production decrease and mitochondrial reactive oxygen species (ROS)-induced damage are the major causes of aging [48]. Many studies suggest that although oxidative damage is an important factor of aging. However, preservation of mitochondrial functions and enhancement of mitochondrial biogenesis are important process to promoting health and lifespan extension [49]. Furthermore, nutrition has a strong influence on the health status. The effect of fasting and protein restriction on the slow aging and increase healthy lifespan in several organisms [50]. Studies in invertebrates and rodents reported the effect of caloric or dietary restriction (CR o DR) in extending longevity up to 50% and able to slow down age-related diseases including cancer, cardiovascular (CVD) and neurodegenerative diseases [51]. Moreover, the deficiency of micronutrients (including vitamins and essential minerals such as zinc, copper, selenium) lead to impairments of the immune functions, metabolic harmony and antioxidant in age-related diseases [52]. A direct effect of a reduced caloric intake on the delay of aging phenotypes is documented in several organisms. The role of nutrients in the regulation of human lifespan is not easy to disentangle, influenced by a complex interaction of nutrition with environmental and genetic factors. The individual genetic background is fundamental for mediating the effects of nutritional components on aging. Classical genetic factors able to influence nutrient metabolism are considered those belonging to insulin/insulin growth factor (INS/IGF-1) signaling, TOR signaling and Sirtuins, but also genes involved in inflammatory/immune response and antioxidant activity can have a major role [45].

The relationship between diet, longevity and human health is complex. Nutrition component affect several physiologic processes, assuming a regulatory role

in metabolic pathways crucial for the cell survival such as inflammation or immune function [53]. It is also involved in nutrigenetics (individual polymorphisms gene response to nutrient consumption) and nutrigenomic (affection of nutrient on gene expressions) [54]. Finally, the relationship between diet, longevity and human health is the socio-economic status of individual [55].

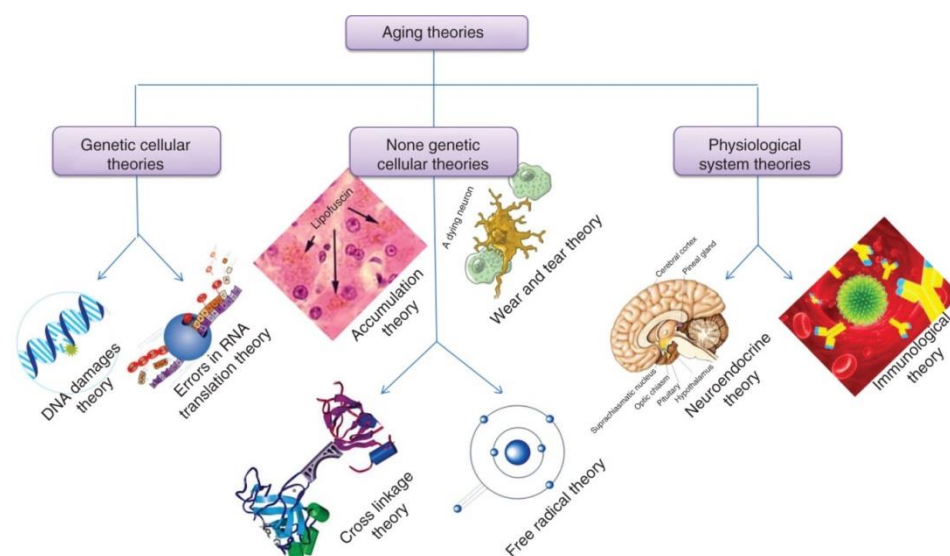


Figure 1. Various mechanisms involved in aging process.(Image from [44])

2.2 Neurite outgrowth

New-born neurons and neural progenitors represent immature spherical cells without neurites. Axons and dendrites were developed by neurons, structurally and morphologically distinct neurites, in developmental stages. *In vitro* neuron model, neuron can produce the lamellipodia (filopodia), spreading around the cell body—stage 1. Next, neuron transforms to roundshape in a cell, surrounded by a mount of short uniform immature processes—stage 2. Several hours later, only one of these processes begins to elongate rapidly and becomes an axon—stage 3. Subsequently axon differentiation, the remaining short processes begin to elongate and differentiate into dendrites—stage 4. The process of polarization is terminated by maturation of formed neurites, dendritic spines morphogenesis, and synapse formation and have 4 or 5 dendrites around the cell body – stage 5 [56] (Figure 2) *In vivo*, cerebellar neurons

were complete development since few weeks after the birth and today need represent an experimental model of postnatal development and axon regeneration. [57] However, the brain has very plasticity and the neural circuits associated with memory and learning may growth and change during a life. Recently, *In vitro* models for examination of neurite outgrowth also included the neuroblastoma cell lines [58]. A number of methods for measurement such as neurite outgrowth, neurite length, and neurite branching, have been developed. Moreover, quantitative assessment of the neurite outgrowth in these assays includes parameters, such as the number of neurites, neurite orientation and neurite length [59].

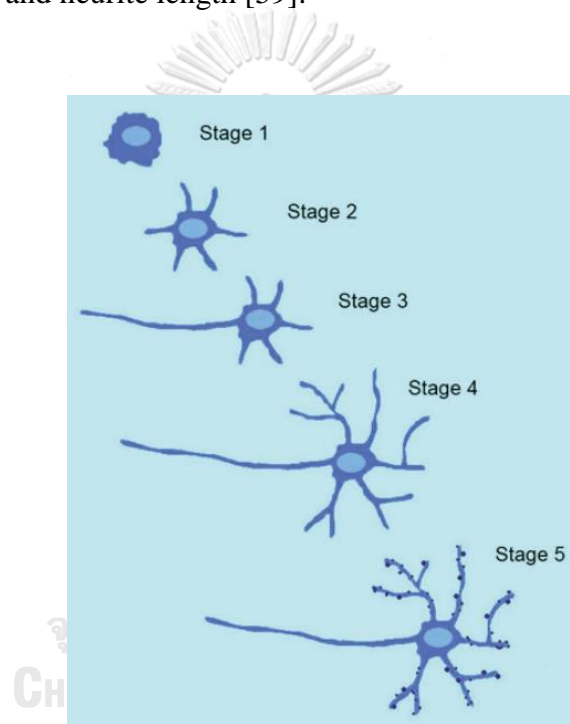


Figure 2. The process of neuron development. A typical *In vitro* cultured neuron development includes 5 stages (Image from [56]).

2.3 Molecular and cellular theory of neurite outgrowth

Neurite outgrowth is an important step in the differentiation of neurons, which start at the cell body extends outside of functional synapses for response to extracellular signals, neurite outgrowth processes relate to add new plasma membranes, generate new cytoplasm, expand and modify the cytoskeleton [60]. Mammalian neurotrophins including NGF, BDNF, neurotrophin 3 (NT3), and neurotrophin 4 (NT4) play major roles in development, maintenance, repairing, and survival of specific neuronal populations. The neurotrophins-induced dimerization of the Trk receptors especially TrkA, leads to activation through transphosphorylation of the cytoplasmic domain kinases and stimulates three major signaling pathways: phosphatidylinositol-3-kinase (PI3K)/Akt, mitogen-activated protein kinase (MAPK), and phospholipase C- γ 1 [61]. Downstream signaling principally promotes survival, growth, and neuronal differentiation and mediates neurogenesis and plasticity in many neuronal populations.

An NGF-mediated signal transmitted from the terminals and distal axons to nuclei regulated phosphorylation of the transcription factor CREB (cyclic adenosine monophosphate response element-binding protein). Internalization of NGF and its receptor (TrkA) transport to the cell body. The tyrosine kinase activity of TrkA was required to maintain it in an autophosphorylated state upon its arrival in the cell body and for propagation of the signal to CREB within neuronal nuclei. Thus, an NGF-TrkA complex is a messenger that delivers the NGF signal from axon terminals to cell bodies of sympathetic neurons [62]. NGF linked to spheres and applied to the cell bodies of sympathetic neurons to induce phosphorylation of the transcription factor cAMP response element binding protein (CREB). However, NGF linked to spheres and applied to the distal axons of sympathetic neurons is incapable of inducing CREB phosphorylation, demonstrating that the retrograde signal to CREB requires internalization. Similarly, inhibition of internalization with a dominant negative form of dynamin attenuates the appearance of both phospho-CREB and phospho-Erk5 (extracellular signal-regulated kinase 5) in cell bodies of sensory neurons following application of neurotrophin to distal axons. Thus, endocytosis is required for many aspects of retrograde signaling [63].

2.3.1 MEK/ERK and PI3K/AKT signaling pathway

Several pathways such as ERK1/2 and PI3K can promote cell survival not only in the nervous system but also in other tissues [64, 65]. Several studies indicated that PI3K and its downstream effector Akt involved in neuronal survival and promoted neurite outgrowth [66]. Recently, the ERK pathway, a part of MAPKs, involved in a number of physiological functions of neurons, proliferation, differentiation, survival, and regulation of response to various growth factors [67]. The activation of ERK1/2 requires phosphorylation of threonine and tyrosine residues that is carried out by the upstream activator kinase, mitogen-activated protein kinase kinase (MEK). Activated ERK1/2 then changes its localization and phosphorylates different target molecules, including transcription regulators and cytoskeletal proteins [68] mediated the neuroprotective activity against neuron damage. ERK1/2 signaling is also important for neuronal differentiation and activation of associated cytoskeletal and synaptic proteins.

Moreover, The recent study reported that MEK/ERK or PI3K/AKT signaling activation was involved in TRPC6 channel-mediated neurite outgrowth in PC12 cells and hippocampal neurons [69], in brimonidine-mediated axon growth after optic nerve injury [70], in BIG1-regulated neurite development [71], in puerarin-regulated neuritogenesis in the neurite extension process [72], and in a natural diarylheptanoid-promoted neuronal differentiation and neurite outgrowth *In vitro* and *In vivo* [73].

2.3.2 PKC pathway activation

Protein kinase C (PKC) is a family of kinases that are involved in regulation of target proteins through the phosphorylation of their serine and/or threonine amino acid residues. PKCs are conserved among eukaryotes and played important roles in several signal transduction cascades. The PKC family consists of at least ten isozymes that are divided into three subfamilies based on their structure and activation mechanisms: conventional, novel, and atypical [74].

One of the PKC subfamilies, atypical PKC (aPKC) has two isoforms, PKC iota (PKC_ι, named PKC λ in mice) and PKC zeta (PKC ζ). aPKC is important for maintaining polarity in cells [75] and in establishing and maintaining polarity for the

development and differentiation of neurons [76], for which axon formation represents an extreme example of cell polarization. During the beginning of axon formation, a complex of aPKC, PAR-3, PAR-6 and a Rac-specific guanine nucleotide exchange factor, mediates the activation of Rac, which controls actin polymerization in the elongating axon [77]. Localization of PAR-3 to the tip of the developing axon is especially important for this process [78].

2.3.3 Teneurin 4

Teneurin (Ten-m/Odz) is a family of type II transmembrane proteins that are highly conserved from invertebrates to mammals. Teneurins compose of an N-terminal intracellular domain and a large C-terminal extracellular domain. In vertebrates, there are Ten-1–4 isoforms, teneurin members are extremely expressed in subpopulations of neurons in the central nervous system (CNS) and also observed in nonneural tissues [79]. Ten-1–4, are expressed in differentiating neurons and Ten-4 is highly expressed in the central nervous system.

Recently, Suzuki et al reported that Ten-4 expression was induced during neurite outgrowth of the neuroblastoma cell line Neuro-2a .Ten-4 protein was localized at the neurite growth cones and Ten-4 overexpression promoted filopodia-like protrusion formation and the length of individual neurite outgrowth through the FAK signaling pathway [8].

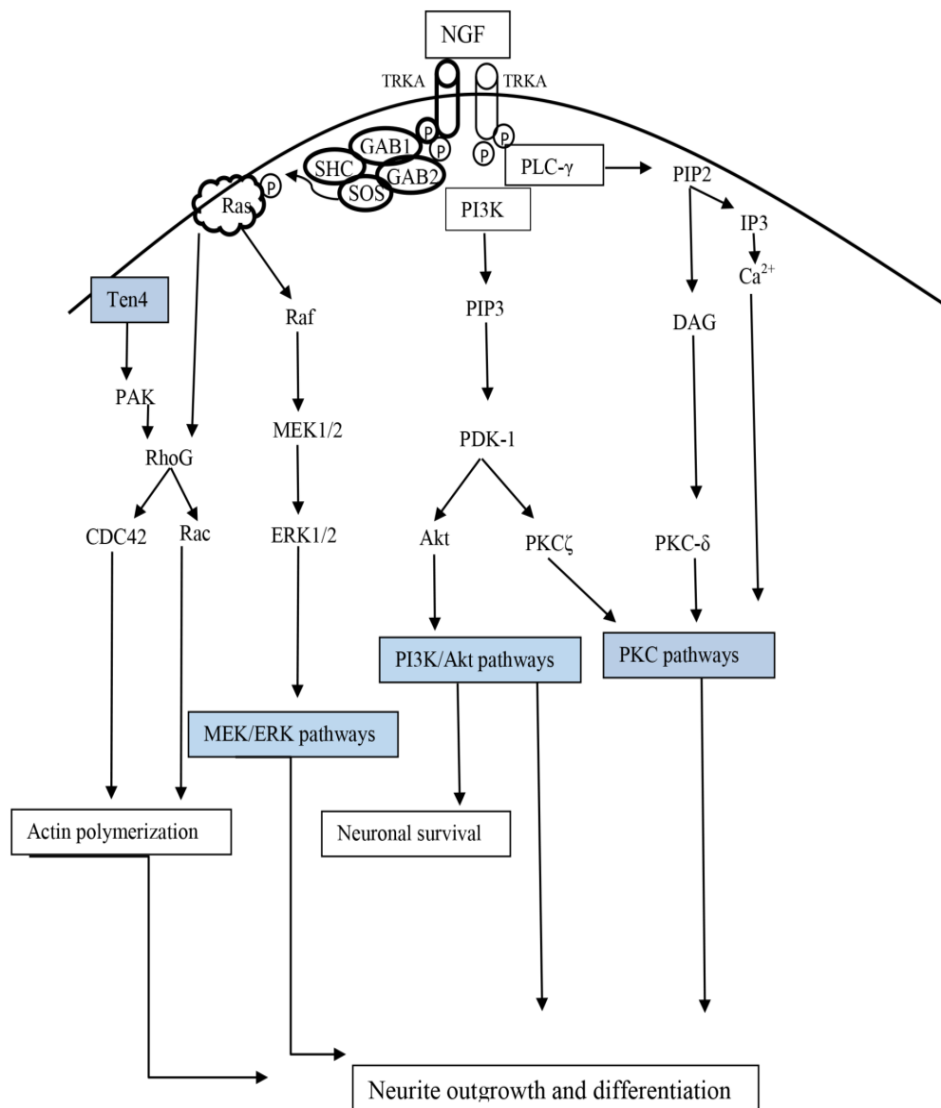


Figure 3. NGF and neurite outgrowth signaling pathways

2.4 Glutamate/H₂O₂ and neurodegeneration

Glutamate, the main excitatory neurotransmitter in the brain, has been recognized as one initiating factor for several neurodegenerative disorders [9, 10]. High levels of glutamate activate structural degradation, ROS/RNS production, mitochondrial and DNA damage, which further lead to neurotoxicity and neuronal cell damage [9, 11]. Glutamate induced neuronal toxicity have been proposed in two pathways [80]. First, excitotoxicity, is mediated by over-stimulation of glutamate receptors resulting increased of extracellular Ca²⁺ influx [81]. Second, oxidative toxicity, is mediated by inhibition of cystine uptake, depletion of intracellular glutathione levels, induction ROS and NADPH oxidase-dependent extracellular hydrogen peroxide (H₂O₂) accumulation [82, 83] (Figure 4).

In the central nervous system (CNS), H_2O_2 has caused lipid peroxidation, mitochondrial dysfunction, and DNA damage leading to neuronal dysfunction through the overproduction of intracellular ROS and malondialdehyde (MDA) [84]. H_2O_2 is one of the major ROSs associated with neurological damage induced by oxidative stress [85]. The excessive generation of ROS induced by glutamate and H_2O_2 leading to oxidative stress and neurotoxicity play a major role in a variety of neurodegenerative diseases, especially Alzheimer's disease (AD) [9, 12].



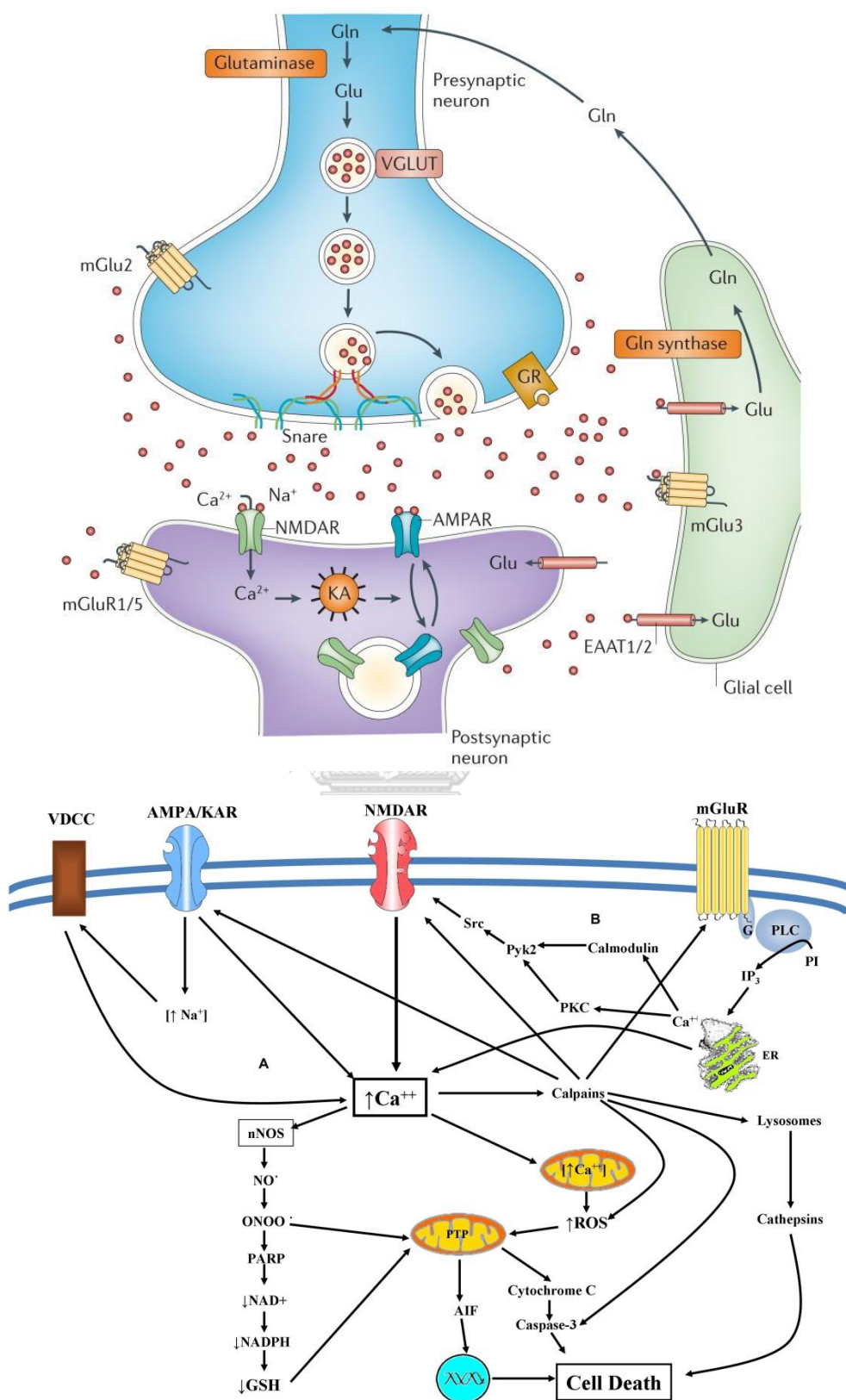


Figure 4. The glutamate synapse and excitotoxicity mediated cell death.(Image from [86], [87])

Neuronal glutamate is synthesized from glutamine (Gln) in glial cells. Glutamate is packaged into synaptic vesicles by vesicular glutamate transporters (vGluT). Glutamate can bind to ionotropic (NMDA, AMPA) and metabotropic (mGluR 1–8) receptors on the membranes of both post-synaptic and pre-synaptic neurons and glial cells. Then, the receptors initiate various responses, including membrane depolarization, activation of intracellular messenger cascades, modulation of local protein synthesis and, eventually, gene expression. Glutamate is cleared from the synapse through excitatory amino acid transporters (EAATs) (EAAT 3–5) on neurons (EAAT 3–5) [86]. Glutamate is converted to glutamine by glutamine synthetase within the astrocyte before being transported to presynaptic neurons, thereby completing the glutamate-glutamine cycle [86].

Under excessive glutamate conditions, consequently over-activates NMDA receptors (NMDA R) trigger an influx of calcium and sodium, which stimulates the production of reactive oxygen species (ROS) such as superoxide (O_2^-), and hydrogen peroxide (H_2O_2) as well as reactive nitrogen species (RNS) such as nitric oxide (NO) and peroxynitrite ($ONOO^-$). High ROS and RNS accumulation induce cell death by activating proteases that damage cellular architecture, peroxidizing lipids, which disrupt membrane integrity, stimulating microglia to produce cytotoxic factors, disrupting mitochondrial function, and inducing pyknosis (chromatin condensation) [87].

2.5 Oxidative stress and age-associated neurodegeneration

Aging is an inevitable natural process accompanied by a progressive accumulation of damage in all constituent macromolecules such as nucleic acids, lipids and proteins [16]. Although the determined mechanisms of aging process are not completely identified, increasing new evidences suggest that aging and age-associated neurodegenerative diseases are considerably associated with ROS [13]. ROS are a group of reactive molecules derived from oxygen which have unpaired valence electrons resulting in generally short-lived and highly reactive [88]. ROS including superoxide (O_2^-), hydrogen peroxide (H_2O_2) and hydroxyl radical (OH \cdot), are generated by both exogenous and endogenous sources. Endogenous sources of ROS generated during normal aerobic respiration of the cells by mitochondria. Exogenous sources of ROS generated by phagocytosis bacteria- or virus-infected cells, generation of by-products in peroxisomes (lipid and fatty acid degradation), and cytochrome P450 [89]. The production of ROS increases during aging, while the endogenous defense mechanisms can decrease. Oxidative stress is the unbalance condition of ROS and antioxidants. Oxidative stress can damage cells by lipid peroxidation, protein oxidation and DNA/RNA damage. These phenomena can lead to neurodegenerative disease [88].

2.6 Antioxidant defense mechanism

2.6.1 Endogenous antioxidant

Generally, the production of ROS is balanced by exogenous and endogenous antioxidant systems. The exogenous antioxidant can be obtained from food sources such as vitamins A, C and E. The endogenous antioxidant system can be divided in two groups, enzymatic and non-enzymatic [90]. The enzymatic group includes superoxide dismutase (SOD), catalase (CAT), glutathione peroxidase (GPx), and glutathione reductase (GR) [90] (Figure 5).

Superoxide dismutase (SOD): The protective mechanisms against ROS were start by SOD, catalyzes the conversion of $O_2^{\cdot-}$ to H_2O_2 and O_2 . Following, the CAT converted H_2O_2 to water and O_2 . Cytosolic copper/zinc-SOD (SOD1), mitochondrial manganese SOD (SOD2), and extracellular SOD (SOD3) are three distinct isoforms of SOD that have been identified [88].

Catalase (CAT): Catalase converted H_2O_2 to water and oxygen using iron or manganese as a cofactor. Catalase is found in the cytoplasm and mitochondria [88].

Glutathione peroxidases (GPX): GPX contains a family of multiple isoenzymes which catalyze the reduction of H_2O_2 and lipid peroxides utilizing GSH as an electron donor. GPX is located in both cytosol and mitochondria. GPX1 exists universally in the cytosol and mitochondria which have been regarded as one of the major antioxidant enzymes in the brain. Studies reported that GPX1 up-regulation is involved in protective responses against neuronal injury [88]. The nonenzymatic group includes glutathione (GSH), the most abundant antioxidant in most of the brain cells, thioredoxin (Trx), vitamins A, E, and C, and selenium [90].

Glutathione (GSH): GSH were synthesized from glutamate, cysteine, and glycine which exert protective function against oxidative stress. GSH is non-enzymatically involved in ROS removal by react with ROS such as $O_2^{\cdot-}$ and $\cdot OH$. Moreover, GSH is the electron donor for the reduction of peroxides in the GPX reaction. GSH counteracted with ROS generating glutathione disulfide (GSSG) and enters a cycle together with GPx and GR. Studies reported that GSH is involved in protective responses against apoptotic cell death and DNA damage by oxidative stress [88].

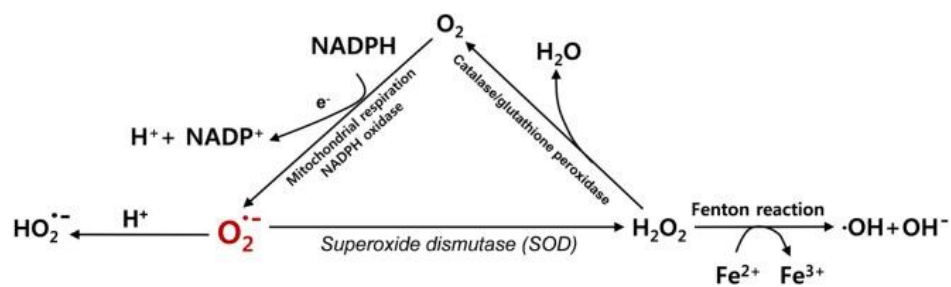


Figure 5. Generation of ROS.(Image from [88])

A by-product of respiratory chain complex in the mitochondria or by NADPH oxidase O_2 cause superoxide ($O_2^{\cdot-}$), which consequently transformed in to hydrogen peroxide (H_2O_2) by superoxide dismutase (SOD) and further transformed to O_2 and H_2O_2 by catalase (CAT) and glutathione (GSH) [88].

2.6.2 SIRT1/Nrf2 signaling pathway

Sirtuin 1 (SIRT1) is a class III histone deacetylase that plays an important role in cell physiological and biochemical processes, including aging, inflammation and neuroprotection [91]. SIRT1 exhibited neuroprotective effects by suppression NF- κ B, prevention amyloid beta-induced toxicity and ameliorate brain inflammatory injury after induction with LPS [92]. Moreover, SIRT1 are involved in the regulation of biological processes of oxidative stress. SIRT1 regulates several important transcription factors, including nuclear erythroid factor 2- related factor 2 (Nrf2), which induced the transcription of antioxidant enzymes and subsequently affected the cellular redox state [92].

Nrf2 translocate to the nucleus and activate the antioxidant response elements (AREs) in the promoter region of many antioxidant genes including heme oxygenase (decycling) 1 (HMOX1), NAD(P)H:quinone oxidoreductase 1 (NQO1), glutamate cysteine ligase complex modifier subunit (GCLM), glutamate-cysteine ligase catalytic subunit (GCLC), and glutathione S-transferase 1 (GSTP1) [92, 93]. Nrf2 mediates and antioxidant enzymes, such as SOD and GST. Accumulating evidences suggest that SIRT1 and Nrf2 involved in CNS redox balance of neurodegenerative disorders by

promoting antioxidant responses [26, 27] (Figure 6). In addition, the enhancing of SIRT1 and Nrf-2/HO-1 expression can protect neurons against oxidative injury in neuronal cells [27]. Many studies reported that SIRT1 promotes the activity of NRF2 and upregulates the expression of NRF2 downstream genes, which protected neurons against oxidative injury in HT22 cells [92, 94].

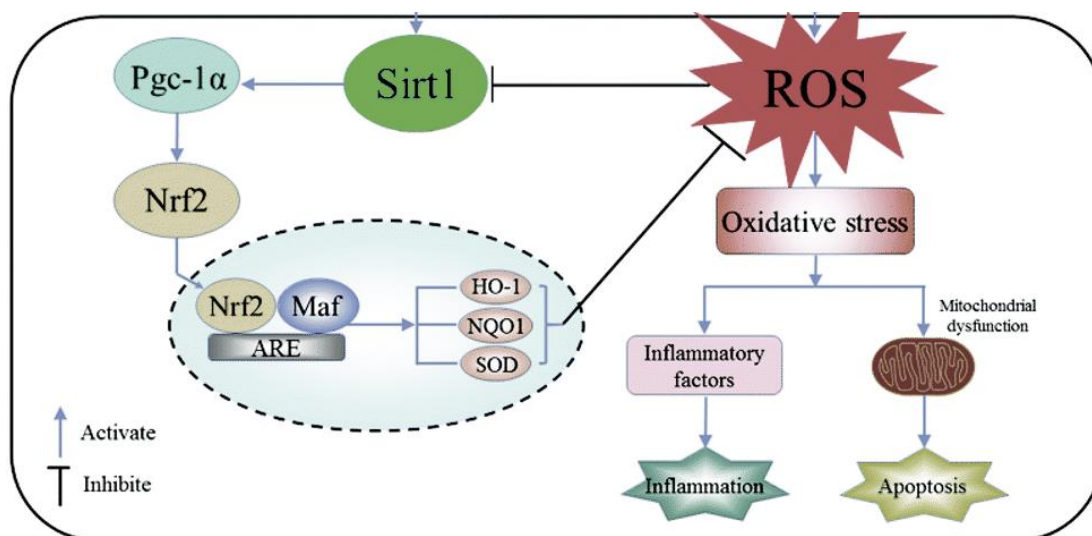


Figure 6. The mechanisms of SIRT1-Nrf2 signaling pathway on oxidative stress resistance properties. (Image from [95]).

2.7 The cultured neuronal cells model

2.7.1 The mouse hippocampal neuronal HT22 cells

In mouse hippocampal neuronal HT22 cells, glutamate can block glutamate-cystine antiporters, resulting in the depletion of the cellular antioxidant glutathione and an increase of ROS, consequence induce neuronal necrosis and apoptosis [10]. These cells lack ionotropic glutamate receptors, also excluding excitotoxicity as a cause for glutamate stimulated neurons death. This makes the HT22 cell line serve as an excellent model of glutamate-induced oxidative neurotoxicity [27]. Therefore, the glutamate-induced cell death in HT22 cells has been widely used as an *In vitro* assay to screen neuroprotective compounds and to elucidate its neuroprotective mechanisms.

2.7.2 The mouse neuroblastoma Neuro-2a cells

The mouse neuroblastoma Neuro-2a cells (Neuro-2a) cells are derived from spontaneous neuroblastoma of mouse and capable to differentiate into neuronal-like cells. Neuro-2a cells are widely established as an *In vitro* model for studying neurite outgrowth [96].

2.8 *Caenorhabditis elegans*; a model for aging and age-related diseases

A major challenge to the identification of effective disease-modifying therapies and life span extension becomes from an insufficient knowledge about the contribution of multiple pathways. Mammalian disease models offer *In vivo* opportunities and extensive similarity to the human, but testing the therapeutic value of small molecules in mammalian model systems is extremely expensive and requires time-consuming experimental designs that can be prohibitive. Over the past decades, the soil nematode *Caenorhabditis elegans* (*C. elegans*) has increasingly been used as a model system to study aging and lifespan extension. The research in the *C. elegans* aging field was focused on the genetics of aging and single gene mutations that increased the life span of the worms. However, there are several different approaches are being used in the *C.elegans* aging field in addition to genetic manipulations that influence life span. For example, environmental manipulations such as caloric restriction and hormetic treatments, evolutionary studies, population studies, models of age-related diseases, and drug screening for compounds that extends life span [97]. Several studies with *C. elegans* have led to new discoveries in neuroscience, signal transduction, cell death, RNA interference, environmental toxicology and biomedical science, among others [98]. Since the discovery of a genetic pathway that appeared to greatly influence aging and stress resistance in *C. elegans* [99], it has also been used extensively as a model organism in studies aiming to unravel lifespan determination.

C. elegans is a small saprophytic nematode of about 1 mm in length in the adult stage. It is a transparent self-fertilizing hermaphrodite, producing both sperm and eggs. *C. elegans* worms have a life cycle of about 3 days and an average lifespan of 18 to 20 days when cultivated *In vitro* on *Escherichia coli* at 20 °C. The postembryonic life cycle of *C. elegans* consists of four larval stages, L1–L4, and

a reproductive stage. Under unfavorable conditions, the L2 stage can enter the dauer larval stage, instead of developing into the regular L3 stage [100]. *C. elegans* shows a number of age-related changes reminiscent of those observed in other organisms. With advancing age worms are less active, display uncoordinated movements, and eventually they stop moving. This appears to be the result of muscle degeneration rather than neuronal defects as the cellular integrity of the nervous system is preserved till very late in life [101]. Other age-related changes include accumulation of lipofuscin, dark pigments, presence of vacuole-like structures, and increased levels of oxidized proteins. It is worth noting that even in an isogenic population great variability in age-related changes between individual worms is observed, suggesting that stochastic factors play a role during nematode aging [102-104].

2.9 Oxidative resistance and longevity pathways in *C.elegans*

2.9.1 The insulin/IGF-1 signaling (IIS) pathway

The insulin/IGF-1 signaling (IIS) pathway's components are highly conserved in worms, flies, and mammals, and the FOXO transcription factor, DAF-16, is the major downstream effector of DAF-2 [105]. The *C. elegans* IIS pathway connects nutrient levels to metabolism, growth, development, longevity, and behavior. This pathway is regulated by insulin-like peptide ligands that bind to the insulin/IGF-1 transmembrane receptor (IGFR) [21, 106]. *DAF-2* was identified for its mutant's dauer constitutive (Daf-C) phenotype, forming the alternative larval state under growth-promoting conditions, while *daf-16* was identified in a Daf-D (dauer defective) mutant that suppressed the *daf-2* mutant's dauer formation [21, 107, 108]. In conditions suitable for growth and reproduction, activation of DAF-2 by binding of an agonist insulin-like ligand initiates a phosphorylation cascade that ultimately inhibits DAF-16 activity (Figure 7).

The AGE-1 PI3K downstream of DAF-2/IGFR also regulates longevity. Activated DAF-2 phosphorylates the phosphoinositide 3-kinase, AGE-1, generating PIP3, recruits the kinases AKT-1, AKT-2, SGK-1, and PDK-1 to the plasma membrane, where PDK-1 phosphorylates AKT and SGK-1 [109, 110]. The AKT-

1/AKT-2/SGK-1 complex phosphorylates the forkhead transcription factor DAF-16 [109, 111], sequestering it in the cytoplasm [112, 113], thus preventing DAF-16 from activating or repressing transcription of its target genes in the nucleus (Figure 6). Inhibitors of this cascade include DAF-18, the phosphoinositide 3-phosphatase PTEN, which antagonizes AGE-1 by dephosphorylating PIP3 [114], and PPTR-1, a regulatory subunit of PP2A that dephosphorylates AKT-1 [115]. The IIS regulation of longevity effects on nematodes similar in flies [116, 117] and mice [118, 119]. The role of IIS in life span control may also extend to humans. Studies in cohorts of Ashkenazi Jewish centenarians have identified non-synonymous polymorphisms in the gene encoding the IGF-I receptor that are associated with longevity [120]. Importantly, cells expressing IGF-1 receptors harboring these polymorphisms exhibit reductions in ligand-dependent Akt phosphorylation, gene regulation, and cell cycle progression compared to cells expressing wild-type IGF-1 receptors, indicating that a reduction in IGF-1 signaling is correlated with longevity in humans [121].

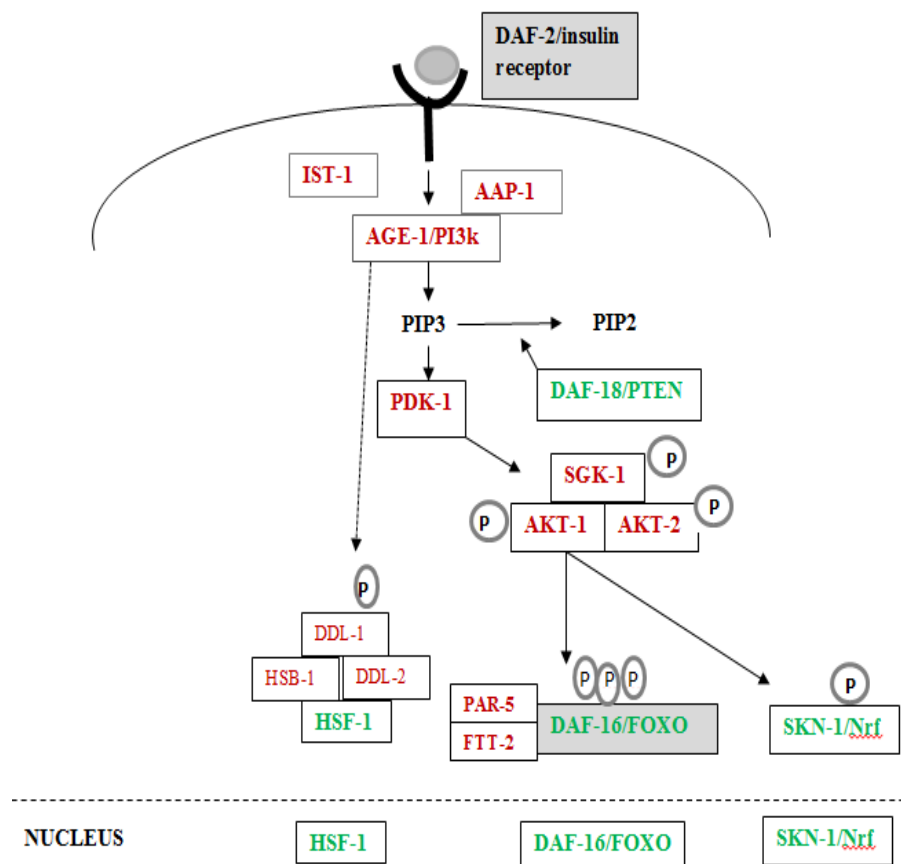


Figure 7. Schematic of *C. elegans* IIS. (Image from [122])

2.9.2 DAF-16/FOXO signaling pathway

C. elegans DAF-16/FOXO is a key node in a diverse array of physiological processes, including development, aging, immunity, stress response, thermotolerance, pathogen resistance, and metabolism. The transcriptional targets of DAF-16 roles in stress-response, antimicrobial, autophagic, and metabolic genes [106] and many of the genes most highly regulated by DAF-16 influence aging [21]. Many of the DAF-16 targets revealed by genome-wide approaches, a large number of these genes may play a role in protection from stresses. First, genes involved in oxidative stress response, such as superoxide dismutases, catalases, and glutathione S-transferases [21]. Second, Heat shock proteins, in particular hsp-16, hsp-12.6, and sip-1 as well as other anti-toxicity genes [123, 124]. And third, genes involved in pathogen resistance, such as lys-7, spp-1, and thaumatins and hypertonic stress resistance [123, 125]. DAF-

16 appears to select specific members of a variety of classes to achieve increased stress protection.

DAF-16 tissue-specific targets to effect different multiple roles. Several lines of evidence suggest that DAF-16 requires other molecules for its activity including c-Jun N-terminal kinase (JNK), CST-1 or Ste20-like kinase and MST1 homolog, Sir2, The 14-3-3 proteins, Heat-shock factor (HSF), β -catenin, SMK-1, HCF-1 and SKN-1 [106]. The fact that both FOXO and insulin/IGF-1 receptors have been identified as genes linked to extreme longevity in recent human centenarian studies [120, 121, 126] suggests that discovering the downstream, tissue-specific FOXO-regulated targets, as in model organisms, will be important for understanding FOXO's role in human longevity and aging. For example, in mice, loss of the insulin receptor in adipose (fat) tissue extends life span [118]. In flies, overexpression of FOXO in the adipose tissue extends life span [127] (Figure 8).

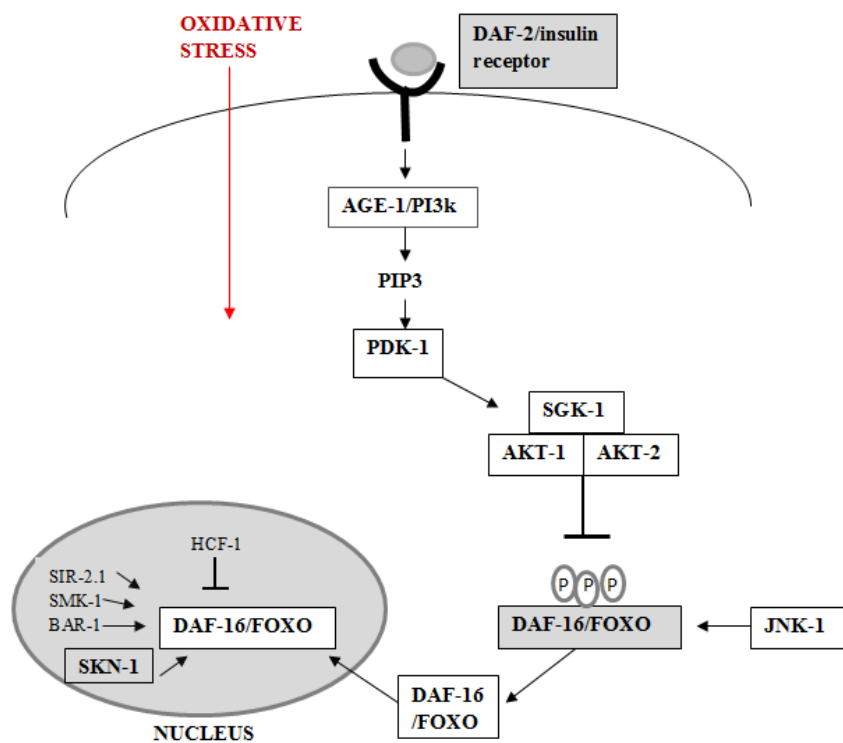


Figure 8. DAF-16 interacts with specific proteins under different stimuli. [128]

2.9.3 The SKN-1/Nrf-2 signaling pathway

The mammalian Nrf/CNC proteins (Nrf1, Nrf2, Nrf3, p45 NF-E2) perform a wide range of cellular protective and maintenance functions. In the nematode *C. elegans*, which offers many advantages for genetic analyses, the Nrf/CNC proteins are represented by their ortholog SKN-1.

The *C. elegans* transcription factor SKN-1/Nrf defends against oxidative stress by activating the conserved phase 2 detoxification systems [129]. Additionally, SKN-1 upregulates numerous other genes involved in growth, nutrient, metabolic signals, detoxification, cellular repair, pathogen resistance, and genes that reduce stress resistance and life span [130]. SKN-1 is expressed in the intestine mediates the phase 2 stress response and the ASI neurons [129]. Similar to the regulation of DAF-16 by insulin signaling, the IIS kinases phosphorylate SKN-1, and reduced IIS leads to constitutive SKN-1 accumulation in intestinal nuclei and target gene activation [131]. Furthermore, SKN-1 contributes to the longevity and stress resistance phenotypes of reduced insulin signaling. These results raise the possibility that SKN-1 acts together with DAF-16 in regulating some processes and target genes. SKN-1 promotes longevity in otherwise WT animals. Loss-of-function *skn-1* mutants have a shortened lifespan [129], and lifespan is extended significantly by more modest SKN-1 overexpression [131]. The aging process also affects SKN-1: during aging the constitutive expression of many SKN-1-regulated genes declines progressively [132], and the responsiveness of SKN-1 target genes to acute oxidative stress is lost [133]. In *Drosophila*, a similar decline in Nrf2 stress responsiveness occurs with aging [134] (Figure 9).

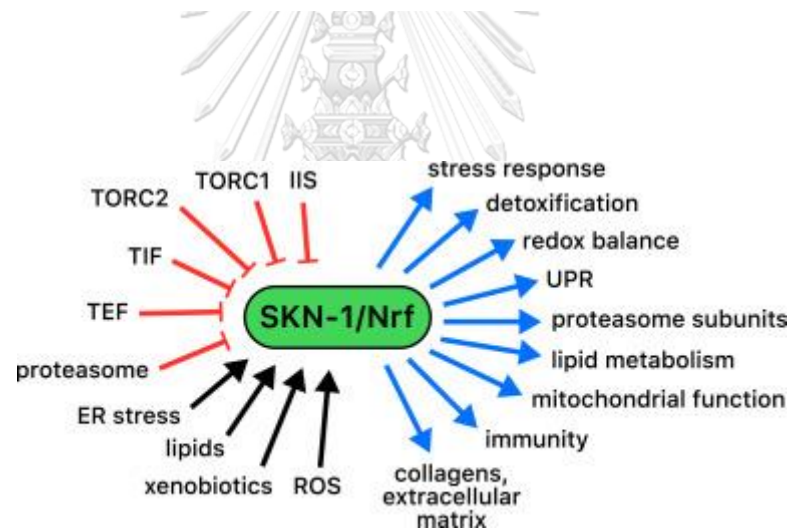
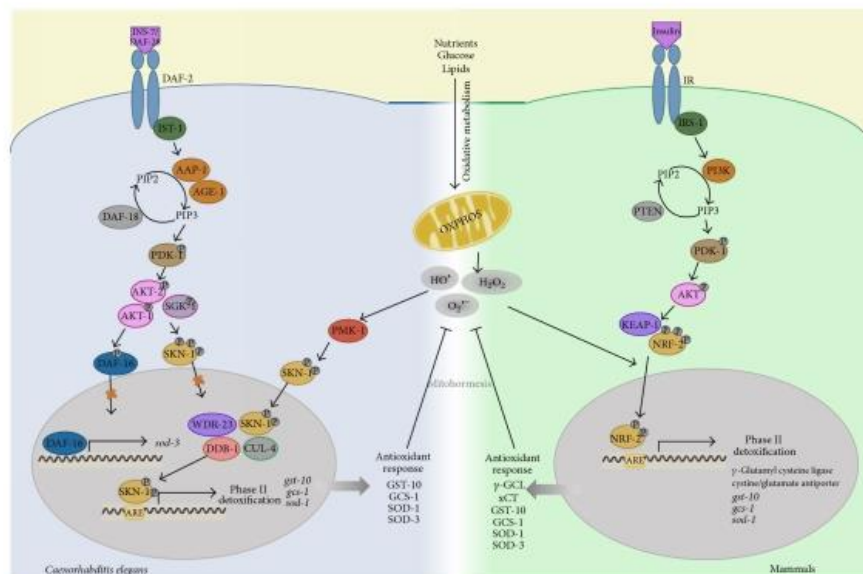


Figure 9. The SKN-1/Nrf2 signaling pathway on stress resistance properties in *C. elegans* and mammals. (Image from [135] [24])

2.10 Thai plant in this study

2.10.1 *Anacardium occidentale*

Anacardium occidentale L (Figure 10), which is called cashew tree or Mamuanghimmaphan in Thai name, is a tropical evergreen tree that produces the cashew seed and the cashew apple which belongs to Anacardiaceae family. The species is originally native to northeastern Brazil and can be found in tropical zone of

East Asia such as Myanmar, Thailand, Cambodia, Vietnam, and Malaysia. Several studies reported that cashew leaves and cashew nut have a great economic and medicinal value. *A. occidentale* has useful for traditional medicine such as in traditional Maya medicine, the leaves or bark of cashew trees can be made into a tea to treat diarrhea.[136] The bark and leave of *A. occidentale L.* are rich in tannins and phenolic compounds can antimicrobial, antibacterial, antioxidant, anti-ulcerogenic , anti-inflammatory,[137] antiulcer, antitumor activity through suppression of hypoxia and angiogenic factors as well as have hypoglycemic effect in diabetic rats and have ability to lower blood glucose levels [138]. Sheela et al. has reported that an ethanolic extract of *A. occidentale L.* leaves suppresses vascular endothelial growth factor (VEGF) induced angiogenesis of both *In vivo* and *In vitro* [139].

Moreover specie of *Anacardium* shows the presence of secondary metabolites including phenols, flavonoids, xanthenes, chalcones, and tannin pyrogallates. Most of secondary metabolites, tannins and flavonoids are related to medicinal use for antibacterial activity treatment of intestinal disturbances and skin lesions. *Anacardium* nut oil has been shown to have an apoptotic effect on tumor cell lines like acute myeloblastic leukemia, breast carcinoma, and cervical epithelial carcinoma [140, 141].



Figure 10. *Anacardium occidentale L.*

2.10.2 *Glochidion zeylanicum*

Glochidion zeylanicum (Gaertn) A. Juss (Figure 11). (GZ) (Phyllanthaceae), which is known as Man pu, Phung mu or Chumset in Thai, can be cultivated in many tropical countries, belongs to Euphorbiaceae family and can be found in tropical zone of East Asia such China, Japan, Myanmar, Thailand, Cambodia, Vietnam, and Malaysia. *Glochidion* species are used as food, local medicinal plants by the leaves. Recently, some studies about *Glochidion* species reported that the roots are used as medicine for coughs and pneumonia, the stem and leaves are used for treating abdominal pain, toothaches and traumatic injuries as well as the leaves are used in the treatment of itches, scabies. Moreover, the local medicinal plants, *Glochidion* plants were used for the treatment of rheumatoid arthritis, influenza, dysentery, impaludism, and dyspepsia [29]. These plants are rich sources of flavanol glucosides, which have a powerful antioxidant [30], anti-inflammation [29], and antitumor potential [31].

According to Kongkachuichai study demonstrated that Mon-pu (*G. perakense*) consisted of high amounts of gallic acid, epicatechingallate and apigenin. Moreover young cashew leaves (*A. occidentale*) also composed of abundant gallic acid, epigallocatechin-3-gallate, epicatechin, quercitin and kaempferol. These plants were rich sources of b-carotene, lutein, total polyphenol, especially gallic acid, and high antioxidant activities plant in Thailand [28]. Furthermore, the total polyphenol content of mon-pu and young cashew leaves are greater than that in blackberries, red kidney beans, and green tea by approximately 2–6 times [142].



Figure 11. *Glochidion zeylanicum* (Gaertn) A. Juss.

2.11 Herbal medicines in anti-aging and neurodegenerative diseases

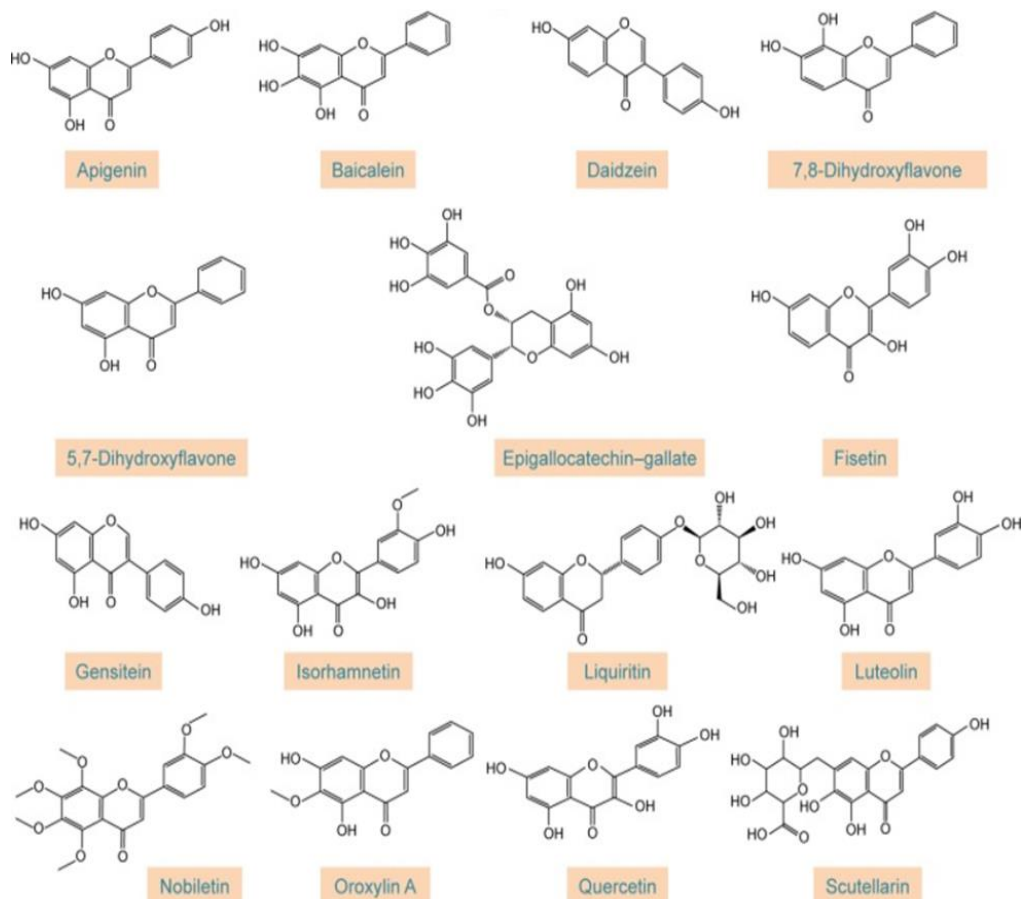
2.11.1 Plant extracts and neuroregenerative properties

Many polyphenolic compounds from natural herbal have been studied on neurite outgrowth promotion in neuronal cell lines. A number of studies have shown that different polyphenols including flavonoids such as genistein, quercetin, liquiritin from *Glycyrrhizae radix* plant, isorhamnetin (a flavonolglycone from *Ginkgo biloba* plant), and acetylated flavonoid glycosides from *Scopariadulcis* together with the stilbenoid compound resveratrol (a polyphenol present in grapes and red wine) can significantly promote neurotrophin (nerve growth factor [NGF] and brain-derived neurotrophic factor [BDNF]) through neurite outgrowth in neuronal cells line [37]. Flavonols including kaempferol, quercetin, and isorhamnetin have capability to enhance the expression levels of the differentiation markers (GAP-43, neurofilament light subunit, synaptophysin, synapsin, and induce neurite outgrowth [143].

Oxidative stress is involved in neurodegenerative diseases including AD and PD. Previous studies have been shown that the polyphenolic compounds exhibited neuroprotective effects in different brain pathologies including neurodegenerative such as Alzheimer's and Parkinson's disease [37]. The antioxidant effect of polyphenols play a role in ROS not only the direct interaction with ROS but also the mechanism of action such as activation of Nrf2 pathway, upregulation of antioxidant enzymes, induction of hypoxia signal transduction (HIF-1- α pathway) [144]. EGCG and catechin [145] and resveratrol [146] have been reported to exert their neuroprotective action through activation of the HIF-1 pathway. The polyphenolics including EGCG, epicatechin, curcumin, resveratrol, quercetin and citrus flavonoids (naringenin and hesperetin) that have neuroprotective effect can cross the blood-brain barrier and localize within the brain tissues (Figure 12). Thus, the neuroprotective and neuromodulatory may have benefit in different brain pathologies [37].

Moreover, the polyphenols from grape juice can improve mild cognitive impairment in elder adults. Previous studies have shown that resveratrol consumption significantly improves memory performance in older adults. The polyphenols compounds are usefully in the brain health during aging [147]. Moreover, in middle-aged, the polyphenols consumption such as catechins, flavonols, and hydroxybenzoic

acids is strongly connected with language and verbal memory. Similarly, other studies indicated that the effects of other polyphenols are helpful on cognitive function and memory in risk for people who have neurodegenerative diseases [37].



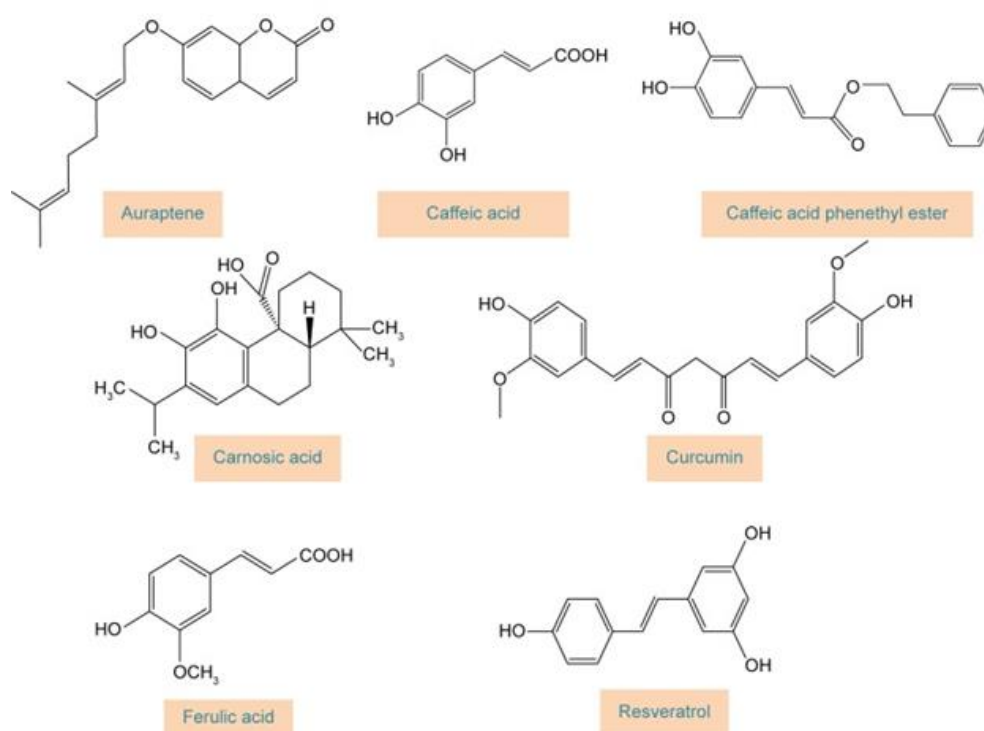


Figure 12. Chemical structures of polyphenols with neurotrophic activity ([37])

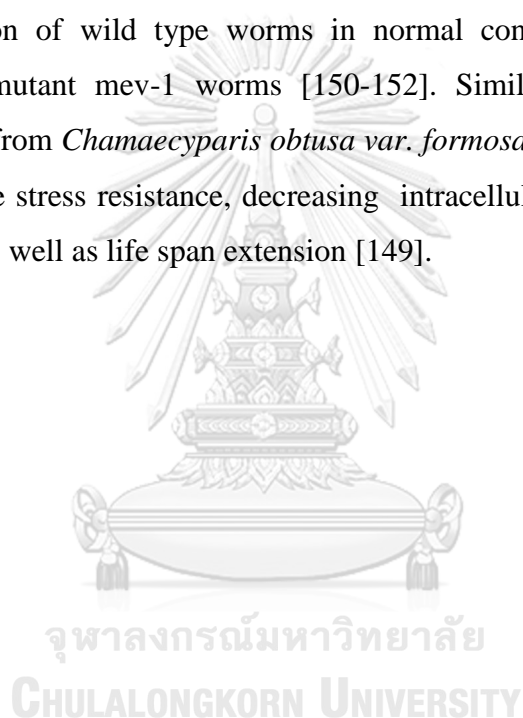
2.11.2 Plant extracts and anti-aging properties

Aging caused by degenerative damages, resulting in the death of an organism ultimately. Recently researches try to develop therapies that delay age-related diseases in human. Natural products have attraction resource with special advantage and few side effects [148]. Several study reported the compound that exhibited anti-aging activity in *C. elegans* models such as resveratrol, α -lipoic acid, astaxanthin, catechin, curcumin, fucoxanthin, spermidine, metformin, caffeine, and rapamycin. Moreover, the antioxidant compound including caffeic acid, coenzyme Q10, gallic acid, oleanolic acid, vitamin E, and vitexin showed the anti-aging and anti-oxidative activity [148].

The insulin/IGF-1 signaling (IIS) pathway and The SKN-1/Nrf-2 signaling pathway are well known as the antioxidant and anti-aging in *C. elegans*. Catechin, caffeic acid, epigallo-catechin gallate, oleanolic acid, rosmarinic acid, sesamin, kaempferol, quercetin, proline, serine, tryptophan and myricetin have been reported in

antioxidant and anti-aging activities via the insulin/IGF-1 signaling (IIS) pathway [148]. Antcin M, baicalein, caffeic acid, sesamin, proline, serine and tryptophan have been reported in antioxidant and anti-aging activities via the the SKN-1/Nrf-2 signaling pathway [148].

Recently, quercetin and flavonoid rich plant extracts have been reported on lifespan extension in *C. elegans* [149-152]. Quercetin has protective effect against oxidative stress by reducing internal oxidative stress and intracellular ROS. Moreover, quercetin show anti-aging effect on reducing lipofuscin accumulation and increasing life span extension of wild type worms in normal condition and hypersensitive oxidative stress mutant *mev-1* worms [150-152]. Similar with Quercetin-3-O- α -rhamnopyranoside from *Chamaecyparis obtusa* var. *formosana* leaves extract that have effect on oxidative stress resistance, decreasing intracellular ROS accumulation and lipofuscin level, as well as life span extension [149].



CHAPTER III

MATERIALS AND METHODS

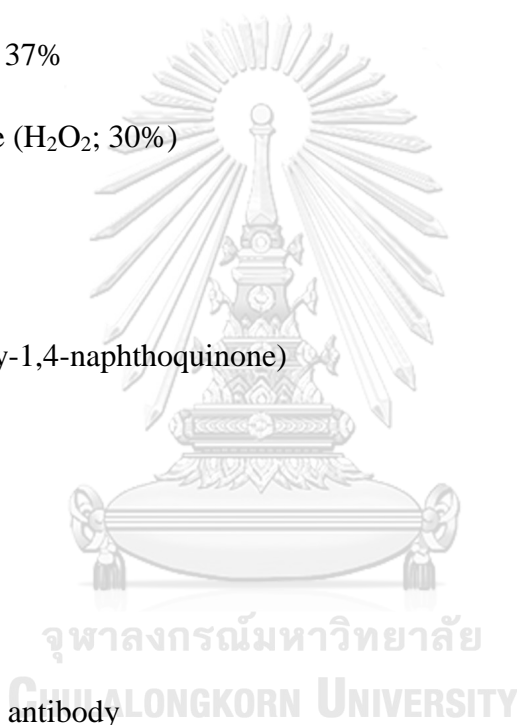
3.1 Materials

3.1.1 Chemicals and reagents

Name	Company, Country
2,2'-Azino-bis(3-ethylbenzothiazoline-6-sulfonic acid) diammonium salt (ABTS)	Sigma-Aldrich, USA
Acetylcholinesterase from electric gel (EC 3.1.1.7, type V-S)	Sigma-Aldrich, USA
30% Acrylamide/Bis solution, 37:5:1	Bio-Rad, USA
Blotting-grade blocker	Bio-Rad, USA
Bovine serum albumin (BSA), Fraction V	GE Healthcare, USA
Bradford reagent	Bio-Rad, USA
Chloroform	Sigma-Aldrich, USA
CytoTox 96® non-radioactive cytotoxicity assay	Promega, USA
Dichloromethane	RCI Labscan, Thailand
Diethyl pyrocarbonate (DEPC)	Sigma-Aldrich, USA
Dimethyl sulfoxide (DMSO)	Sigma-Aldrich, USA

Dulbecco's modified Eagle's medium (DMEM)	Sigma-Aldrich, USA
DNA Ladder 100 bp	Thermo Scientific, USA
2,2-Diphenyl-1-picrylhydrazyl (DPPH)	Sigma-Aldrich, USA
ECL Select Western Blotting detection reagent	GE Healthcare, USA
EGCG (Epigallocatechin gallate) (the purity $\geq 95\%$)	Sigma-Aldrich, Germany
Ethanol	RCI Labscan, Thailand
Fetal bovine serum (FBS)	Sigma-Aldrich, USA
FITC Annexin V Apoptosis Detection Kit with PI	BioLegend, USA
Folin-Ciocalteu phenol reagent	Sigma-Aldrich, USA
Galantamine	Sigma-Aldrich, USA
GAP43 antibody	Abcam, UK
Gallic acid	TCI America, USA
GBX Developer/Fixer	Kodak, USA
Glycine	GE Healthcare, USA

Goat anti-rabbit IgG, HRP-linked antibody	Cell Signaling Technology, USA
2', 7'-dichlorodihydrofluorescein diacetate (H ₂ DCFDA)	Molecular Probes, USA
Hank's balanced salt solution (HBSS)	Gibco, USA
Hexane	RCI Labscan, Thailand
Hydrochloric acid, 37%	Merck, Germany
Hydrogen peroxide (H ₂ O ₂ ; 30%)	Merck, Germany
Isopropanol	Sigma-Aldrich, USA
Juglone (5-hydroxy-1,4-naphthoquinone)	Sigma-Aldrich GmbH, Germany
L-ascorbic acid	Calbiochem, USA
L-glutamic acid	Sigma-Aldrich, USA
Mouse anti-β-actin antibody	Cell Signaling Technology, USA
Quercetin	Sigma-Aldrich, USA
Methanol	RCI Labscan, Thailand
3-(4,5-dimethylthiazol-2-yl)-2,5-diphenyltetrazoliumbromide	Biobasic, Canada (MTT)



Nuclear factor-E2-related factor 2 (Nrf2) antibody	Cell Signaling Technology, USA
Oligo(dT)17 Primer	Bioneer, South Korea
Paraformaldehyde	Sigma-Aldrich, USA
Penicillin/Streptomycin solution	Gibco, USA
Phosphate buffered saline (PBS)	Hyclone, USA
Potassium carbonate (K_2CO_3)	Merck, Germany
Potassium persulphate ($K_2S_2O_8$)	Sigma-Aldrich, USA
Primers	Bioneer, South Korea
Protein ladder	Thermo Scientific, USA
PVDF membrane	GE Healthcare, USA
qPCR PreMix	Bioneer, South Korea
RT PreMix	Bioneer, South Korea
Sirtuin 1 (SIRT1) antibody	Cell Signaling Technology, USA
Sodium acetate (NaOAc)	Sigma-Aldrich, USA



Sodium azide	AppliChem GmbH, Germany
Sodium carbonate (Na ₂ CO ₃)	Merck, Germany
Sodium chloride (NaCl)	Merck, Germany
Sodium dodecyl sulfate (SDS)	Ajax Finechem, Austarlia
Sodium hydroxide (NaOH)	Merck, Germany
Sodium sulfate (Na ₂ SO ₄)	Merck, Germany
Tetramethylethylenediamine (TEMED)	Merck, Germany
Teneurin-4 antibody	R&D Systems, Inc., Canada
Tris base	Vivantis Technologies, Malaysia
Tris-HCl	Sigma-Aldrich, USA
Trizol reagent	Invitrogen, USA
Triton X-100	Merck, Germany
Trypan Blue Solution, 0.4%	Gibco, USA
Trypsin-EDTA	Hyclone, USA
Tryptone	Thermo Scientific, USA
Tween 20	Vivantis Technologies, Malaysia

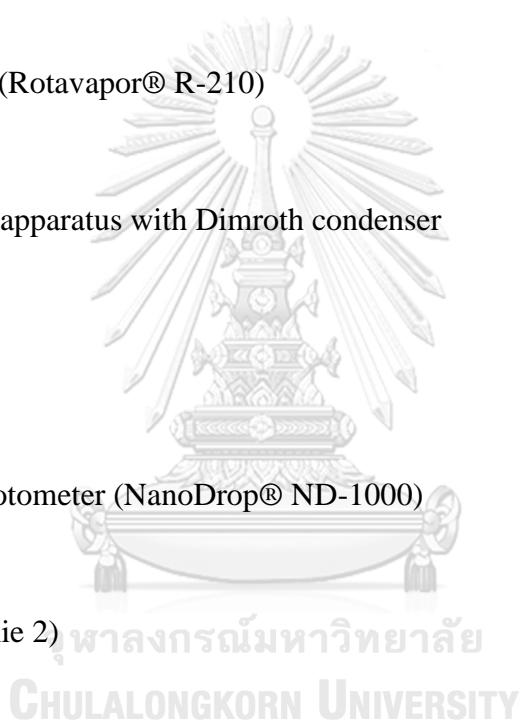
3.1.2 Tools and devices

Name	Company, Country
Adhesive optical sealing film	Bioneer, South Korea
Analytical balance	Mettler Toledo, Switzerland
Autoclave	Hirayama, Japan
Autopipette	Gilson, France
Benchtop centrifuge (Hettich® Universal 320R)	Sigma-Aldrich, USA
Block heater	Wealtec, USA
Cell culture flask (25 and 75 cm ³)	Corning, USA
Cell culture plate, flat bottom with lid (6-, 12-, 96-well)	Corning, USA
Cell culture plate, black, flat bottom with lid (96-well)	Corning, USA
Centrifuge tube (15 and 50 mL)	Corning, USA
Centrifugal evaporator (miVac Quattro)	Genevac, UK
CO ₂ incubator (Forma Series II 3110)	Thermo Scientific, USA
Disposable serological pipettes (5, 10, 25 mL)	Corning, USA
Electrophoresis power supply	Bio-Rad, USA
Extraction thimble cellulose (Whatman™)	GE Healthcare, USA
Filter tips (ART® 10, 100, 200, 1000 µL)	Thermo Scientific, USA

Filter paper no.1 (Whatman™)	GE Healthcare, USA
Fluorescence microscope (Axio Observer A1)	Carl Zeiss, Germany
Fluorescence microscope (BIOREVO BZ-9000)	Keyence Deutschland GmbH, Germany
Freezer (-20°C)	Sanyo Electric, Japan
Freezer (-80°C)	Lyofreeze, USA
Fused-silica capillary column (Agilent HP-5MS, 30 m × 0.25 mm, i.d., 0.25 µm film thickness)	Agilent Technologies, USA
Hemocytometer	Hausser Scientific, USA
Incubator	Memmert, Germany
Inverted microscope	Olympus Optical, Japan
Laboratory glass bottles (Duran®)	DWK Life Sciences, Germany
Laminar flow cabinet	Haier, China
Laminar flow cabinet	ESI Flufrance, France
Laminar flow clean bench	Esco, Singapore

Light microscope	Olympus Optical, Japan
Liquid nitrogen tank	Taylor Wharton, USA
Mass selective detector (Agilent 5973)	Agilent Technologies, USA
Micro high speed refrigerated centrifuge (VS-15000CFNII)	Vision Scientific, South Korea
Microcentrifuge tube (0.2 and 0.6 mL)	Axigen Scientific, USA
Microcentrifuge tube (1.5 mL)	Biologix Research, USA
Microplate reader (EnSpire® multimode)	Perkin-Elmer, USA
Microplate reader (Synergy™ Mx)	BioTek Instruments, USA
Mini Trans-Blot® Electrophoretic Transfer cell	Bio-Rad, USA
Multichannel pipette	Gilson, France
PCR tube (0.2 mL opaque white 8-strip)	Bioneer, South Korea
pH meter	Mettler Toledo, Switzerland
Pipette Controller	Eppendorf, Germany
Pipette tips (10 µL)	Sorenson, USA

Pipette tips (200 and 1000 μ L)	Corning, USA
Real-time quantitative thermal block (Exicycler™ 96)	Bioneer, South Korea
Refrigerator (4°C)	Sharp, Japan
Rotary evaporator (Laborota 4001) Instruments,	Heidolph Germany
Rotary evaporator (Rotavapor® R-210)	Buchi, Switzerland
Soxhlet extraction apparatus with Dimroth condenser	Lenz Laborglas, Germany
Stereomicroscope	Nikon Corporation, Japan
UV-Vis spectrophotometer (NanoDrop® ND-1000) USA	Thermo Scientific, Scientific Industries, USA
Vortex mixer (Genie 2)	FinePCR, South Korea
Vortex mixer (FINEVORTEX)	Memmert, Germany
Waterbath	



3.1.3 Plant materials

The leaves of *Anacardium occidentale* L. (AO) and *Glochidion zeylanicum* (Gaertn) A. Juss. (GZ) were collected from Jana district, Songkhla Province, in southern Thailand and were stored as a voucher specimen at the herbarium of Kasin Suvatabhandhu (Department of Botany, Faculty of Science, Chulalongkorn University, Thailand).

3.1.3.1 *Anacardium occidentale* L. (AO)

Family: Anacardiaceae

Common name: Mamuanghimmaphan (in Thai), Cashew (in English)

Herbarium voucher number: No. BCU-015863



Figure 13. *Anacardium occidentale* L. Leaf

3.1.3.2 *Glochidion zeylanicum* (Gaertn) A. Juss (GZ)

Family: Phyllanthaceae

Common name: Man pu, Phung mu or Chumset (in Thai)

Herbarium voucher number: No. BCU-016061



Figure 14. *Glochidion zeylanicum* (Gaertn) A. Juss. Leave

3.1.4 The cultured neuronal cell models

The HT22 cells and Neuro-2a cells (Figure 15) were used to examine neuroprotective and neuritogenesis properties on neuronal cell models in this study.

The mouse hippocampal neuronal HT22 cells have been used to study neuroprotective properties. These cells lack ionotropic glutamate receptors and are resistant to excitotoxicity as a cause for glutamate-stimulated neuronal death [10]. HT22 cell line was a generous gift from Professor David Schubert at the Salk Institute, San Diego, CA, USA.

The mouse neuroblastoma Neuro-2a cells have been extensively used to study neuronal differentiation and neurite growth [40]. Neuro-2a cell line was obtained from Health Science Research Resources Bank, Osaka, Japan

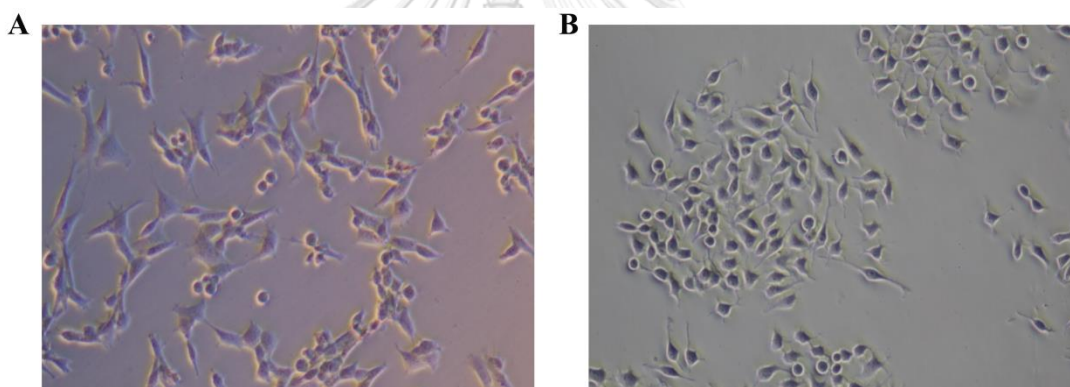


Figure 15. The morphology of cultured neuronal. (A) HT22 and (B) Neuro-2a cells

3.1.5 The *C. elegans* models

The nematode *C. elegans* were used to examine oxidative stress resistance properties and anti-aging in this study.

The strains N2 (wild-type) (Figure 16), TK-22 (*mev-1*[*kn1*]III), TJ375 (*gpIs1*[*hsp-16-2*::GFP]), CF1553 (*mul84*[*pAD76*(*sod-3*::GFP)]), TJ356 (*zIs356* [*daf-16p*::*daf-16a/b*::GFP+*rol-6*]), CF1038 (*daf-16*[*mu86*]I), BA17 (*fem-1*[*hc17*]IV), EU1 (*skn-1*[*zu67*]), CL2166 ([*pAF15*]*gst-4p*::GFP::NLS) , LD1(*ldls7*) and *Escherichia coli* OP50 were obtained from the Caenorhabditis Genetics Center at the University of Minnesota, USA. All strains were cultured at Prof. Dr. Michael Wink's laboratory, Institute of Pharmacy and Molecular Biotechnology, Heidelberg University, Germany.

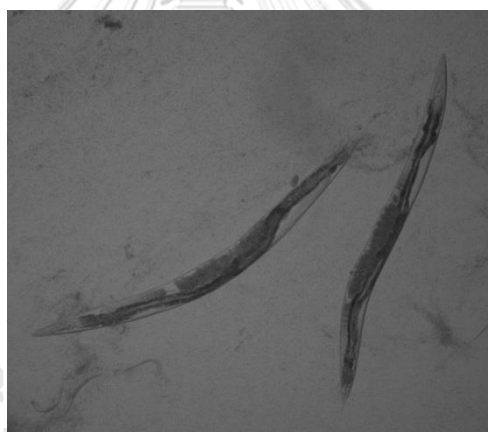


Figure 16. *C. elegans* wild-type (N2)

3.2 Methods

3.2.1 Plant extraction

The leaves of *A. occidentale* L. and *G. zeylanicum* were shade dried and agitated using blender. The extracts were extracted sequentially with 400 mL hexane, dichloromethane and methanol by Soxhlet for 36 h. The extracts were evaporated at 35-45 °C after filtration using Whatman No. 1 filter paper. The extracts were calculate percent yield of the final product [153, 154] (Figure 17).

The residue was dissolved in dimethyl sulfoxide (DMSO) to a final concentration of 100 mg/mL as stock solution and stored at -20 °C until needed for analysis. The extraction yields of AO hexane, dichloromethane and methanol extracts were 1.21%, 0.46%, and 15.97%, respectively. The extraction yields of GZ hexane, dichloromethane and methanol extracts were 0.74%, 0.33%, and 11.78%, respectively.

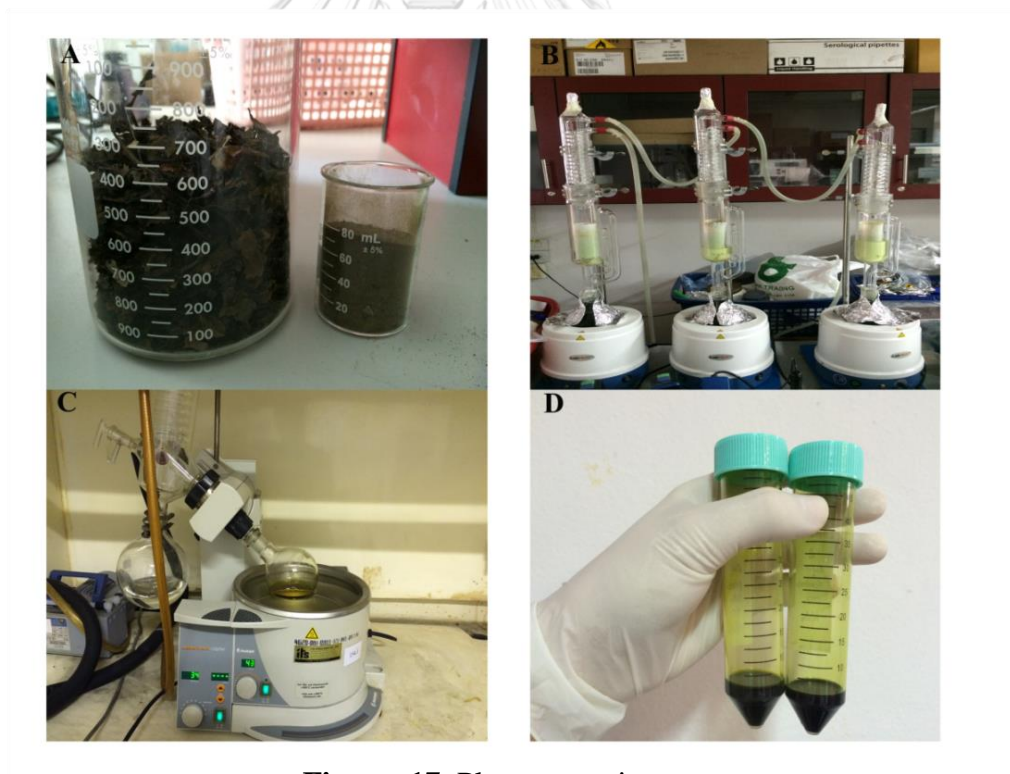


Figure 17. Plant extraction

(A) The extracts powder after agitated by blender, (B) Soxhlet extraction, (C) Evaporation, (D) Plant Extracts

3.2.2 Phytochemical analysis

3.2.2.1 Gas/Liquid Chromatography-Mass Spectrometry analysis

The hexane and methanol extracts were submitted to screening and phytochemical analysis by using GLC-MS and LC-MS (Gas/Liquid Chromatography-Mass Spectrometry) at the Institute of Systems Biology (University Kebangsaan Malaysia, Malaysia).

For GLC-MS chromatographic separation was carried out on a Clarus 600 GC-MS system (Perkin Elmer, Shelton, CT, USA) separated with a 30 m × 0.25 mm × 0.25 µm Elite-5MS column (Perkin Elmer, USA). The temperature of the oven was set at 40 °C and was increased by 5 °C/min until it reached 250 °C, and the carrier gas was helium at a constant flow of 1 mL/min. The MS parameters used were electron impact mode (EI) following an ionization voltage of 70 eV, an ion source temperature of 200 °C and a scan range of 40–600 Da. The National Institute of Standards and Technology (NIST, version 2.0, Gaithersburg, MD, USA) database was used for the identification of compounds by exceeding the signal-to-noise ratio (S/N) of 100 and comparing the volatile information based on the compounds compound name. Match and reverse match values below 800 were filtered [153, 154].

For LC-MS, chromatographic separation was carried out on a Dionex™ UltiMate 3000 UHPLC system (Thermo Scientific) equipped with an Acclaim™ Polar Advantage II C18 column (3 × 150 mm, 3 µm particle size) (Thermo Scientific, USA) by using a 1 µL injection volume. The mobile phase comprised 0.1% formic acid in water (solvent A) and 100% acetonitrile (solvent B), which had a flow rate of 400 µL/min for 22 min. At 0-3 min, 3-10 min, 10-15 min, and 15-22 min; 5% B, 80% B, 80% B, and 5% B were used for the gradient elution, respectively. High-resolution MS analysis was carried out in the positive electrospray ionization mode using a MicroTOF-Q III (Bruker Daltonik GmbH, Bremen, Germany). A capillary voltage of 4500 V, drying gas flow of 8 L/min, an ion source temperature of 200 °C, a nebulizer pressure of 1.2 bar, an end plate offset of –500 V, and a scan range from m/z 50 to 1000 were used as parameters for the instrument. The METLIN and KNApSACk databases were used for the identification of compounds by comparing the observed m/z values with the calculated mass values from previously published

data. The abundance of individual compounds was calculated from the percentage of peak area relative to the total area of all peaks in the chromatograms [153, 154].

The secondary metabolites of the hexane extract were further submitted to characterize and quantify the bioactive compounds by GLC-MS (Gas/Liquid Chromatography-Mass Spectrometry) at RSU Science and Technology Research Equipment Center (Rangsit University, Thailand). GLC-MS analysis, chromatographic separation was carried out on a Clarus 600 GC-MS system (Perkin Elmer, Shelton, CT, USA) equipped with a 30 m × 0.25 mm × 0.25 μm Elite-5MS column (Perkin Elmer, USA). The temperature of the oven was set at 40 °C and was increased by 5 °C/min until it reached 250 °C, and the carrier gas was helium at a constant flow of 1 mL/min. The MS parameters: electron impact mode (EI) at an ionization voltage of 70 eV, an ion source temperature of 200 °C and a scan range of 40–600 Da [153, 154].

3.2.2.2 High Performance Liquid Chromatography (HPLC) analysis

The secondary metabolites of the methanol extract were further submitted to characterize and quantify the bioactive compounds by HPLC (High-Performance Liquid Chromatography) at RSU Science and Technology Research Equipment Center (Rangsit University, Thailand).

HPLC analysis, the chromatography was carried out on SHIMADZU LC-10 HPLC equipped with an analytical C18 reversed-phase column (ODS3 C18, 4.6 × 250 mm i.d., 5-micrometer particle size) and UV detector (best condition at 220 nm). The mobile phase consists of 0.02 M sodium acetate, buffered to a pH of 4 with 0.0125 M citric acid, containing 0.042 M methanesulfonic acid and 0.1 mM EDTA. The flow rate was set at 1 mL/min. The working standard solutions were freshly prepared in 0.05 M perchloric acid containing 0.1 mM Na₂EDTA on ice and stored at –20 °C before using. Peaks were identified by comparing the retention time of each peak in the sample solution, where each individual peak was further compared to the standard solution of gallic acid, catechin, epigallocatechin gallate (EGCG), oxyresveratrol, quercetin, octadecatrienolic acid (linolenic acid), and hexadecanoic

(palmitic acid) (Sigma-Aldrich, USA) served as an internal standard. The calibration curves of internal standard compounds were constructed for quantification [153, 154].

3.2.3 Determination of antioxidant properties *In vitro*

3.2.3.1 Radical scavenging activity

The stable radical DPPH (DPPH•) and the stable cation radical ABTS (ABTS•+) were used for measuring free radical scavenging activity. Briefly, the reaction consisted of DPPH• or ABTS• + solution and the extract (1 mg/mL) at a 1:1 ratio. After incubation in the dark for 30 min, the absorbance was read at 517 nm or 734 nm using an EnSpire® Multimode Plate Reader (Perkin-Elmer, USA) and a UV-VIS Spectrophotometer with ascorbic acid (vitamin C) at various concentrations used as a standard. Vitamin C and EGCG were used as positive controls. Radical scavenging activity was expressed as the percent inhibition of the radical calculated by the following equation: % Radical scavenging activity = [(Abs of control- Abs of sample) × 100/ Abs of control]. The antioxidant capacity was expressed as an EC₅₀ value [153, 154].

3.2.3.2 Total phenolic content

The Folin Ciocalteu method was used to determine the total phenolic content. In brief, 50 µL of the extract (1 mg/mL) was mixed with 50 µL of a fold diluted Folin-Ciocalteu phenol reagent. After 20 min, the mixture was neutralized by the addition of 50 µL of a 7.5% (w/v) Na₂CO₃ solution and incubated in the dark for 20 min. Then, the absorbance was measured at 760 nm. Gallic acid was used as a standard for the calibration curve. The total phenolic content was expressed as gallic acid equivalents (GAE/mg of plant extracts) [153, 154].

3.2.3.3 Total flavonoid content

An aluminum chloride colorimetric method was used to measure the total flavonoid content. In brief, 50 µL of the extract (1 mg/mL) was mixed with 150 µL of 95% ethanol, 10 µL of 10% (v/v) AlCl₃ solution and 10 µL of 1 M NaOAc solution. Then, the mixture was incubated in the dark for 40 min, and the absorbance was measured at 415 nm. The total flavonoid content was calculated from a calibration curve using

quercetin as a standard, and the results are expressed as quercetin equivalents (QE/mg of plant extracts) [153, 154].

3.2.3.4 Cell-based antioxidant measurement

ROS production was quantified by the DCFH-DA method. After treatment, 10 μ M H₂DCFDA was added to the culture medium and incubated for 30 min at 37 °C, followed by washing with Hank's balanced salt solution (HBSS). The fluorescence intensity (excitation = 485 nm; emission = 535 nm) was measured using an EnSpire® Multimode Plate Reader (Perkin-Elmer). Data were expressed as the percentage of fluorescence intensity of treated cells relative to the untreated control.

3.2.4 Cell culture and treatment condition

HT22 cells (The Salk Institute, San Diego, CA, USA) were maintained in DMEM supplemented with 10% (v/v) fetal bovine serum and 1% penicillin/streptomycin. Neuro-2a cells (Health Science Research Resources Bank, Osaka, Japan) were maintained in DMEM and HamF12 supplemented with 10% (v/v) fetal bovine serum and 1% penicillin/streptomycin. Cells were incubated under at 37 °C in a humidified incubator with 5% CO₂.

HT22 and Neuro-2a cells were treated with different concentrations of the AO/GZ hexane extracts (10-50 μ g/mL) and the AO/GZ methanol extracts (0.5-10 μ g/mL) for 48 h. To induce cell toxicity, glutamate or H₂O₂, were added to the culture medium. Stock solutions of glutamate and H₂O₂ were prepared in DMEM. Stock solutions of the extracts were prepared in DMSO. For the untreated control group, cells were treated with 0.1% (v/v) DMSO.

3.2.5 Determination of cell viability

Cell viability was evaluated by using MTT and LDH assay. To perform the MTT assay, after each treatment, 0.5 mg/mL MTT were added to the culture medium and incubated for 3 h at 37 °C. Then, all solution was removed and the formazan crystals were solubilized by DMSO-ethanol mixture (1:1, v/v). The absorbance at 550 nm was measured using an EnSpire® Multimode Plate Reader (Perkin-Elmer, Waltham, MA, USA). Results were expressed as a percentage of cells relative to the untreated control.

For LDH assay, the activity of LDH release into culture medium was measured using the CytoTox 96® assay (Promega) according to the manufacturer's instructions. After each treatment, the culture supernatant was incubated with a substrate mix for 30 min in the dark at RT, followed by the addition of a stop solution. The absorbance at 490 nm was read using an EnSpire® Multimode Plate Reader (Perkin-Elmer, Waltham, MA, USA). Results were expressed as a percentage of maximum LDH release obtained by complete cell lysate.

3.2.6 RNA isolation and quantitative RT-PCR

Total RNA was extracted using Trizol reagent (Invitrogen) following the manufacturer's instructions. The amount of RNA was determined by measuring the absorbance at 260 nm. 1 µg of total RNA was used for cDNA synthesis using AccuPower RT PreMix (Bioneer) and oligo (dT). All real-time PCR reactions were performed in an Exicycler™ 96 (Bioneer). PCR conditions: 95 °C for 15 min, followed by 45-55 cycles of denaturation at 95 °C for 15 s and primer annealing/extension at 55 °C for 30 s. A melting curve analysis was performed to determine primer specificity [10, 93]. The relative expression of each gene was normalized against the internal control gene (β -actin) and expression levels were analyzed using the $2^{-\Delta\Delta CT}$ method.

Table 1. List of the gene-specific sequences of primers in this study.

Gene	Sequence of primer	Product size (bp)
SOD1	Forward: 5'-CAGGACCTCATTTTAATCCTCAC-3' Reverse: 5'-CCCAGGTCTCCAACATGC-3'	76
SOD2	Forward: 5'-CTGGACAAACCTGAGCCCTA-3' Reverse 5'-TGATAGCCTCCAGCAACTCTC-3'	62
CAT	Forward: 5'-CAGCGACCAGATGAAGCA-3' Reverse: 5'-CTCCGGTGGTCAGGACAT-3'	68
GPx	Forward: 5'-ACAGTCCACCGTGTATGCCTTC-3' Reverse: 5'-CTCTTCATTCTTGCCATTCTCCTG-3'	238
GSTo1	Forward: 5'-CAGCGATGTCGGGAGAAT-3' Reverse: 5'-GGCAGAACCTCATGCTGTAGA-3'	102
GSTa2	Forward: 5'-TCTGACCCCTTTCCCTCTG-3' Reverse: 5'-GCTGCCAGGATGTAGGAACT-3'	85
NQO1	Forward: 5'-CGACAACGGTCCTTTCCAGA-3' Reverse: 5'-TCCCAGACGGTTTCCAGAC-3'	253
GCLM	Forward: 5'-GGAGCTTCGGGACTGTATCC-3' Reverse: 5'-AACTCCAAGGACGGAGCAT-3'	236
EAAT3	Forward: 5'-ATGATCTCGTCCAGTTCGGC-3' Reverse: 5'-TGACGATCTGCCC AATGCTT-3'	202
GAP43	Forward: 5'-AGCCTAAACAAGCCGATGTG-3' Reverse: 5'-GGTTTGGCTTCGTCTACAGC-3'	157
Ten4	Forward: 5'-GTGGACAAGTTTGGGCTCAT -3' Reverse: 5'-GGGTTGATGGCTAAGTCTGT -3'	185
β -actin	Forward: 5'-GGCTGTATTCCCCTCCATCG-3' Reverse: 5'-CCAGTTGGTAACAATGCCATGT-3'	154

3.2.7 Western blot analysis

Whole cell lysates were prepared in 1X RIPA buffer according to the manufacturer's protocol. Total protein concentrations were quantified by the Bradford assay. An equal amount of protein (20 μ g) was separated on 6-10% SDS polyacrylamide gel and then transferred to PVDF membranes. After blocking for 2 h with 5% skim milk in TBS-T (Tris-buffered saline, 0.1% Tween 20), the membranes were allowed to incubate overnight at 4 °C with primary antibodies specific for SIRT1 (1:2000), Nrf2(1:8000), GAP43 (1: 8000), Ten-4 (1: 2000) or β -actin (1:16,000). Membranes were incubated with HRP-conjugated secondary antibodies (1:10,000) at room

temperature for 60 min. Specific protein bands were visualized using the DCP-T300 brother scanner and evaluated using ImageJ software (National Institutes of Health, Bethesda, MD).

3.2.8 Measurement of neurite outgrowth and neurite-bearing cells

A neurite outgrowth stimulation assay was performed according to Eik et al [155]. Neuro-2a cells (15000 cells/well) were seeded in 6 well tissue culture plates in 10% FBS medium for 12-18 h. Media were carefully removed and washed by PBS. After that, the cells were treated with different concentrations of AOH extract (0.25-1 $\mu\text{g}/\text{mL}$) and AOM extract (0.5-10 $\mu\text{g}/\text{mL}$) in starving condition (1% FBS medium) for 48 h.

The Neuro-2a cells (100 cells /treatment) were randomly photographed using a bright-field microscope under 10X magnification. The cells were marked as differentiated if one or more neurites were longer than the diameter of the cell body [4]. The length of neurite was measured from cell membrane of body cell to the end of the growth cone and the percentage of neurite-bearing cells was quantified by ImageJ software (National Institutes of Health, Bethesda, MD). The expression of a specific neuronal differentiation marker, growth-associated protein 43 (GAP43) was investigated by real-time PCR and Western blot analysis. The cells in complete growth medium (10% FBS) were used as the negative control and the cells in starving condition (1% FBS) medium were used as the control. The cells were treated with 20 μM retinoic acid regarding the positive control.

3.2.9 Knockdown of Teneurin-4 expression

For knockdown of Teneurin-4 (Ten-4), On-Target Plus small interfering RNA (siRNA), which contains the targeting sequence of Ten-4 (Thermo Fisher Scientific), was used. Specific siRNAs of the Ten-4 gene were designed according to Suzuki et al [8] (Sense: 5'- GAUUGUGGCAAACUAGUAU-3', Antisense: 5'- AUACUAGUUUGCCACAAUC-3'). Transfection of Neuro-2a cells was accomplished using Lipofectamine® 2000 (Invitrogen; Thermo Fisher Scientific, Inc.). The negative control group was transfected with AccuTarget™ Negative Control siRNA (Thermo Fisher Scientific) in Neuro-2a cells. The knockdown efficiency was assessed by quantitative RT-PCR (Figure. 18).

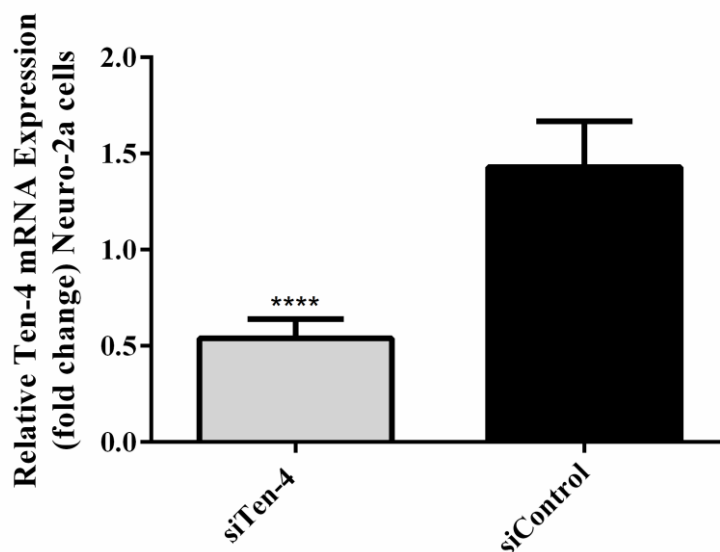


Figure 18. Knockdown efficiency of Ten-4 by siRNA

Ten-4 mRNA expression significantly decreased in siTen-4-Neuro-2a cells (62.26% compared to siCont-Neuro-2a cells). β -actin was used as the internal control for RT-PCR assay. All data were normalized to 10% FBS control levels in siCont-Neuro-2a cells and shown as the mean \pm SEM in at least three independent experiments. ****p < 0.0001 compared to the siCont-Neuro-2a cells in 1% FBS by one-way ANOVA following Bonferroni's method (posthoc).

3.2.10 *C. elegans* culture and treatment condition

The *C. elegans*, all strains were maintained in nematode growth medium (NGM) agar plates at 20 °C except for the BA17 strain, which was maintained at 25 °C to prevent egg laying. The worms were seeded with living *E. coli* OP50 as a food source. A liquid medium was used for some experiments using S-medium, which was prepared by mixing with *E. coli* OP50 (DO600 = 1.0).

Age-synchronized populations of *C. elegans* were obtained by hypochlorite treatment. Worms grown on NGM agar were washed with sterile water and treated with 5 M NaOH and 5% NaOCl at a ratio of 1:2 for 8-10 min for lysis and decontamination. The lysate was pelleted by centrifugation (1200 rpm, 2 min) to obtain eggs. The eggs were separated in the pellet layer, and the pellets were washed with sterile water at a ratio of 1:2, followed by centrifugation (1200 rpm, 2 min). The upper layer of water

was removed, the egg pellet was collected, and eggs were allowed to hatch in M9 buffer [36].

For the treatment group, the toxicity and antibacterial tests were conducted to determine the non-toxic concentration of the extracts with *E. coli* OP50 (Figure 19). Worms were treated with appropriate concentrations of the extracts: 25, 50 and 100 $\mu\text{g}/\text{mL}$ AO/GZ hexane extract; 25, 50 and 100 $\mu\text{g}/\text{mL}$ AO/GZ dichloromethane extract; and 1, 2.5 and 5 $\mu\text{g}/\text{mL}$ AO/GZ methanol extract. For the control group, worms were treated with 1% (v/v) DMSO. For the positive control group, worms were treated with 25 $\mu\text{g}/\text{mL}$ EGCG in all experiments except the lifespan assay, in which worms were treated with 100 $\mu\text{g}/\text{mL}$ EGCG [153, 154, 156].

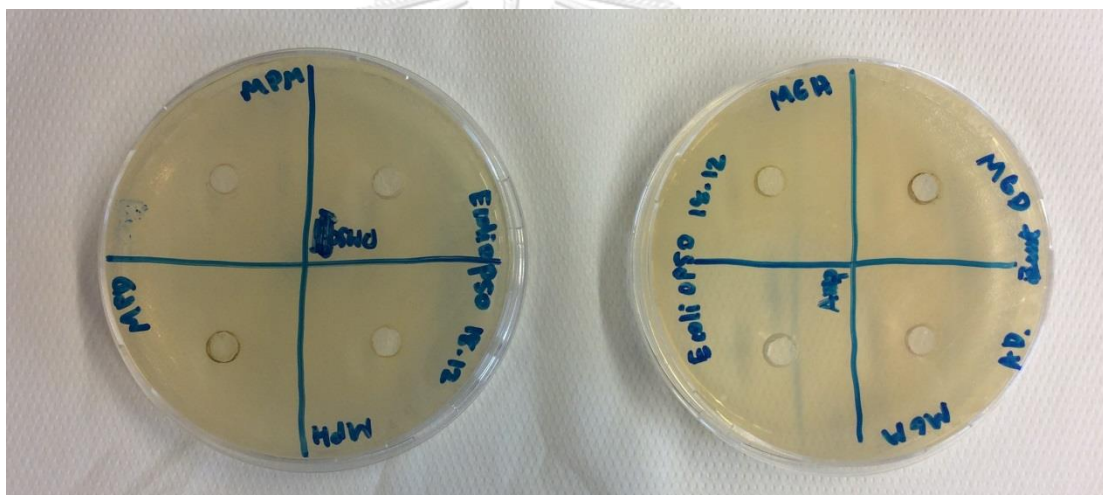


Figure 19. The toxicity tests

The wild-type (N2) worm were treated with different concentrations of the extracts as follows: 25, 50 and 100 $\mu\text{g}/\text{mL}$ AO/GZ hexane extracts; 25, 50 and 100 $\mu\text{g}/\text{mL}$ AO/GZ dichloromethane extracts; and 1, 2.5 and 5 $\mu\text{g}/\text{mL}$ AO/GZ methanol extracts did not exhibited toxicity effect. Moreover, The *E. coli* OP50 treated with high concentration of 500 $\mu\text{g}/\text{mL}$ AO/GZ dichloromethane extracts, 500 $\mu\text{g}/\text{mL}$ AO/GZ hexane extracts and 100 $\mu\text{g}/\text{mL}$ AO/GZ methanol extracts did not exhibited antibacterial effect.

3.2.11 Determination of survival rate under juglone-induced oxidative stress

To analyze the survival rate under oxidative stress conditions, L1 larvae of wild-type (N2) and transgenic (CF1038, EU1) worms were treated with the extracts of different concentrations in S-medium for 48 h; each group contained 80 individuals. Each group was treated with 80 μ M pro-oxidant juglone for 24 h. Then, dead and live worms were counted [153, 154, 156]. The worms were considered dead when they failed to respond to a gentle touch with a platinum wire on their bodies [36].

3.2.12 Measurement of intracellular ROS in *C. elegans*

To measure the intracellular ROS accumulation in *C. elegans*, L1 larvae of wild-type (N2) and transgenic (CF1038, EU1) worms were treated with plant extracts of different concentrations in S-medium for 48 h; each group comprised of 50-100 individuals. After treatment, the worms were pelleted by centrifugation, added to 50 μ M 2,7-dichlorodihydrofluorescein-diacetate (H₂DCF-DA) solution and incubated in the dark at 20 °C for 1 h. After incubation, worms were paralyzed using 10 mM sodium azide and mounted on a microscopic glass slide. Worms were randomly photographed (30 worms/group) using a BIOREVO BZ-9000 fluorescence microscope (Keyence Deutschland GmbH, Neu-Isenburg, Germany) [153, 154, 156]. The relative fluorescence of the whole body was measured and evaluated as the mean fluorescence intensity using ImageJ software (National Institutes of Health, Bethesda, MD).

3.2.13 Quantification of HSP-16.2::GFP, GST-4::GFP and SOD-3::GFP expression

The TJ375, CL2166 and CF1553 transgenic worms, which have a gene promoter fused with a GFP reporter, were used to measure the expression of HSP-16.2, GST-4 and SOD-3, respectively. L1 larvae were treated with plant extracts of different concentrations in S-medium at 20 °C; each group contained 50-100 worms. The TJ375 and CL2166 transgenic worms were incubated for 72 h and 48 h, respectively. Then, the worms were exposed to a nonlethal dose of 20 μ M juglone for 24 h. The CF1553 worms were incubated for 72 h. After that, all worms were submitted to fluorescence microscopy as described before [153, 154, 156].

3.2.14 Determination of subcellular localization of DAF-16 and SKN-1

To determine the localization of the transcription factors DAF-16 and SKN-1, TJ356 and EU1 transgenic strains were used, respectively. L1 larvae were treated with plant extracts of different concentrations in S-medium at 20 °C for 72 h; each group contained 50-100 larvae. After incubation, worms were submitted to fluorescence microscopy as described before [153, 154, 156].

3.2.15 Measurement of brood size assay

To analyze the potential toxic effect of the extracts on the reproductive system, brood size was measured. Synchronized N2 worms at the L4 larval stage were sorted and placed one by one on each NGM agar plate. The plates were supplemented with different concentrations of plant extracts in *E. coli* OP50 and incubated at 20 °C for 24 h. The adult worms were transferred to fresh medium every day during the reproductive phase to separate them from their progeny [153, 154, 156]. The eggs were counted using a dissecting microscope every day for 4 days to obtain a mean brood size [36].

3.2.16 Measurement of body length and body surface area

To detect the putative effect of dietary restriction by the extracts treatment, the body lengths and body surface area of the worms were measured. For body length measurement, synchronized and treated worms were analyzed in the same way as in the brood size assay. After treatment, day 1 adult worms were paralyzed by using 10 mM sodium azide and mounted on a microscopic glass slide. Thirty worms were randomly photographed using a 10× objective lens of a bright-field microscope. The body length of worms were analyzed by using the software BZ-II Analyzer (Keyence Corp.) and reported in micrometers. For body surface area measurement, BA17 transgenic worms in the L1 larval stage were treated with plant extracts of different concentrations in S-medium at 25 °C; each group contained 50-100 individuals. The media were changed every second day. On day 8, worms were photographed and measured the body surface area by ImageJ software (National Institutes of Health, Bethesda, MD) [153, 154, 156].

3.2.17 Quantification of lipofuscin

To measure the accumulation of the autofluorescent pigment lipofuscin, BA17 transgenic worms were used. Synchronized and treated worms were analyzed in the same way as in the body surface area assay. After treatment until day 16, the worms were paralyzed with 10 mM sodium azide and mounted on a glass slide. Thirty worms were randomly photographed by using a BIOREVO BZ-9000 fluorescence microscope (λ_{ex} 360/20 nm, λ_{em} 460/38 nm) [153, 154, 156].

3.2.18 Measurement of pharyngeal pumping rate

To determine a potential age-related decline in muscle function, pharyngeal pumping rates were measured. Synchronized worms at the L4 larval stage were sorted and placed one by one on each NGM agar plate. The plates were supplemented with different concentrations of plant extracts in *E. coli* OP50 and incubated at 20 °C for 24 h. L4 larva stage worms were treated with the extracts for 24 h, except for the control group. Each group contained 30-50 individuals. The adult worms were transferred to fresh medium with treatment every day during the reproductive phase prior to separation from their progeny. After that, the adult worms were transferred to fresh medium with treatment every second day. Pharyngeal pumping was analyzed on days 6, 8, 10, and 12 by counting the pumping frequency of the terminal pharyngeal bulb of each single worm for 60 s. The dissection microscope was used to measure the pumping rate of at least 20 worms from each group [153, 154, 156]. When the worms were crawling on the *E. coli* OP50 lawn, the pumping frequency was recorded and represented as pumps min^{-1} [36].

3.2.19 Measurement of lifespan

To determine the lifespan, wild-type (N2) and transgenic (TK22) worms were used. Synchronized worms at the L4 larval stage were sorted and placed one by one on each NGM agar plate. The plates were supplemented with different concentrations of plant extracts in *E. coli* OP50 and incubated at 20 °C for 24 h. Each group contained 30-50 individuals. The worms were counted every day and were presented as a percentage of surviving worms. Worms that failed to respond to a gentle touch with a platinum wire were scored as dead and excluded from the plates. The worms with internally hatched progeny or extruded gonads were scored as censors and discarded from the assay [153, 154, 156].

3.2.20 Statistical analysis

Measurements are presented as the mean of three independent runs (mean \pm SEM) and performed with Graphpad Prism 6. Statistical comparison between control and treatments were performed by a one-way ANOVA following Bonferroni's method (post hoc). Lifespan data were determined by log-rank (Mantel-Cox) tests followed by the Gehan-Breslow-Wilcoxon test. All the experiments were performed at least three times. Differences between the data were considered significant at $p < 0.05$.

CHAPTER IV

RESULTS

4.1 Phytochemical constituents of AO and GZ extracts

The extraction of AO and GZ leaves was carried out by using a Soxhlet with different solvents including hexane, dichloromethane and methanol. The extraction yields of AOH, AOD and AOM were 1.21%, 0.46%, and 15.97%, respectively. The extraction yields of GZH, GZD and GZM were 0.74%, 0.33%, and 11.78%, respectively. The secondary metabolites of the hexane and methanol extracts were characterized and quantified by GLC-MS (Gas/Liquid Chromatography-Mass Spectrometry) and HPLC (High-Performance Liquid Chromatography).

Qualitative phytochemical screening, GLC-MS and LC-MS were firstly determined in the extracts from hexane and methanol extractions. Chromatographic peaks were analyzed for identification possible bioactive compounds based on searching m/z values of molecular ion peaks in the positive mode $[M + H]^+$ and comparing with databases. This study reported phytochemical compounds from the extracts proposed as bioactive compound that have neuroprotective effects, antioxidant activity, and anti-aging that were reported in the literature. GC-MS results show more than 50 isolated peaks in the chromatogram of AOH and GZH extract (Figure. 20-21), the peaks of possible bioactive compounds show by number and detailed in Table 2 and 3. AOH extracts exhibited eight secondary metabolites including copaene, caryophyllene, heneicosane, n-hexadecanoic acid or palmitic acid, phytol, 9,12,15-octadecatrienoic acid, (Z,Z,Z)- or α -linolenic acid, octadecanoic acid or stearic acid and monounsaturated anacardic acid. GZH extracts exhibited seven secondary metabolites including pentadecanoic acid, n-hexadecanoic acid, phytol, octadecatrienoic acid, octadecanoic acid, hexanedioic acid and benzoic acid.

LC-MS results show more than 120 isolated peaks and 76 isolated peaks in the chromatogram of AOM and GZM extract, respectively (Figure. 20-21), the peaks of possible bioactive compounds show by number and detailed in Table 4 and 5. AOM

extracts exhibited seven compounds including salicylic acid, l-phenylalanine, quercetin 3-O-glucoside, quercetin 3-(2-galloylglucoside), quercetin 3-arabioside, quercitrin / kaempferol-7-O-glucoside and α -CEHC, tocopherols. GZM extracts exhibited eight compounds including l-proline, resveratrol 4'-methyl ether, quinic acid, gallic acid, quercitrin/kaempferol 3- α -d-glucoside, ginkgolide b, glycitin, and catechin. Quantitative phytochemical analysis, GLC-MS and HPLC were used in the extracts from hexane and methanol extractions (Figure 20-21, Table 6-7).

GLC-MS profiles represented main compounds in AOH and GZH extracts. AOH extracts exhibited palmitic acid (8495.95 mg/100 g of crude extract) and α -linolenic acid (4073.13 mg/100 g of crude extract). GZH extracts exhibited palmitic acid (8495.95 mg/100 g of crude extract) and α -linolenic acid (4073.13 mg/100 g of crude extract). Moreover, HPLC showed the presence of bioactive compounds in AOM and GZM extracts. AOM extracts exhibited gallic acid (305.92 mg/100 g of crude extract), catechin (1924.13 mg/100 g of crude extract) and quercetin-3-O -glucoside (707.10 mg/100 g of crude extract). GZM extracts exhibited gallic acid (2998.634 mg/100 g of crude extract), catechin (36714.74 mg/100 g of crude extract), oxyresveratrol (2.17 mg/100 g of crude extract), and quercetin (8.33 mg/100 g of crude extract). This research is the first report about the bioactive compounds (flavonoid glycoside) in AOM (gallic acid, catechin and quercetin) and GZM (gallic acid and catechin) leaf extracts (Figure 22).

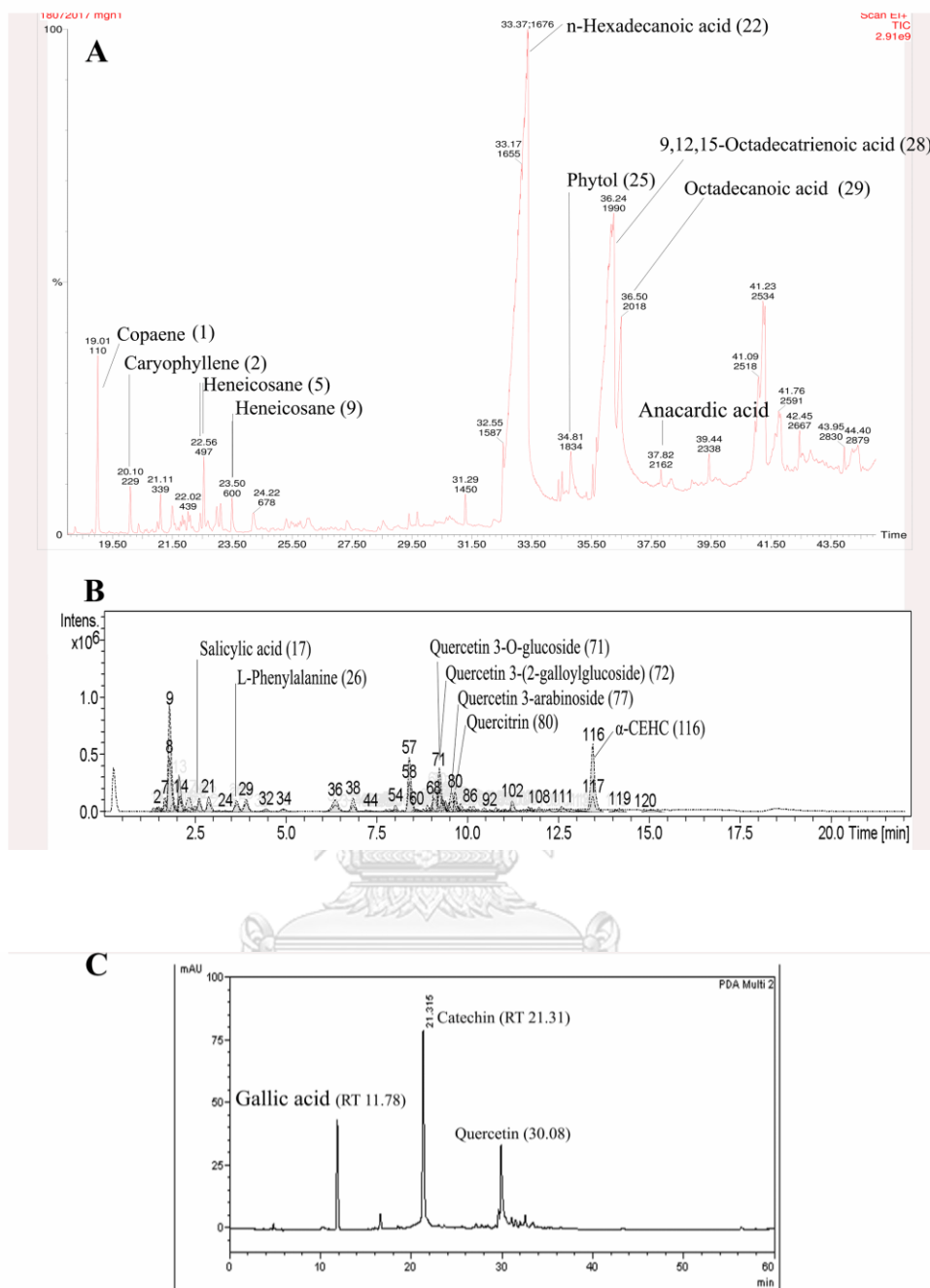


Figure 20. Phytochemical constituents of AO extracts.

(A) GLC-MS profile of the AOH extract. (B) LC-MS run of the AOM extract.
(C) HPLC chromatogram of AOM extract.

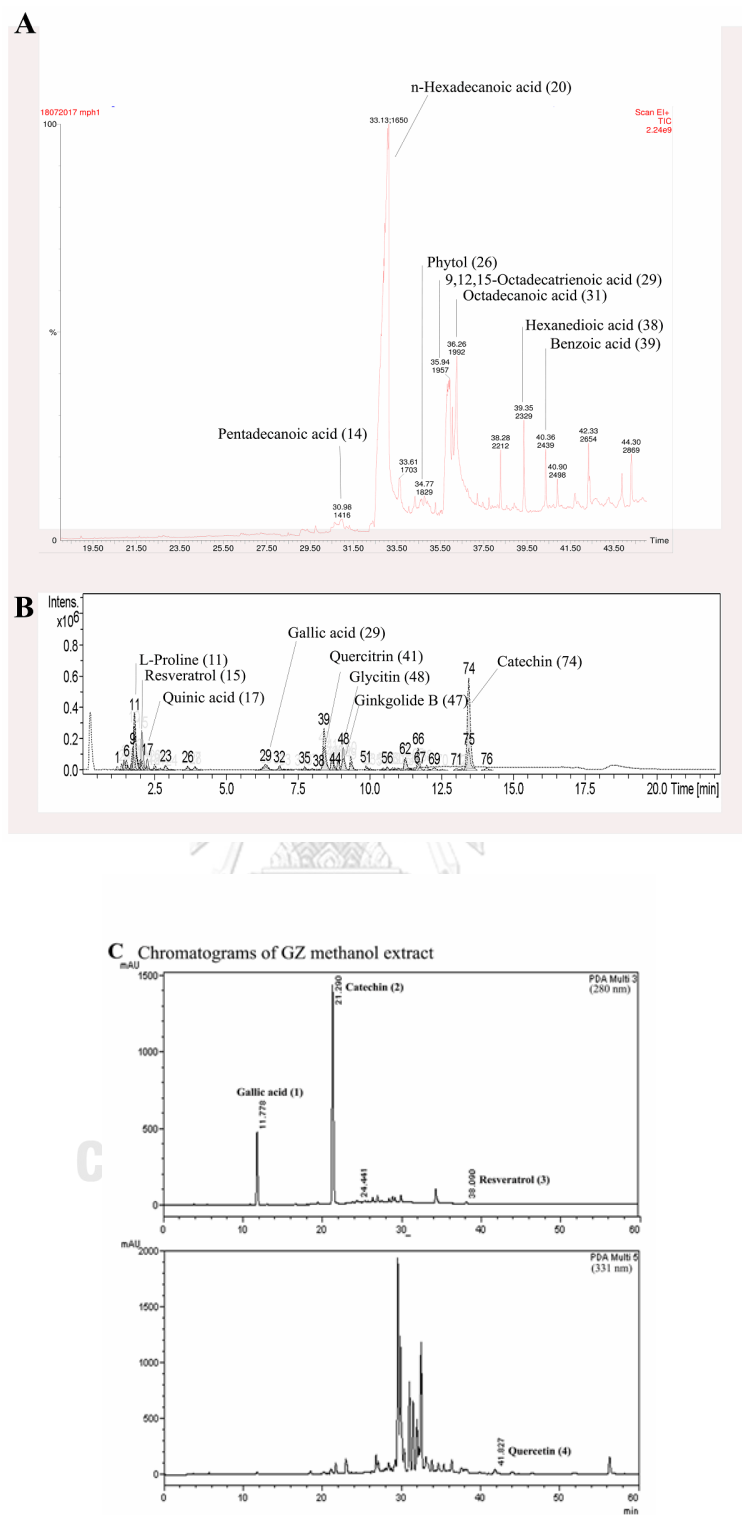


Figure 21. Phytochemical constituents of GZ extracts.

(A) GLC-MS profile of the GZH extract. (B) LC-MS run of the GZM extract.
(C) HPLC chromatogram of GZM extract.

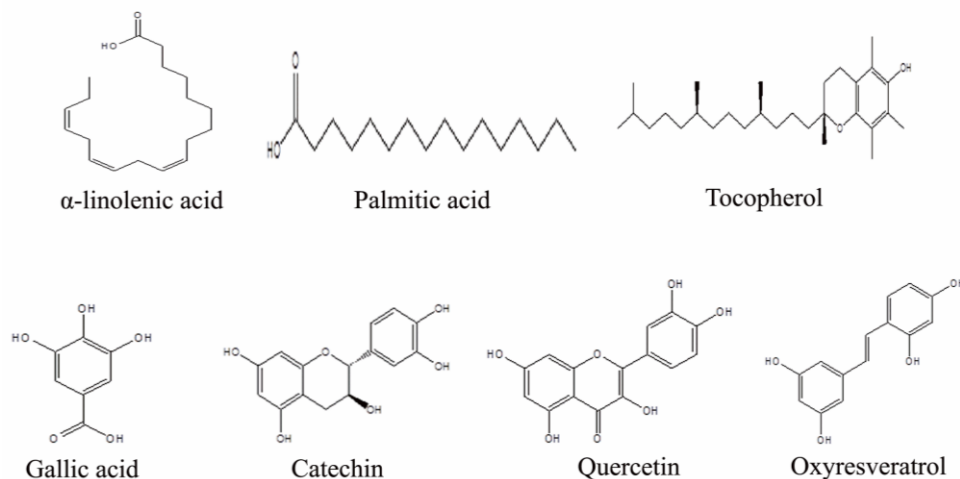


Figure 22. The structure of major compounds found in AO and GZ extracts.

(A) The bioactive compounds in AOH and GZH extracts.

(B) The bioactive compounds in AOM and GZM extracts.

Table 2. Proposed phytochemical constituents in the AOH extract using GC-MS

Peak No.	Rt(min)	Area (%)	Proposed compound	Match	Prob.
1	19.0080	1.565	Copaene	926	33.1000
2	20.0990	0.457	Caryophyllene	942	32.7000
5	22.0240	0.175	Heneicosane	824	11.4000
9	23.5000	0.389	Heneicosane	901	15.9000
22	33.3660	41.807	n-Hexadecanoic acid or Palmitic acid	893	68.8000
25	34.8150	0.801	Phytol	824	23.1000
28	36.2450	19.606	9,12,15-Octadecatrienoic acid, (Z,Z,Z)- or α -Linolenic acid	833	40.6000
29	36.5020	6.914	Octadecanoic acid or Stearic acid	875	87.5000
31	37.8220	0.345	Monounsaturated anacardic acid	788	9.2000

Library: MAINLIB

Table 3. Proposed phytochemical constituents in the GZH extract using GLC-MS

Peak No.	Rt (min)	Area (%)	Proposed compound	Match	Prob.
14	30.9820	1.0160	Pentadecanoic acid	755	68.30
20	33.1280	48.3180	n-Hexadecanoic acid or Palmitic acid	897	71.50
26	34.7690	0.6850	Phytol	798	42.30
29	35.9420	11.0570	9,12,15-Octadecatrienoic acid, (Z,Z,Z)- or α -Linolenic acid	812	9.90
31	36.2630	10.9150	Octadecanoic acid or Stearic acid	900	89.60
38	39.3530	1.6730	Hexanedioic acid, mono(2-ethylhexyl)ester or Adipic acid	808	79.00
39	40.3620	1.0370	Benzoic acid, 3-methyl-2-trimethylsilyloxy-, trimethylsilyl ester	591	607.00

*Library: MAINLIB, *mg/100 g of crude extract*

Table 4. Proposed phytochemical constituents in the AOM extract using LC-MS

Peak No.	Rt (min)	[M + H] ⁺ (m/z)	Area (%)	Proposed compound	Theoretical mass	Mass error (ppm)
17	2.3	139.0395	2.0142	Salicylic acid	138.0320	3
26	3.7	166.0856	1.4076	L-Phenylalanine	165.0790	3
71	9.2	465.1032	4.0410	Quercetin 3-O-glucoside	464.0960	0
72	9.3	617.1136	1.3883	Quercetin 3-(2-galloylglucoside)	616.1060	0
77	9.6	435.0922	2.0603	Quercetin 3-arabinoside	434.0850	0
80	9.7	449.1078	1.6803	Quercitrin / Kaempferol-7-O-glucoside	448.1010	0
116	13.4	279.1587	7.4592	α -CEHC,tocopherols	278.1528	1

Database: METLIN (CA, USA) and KNApSack Keyword Search Web Version 1.000.01

Table 5. Proposed phytochemical constituents in the GZH extract using LC-MS

Peak No.	Rt (min)	[M + H] ⁺ (m/z)	Area (%)	Proposed compound	Theoretical mass	Mass error (ppm)
11	1.8	116.0723	13.9908	L-Proline	115.0633	5
15	2.1	242.1015	4.68035	Resveratrol 4'-methyl ether	219.1107	6
17	2.3	193.0700	1.34899	Quinic acid	192.0634	3
29	6.4	171.0290	1.72094	Gallic acid	170.0215	1
41	8.7	449.1092	3.81108	Quercitrin or Kaempferol 3-alpha/beta-D-galactoside or Kaempferol 3-alpha/beta-D-glucoside	448.1006	3
47	9.1	447.1272	1.73585	Ginkgolide B	424.1383	2
48	9.1	447.1294	3.08348	Glycitin	446.1213	1
74	13.4	290.8464	18.7542	Catechin	290.0790	1

Database: METLIN (CA, USA) and KNApSack Keyword Search Web Version 1.000.01

Table 6. Individual phytochemical constituents in the AO extract using HPLC

Rt (min)	Compound	Concentration*
30.8	Palmitic acid	8495.95
34.8	α -linolenic acid	4073.13
11.7	Gallic acid	305.92
21.1	Catechin	1924.13
41.8	Quercetin	707.10

*mg/100 g of crude extract

Table 7. Individual phytochemical constituents in the GZ extract using HPLC

Rt (min)	Compound	Concentration*
30.8	Palmitic acid	3727.26
34.8	α -linolenic acid	429.55
11.7	Gallic acid	2998.63
21.1	Catechin	36714.74
37.3	Oxyresveratrol	2.17
41.8	Quercetin	8.33

*mg/100 g of crude extract

4.2 Antioxidant properties of AO and GZ extracts

4.2.1 The antioxidant properties (*In vitro*)

To analyse the antioxidant properties of the extracts *In vitro*, the radical scavenging activity by DPPH and ABTS assays, total phenolic content and total flavonoid content were examined. The AO extracts showed antioxidant activity. Among these AOM extract exhibited powerful antioxidant activity *In vitro*. The result from DPPH and ABTS assay, AO methanol extract effectively scavenged the radical by 90.62% (EC₅₀ = 11.32 µg/mL) and 99.36% (EC₅₀ = 5.94 µg/mL), respectively (Figure 23, Table 8). In accordance with the antioxidant activities, AOM extract exhibited high phenolic (160.35 GAE/g dry weight sample) and flavonoid (46.96 QE/g dry weight sample) contents (Figure 23, Table 8). Moreover, the result from ABTS assay, AOH extract showed radical scavenging activity by 61.03% (EC₅₀ = 11.50 µg/mL) (Figure 23, Table 8).

The GZ extracts showed antioxidant activity. Among these GZM extract exhibited powerful antioxidant activity *In vitro*. The result from DPPH and ABTS assay, GZ methanol extract effectively scavenged the radical by 86.66% (EC₅₀ = 65.27 µg/mL) and 93.98% (EC₅₀ = 63.45 µg/mL), respectively (Figure 24, Table 9). In accordance with the antioxidant activities, AOM extract exhibited high phenolic (162.81 GAE/g dry weight sample) and flavonoid (52.50 QE/g dry weight sample) contents (Figure 24, Table 9). However, the dichloromethane extracts (AZD and GZD) did not exhibit antioxidant activity, so this extracts were omitted for the subsequent experiments.

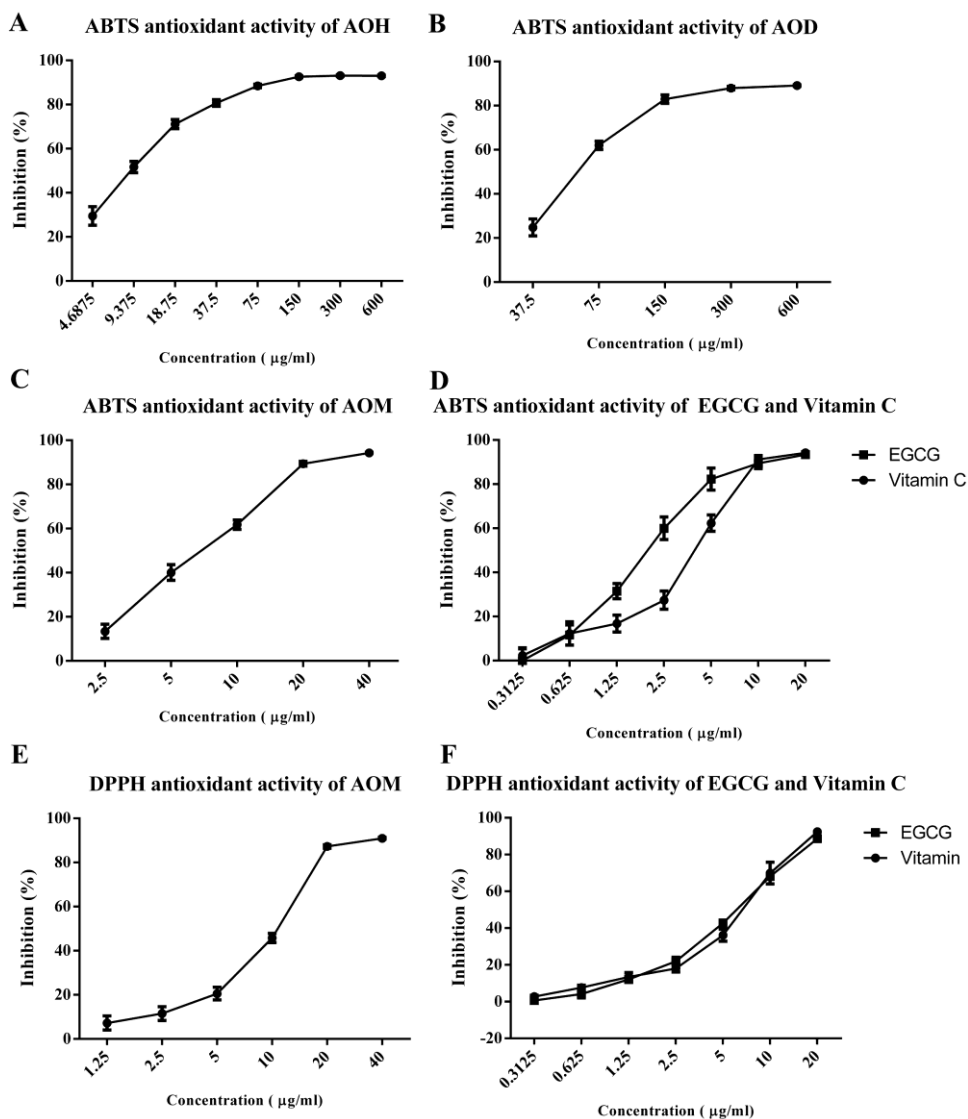


Figure 23. The *In vitro* antioxidant properties of AO extracts.

ABTS radical scavenging activity of AOH (4.69-600 $\mu\text{g/mL}$)(A), AOD (37.5-600 $\mu\text{g/mL}$)(B), AOM (2.5-40 $\mu\text{g/mL}$)(C), EGCG and vitamin C (0.31-20 $\mu\text{g/mL}$)(D) DPPH radical scavenging activity of AOM (1.25-40 $\mu\text{g/mL}$)(E), EGCG and vitamin C (0.31-20 $\mu\text{g/mL}$)(F).

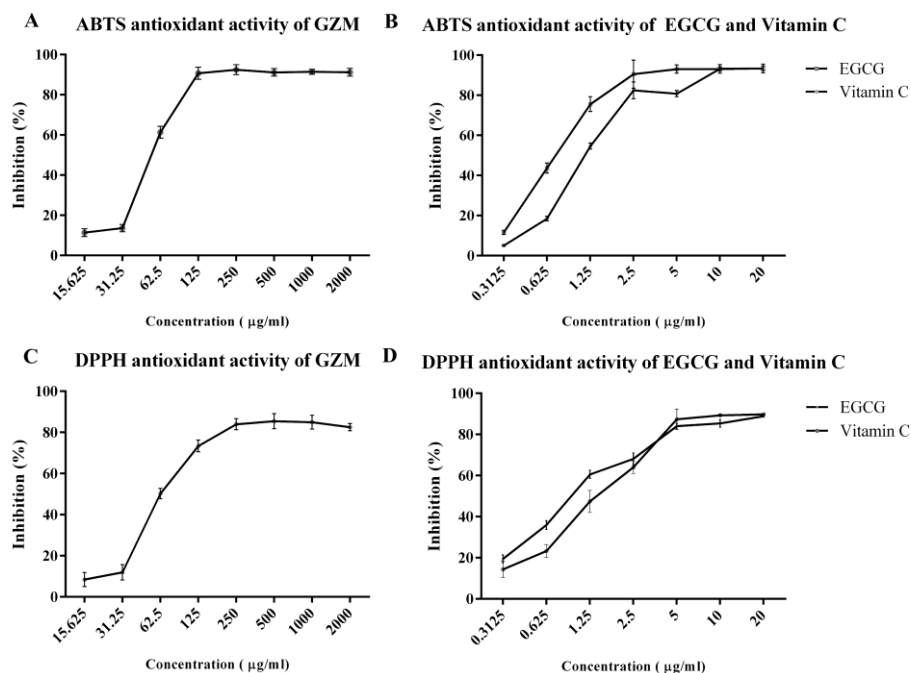


Figure 24. The *In vitro* antioxidant properties of GZ extracts.

ABTS radical scavenging activity of GZM (15.625-2000 µg/mL)(A), EGCG and vitamin C (0.31-20 µg/mL)(B) DPPH radical scavenging activity of GZM (15.625-2000 µg/mL)(C), EGCG and vitamin C (0.31-20 µg/mL)(D).

Table 8. The antioxidant properties of AO extracts (*In vitro*)

Extract	Total Phenolics mg GAE/g **	Total Flavonoids mg QE/g **	DPPH scavenging assay		ABTS scavenging assay	
			%Radical Scavenging activity*	EC ₅₀ (µg/mL)	%Radical Scavenging activity*	EC ₅₀ (µg/mL)
AOH	27.00 ± 2.12	2.26 ± 0.14	0.33 ± 1.31	-	61.03 ± 2.70	11.50 ± 3.85
AOD	12.70 ± 2.13	0.17 ± 0.36	0.05 ± 3.75	-	42.93 ± 8.13	74.04 ± 9.83
AOM	160.35 ± 0.83	46.96 ± 0.09	90.62 ± 0.64	11.32 ± 0.45	99.36 ± 3.29	5.94 ± 1.03
Vitamin C	-	-	-	7.91 ± 1.34	-	4.76 ± 0.71
EGCG	-	-	-	6.89 ± 0.33	-	2.59 ± 0.40

AOH: 1 mg/mL AO hexane extract, AOD: 1 mg/mL AO dichloromethane extract, AOM: 1 mg/mL AO methanol extract * of 1 mg/mL extract, ** dry weight sample, Values are expressed as the mean ± SD (n = 3)

Table 9. The antioxidant properties of GZ extracts (*In vitro.*)

Extract	Total Phenolics mg GAE/g **	Total Flavonoids mg QE/g **	DPPH scavenging assay		ABTS scavenging assay	
			%Radical Scavenging activity*	EC ₅₀ (µg/mL)	%Radical Scavenging activity*	EC ₅₀ (µg/mL)
GZH	7.33 ± 2.29	3.77 ± 1.37	14.75 ± 3.02	-	21.64 ± 1.13	-
GZD	8.49 ± 0.62	0.35 ± 0.27	12.17 ± 2.56	-	22.50 ± 1.18	-
GZM	162.81 ± 3.64	52.50 ± 2.29	86.66 ± 0.44	65.27 ± 11.63	93.98 ± 0.05	63.45 ± 1.14
Vitamin C	-	-	-	1.28 ± 0.12	-	1.38 ± 0.02
EGCG	-	-	-	0.95 ± 0.08	-	0.95 ± 0.02

GZH; 1 mg/mL of GZ hexane extract, GZD; 1 mg/mL GZ dichloromethane extract, GZM; 1 mg/mL GZ methanol extract. * of 1 mg/mL extract, ** dry weight sample, Values are expressed as the mean ± SD (n = 3)

4.2.2 The antioxidant properties in cells

To analyse the antioxidant activities of the extracts in cells, the intracellular ROS levels were measured using DCFH-DA in cultured neuronal (HT22 and Neuro-2a) cells. Intracellular ROS level was significantly elevated in HT22 (approximately 1.7 fold) and Neuro-2a (approximately 1.9 fold) cells after exposure to glutamate, compared to the control.

The HT22 cells treated with 10, 25, and 50 µg/ml AOH extracts exhibited a reduced intracellular ROS levels of 35.06%, 31.69%, and 33.56%, respectively (adjusted $p < 0.0001$). The cells treated with 0.5, 1, and 10 µg/ml AOM extracts exhibited a reduced intracellular ROS levels of 32.35%, 27.74%, and 27.59%, respectively (adjusted $p < 0.0001$) (compared to the glutamate treated control) (Figure 25).

The Neuro-2a cells treated with 10, 25, and 50 µg/ml AOH extracts exhibited a reduced intracellular ROS levels of 34.56%, 28.81%, and 33.59%, respectively (adjusted $p < 0.0001$). The cells treated with 0.5, 1, and 10 µg/ml AOM extracts exhibited a reduced intracellular ROS levels of 46.24%, 45.51%, and 40.86%, respectively (adjusted $p < 0.0001$) (compared to the glutamate treated control) (Figure 25).

In addition, the HT22 cells treated with 10, 25, and 50 $\mu\text{g/ml}$ GZH extracts exhibited a reduced intracellular ROS levels of 37.50%, 42.85%, and 43.94%, respectively (adjusted $p < 0.0001$). The cells treated with 0.5, 1, and 10 $\mu\text{g/ml}$ GZM extracts exhibited a reduced intracellular ROS levels of 31.04%, 33.91%, and 33.75%, respectively (adjusted $p < 0.0001$) (compared to the glutamate treated control) (Figure 26).

The Neuro-2a cells treated with 10, 25, and 50 $\mu\text{g/ml}$ GZH extracts exhibited a reduced intracellular ROS levels of 45.72%, 45.06%, and 45.59%, respectively (adjusted $p < 0.0001$). The cells treated with 0.5, 1, and 10 $\mu\text{g/ml}$ GZM extracts exhibited a reduced intracellular ROS levels of 40.08%, 39.65%, and 43.11%, respectively (adjusted $p < 0.0001$) (compared to the glutamate treated control) (Figure 26).

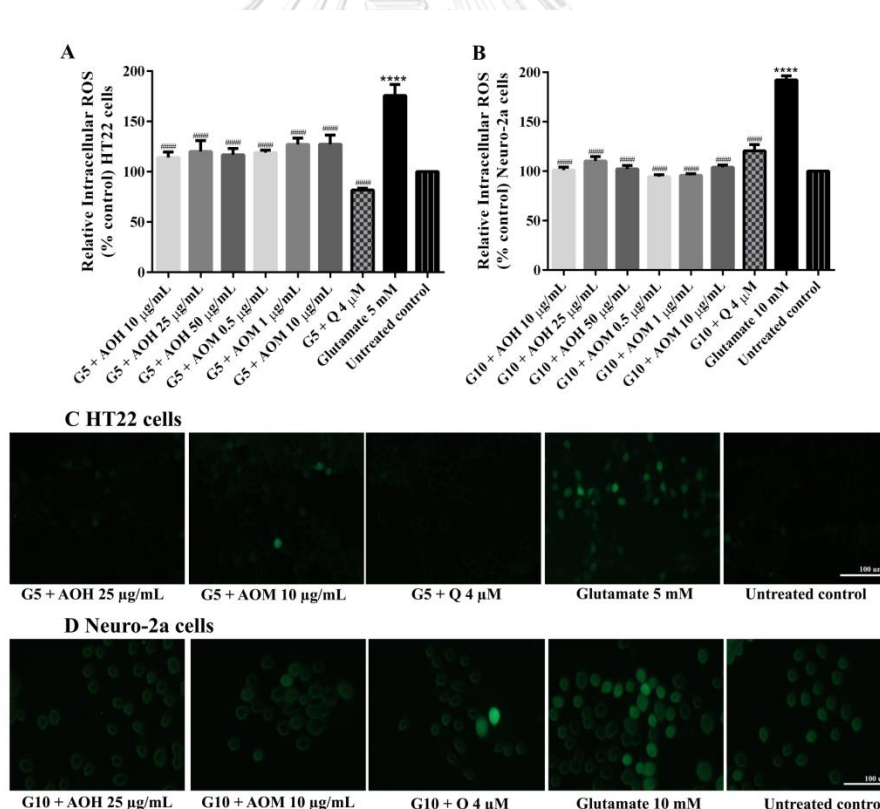


Figure 25. The antioxidant properties of AO extracts in cells.

AO extract treatment reduced ROS levels in HT22 (A) and Neuro-2a (B) cells when compared to glutamate-treated cells. Representative fluorescence micrographs of HT22 (C) and Neuro-2a (D) cells stained with DCFH-DA were observed under a fluorescence microscope (10 \times). Samples were exposed to glutamate (G5:5 mM glutamate, G10:10 mM glutamate) to induce oxidative stress.

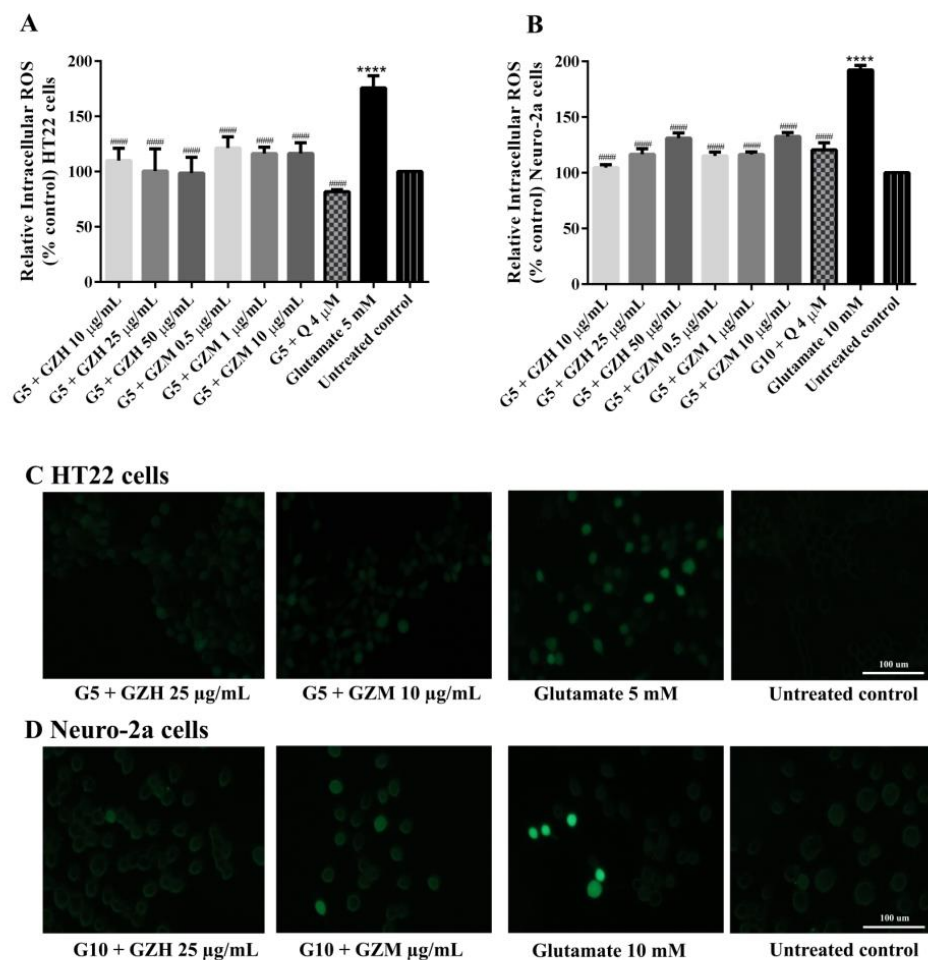


Figure 26. The antioxidant properties of GZ extracts in cells.

GZ extract treatment reduced ROS levels in HT22 (A) and Neuro-2a (B) cells when compared to glutamate-treated cells. Representative fluorescence micrographs of HT22 (C) and Neuro-2a (D) cells stained with DCFH-DA were observed under a fluorescence microscope (10 \times). Samples were exposed to glutamate (G5:5 mM glutamate, G10:10 mM glutamate) to induce oxidative stress.

4.2.3 The antioxidant properties (*In vivo*)

To analyze the antioxidant activities of the extracts *In vivo*, the intracellular ROS accumulation levels were measured in wild-type *C. elegans* using H2DCF-DA. The wild-type worms treated with 25 µg/mL AOH extract exhibited a reduced intracellular ROS accumulation of 45.24% (adjusted $p < 0.0001$). The wild-type worms treated with 1.0 and 2.5 µg/mL AOM extracts had a reduced intracellular ROS accumulation of 67.22% and 58.10%, respectively (adjusted $p < 0.0001$) (compared to the control group) (Figure 27).

In addition, the wild-type worms treated with 25 µg/mL GZH extract exhibited a reduced intracellular ROS accumulation of 41.33% (adjusted $p < 0.0001$). The wild-type worms treated with 1.0 and 2.5 µg/mL GZM extracts had a reduced intracellular ROS accumulation of 63.54% and 42.47%, respectively (adjusted $p < 0.0001$) (compared to the control group) (Figure 28).

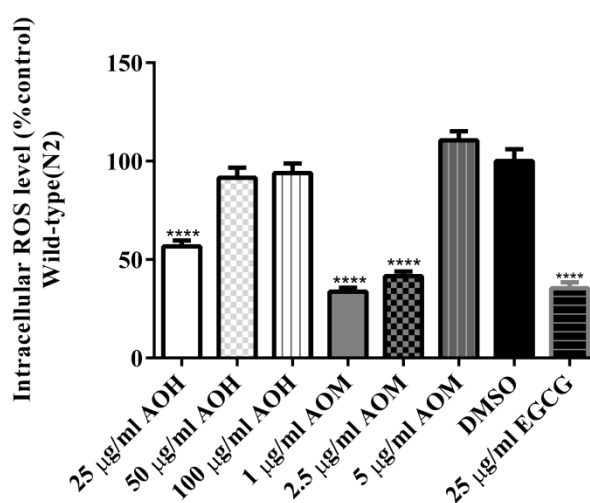


Figure 27. Effect of AO extracts on intracellular ROS in wild-type worms.

AO extract treatment reduced ROS levels in N2 worms when compared to the DMSO control group. Worms were treated with different concentrations of hexane (AOH) and methanol extracts (AOM). DMSO and EGCG were used as the solvent control and positive control groups, respectively. Data are presented as the mean \pm SEM ($n = 80$, replicated three times). * $p < 0.05$, ** $p < 0.01$, *** $p < 0.001$ and **** $p < 0.0001$, compared to the DMSO control by one-way ANOVA following Bonferroni's method (post hoc).

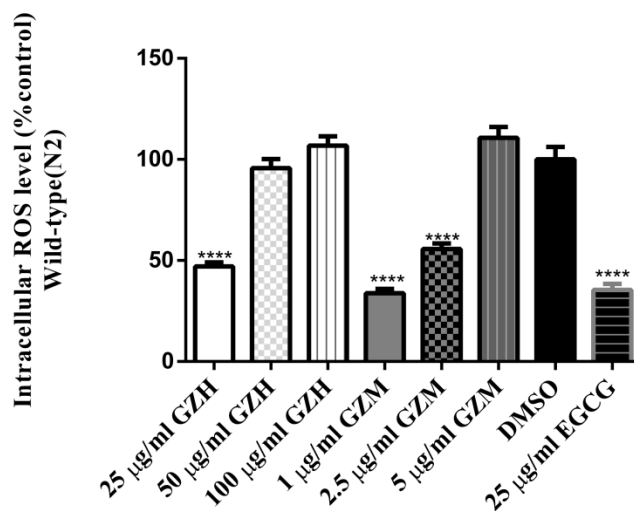


Figure 28. Effect of GZ extracts on intracellular ROS in wild-type worms.

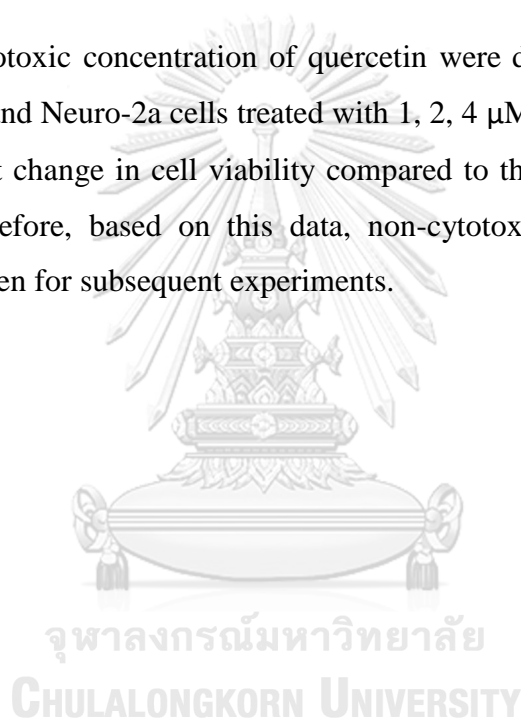
GZ extract treatment reduced ROS levels in N2 worms when compared to the DMSO control group. Worms were treated with different concentrations of hexane (AOH) and methanol extracts (AOM). DMSO and EGCG were used as the solvent control and positive control groups, respectively. Data are presented as the mean \pm SEM ($n = 80$, replicated three times). * $p < 0.05$, ** $p < 0.01$, *** $p < 0.001$ and **** $p < 0.0001$, compared to the DMSO control by one-way ANOVA following Bonferroni's method (post hoc).

4.3 Neuroprotective effects of AO and GZ extracts

To analyze cytotoxicity of the extracts in cultured neuronal (HT22 and Neuro-2a) cells, the MTT assay was explored. The HT22 and Neuro-2a cells treated with AO extracts (AOH 10-50 $\mu\text{g}/\text{mL}$, AOM 0.5-10 $\mu\text{g}/\text{mL}$) for 48 h did not cause a significant change in cell viability compared to the control group ($p \geq 0.05$) (Figure 29).

The HT22 and Neuro-2a cells treated with GZ extracts (GZH 10-50 $\mu\text{g}/\text{mL}$, GZM 0.5-10 $\mu\text{g}/\text{mL}$) for 48 h did not cause a significant change in cell viability compared to the control group ($p \geq 0.05$) (Figure 29).

Next, the non-cytotoxic concentration of quercetin were determined using the MTT assay. The HT22 and Neuro-2a cells treated with 1, 2, 4 μM quercetin for 48 h did not cause a significant change in cell viability compared to the control group ($p \geq 0.05$) (Figure 29). Therefore, based on this data, non-cytotoxic concentrations of each extracts were chosen for subsequent experiments.



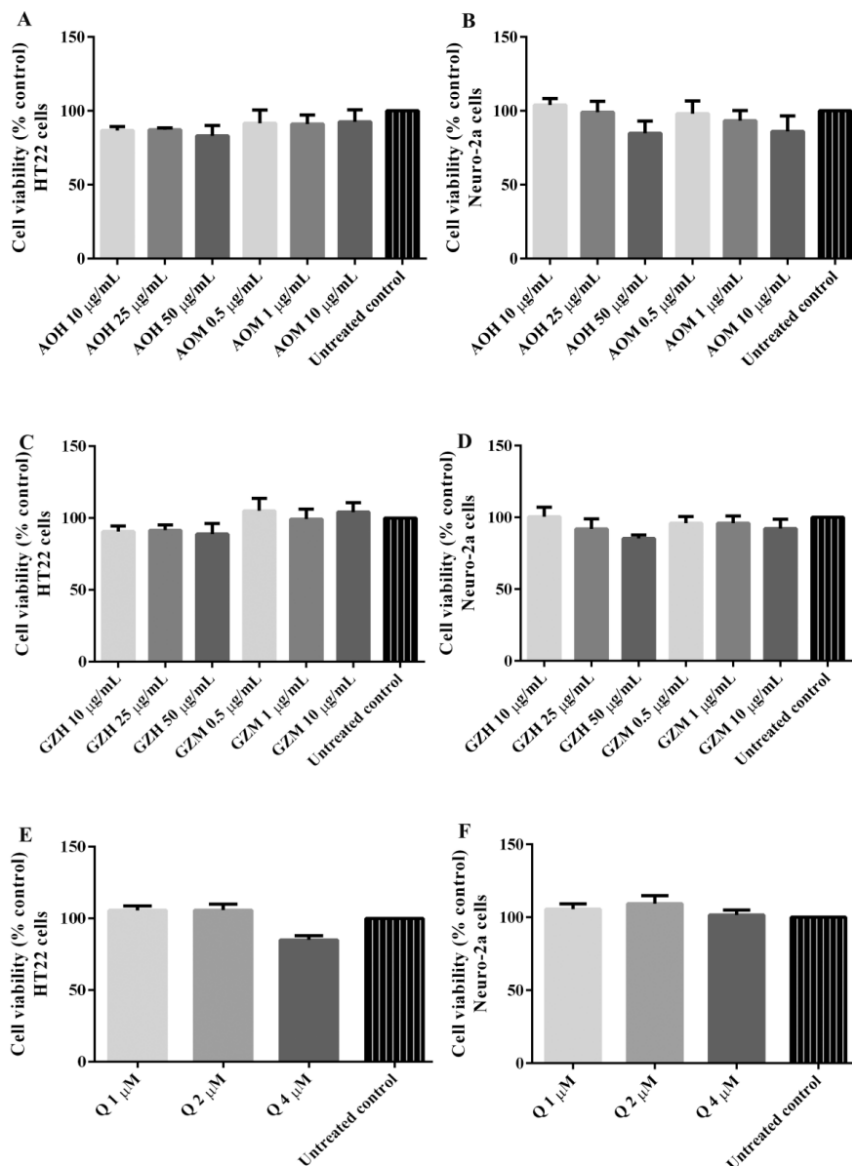


Figure 29. Cytotoxicity of the extracts in cultured neuronal cells.

Cell viability after treatment with different concentrations of AO (**AB**), GZ (**CD**) extracts quercetin (**EF**) in HT22 and Neuro-2a cells. All data are shown as the mean \pm SEM at least three independent experiments. **** $p < 0.0001$ compared to the untreated control by one-way ANOVA following Bonferroni's method (posthoc).

4.3.1 Protective effects against H₂O₂-induced toxicity

To determine an optimum condition of H₂O₂ toxicity in HT22 and Neuro-2a cells, cells were exposed to H₂O₂ (50-400 μ M for HT22 cells and 100-600 μ M for Neuro-2a cells) for 5-90 min. IC₅₀ values for H₂O₂ were 200 μ M (15 min) and 400 μ M (15 min) in HT22 and Neuro-2a cells, respectively (Figure 30AB). Thus, for H₂O₂ treatment the IC₅₀ concentrations were chosen for subsequent experiments.

To determine protective effects against H₂O₂-induced toxicity, quercetin was used as a positive control. The HT22 and Neuro-2a cells treated with 200-400 μ M H₂O₂ alone significantly reduced cell viability by approximately 50% (Figure 30EF). The HT22 and Neuro-2a cells treated with 1, 2, 4 μ M quercetin for 24 h and exposed to 200-400 μ M H₂O₂, significantly lower H₂O₂-induced cell death in a concentration-dependent manner (Figure 30EF). Thus, the positive control concentration was chosen at 4 μ M quercetin.

The HT22 cells treated with 10, 25, and 50 μ g/ml AOH extracts significantly increased cell survival by 46.05%, 53.80% and 20.16%, respectively (adjusted $p < 0.0001$) (compared to the H₂O₂ treated control) (Figure 31AB). The Neuro-2a cells treated with 10 and 25 μ g/ml AOH extracts significantly increased cell survival by 39.37% and 25.85%, respectively (adjusted $p < 0.0001$) (compared to the H₂O₂ treated control) (Figure 31CD).

The HT22 cells treated with 0.5, 1, and 10 μ g/ml AOM extracts significantly increased cell survival by 43.10%, 42.42% and 51.13%, respectively (adjusted $p < 0.0001$) (compared to the H₂O₂ treated control) (Figure 31AB). The Neuro-2a cells treated with 0.5, 1 and 10 μ g/ml AOM extracts significantly increased cell survival by 17.01%, 32.99% and 41.90%, respectively (adjusted $p < 0.0001$) (compared to the H₂O₂ treated control) (Figure 31CD).

In addition, The HT22 cells treated with 10, 25, and 50 μ g/ml GZH extracts significantly increased cell survival by 32.48%, 21.19% and 31.52%, respectively (adjusted $p < 0.0001$) (compared to the H₂O₂ treated control) (Figure 32AB). The Neuro-2a cells treated with 10, 25, and 50 μ g/ml GZH extracts significantly increased

cell survival by 19.70%, 20.91% and 19.94%, respectively (adjusted $p < 0.0001$) (compared to the H_2O_2 treated control) (Figure 32CD).

The HT22 cells treated with 0.5, 1, and 10 $\mu\text{g/ml}$ GZM extracts significantly increased cell survival by 60.72%, 52.75% and 56.03%, respectively (adjusted $p < 0.0001$) (compared to the H_2O_2 treated control) (Figure 32AC). The Neuro-2a cells treated with 1 $\mu\text{g/ml}$ GZM extracts significantly increased cell survival by 24.15%, respectively (adjusted $p < 0.01$) (compared to the H_2O_2 treated control) (Figure 32BD).

The Results were in a similar range as the positive control quercetin (79.78% survival in HT22 cells and 80.14% survival in Neuro-2a cells), which is a well-known neuroprotective compound (Park et al., 2019a), and were confirmed by LDH assay (Figure 31BD, 32BD) as well as morphological examination (Figure 31EF, 32EF). The results suggest that the AO and GZ extracts have a neuroprotective effect against H_2O_2 -induced neuronal cell death.

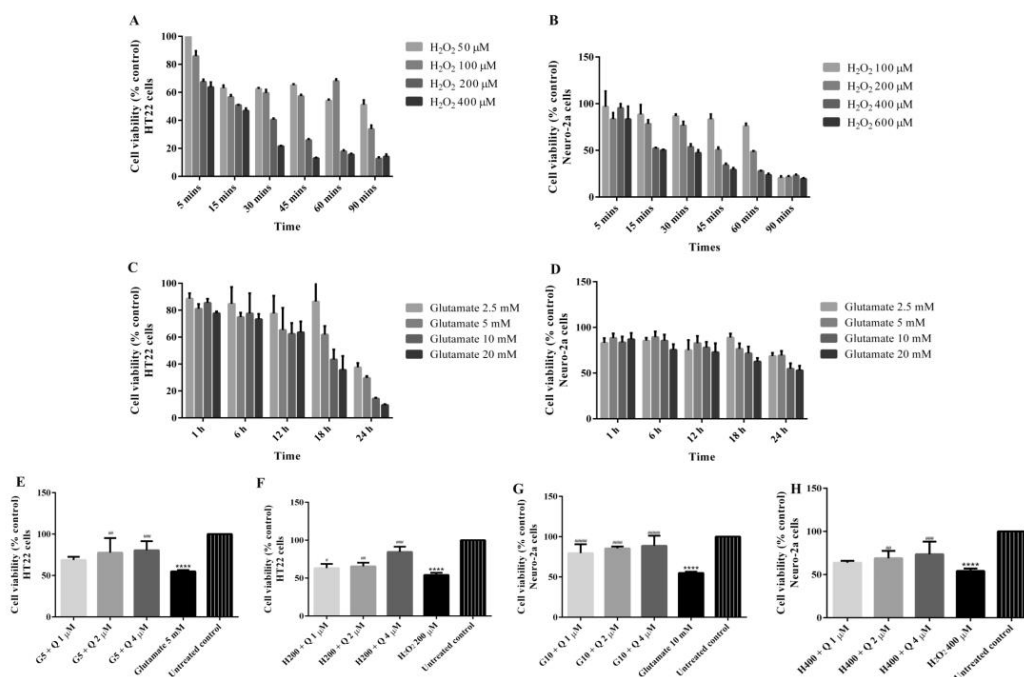


Figure 30. The optimum condition of H₂O₂, glutamate and quercetin in HT22 and Neuro-2a cells.

Cell viability after treatment with different concentrations of H₂O₂ (AB), glutamate (CD) for different times in HT22 and Neuro-2a cells. Cell viability after treatment with different concentrations of quercetin extracts and exposed to H₂O₂ (FH) or glutamate (EG) in HT22 and Neuro-2a cells. Samples were exposed to glutamate (G5: 5 mM glutamate, G10: 10 mM glutamate) to induce toxicity. All data are shown as the mean \pm SEM at least three independent experiments. *** $p < 0.0001$ compared to the untreated control; # $p < 0.05$, ## $p < 0.01$, ### $p < 0.001$ and #### $p < 0.0001$, compared to the glutamate treated cells by one-way ANOVA following Bonferroni's method (posthoc).

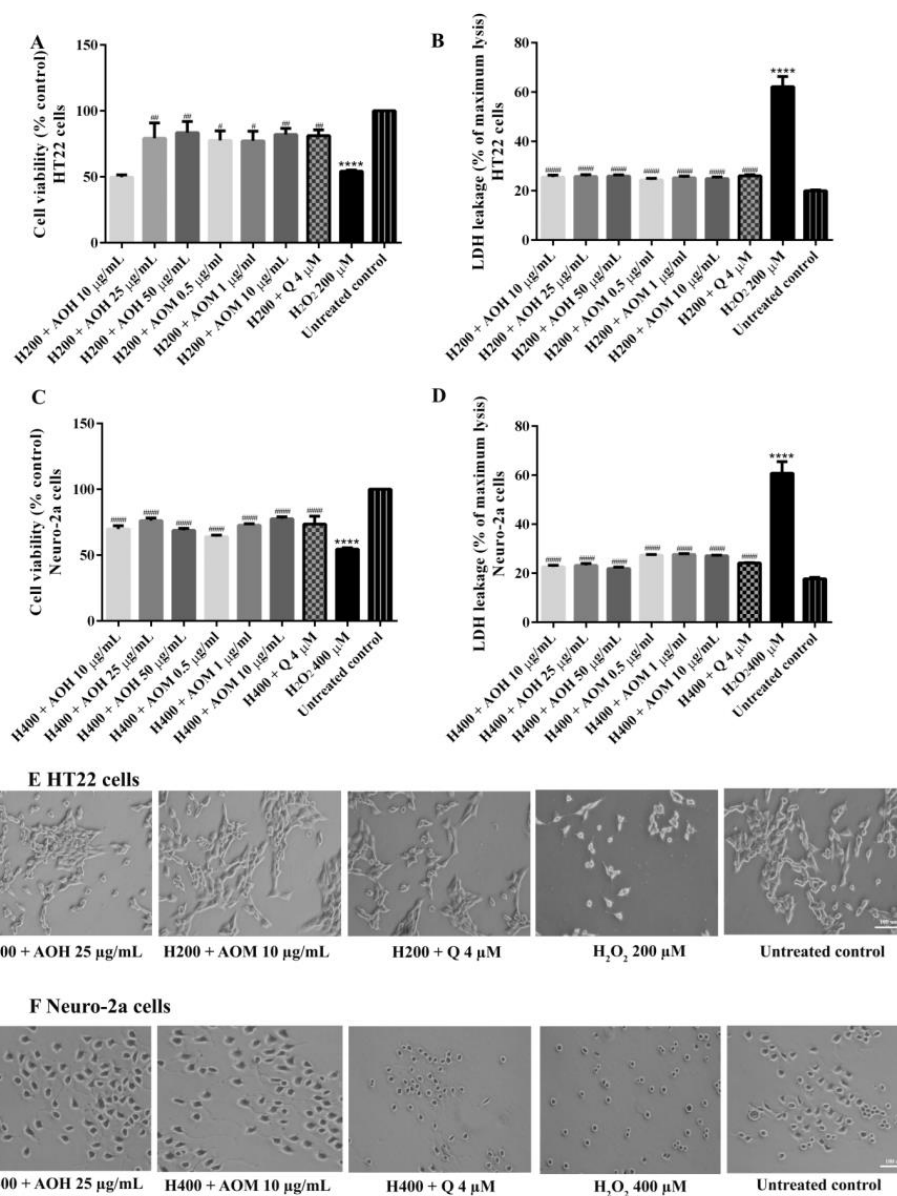


Figure 31. Protective effects of AO extracts against H₂O₂-induced toxicity in HT22 and Neuro-2a cells.

Cell viability after treatment with different concentrations of AO extracts and H₂O₂ in HT22 (**AB**) and Neuro-2a cells (**CD**). Cell morphology of HT22 (**E**) and Neuro-2a (**F**) cells was observed under microscope at 5 \times magnification. Samples were exposed to H₂O₂ (H200: 200 μ M H₂O₂, H400: 400 μ M H₂O₂) to induce toxicity. All data are shown as the mean \pm SEM at least three independent experiments. **** p < 0.0001 compared to untreated control; # p < 0.05, ## p < 0.01, ### p < 0.001, and #### p < 0.0001, compared to the glutamate treated cells by one-way ANOVA following Bonferroni's method (post hoc).

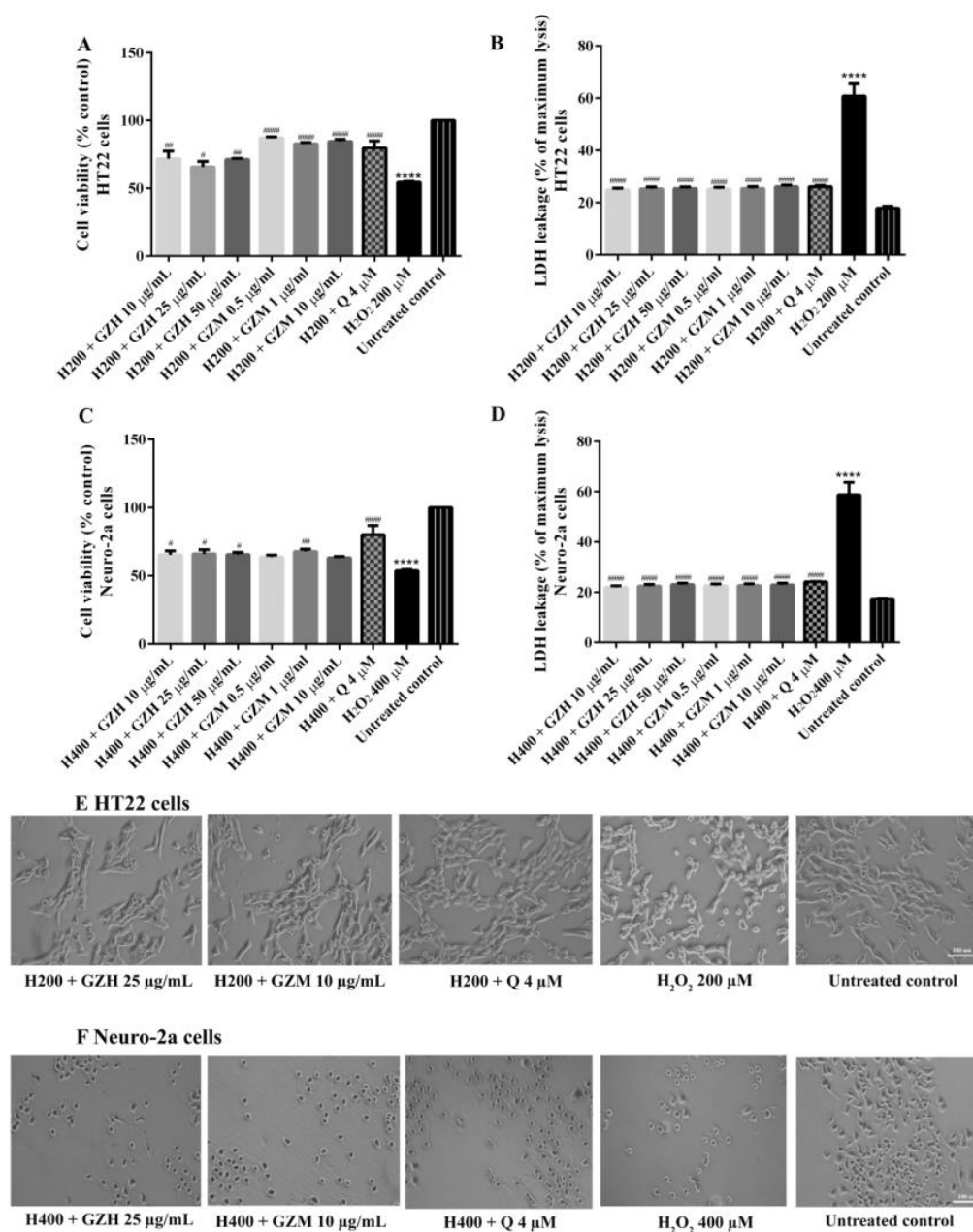


Figure 32. Protective effects of GZ extracts against H₂O₂-induced toxicity in HT22 and Neuro-2a cells.

Cell viability after treatment with different concentrations of GZ extracts and H₂O₂ in HT22 (AB) and Neuro-2a cells (CD). Cell morphology of HT22 (E) and Neuro-2a (F) cells was observed under microscope at 5 \times magnification. Samples were exposed to H₂O₂ (H200: 200 μM H₂O₂, H400: 400 μM H₂O₂) to induce toxicity. All data are shown as the mean \pm SEM at least three independent experiments. **** p < 0.0001 compared to untreated control; # p < 0.05, ## p < 0.01, ### p < 0.001, and #### p < 0.0001, compared to the glutamate treated cells by one-way ANOVA following Bonferroni's method (post hoc).

4.3.2 Protective effects against glutamate-induced toxicity

To determine an optimum condition of glutamate toxicity in HT22 and Neuro-2a cells, cells were exposed to 2.5-20 mM glutamate for 1-24 h. IC₅₀ values for glutamate were 5 mM (18 h) and 10 mM (24 h) in HT22 and Neuro-2a cells, respectively (Figure 22). Thus, for glutamate treatment, IC₅₀ concentrations were chosen for subsequent experiments

To determine protective effects against glutamate -induced toxicity, quercetin was used as a positive control. The HT22 and Neuro-2a cells treated with 5-10 mM glutamate alone significantly reduced cell viability by approximately 50% (Figure 30CD). The HT22 and Neuro-2a cells treated with 1, 2, 4 μ M quercetin for 24 h and exposed to 5-10 mM glutamate, significantly lower glutamate-induced cell death in a concentration-dependent manner (Figure 30EG). Thus, the positive control concentration was chosen at 4 μ M quercetin.

The HT22 cells treated with 10, 25, and 50 μ g/ml AOH extracts significantly increased cell survival by 71.94%, 68.23% and 43.70%, respectively (adjusted $p < 0.0001$) (compared to the glutamate treated control) (Figure 33AB). The Neuro-2a cells treated with 10, 25, and 50 μ g/ml AOH extracts significantly increased cell survival by 45.92%, 54.28% and 23.70%, respectively (adjusted $p < 0.0001$) (compared to the glutamate treated control) (Figure 33 CD).

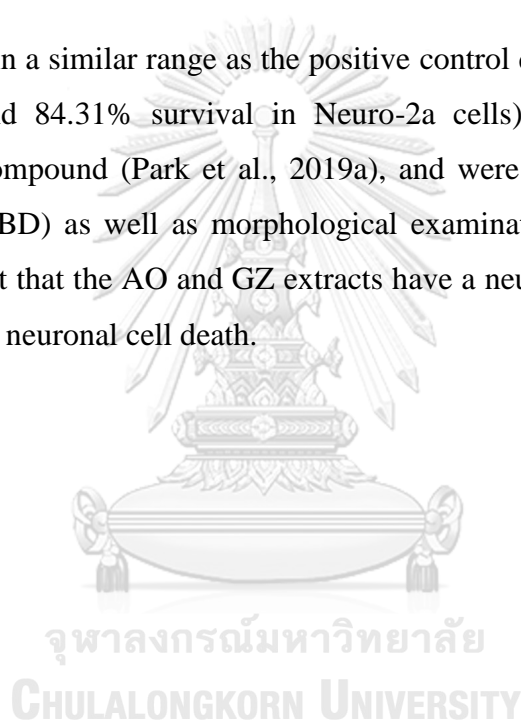
The HT22 cells treated with 0.5, 1, and 10 μ g/ml AOM extracts significantly increased cell survival by 72.65%, 73.94% and 77.41%, respectively (adjusted $p < 0.0001$) (compared to the glutamate treated control) (Figure 33AB). The Neuro-2a cells treated with 0.5, 1 and 10 μ g/ml AOM extracts significantly increased cell survival by 38.61%, 44.90% and 42.41%, respectively (adjusted $p < 0.0001$) (compared to the glutamate treated control) (Figure 33CD).

In addition, The HT22 cells treated with 10, 25, and 50 μ g/ml GZH extracts significantly increased cell survival by 67.39%, 40.93% and 39.17%, respectively (adjusted $p < 0.0001$) (compared to the glutamate treated control) (Figure 34AB). The Neuro-2a cells treated with 10, 25, and 50 μ g/ml GZH extracts significantly increased

cell survival by 32.78%, 39.08% and 28.69%, respectively (adjusted $p < 0.0001$) (compared to the glutamate treated control) (Figure 34CD).

The HT22 cells treated with 0.5, 1, and 10 $\mu\text{g/ml}$ GZM extracts significantly increased cell survival by 43.21%, 34.89% and 37.30%, respectively (adjusted $p < 0.0001$) (compared to the glutamate treated control) (Figure 34 AB). The Neuro-2a cells treated with 0.5, 1 and 10 $\mu\text{g/ml}$ GZM extracts significantly increased cell survival by 39.91%, 52.09% and 63.72%, respectively (adjusted $p < 0.0001$) (compared to the glutamate treated control) (Figure 34CD).

The Results were in a similar range as the positive control quercetin (87.76% survival in HT22 cells and 84.31% survival in Neuro-2a cells), which is a well-known neuroprotective compound (Park et al., 2019a), and were confirmed by LDH assay (Figure 33BD, 34BD) as well as morphological examination (Figure 33EF, 34EF). The results suggest that the AO and GZ extracts have a neuroprotective effect against glutamate-induced neuronal cell death.



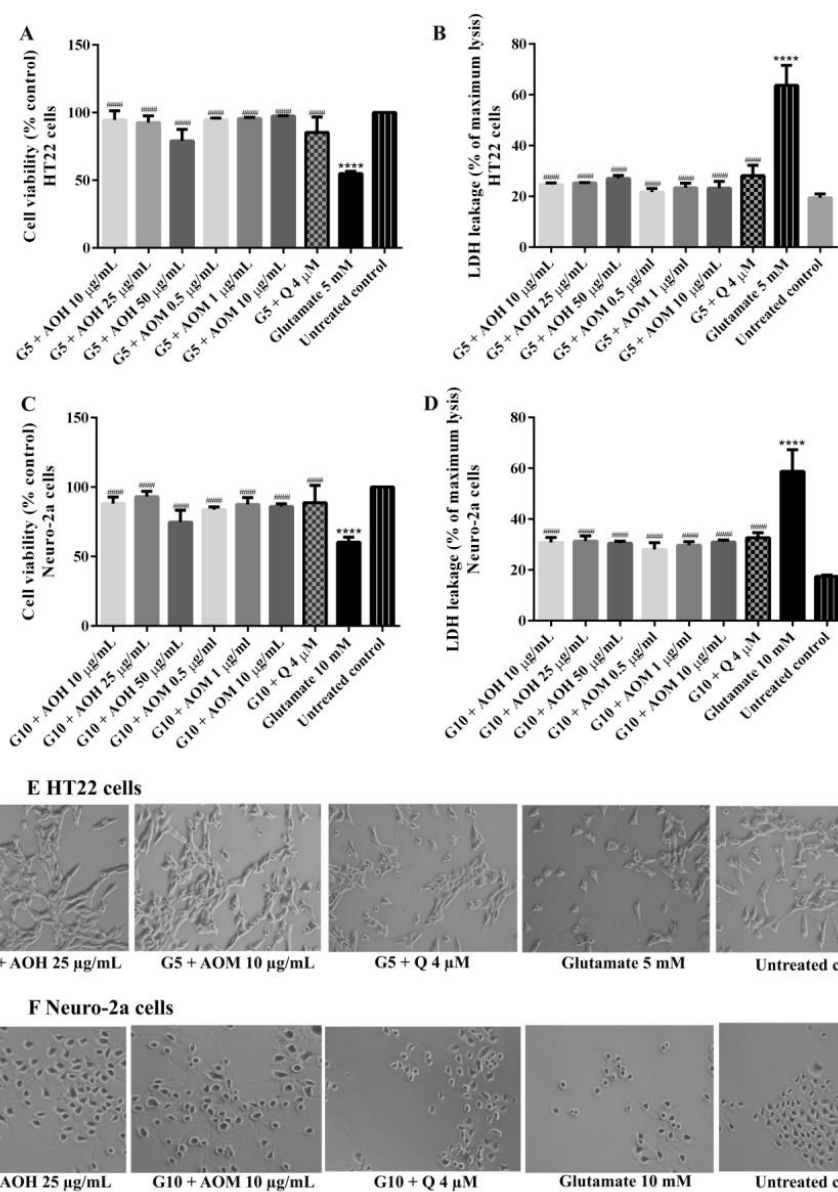


Figure 33. Protective effects of AO extracts against glutamate-induced toxicity in HT22 and Neuro-2a cells.

Cell viability after treatment with different concentrations of AO extracts and exposed to glutamate in HT22 (**AB**) and Neuro-2a cells (**CD**). Cell morphology of HT22 (**E**) and Neuro-2a (**F**) cells were observed under a microscope at 5 \times magnification. Samples were exposed to glutamate (G5: 5 mM glutamate, G10: 10 mM glutamate) to induce toxicity. All data are shown as the mean \pm SEM at least three independent experiments. **** p < 0.0001 compared to the untreated control; # p < 0.05, ## p < 0.01, ### p < 0.001 and #### p < 0.0001, compared to the glutamate treated cells by one-way ANOVA following Bonferroni's method (posthoc).

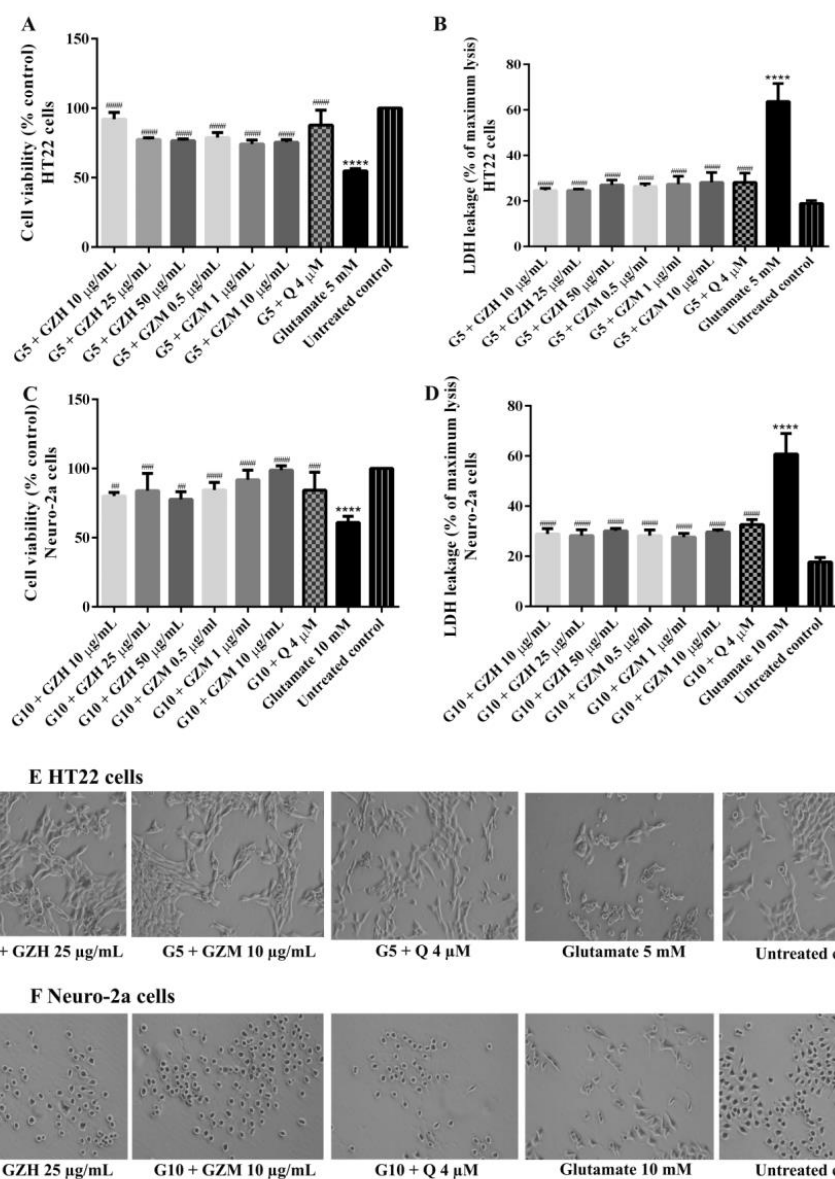


Figure 34. Protective effects of GZ extracts against glutamate-induced toxicity in HT22 and Neuro-2a cells.

Cell viability after treatment with different concentrations of GZ extracts and exposed to glutamate in HT22 (**AB**) and Neuro-2a cells (**CD**). Cell morphology of HT22 (**E**) and Neuro-2a (**F**) cells were observed under a microscope at 5 \times magnification. Samples were exposed to glutamate (G5: 5 mM glutamate, G10: 10 mM glutamate) to induce toxicity. All data are shown as the mean \pm SEM at least three independent experiments. **** p < 0.0001 compared to the untreated control; # p < 0.05, ## p < 0.01, ### p < 0.001 and #### p < 0.0001, compared to the glutamate treated cells by one-way ANOVA following Bonferroni's method (posthoc).

4.4 Oxidative stress resistance properties of AO and GZ extracts

To investigate the oxidative stress resistance properties of the extracts, the survival of worm were analyzed under oxidative stress conditions. The wild-type (N2) worm treated with 80 μM juglone for 24 h significantly reduced survival rate by 79% when compare to the control group (21% survival) ($p < 0.0001$) (Figure 35).

The survival rate for wild-type worms pretreated with 25 and 50 $\mu\text{g/mL}$ AOH extract increased by 36.71% ($p < 0.05$) and 49.15% ($p < 0.0001$), respectively. Moreover, the survival rate for wild-type worms pretreated with 1.0 and 2.5 $\mu\text{g/mL}$ AOM extract increased by 40.89% ($p < 0.01$) and 45.48% ($p < 0.001$), respectively (Figure 35A).

In addition, the survival rate for wild-type worms pretreated with 25 and 50 $\mu\text{g/mL}$ GZH extract increased by 42.23% ($p < 0.05$) and 43.95% ($p < 0.01$), respectively. Moreover, the survival rate for wild-type worms pretreated with 1.0 and 2.5 $\mu\text{g/mL}$ GZM extract increased by 37.49% ($p < 0.05$) and 48.83% ($p < 0.0001$), respectively (Figure 35B).

However, higher concentrations of AO extracts (≥ 100 $\mu\text{g/mL}$ hexane extract and ≥ 5 $\mu\text{g/mL}$ methanol extract) did not significantly increase the survival rate of the worms under oxidative conditions compared to the DMSO reagent control group, possibly due to their pro-oxidant activity *In vivo* (Figure 36).

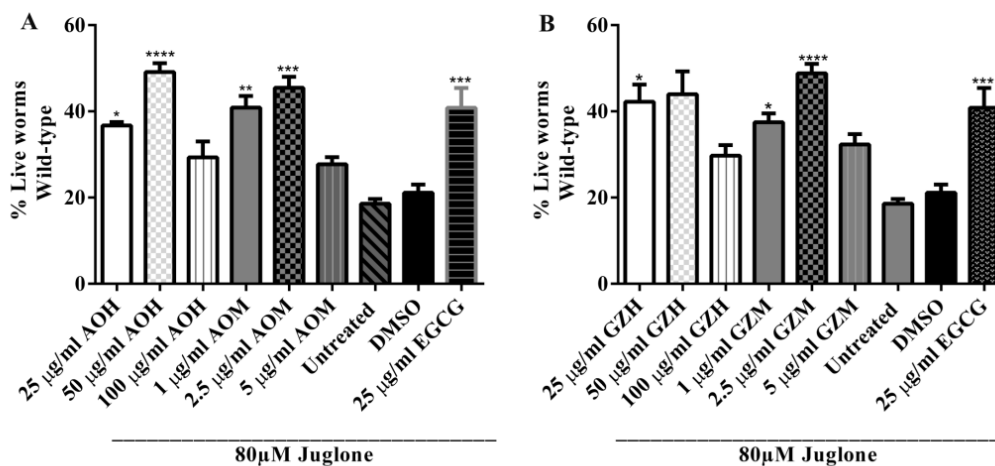


Figure 35. Effect of AO and GZ extracts on the survival rate of wild-type worms under oxidative stress induced by juglone.

AO (A) and GZ (B) extracts protect against oxidative stress in wild-type *C. elegans* as evidenced by the survival rate of wild-type (N2) worms, which was significantly enhanced after pretreatment with the extracts. Worms were treated with AO hexane and methanol extracts at different concentrations. DMSO and EGCG were used as the solvent control and positive control groups. Data are presented as the mean \pm SEM (n = 80, replicated three times). ** $p < 0.01$ and **** $p < 0.001$, compared to the DMSO control by one-way ANOVA following Bonferroni's method (post hoc).

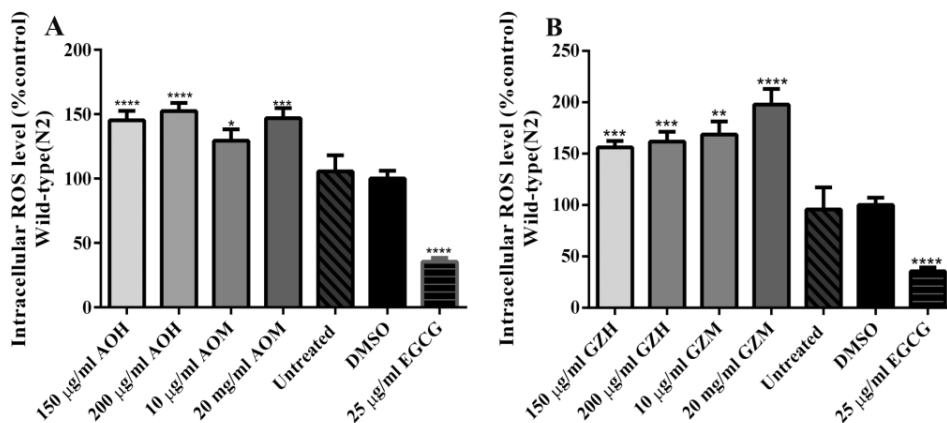


Figure 36. Pro-oxidant effect of AO and GZ extracts on intracellular ROS in wild-type worms.

High concentrations of AO (**A**) and GZ (**B**) extracts (150 and 200 μmL AOH, GZH; 10 and 20 $\mu\text{g/mL}$ AOM, GZM) treatment increased ROS levels in N2 worms when compared to the DMSO control group. Data are presented as the mean \pm SEM (n = 80, replicated three times). * $p < 0.05$, ** $p < 0.01$, *** $p < 0.001$ and **** $p < 0.0001$, compared to the DMSO control by one-way ANOVA following Bonferroni's method (post hoc).

4.5 Anti-aging properties of AO and GZ extracts

4.5.1 The autofluorescent pigment lipofuscin

To investigate the possible influence of the extracts on aging in *C. elegans*, the accumulation of the autofluorescent pigment lipofuscin and the pharyngeal pumping rate were measured in BA17 and wild-type worms, respectively.

The wild-type worms treated with 25, 50 and 100 $\mu\text{g}/\text{mL}$ AOH had a significantly lower level of lipofuscin (11.96%, $p < 0.0001$; 17.55%, $p < 0.0001$ and 12.62%; $p < 0.0001$, respectively). A similar result was obtained for wild-type worms treated with 1.0, 2.5 and 5 $\mu\text{g}/\text{mL}$ AOM extract (Figure 29) (reduction of lipofuscin by 12.25%, $p < 0.0001$; 18.48%, $p < 0.0001$; and 8.39% $p < 0.01$, respectively) (Figure 37A).

In addition, the wild-type worms treated with 25, 50 and 100 $\mu\text{g}/\text{mL}$ GZH had a significantly lower level of lipofuscin (12.06%, $p < 0.0001$; 14.19%, $p < 0.0001$ and 21.70%; $p < 0.0001$, respectively). A similar result was obtained for wild-type worms treated with 1.0, 2.5 and 5 $\mu\text{g}/\text{mL}$ GZM extract (Figure 29) (reduction of lipofuscin by 7.54%, $p < 0.01$; 12.12%, $p < 0.0001$; and 8.17% $p < 0.01$, respectively). These effects are in a similar range as that of 25 $\mu\text{g}/\text{mL}$ EGCG (21.58%, $p < 0.0001$) (Figure 37B).

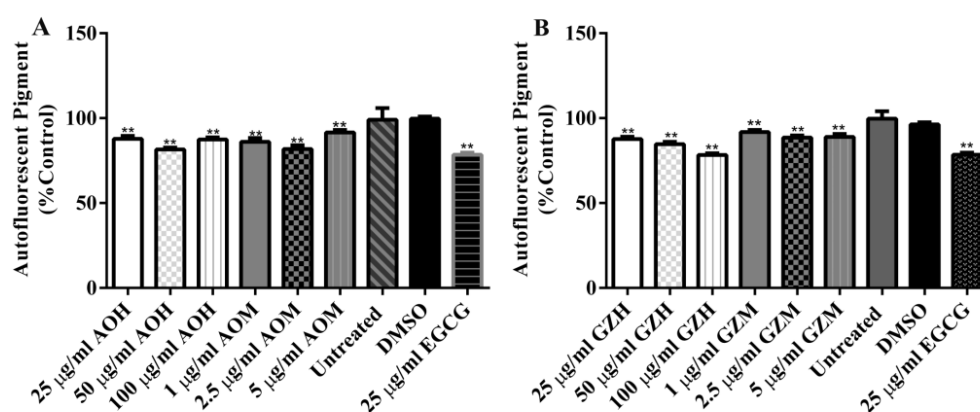


Figure 37. Effect of AO and GZ extracts on age-related markers (lipofuscin).

AO (**A**) and GZ (**B**) attenuated the autofluorescent pigment lipofuscin in BA17 worms. Autofluorescent granules were measured under the blue wavelength band. Data are presented as the mean \pm SEM ($n = 100$). DMSO and EGCG were used as the solvent control and positive control group, respectively. Data are presented as the mean \pm SEM ($n = 30$, replicated three times). $**p < 0.01$ and $***p < 0.001$, compared to the DMSO control by one-way ANOVA following Bonferroni's method (post hoc).

4.5.2 The pharyngeal pumping rate

To investigate the influence of AO extracts on muscle function activity, the pharyngeal pumping rate (a marker for aging) was examined in wild-type worms.

On days 5, the pharyngeal pumping rates of the worms treated with 25, 50 and 100 $\mu\text{g/mL}$ AOH extracts were 250.6%, 243% and 233.4%, respectively ($p < 0.0001$). The pharyngeal pumping rates of the worms treated with 1, 2.5 and 5 $\mu\text{g/mL}$ AOM extracts were 252.8%, 266.65% and 288.99%, respectively. These rate were higher than the rate of the worms in the control group (113.90%) ($p < 0.0001$).

On days 8, the pharyngeal pumping rates of the worms treated with 25, 50 and 100 $\mu\text{g/mL}$ AOH extracts were 260.15%, 253.25% and 221.7%, respectively ($p < 0.0001$). The pharyngeal pumping rates of the worms treated with 1, 2.5 and 5 $\mu\text{g/mL}$ AOM extracts were 231.25%, 222% and 272.6%, respectively. These rate were higher than the rate of the worms in the control group (107.42%) ($p < 0.0001$).

On days 10, the pharyngeal pumping rates of the worms treated with 25, 50 and 100 $\mu\text{g/mL}$ AOH extracts were 206.84%, 197.85% and 187.1%, respectively ($p < 0.0001$). The pharyngeal pumping rates of the worms treated with 1, 2.5 and 5 $\mu\text{g/mL}$ AOM extracts were 203.03%, 232.6% and 184.3%, respectively. These rate were higher than the rate of the worms in the control group (86.03%) ($p < 0.01$).

On days 12, the pharyngeal pumping rates of the worms treated with 25 $\mu\text{g/mL}$ AOH extracts were 165.71% ($p < 0.05$). The pharyngeal pumping rates of the worms treated with 1 $\mu\text{g/mL}$ AOM extracts were 222.2%. These rate were higher than the rate of the worms in the control group (72.29%) ($p < 0.05$) (Figure 38).

In addition, On days 5, the pharyngeal pumping rates of the worms treated with 25, 50 and 100 $\mu\text{g/mL}$ GZH extracts were 241.09%, 208.27% and 215.59%, respectively

($p < 0.0001$). The pharyngeal pumping rates of the worms treated with 1, 2.5 and 5 $\mu\text{g/mL}$ GZM extracts were 235.77%, 249.70% and 274.20%, respectively. These rate were higher than the rate of the worms in the control group (113.90%) ($p < 0.0001$).

On days 8, the pharyngeal pumping rates of the worms treated with 25, 50 and 100 $\mu\text{g/mL}$ GZH extracts were 267.55%, 207.54% and 234.57%, respectively ($p < 0.0001$). The pharyngeal pumping rates of the worms treated with 1, 2.5 and 5 $\mu\text{g/mL}$ GZM extracts were 208.68%, 207.3% and 197.75%, respectively. These rate were higher than the rate of the worms in the control group (107.42%) ($p < 0.0001$).

On days 10, the pharyngeal pumping rates of the worms treated with 25, 50 and 100 $\mu\text{g/mL}$ GZH extracts were 173.40%, 204.30% and 189.05%, respectively ($p < 0.0001$). The pharyngeal pumping rates of the worms treated with 1, 2.5 and 5 $\mu\text{g/mL}$ GZM extracts were 195.9%, 188.68% and 197.33%, respectively. These rate were higher than the rate of the worms in the control group (86.03%) ($p < 0.01$).

On days 12, the pharyngeal pumping rates of the worms treated with 25 $\mu\text{g/mL}$ GZH extracts were 156.71% ($p < 0.05$). The pharyngeal pumping rates of the worms treated with 1 $\mu\text{g/mL}$ GZM extracts were 148.12%. These rate were higher than the rate of the worms in the control group (72.29%) ($p < 0.05$) (Figure 39).

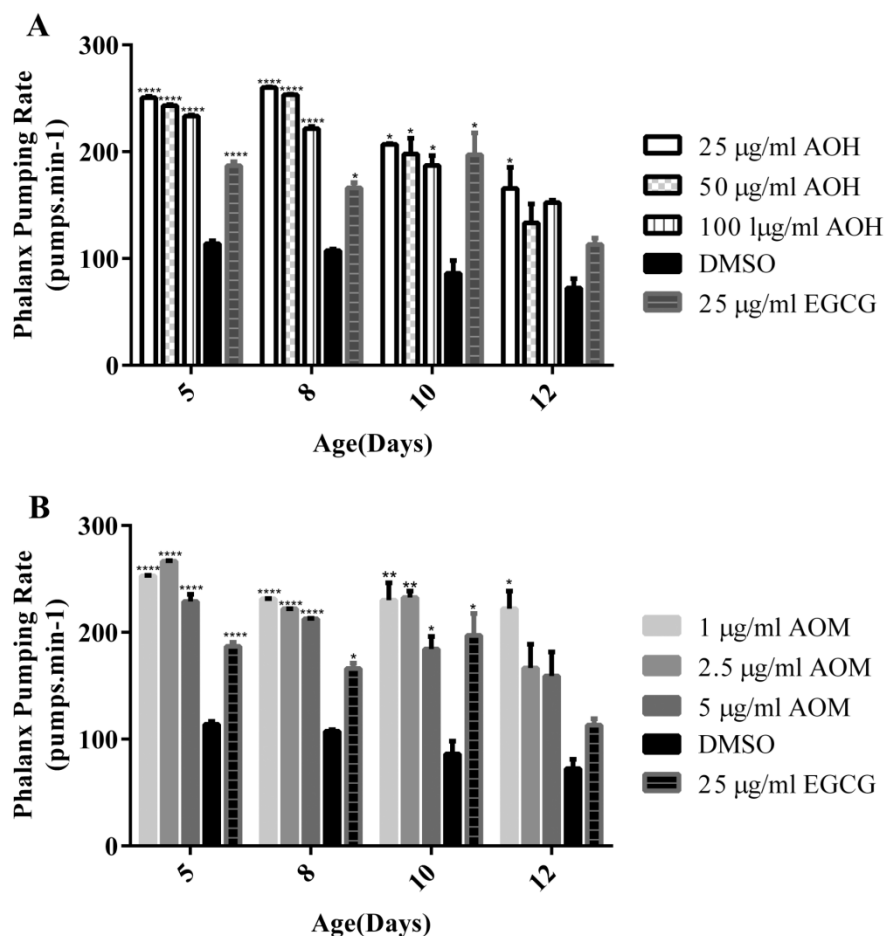


Figure 38. Effect of AO extracts on age-related markers (pharyngeal pumping).

AOH (A) and AOM (B) improve the pharyngeal pumping rate throughout the *C. elegans* aging process. Data are presented as the mean \pm SEM (n = 100). DMSO and EGCG were used as the solvent control and positive control group, respectively. Data are presented as the mean \pm SEM (n = 30, replicated three times). ** $p < 0.01$ and *** $p < 0.001$, compared to the DMSO control by one-way ANOVA following Bonferroni's method (post hoc).

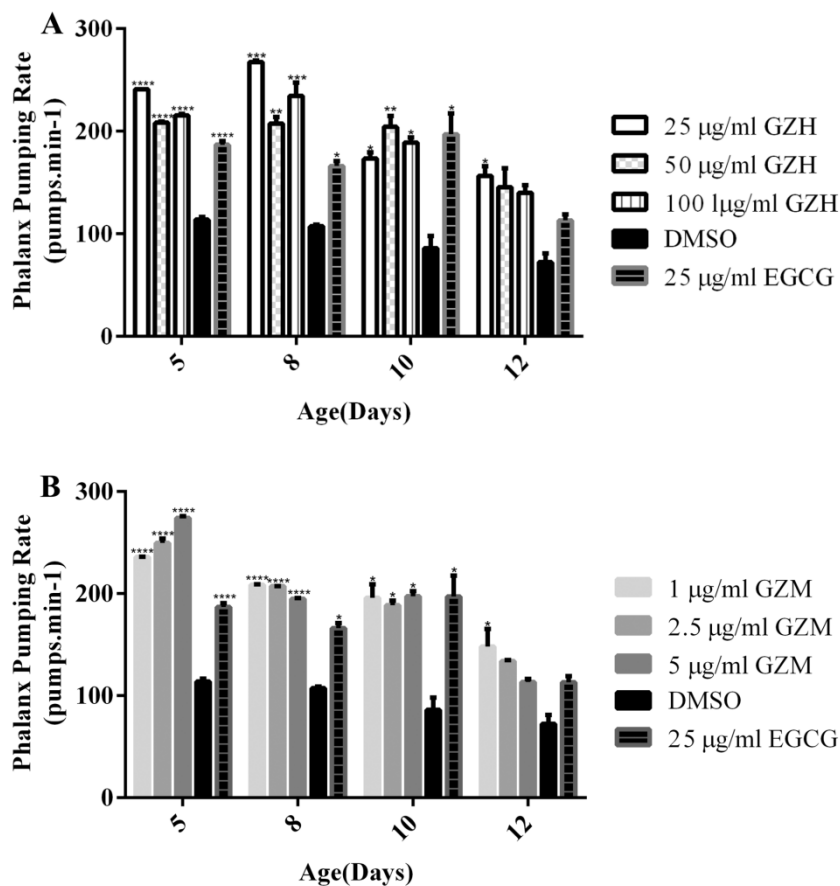


Figure 39. Effect of GZ extracts on age-related markers (pharyngeal pumping).

GZH (A) and GZM (B) improve the pharyngeal pumping rate throughout the *C. elegans* aging process. Data are presented as the mean \pm SEM (n = 100). DMSO and EGCG were used as the solvent control and positive control group, respectively. Data are presented as the mean \pm SEM (n = 30, replicated three times). ** p < 0.01 and *** p < 0.001, compared to the DMSO control by one-way ANOVA following Bonferroni's method (post hoc).

4.5.3 Dietary restriction (DR) effects

Aging can be influenced by dietary restriction (DR). To investigate the dietary restriction interfering by the extracts, the brood size and body lengths of the nematodes were measured. Brood size and body length in wild type worms were not affected by different concentrations of the AO and GZ hexane, dichloromethane and methanol extracts (Figure 40-41). These data indicated that the effects extracts were not caused by DR.

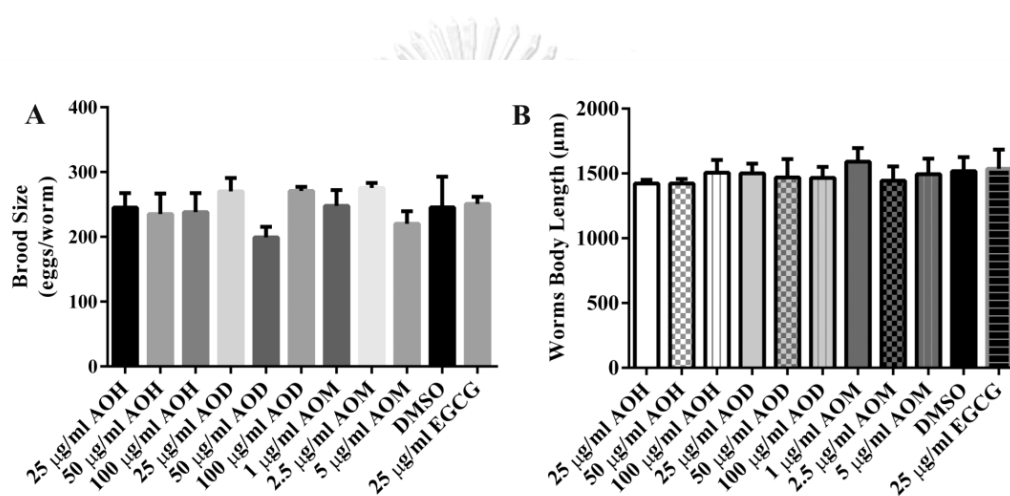


Figure 40. Dietary restriction (DR) effects of AO extracts.

Brood size (A) and body length (B) of wild-type worms after AO extracts treatment. Treatment with AO had no effect on egg laying activity and body length. The results are expressed as the mean \pm SEM from three independent experiments ($n = 30$). Treatment groups are compared to the DMSO control by one-way ANOVA following Bonferroni's method (post hoc).

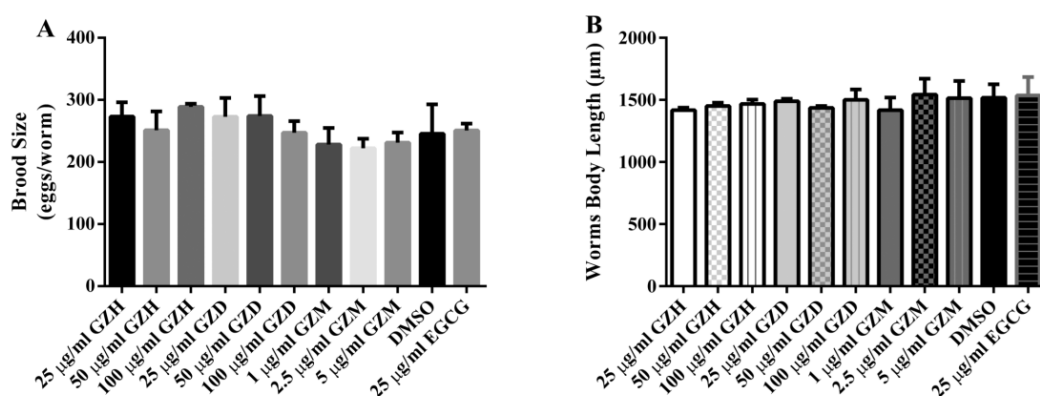


Figure 41. Dietary restriction (DR) effects of GZ extracts

Brood size (A) and body length (B) of wild-type worms after GZ extracts treatment. Treatment with GZ had no effect on egg laying activity and body length. The results are expressed as the mean \pm SEM from three independent experiments ($n = 30$). Treatment groups are compared to the DMSO control by one-way ANOVA following Bonferroni's method (post hoc).

4.5.4 Lifespan

To investigate the extracts can influence longevity, the life-span assay were carried out in the wild-type (N2) and Mev-1 mutants (TK22) (A mutation in succinate dehydrogenase cytochrome b causes oxidative stress and short lifespan) worms. The wild-type worms treated with 50 $\mu\text{g}/\text{mL}$ AOH and 1 $\mu\text{g}/\text{mL}$ AOM extracts significantly increased the mean lifespan of the N2 worms by 20.31% ($p < 0.001$) and 3.36% ($p < 0.01$), respectively (Figure 42AB, Table 10).

In addition, The wild-type worms treated with 100 $\mu\text{g}/\text{mL}$ GZH, 1 and 5 $\mu\text{g}/\text{mL}$ GZM extracts significantly increased the mean lifespan of the N2 worms by 15.71% ($p < 0.01$), 15.42% ($p < 0.05$) and 15.53% ($p < 0.01$), respectively (Figure 42CD, Table 11).

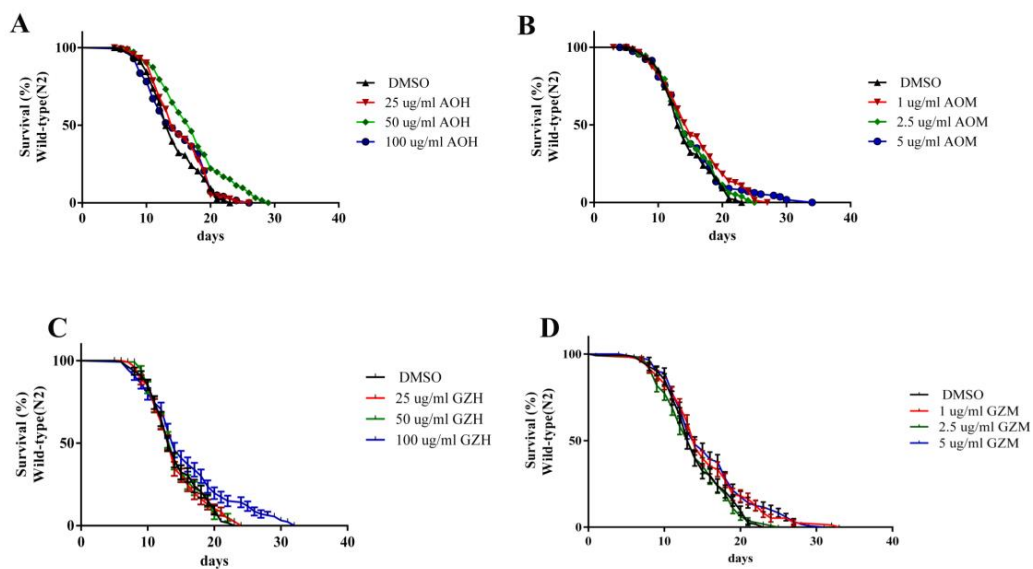


Figure 42. Effect of AO and GZ extracts on the lifespan of wild-type worms.

Survival curves of the worms at 20 °C on the plate treated with AOH (A), AOM (B), GZH (C), and GZM (D) at different concentrations. Survival plots were drawn by GraphPad Prism 6.0.

Table 10. Results and statistical analyses of the AO extracts treated *C. elegans* in lifespan assay

Strain	Treatment	Mean life span (day) \pm SE	Maximum	Percentage of increased	P value	P value summary	Worms (N)	censored
			lifespan (days)	lifespan (vs control)	(vs control)			
N2	DMSO control	14.28 \pm 0.36					N=120	N=8
N2	25 mg/ml AOH	14.91 \pm 0.31	26	4.41	0.13	ns	N=126	N=18
N2	50 mg/ml AOH	17.18 \pm 0.44	33	20.31	< 0.0001	****	N=137	N=8
N2	100 mg/ml AOH	15.04 \pm 0.44	26	5.32	0.27	ns	N=126	N=2
N2	1 mg/ml AOM	14.76 \pm 0.47	29	3.36	0.01	**	N=107	N=22
N2	2.5 mg/ml AOM	14.63 \pm 0.43	29	2.45	0.27	ns	N=104	N=9
N2	5 mg/ml AOM	15.16 \pm 0.49	34	6.16	0.21	ns	N=111	N=9
TK22	DMSO control	9.67 \pm 0.41					N=33	N=4
TK22	25 mg/ml AOH	9.58 \pm 0.30	15	-0.91	0.26	ns	N=38	N=2
TK22	50 mg/ml AOH	9.97 \pm 0.47	16	3.16	0.85	ns	N=36	N=2
TK22	100 mg/ml AOH	10.76 \pm 0.60	17	11.31	0.12	ns	N=25	N=4
TK22	1 mg/ml AOM	9.96 \pm 0.46	17	3.02	0.62	ns	N=49	N=4
TK22	2.5 mg/ml AOM	10.97 \pm 0.57	18	13.48	0.12	ns	N=38	N=1
TK22	5 mg/ml AOM	9.79 \pm 0.56	17	1.23	0.56	ns	N=42	N=4

N2; Wild type , TK22 ; *mev-1(kn1)*

Table 11. Results and statistical analyses of GZ extracts treated *C. elegans* in lifespan assay

Strain	Treatment	Mean lifespan (day) \pm SEM	Maximum lifespan (days)	Percentage of increased lifespan (vs control)	P value (vs control)	P value summary	Worm (N)
N2	DMSO control	14.28 \pm 0.3599	21				N=120
N2	25 μ g/mL GZH	13.93 \pm 0.3507	24	-2.45098	0.901	ns	N=121
N2	50 μ g/mL GZH	14.21 \pm 0.3805	24	-0.490196	0.833	ns	N=105
N2	100 μ g/mL GZH	15.71 \pm 0.5486	32	10.014006	0.0056	**	N=132
N2	1.0 μ g/mL GZM	15.42 \pm 0.4908	29	7.9831933	0.0139	*	N=127
N2	2.5 μ g/mL GZM	12.55 \pm 0.4489	29	-12.11485	0.7191	ns	N=112
N2	5 μ g/mL GZM	15.53 \pm 0.4635	34	8.7535014	0.0066	**	N=132
TK22	DMSO control	9.667 \pm 0.4144	15				N=33
TK22	25 μ g/mL GZH	9.429 \pm 0.4126	16	-2.46198407	0.6491	ns	N=35
TK22	50 μ g/mL GZH	9.581 \pm 0.3525	15	-0.889624496	0.816	ns	N=31
TK22	100 μ g/mL GZH	10.37 \pm 0.5288	17	7.272163029	0.4833	ns	N=27
TK22	1.0 μ g/mL GZM	11.54 \pm 0.5245	17	19.37519396	0.1071	ns	N=39
TK22	2.5 μ g/mL GZM	11.31 \pm 0.5236	18	16.99596566	0.1798	ns	N=39
TK22	5 μ g/mL GZM	10.88 \pm 0.5015	17	12.54784318	0.4237	ns	N=41

N2; Wild-type, TK22 ; *mev-1(kn1)*

GZH; GZ hexane extract, GZM; GZ methanol extract

The lifespan assay was carried out with wild-type (N2) and *mev-1(kn-1)* worms at 20 °C. P-value log rank as compared to the control worms; the mean lifespan in days is the average number of days the worms survived in each group. Each treatment was compared to the control by the non-parametric log rank (Mantel–Cox) tests.

4.6 The underlying mechanisms of AO and GZ extracts (*In vivo*)

4.6.1. Antioxidant gene expression

To investigate the neuroprotective effects of the extracts on glutamate-induced oxidative stress through endogenous antioxidant enzymes, the expression of antioxidant and phase II enzymes gene expression were measured. The neuroprotective results showed that 25 µg/mL AOH extract and 10 µg/mL AOM extract exhibited a powerful neuroprotective effect in HT22 and Neuro-2a cells (Figure 20 and 24). Thus, these concentrations were used for the following experiments.

The HT22 cells treated with 25 µg/ml AOH extracts significantly increased GSTa2, GSTo1, GPx, and SOD1 mRNA expression by 77% ($p < 0.0001$), 39% ($p < 0.05$), 46% ($p < 0.05$), and 82% ($p < 0.001$), respectively (Figure 43AB). The Neuro-2a cells treated with 25 µg/ml AOH extracts significantly increased GSTa2, GSTo1, GPx, SOD1 and SOD2 mRNA expression by 251% ($p < 0.0001$), 80% ($p < 0.0001$), 32% ($p < 0.05$), 80% ($p < 0.001$) and 32% ($p < 0.01$), respectively (Figure 43CD).

The HT22 cells treated with 10 µg/ml AOM extracts significantly increased GSTa2, GSTo1, GPx, and SOD1 mRNA expression by 46% ($p < 0.01$), 50% ($p < 0.05$), 50% ($p < 0.05$), and 62% ($p < 0.01$), respectively (Figure 43AB). The Neuro-2a cells treated with 10 µg/ml AOM extracts significantly increased GSTa2, GSTo1, GPx, SOD1 and SOD2 mRNA expression by 36% ($p < 0.01$), 49% ($p < 0.01$), 32% ($p < 0.01$), 46% ($p < 0.01$) and 67% ($p < 0.0001$), respectively (Figure 43CD).

In addition, The HT22 cells treated with 1 µg/ml GZH extracts significantly increased GSTa2, GSTo1, GPx, SOD1 and SOD2 mRNA expression by 41% ($p < 0.05$), 103% ($p < 0.0001$), 85% ($p < 0.0001$), 240% ($p < 0.0001$) and 97% ($p < 0.0001$), respectively (Figure 44AB). The Neuro-2a cells treated with 1 µg/ml GZH extracts significantly increased GSTa2, GSTo1, GPx, SOD1 and SOD2 mRNA expression by 80% ($p < 0.0001$), 45% ($p < 0.0001$), 30% ($p < 0.001$), 36% ($p < 0.001$), and 90% ($p < 0.0001$), respectively (Figure 44CD).

The HT22 cells treated with 10 µg/ml GZM extracts significantly increased GSTa2, GSTo1, GPx, and SOD1 mRNA expression by 55% ($p < 0.01$), 86% ($p < 0.01$), 60% (p

<0.01), and 100% ($p < 0.0001$), respectively (Figure 44AB). The Neuro-2a cells treated with 10 $\mu\text{g/ml}$ GZM extracts significantly increased GSTa2, GSTo1, GPx, SOD1 and SOD2 mRNA expression by 78% ($p < 0.0001$), 38% ($p < 0.0001$), 45% ($p < 0.001$), 38% ($p < 0.001$) and 42% ($p < 0.01$), respectively (Figure 44CD). However, the expression of the CAT gene was not significantly changed in either HT22 or Neuro-2a cells after treatment with the AO and GZ extracts.

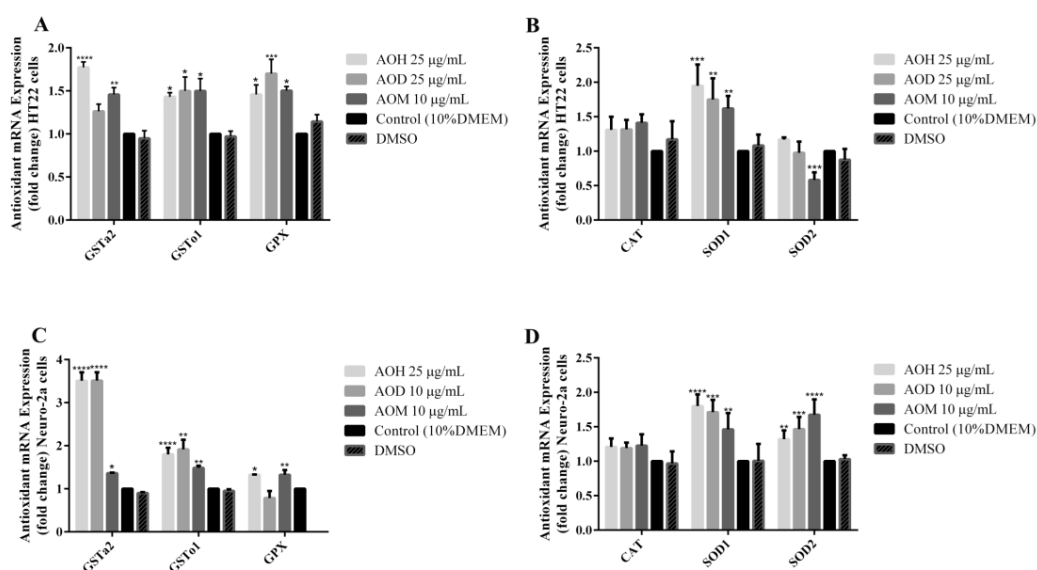


Figure 43. The effect of AO extracts on antioxidant gene expression in HT22 and Neuro-2a cells.

AO extract treatment increased endogenous antioxidant gene expression in HT22 (AB) and Neuro-2a (CD) cells when compared to untreated control. β -actin was used as the internal control for RT-PCR assay. All data are shown as the mean \pm SEM at least three independent experiments. * $p < 0.05$, ** $p < 0.01$, *** $p < 0.001$ and **** $p < 0.0001$, compared to the untreated control by one-way ANOVA following Bonferroni's method (posthoc).

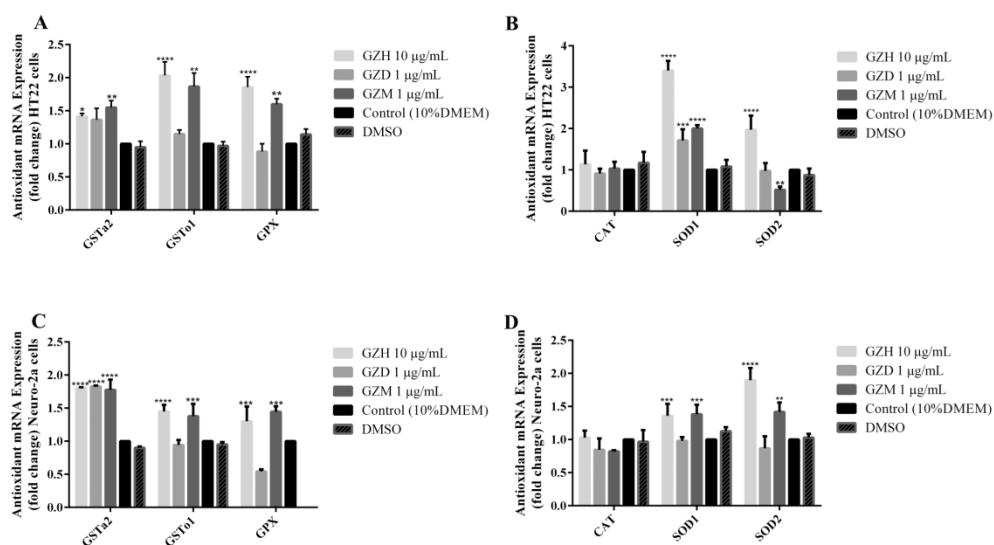


Figure 44. The effect of GZ extracts on antioxidant gene expression in HT22 and Neuro-2a cells.

GZ extract treatment increased endogenous antioxidant gene expression in HT22 (AB) and Neuro-2a (CD) cells when compared to untreated control. β -actin was used as the internal control for RT-PCR assay. All data are shown as the mean \pm SEM at least three independent experiments. * $p < 0.05$, ** $p < 0.01$, *** $p < 0.001$ and **** $p < 0.0001$, compared to the untreated control by one-way ANOVA following Bonferroni's method (posthoc).

4.6.2 SIRT1 and Nrf2 signaling pathway

To investigate the underlying mechanisms of the extracts, the SIRT1/Nrf2 signaling pathway were studied. The effects on SIRT1 expression were firstly examined by RT-PCR and WB analysis. The HT22 and Neuro-2a cells treated with 10 μ g/ml AOM extracts significantly increased SIRT1 mRNA expression by 463% ($p < 0.0001$), 44% ($p < 0.05$) and 46% ($p < 0.01$), respectively. The results were confirmed by WB analysis; the Neuro-2a cells treated with 10 μ g/ml AOM extracts significantly increased SIRT1 protein expression by 56% ($p < 0.01$), respectively (Figure 45).

In addition, The HT22 cells treated with 1 μ g/ml GZH and 10 μ g/ml GZM extracts significantly increased SIRT1 mRNA expression by 250% ($p < 0.0001$) and 64% ($p < 0.05$), respectively. The Neuro-2a cells treated with 1 μ g/ml GZH and 10 μ g/ml GZM extracts significantly increased SIRT1 mRNA expression by 19% ($p < 0.05$) and

50% ($p < 0.0001$), respectively. The results were confirmed by WB analysis; the Neuro-2a cells treated with 1 $\mu\text{g/ml}$ GZH and 10 $\mu\text{g/ml}$ GZM extracts significantly increased SIRT1 protein expression by 63% ($p < 0.05$) and 52% ($p < 0.05$), respectively (Figure 46).

Next, the effects on Nrf2 expression were examined by WB analysis. The HT22 and Neuro-2a cells treated with 10 $\mu\text{g/ml}$ AOM extracts significantly increased Nrf2 protein expression by 71% ($p < 0.0001$) (Figure 47). In addition, The HT22 cells treated with 1 $\mu\text{g/ml}$ GZH and 10 $\mu\text{g/ml}$ GZM extracts significantly increased Nrf2 protein expression by 46% ($p < 0.05$) and 60% ($p < 0.01$), respectively (Figure 48).

To further elucidate the mechanisms of the extracts, the antioxidant-related target genes (NQO1, GCLM, and EAAT3) that are regulated by the SIRT1-Nrf2 signaling pathway were measured. The HT22 cells treated with 25 $\mu\text{g/ml}$ AOH extracts significantly increased NQO1, GCLM, and EAAT3 mRNA expression by 59% ($p < 0.0001$), 88% ($p < 0.0001$) and 77% ($p < 0.0001$), respectively. The Neuro-2a cells treated with 25 $\mu\text{g/ml}$ AOH extracts significantly increased NQO1, GCLM, and EAAT3 mRNA expression by 86% ($p < 0.0001$), 99% ($p < 0.001$) and 191% ($p < 0.001$), respectively (Figure 47).

The HT22 cells treated with 10 $\mu\text{g/ml}$ AOM extracts significantly increased NQO1, GCLM, and EAAT3 mRNA expression by 68% ($p < 0.0001$), 41% ($p < 0.05$) and 110% ($p < 0.0001$), respectively. The Neuro-2a cells treated with 10 $\mu\text{g/ml}$ AOM extracts significantly increased NQO1, GCLM, and EAAT3 mRNA expression by 187% ($p < 0.0001$), 56% ($p < 0.01$) and 56% ($p < 0.01$), respectively (Figure 47).

In addition, the HT22 cells treated with 1 $\mu\text{g/ml}$ GZH extracts significantly increased NQO1, GCLM, and EAAT3 mRNA expression by 70% ($p < 0.001$), 67% ($p < 0.001$) and 157% ($p < 0.0001$), respectively. The Neuro-2a cells treated with 1 $\mu\text{g/ml}$ GZH extracts significantly increased NQO1, GCLM, and EAAT3 mRNA expression by 78% ($p < 0.0001$), 46% ($p < 0.0001$) and 58% ($p < 0.01$), respectively (Figure 48).

The HT22 cells treated with 10 $\mu\text{g/ml}$ GZM extracts significantly increased GCLM and EAAT3 mRNA expression by 78% ($p < 0.0001$) and 59% ($p < 0.01$), respectively.

The Neuro-2a cells treated with 10 $\mu\text{g/ml}$ GZM extracts significantly increased GCLM, and EAAT3 mRNA expression by 36% ($p < 0.0001$) and 222% ($p < 0.0001$), respectively (Figure 48).

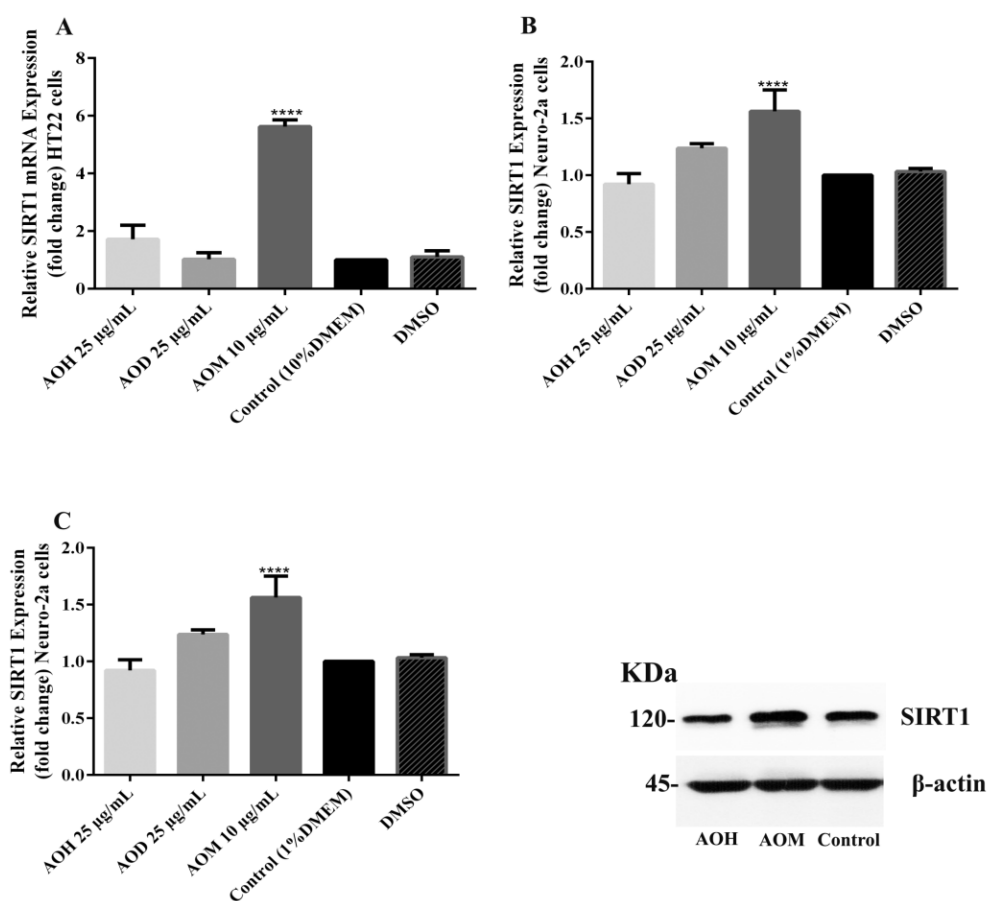


Figure 45. Effect of AO extracts on SIRT1 signaling pathway.

AO methanol extract treatment increased the SIRT1 mRNA gene expression in HT22 (**A**) and Neuro-2a (**B**) cells. Moreover, AOM extract increased the SIRT1 protein expression (**C**) in Neuro-2a cells. Whole-cell lysates were subjected to western blot analysis of the SIRT1 after AO extract treatment. β -actin was used as endogenous loading control for western blot assay and internal control for RT-PCR assay. All data were normalized to endogenous control levels and shown as mean \pm SEM at least three independent experiments. * $p < 0.05$, ** $p < 0.01$, *** $p < 0.001$ and **** $p < 0.0001$, compared to the untreated control by one-way ANOVA following Bonferroni's method (post hoc).

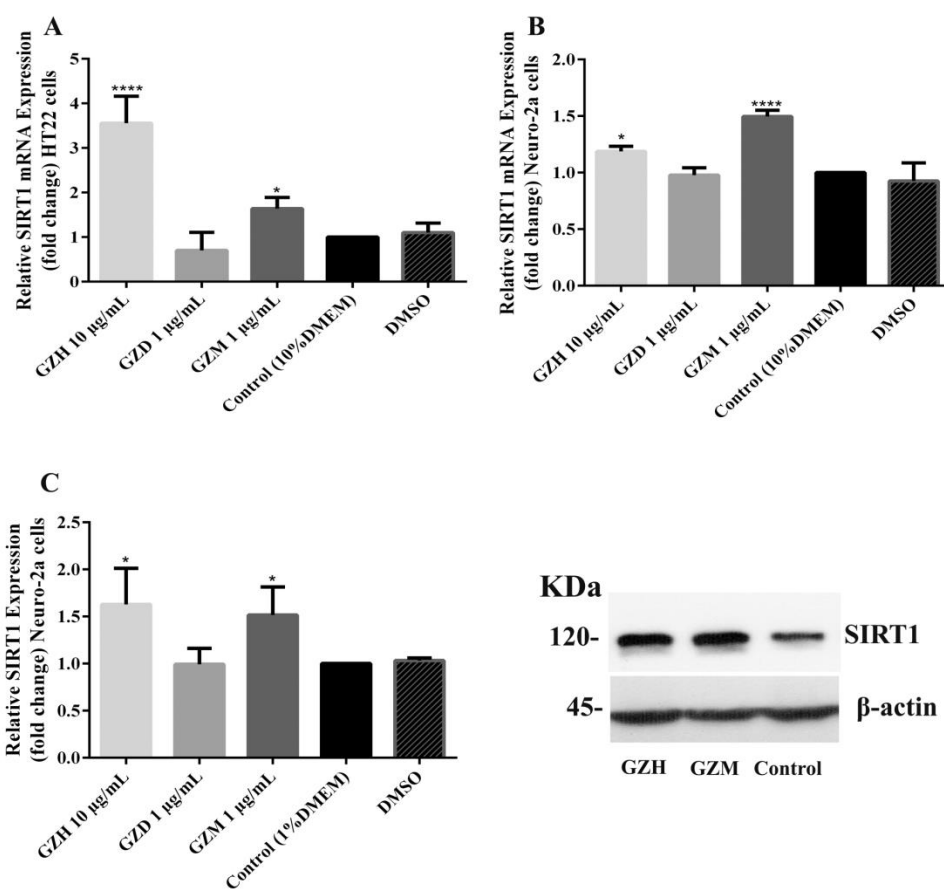


Figure 46. Effect of GZ extracts on SIRT1 signaling pathway.

GZ methanol extract treatment increased the SIRT1 mRNA gene expression in HT22 (A) and Neuro-2a (B) cells. Moreover, GZM extract increased the SIRT1 protein expression (C) in Neuro-2a cells. Whole-cell lysates were subjected to western blot analysis of the SIRT1 after GZ extracts treatment. β -actin was used as endogenous loading control for western blot assay and internal control for RT-PCR assay. All data were normalized to endogenous control levels and shown as mean \pm SEM at least three independent experiments. * p < 0.05, ** p < 0.01, *** p < 0.001 and **** p < 0.0001, compared to the untreated control by one-way ANOVA following Bonferroni's method (post hoc).

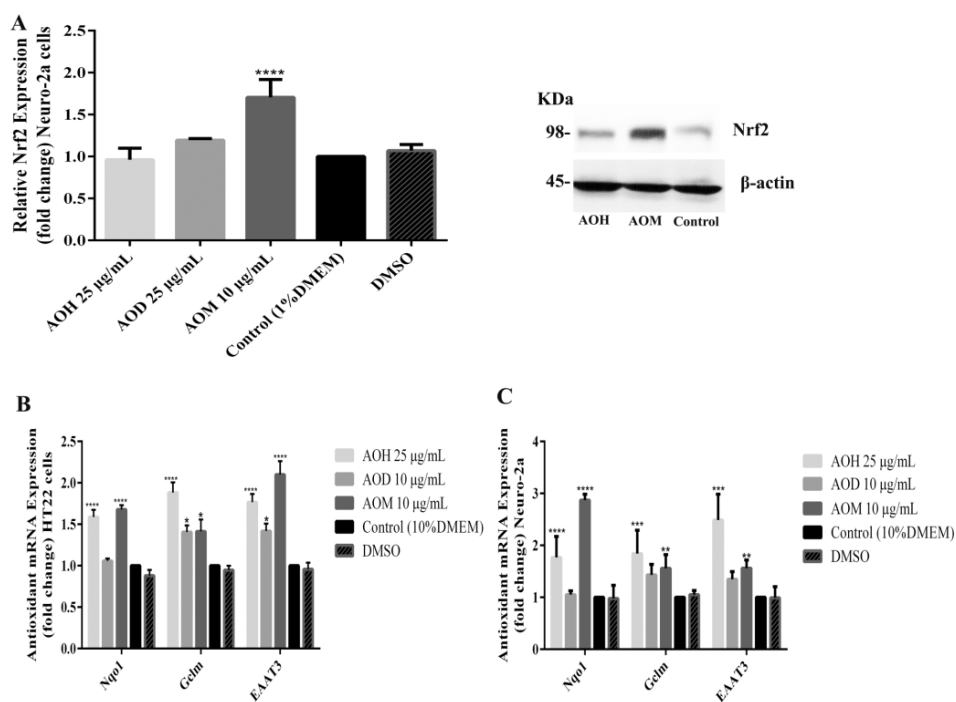


Figure 47. Effect of AO extracts on Nrf2 signaling pathway.

AO methanol extract treatment increased the Nrf2 expression (**A**) and antioxidant-related target genes in HT22 (**B**) and Neuro-2a cells (**C**) when compared to the untreated control. Whole-cell lysates were subjected to western blot analysis of the Nrf2 level after AO extract treatment. β -actin was used as endogenous loading control for western blot assay and internal control for RT-PCR assay. All data were normalized to endogenous control levels and shown as mean \pm SEM at least three independent experiments. * $p < 0.05$, ** $p < 0.01$, *** $p < 0.001$ and **** $p < 0.0001$, compared to the untreated control by one-way ANOVA following Bonferroni's method (post hoc).

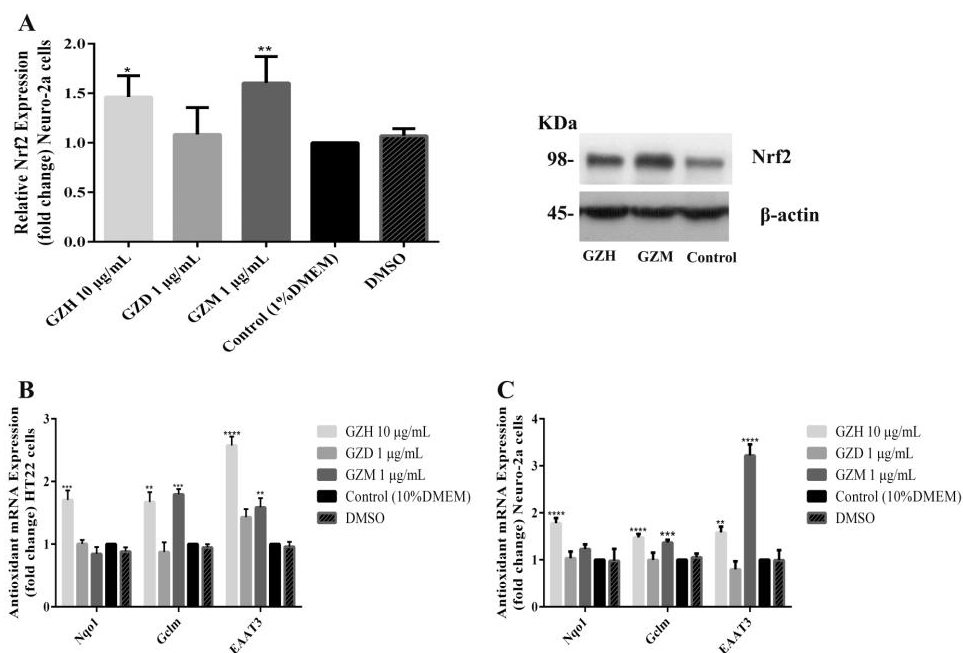


Figure 48. Effect of GZ extracts on Nrf2 signaling pathway.

GZH and GZM extracts treatment increased the Nrf2 expression (A) and antioxidant-related target genes in HT22 (B) and Neuro-2a cells (C) when compared to the untreated control. Whole-cell lysates were subjected to western blot analysis of the Nrf2 level after GZ extracts treatment. β -actin was used as endogenous loading control for western blot assay and internal control for RT-PCR assay. All data were normalized to endogenous control levels and shown as mean \pm SEM at least three independent experiments. * $p < 0.05$, ** $p < 0.01$, *** $p < 0.001$ and **** $p < 0.0001$, compared to the untreated control by one-way ANOVA following Bonferroni's method (post hoc).

4.7 The underlying mechanisms of AO and GZ extracts (*In vivo*)

4.7.1 *HSP-16.2* gene expression

To determine the mechanism of antioxidant activities, the protective activities of the extracts against oxidative stress were studied in *C. elegans*. The effects of the extracts on heat shock protein 16.2 (*HSP-16.2*) gene expression were studied. In nematodes, the promoter for *HSP-16.2* was joined with GFP (strain TJ375). Under oxidative stress conditions (20 μ M juglone), *HSP-16.2* induction was visualized by a high intensity of GFP fluorescence in the head of the transgenic worms.

However, the TJ375 worms treated with 25, 50 and 100 μ g/mL AOH extracts significantly decreased the fluorescence intensity of GFP by 64.90%, 67.77% and 45.86% ($p < 0.0001$), respectively. A similar result was obtained for TJ375 worms treated with 1.0, 2.5 and 5 μ g/mL AOM extracts significantly decreased the fluorescence intensity of GFP by 78.04%, 68.27% and 22.32% ($p < 0.0001$), respectively (Figure 49).

In addition, the TJ375 worms treated with 25, 50 and 100 μ g/mL GZH extracts significantly decreased the fluorescence intensity of GFP by 54.94%, 52.27% and 62.88% ($p < 0.0001$), respectively. A similar result was obtained for TJ375 worms treated with 1.0, 2.5 and 5 μ g/mL GZM extracts significantly decreased the fluorescence intensity of GFP by 67.09%, 32.13% and 36.70% ($p < 0.0001$), respectively (Figure 50). *HSP-16.2* expression under juglone-induced oxidative stress was suppressed in worms by AO and GZ extracts similar to 25 μ g/mL EGCG (61.91%, $p < 0.0001$). These data indicate that the extracts are bioavailable and exhibit *In vivo* antioxidant properties.

4.7.2 *SOD-3* gene expression

The effects of the extracts on superoxide dismutase 3 (*SOD-3*) gene expression were studied. In nematodes, the promoter for *SOD-3* was joined with GFP (strain CF1553). The gene expressions are representing follow the fluorescence intensity. The CF1553 worms treated with 25, 50 and 100 μ g/mL AOH extracts significantly increased the fluorescence intensity of GFP 25.41% ($p < 0.0001$), 23.70% ($p < 0.0001$) and 22.64% ($p < 0.01$), respectively. A similar result was obtained for CF1553 worms treated with

1.0, 2.5 and 5 $\mu\text{g}/\text{mL}$ AOM extracts significantly increased the fluorescence intensity of GFP by 27.37% ($p < 0.001$), 29.11% ($p < 0.001$) and 24.87% ($p < 0.01$), respectively (Figure 49).

In addition, the CF1553 worms treated with 25 $\mu\text{g}/\text{mL}$ GZH extracts significantly increased the fluorescence intensity of GFP 16.47% ($p < 0.001$). A similar result was obtained for CF1553 worms treated with 1.0 and 2.5 GZM extracts significantly increased the fluorescence intensity of GFP 18.03% ($p < 0.001$) and 16.42% ($p < 0.01$) and 24.87% ($p < 0.01$), respectively (Figure 50). The effects of the extracts on *SOD-3* gene expression was similar to the EGCG treatment (13.39%, $p < 0.05$). These data indicate that the AO and GZ extracts can increase the *In vivo* antioxidant effect by inducing antioxidant enzymes.

4.7.3 *GST-4* gene expression

The effects of the extracts on glutathione S-transferase 4 gene (*GST-4*) gene expression were studied. In nematodes, the promoter for *GST-4* was joined with GFP (strain CL2166). The gene expressions are representing follow the fluorescence intensity. The CL2166 worms treated with 25 and 50 $\mu\text{g}/\text{mL}$ AOH extracts significantly increased the fluorescence intensity of GFP 41.99% ($p < 0.0001$) and 17.68% ($p < 0.01$), respectively. A similar result was obtained for CL2166 worms treated with 1.0, 2.5 and 5 $\mu\text{g}/\text{mL}$ AOM extracts significantly increased the fluorescence intensity of GFP by 27.38% ($p < 0.0001$), 23.80% ($p < 0.0001$) and 50.19% ($p < 0.0001$), respectively (Figure 49).

In addition, the CL2166 worms treated with 25 $\mu\text{g}/\text{mL}$ GZH extracts significantly increased the fluorescence intensity of GFP 17.47% ($p < 0.001$). A similar result was obtained for CL2166 worms treated with 1.0, 2.5 and 5 $\mu\text{g}/\text{mL}$ GZM extracts significantly increased the fluorescence intensity of GFP by 29.80% ($p < 0.001$), 57.41% ($p < 0.0001$) and 54.20% ($p < 0.0001$), respectively (Figure 50). These data indicate that the AO and GZ extracts can increase the *In vivo* antioxidant effect by inducing antioxidant enzymes.

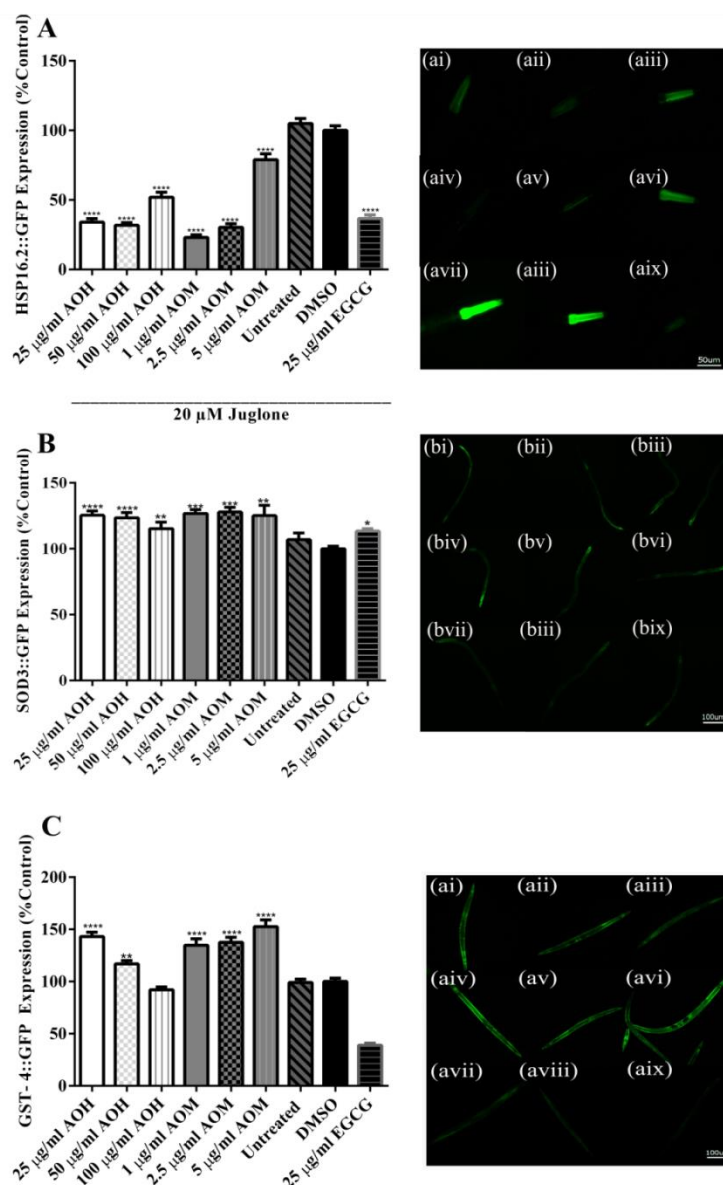


Figure 49. Effect of AO extracts on the stress resistance genes in *C. elegans*.

AO extracts decreased HSP 16.2 expression in mutant TJ375 worms [HSP-16.2::GFP(gplsI)] under oxidative stress induced by juglone (A). AO extracts increased SOD-3 expression in mutants CF1553 [(pAD76) sod-3p::GFP + rol-6] (B) and AO extracts treatment increased GST-4 expression in mutants CL2166 [(pAF15)gst-4p::GFP::NLS] under oxidative stress induced by juglone (C).

aii-aix and **bii-bix**: representative pictures of GFP fluorescence in worms treated with 25 µg/mL AOH (**aii/bii**); 50 µg/mL AOH (**aiii/biii**); 100 µg/mL AOH (**aiv/biv**); 1 µg/mL AOM (**av/bv**); 2.5 µg/mL AOM (**avi/bvi**); 5 µg/mL AOM (**avii/bvii**); Untreated control (**aviii/bviii**); DMSO solvent control (**aix/bix**); and 25 µg/mL EGCG (**ax/bx**).

The GFP mean pixel density for each group was calculated from the mean value of the 30 worms that were randomly selected. Data were obtained from three independent experiments and are presented as the mean \pm SEM. DMSO and EGCG were used as the solvent control and positive control group, respectively. $*p < 0.05$, $**p < 0.01$, $** *p < 0.001$ and $****p < 0.0001$, compared to the DMSO control; # $p < 0.05$ compared to the EGCG positive control by one-way ANOVA following Bonferroni's method (post hoc).

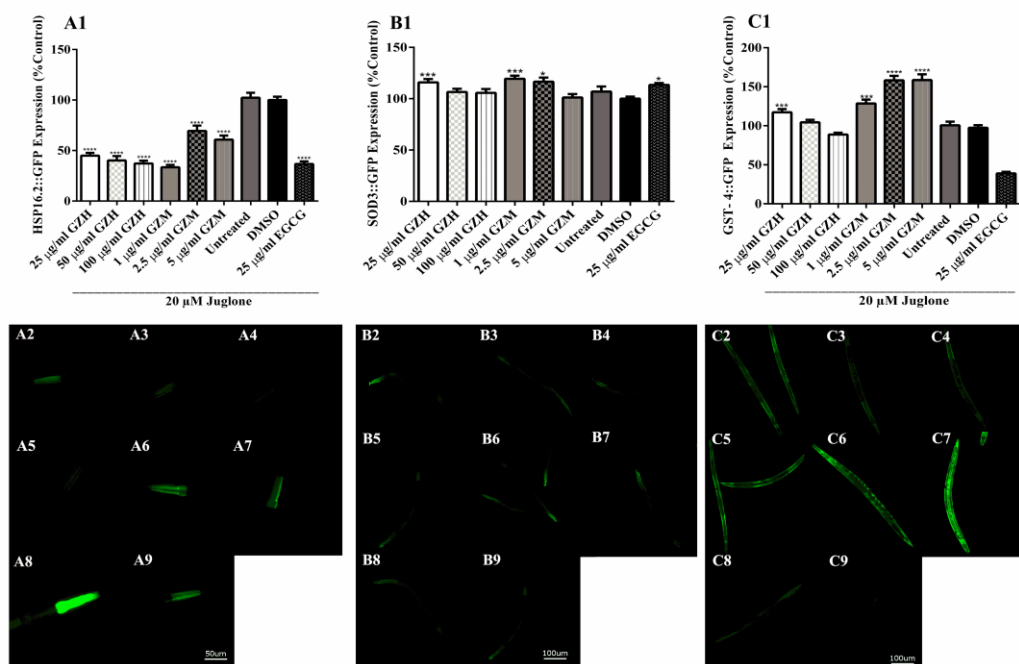


Figure 50. Effect of GZ extracts on stress resistance genes in *C. elegans*.

GZ extracts decreased HSP 16.2 expression in mutant TJ375 worms [HSP-16.2::GFP(gplsI)] under oxidative stress induced by juglone (A) GZ extracts increased SOD-3 expression in mutants CF1553 [(pAD76) sod-3p::GFP + rol-6] (B) and GZ extracts treatment increased GST-4 expression in mutants CL2166 [(pAF15)gst-4p::GFP::NLS] under oxidative stress induced by juglone (C).

A2-A9, B2-B9, C2-C9: representative pictures of GFP fluorescence in worms treated with 25 µg/mL GZH (A2/B2/C2); 50 µg/mL GZH (A3/B3/C3); 100 µg/mL GZH (A4/B4/C4); 1 µg/mL GZM (A5/B5/C5); 2.5 µg/mL GZM (A6/B6/C6); 5 µg/mL GZM (A7/B7/C7); DMSO solvent control (A8/B8/C8); and 25 µg/mL EGCG (A9/B9/C9). The GFP mean pixel density for each group was calculated from the mean value of the 30 worms that were randomly selected. Data were obtained from three independent experiments and are presented as the mean \pm SEM. DMSO and EGCG were used as the solvent control and positive control group, respectively. $*p < 0.05$, $**p < 0.01$, $** *p < 0.001$ and $****p < 0.0001$, compared to the DMSO control; # $p < 0.05$ compared to the EGCG positive control by one-way ANOVA following Bonferroni's method (post hoc).

4.7.4 DAF-16/FoxO transcription factor

To investigate whether the extracts mediate their antioxidant activity through the DAF-16/FoxO pathway, the DAF-16 loss-of-function mutant (CF1038) worms were used in survival assays and intracellular ROS accumulation, and TJ356 transgenic worms were used in the DAF-16 subcellular localization assay.

The CF1038 worms treated with all concentrations of the AO and GZ extracts did not exhibit an increased survival rate under oxidative stress nor a decreased intracellular ROS accumulation level when compared to the DMSO control (Figure 53-54). These data indicate that the AO and GZ extracts failed to increase the survival rate under oxidative stress and attenuate intracellular ROS levels in DAF-16 loss-of-function mutants.

The TJ356 worms treated with 25, 50 and 100 $\mu\text{g}/\text{mL}$ AOH extracts significantly increased the level of nuclear location of DAF-16::GFP by 59.73%, 63.74% and 57.45%, ($p < 0.0001$) respectively. The TJ356 worms treated with 1.0, 2.5 and 5 $\mu\text{g}/\text{mL}$ AOM, a similar pattern of nuclear location was observed [nuclear localization 49.68% ($p < 0.001$), 58.74% ($p < 0.0001$) and 68.17% ($p < 0.0001$), respectively]. These data show a strong nuclear localization of DAF-16 compared to the control group (13.56%). These effects are similar to that of 25 $\mu\text{g}/\text{mL}$ EGCG as a positive control (45.95%, $p < 0.01$). Interestingly, 5 $\mu\text{g}/\text{mL}$ AOM extract increased the nuclear location of DAF-16::GFP stronger than EGCG (Figure 51).

In addition, The TJ356 worms treated with 25, 50 and 100 $\mu\text{g}/\text{mL}$ GZH extracts significantly increased the level of nuclear location of DAF-16::GFP by 61.03, 60.32% and 74.18%, ($p < 0.0001$) respectively. The TJ356 worms treated with 1.0, 2.5 and 5 $\mu\text{g}/\text{mL}$ GZM, a similar pattern of nuclear location was observed [nuclear localization 51.56% ($p < 0.001$), 66.68% ($p < 0.0001$) and 69.51% ($p < 0.0001$), respectively]. These data show a strong nuclear localization of DAF-16 compared to the control group (13.56%). These effects are similar to EGCG positive control (Figure 51). Taken together, survival assays, intracellular ROS accumulation and DAF-16 subcellular localization assays strongly suggest that AO and GZ extracts

mediate antioxidant activity and stress resistance in *C. elegans* via the DAF-16/FoxO pathway.

4.7.5 SKN-1/Nrf-2 transcription

To further investigate whether the extracts exhibit their antioxidant activity through the SKN-1 signaling pathway, the SKN-1 loss-of-function mutant (EU1) was used in survival assays and intracellular ROS accumulation and LD1 transgenic worms were used in the SKN-1 subcellular localization assay.

The EU1 worms treated with all concentrations of the AO and GZ extracts did not exhibit an increased survival rate under oxidative stress nor a decreased intracellular ROS accumulation level when compared to the control group (Figure 53-54). These data indicate that the AO and GZ extracts failed to increase the survival rate under oxidative stress and attenuate intracellular ROS levels in SKN-1 loss-of-function mutants. Moreover, the SKN-1 pathway is apparently involved in the oxidative stress response, similar to the DAF-16 pathway.

The LD1 worms treated with 1.0, 2.5 and 5 $\mu\text{g}/\text{mL}$ AOM extracts significantly increased the level of nuclear location of SKN-1::GFP by 28.49% ($p < 0.001$), 22.55% ($p < 0.01$) and 24.10% ($p < 0.01$), respectively (Figure 51). In addition, the LD1 worms treated with 1.0 and 2.5 $\mu\text{g}/\text{mL}$ GZM extracts significantly increased the level of nuclear location of SKN-1::GFP by 24.07% ($p < 0.05$) and 27.64% ($p < 0.01$), respectively (Figure 52). However, the AOH and GZH extracts did not exhibit the significantly different of SKN-1 nuclear location when compare to the control group. These findings strongly suggest that AO and GZ extracts exert their antioxidant activity and stress resistance effects in *C. elegans* also via the SKN-1 signaling pathway.

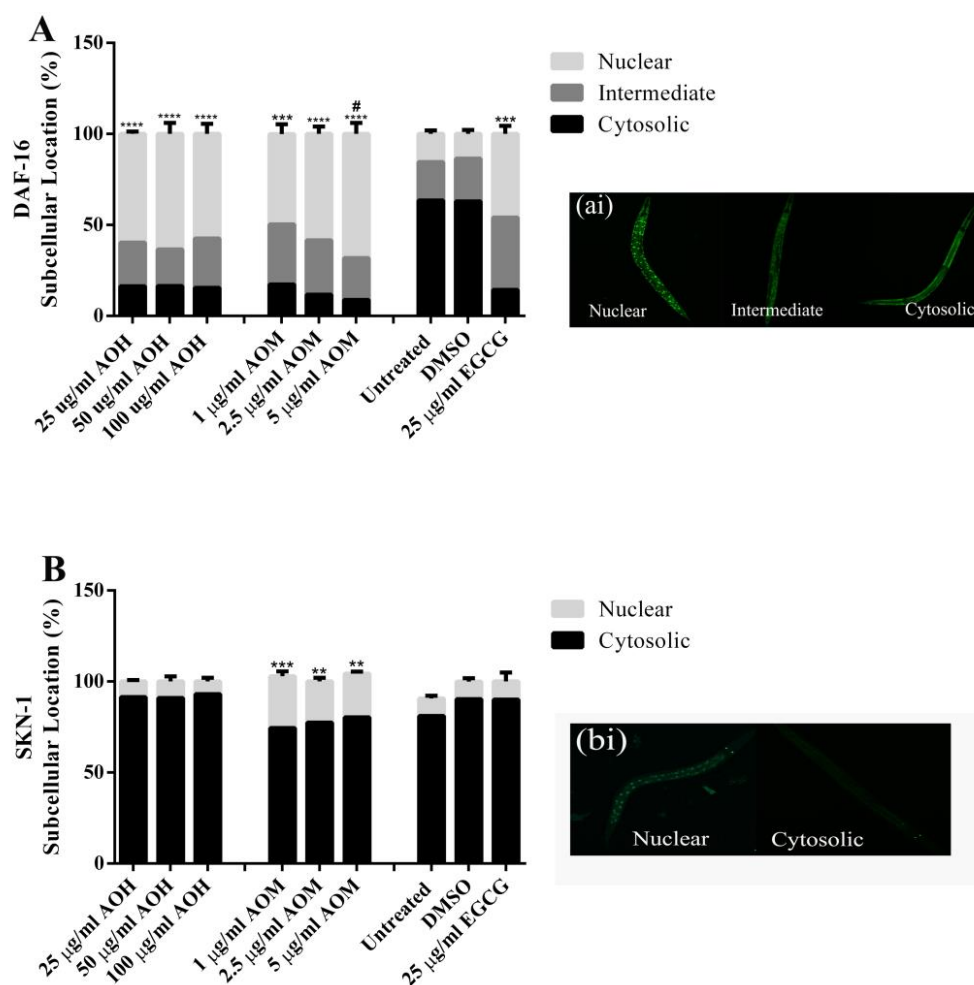


Figure 51. Effect of AO extracts on nuclear localization of DAF-16 and SKN-1.

AO extracts induced a significant translocation of DAF-16::GFP in mutant TJ356 worms [daf-16p::daf-16a/b::GFP + rol-6] after pre-treatment with the extract for 72 h (A). Representative fluorescent images of the subcellular location of DAF-16 in the nucleus, intermediate and cytosolic regions (Ai). AO extracts induced a significant translocation of SKN-1::GFP in mutant LD1 worms after pre-treatment with the extract for 72 h (B). Representative fluorescent images of the subcellular location of SKN-1 in the nucleus and cytosolic regions (Bi). The nuclear localizations of DAF-16 and SKN-1 when treated with the DMSO control were 13.56% and 1.50%, respectively.

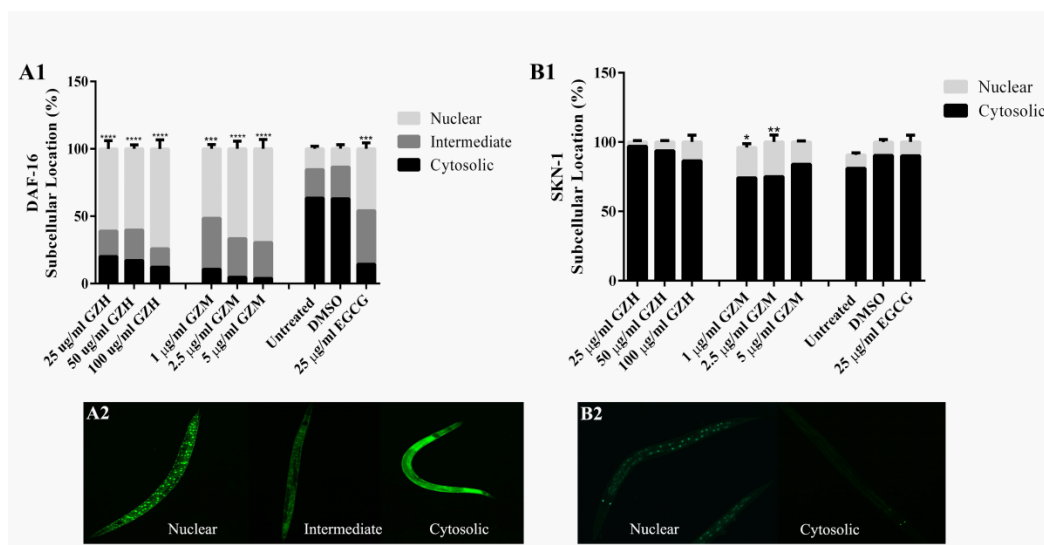


Figure 52. Effect of GZ extracts on nuclear localization of DAF-16 and SKN-1.

GZ extracts induced a significant translocation of DAF-16::GFP in mutant TJ356 worms [daf-16p::daf-16a/b::GFP + rol-6] after pre-treatment with the extract for 72 h (**A1**). Representative fluorescent images of the subcellular location of DAF-16 in the nucleus, intermediate and cytosolic regions (**A2**). GZ extracts induced a significant translocation of SKN-1::GFP in mutant LD1 worms after pre-treatment with the extract for 72 h (**B1**). Representative fluorescent images of the subcellular location of SKN-1 in the nucleus and cytosolic regions (**B2**). The nuclear localizations of DAF-16 and SKN-1 when treated with the DMSO control were 13.56% and 1.50%, respectively.

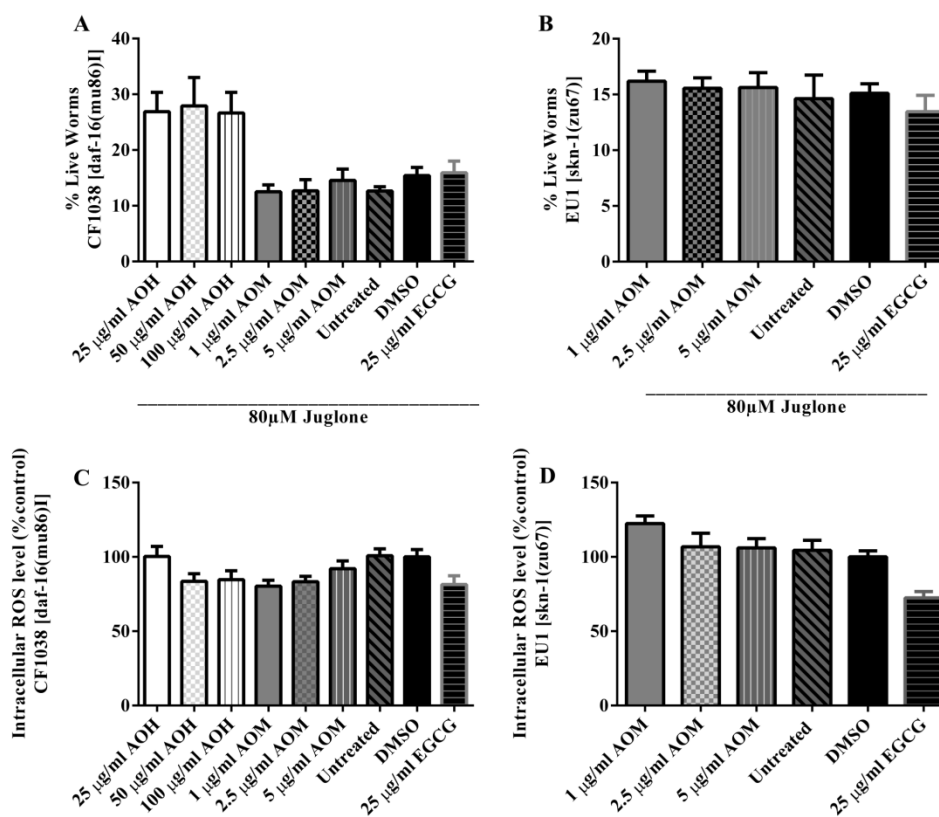


Figure 53. Effect of AO extracts on oxidative stress resistance properties of CF1038 and EU1 worms under oxidative stress induced by juglone.

The AO extracts failed to increase the survival rate (**AB**) and decrease intracellular ROS accumulation (**CD**) in CF1038 (**AC**) and EU1 (**BD**) worms. Worms were treated with AO hexane and methanol extracts at different concentrations. DMSO and EGCG were used as the solvent control and positive control groups. Data are presented as the mean \pm SEM ($n = 80$, replicated three times). ** $p < 0.01$ and *** $p < 0.001$, compared to the DMSO control by one-way ANOVA following Bonferroni's method (post hoc).

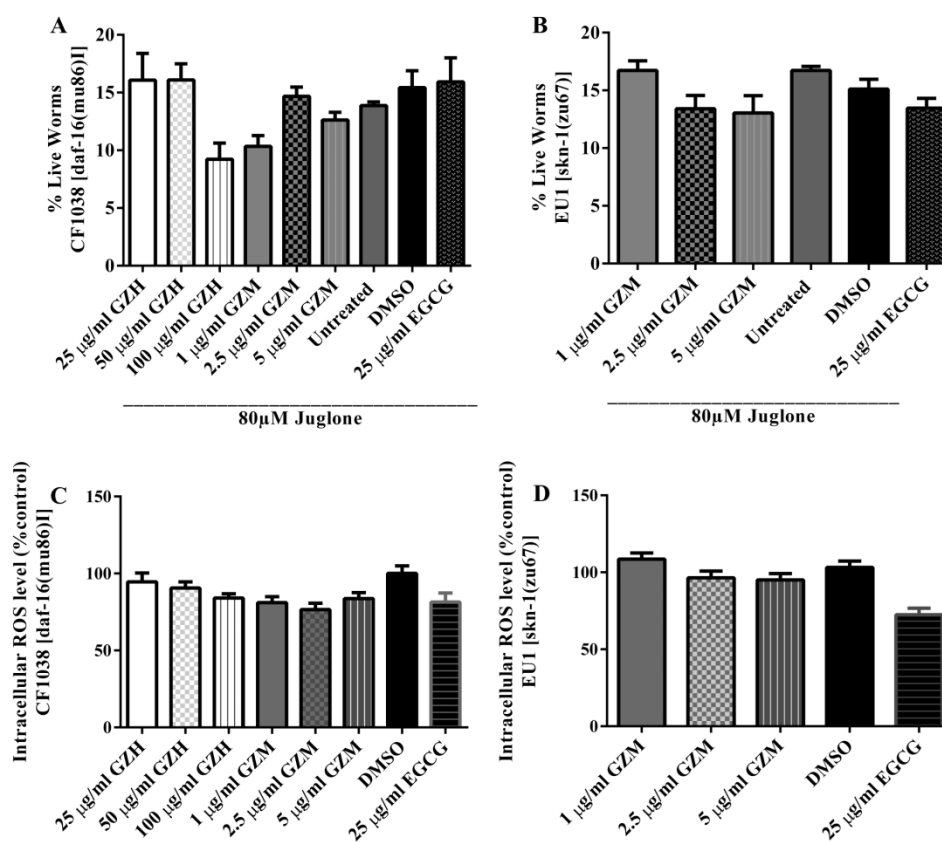


Figure 54. Effect of GZ extracts on oxidative stress resistance properties of CF1038 and EU1 worms under oxidative stress induced by juglone.

The GZ extracts failed to increase the survival rate (**AB**) and decrease intracellular ROS accumulation (**CD**) in CF1038 (**AC**) and EU1 (**BD**) worms. Worms were treated with GZ hexane and methanol extracts at different concentrations. DMSO and EGCG were used as the solvent control and positive control groups. Data are presented as the mean \pm SEM (n = 80, replicated three times). ** $p < 0.01$ and *** $p < 0.001$, compared to the DMSO control by one-way ANOVA following Bonferroni's method (post hoc).

4.7.6 Lifespan

To study whether the antioxidant effects of the extracts can influence longevity, the lifespan assay were explored in *Mev-1* mutants (TK22) (A mutation in succinate dehydrogenase cytochrome b causes oxidative stress and short lifespan) worms.

The AO and GZ extracts exhibited the lifespan extending effects in wild-type (N2) worms However, The AO and GZ extracts failed to extend the mean lifespan of TK22 worms (Figures 55). These data indicated that the lifespan extension effect of the extracts are likely not based on the oxidative stress resistance and antioxidant effect alone, the extracts may be influence longevity via the DAF-16 pathway.

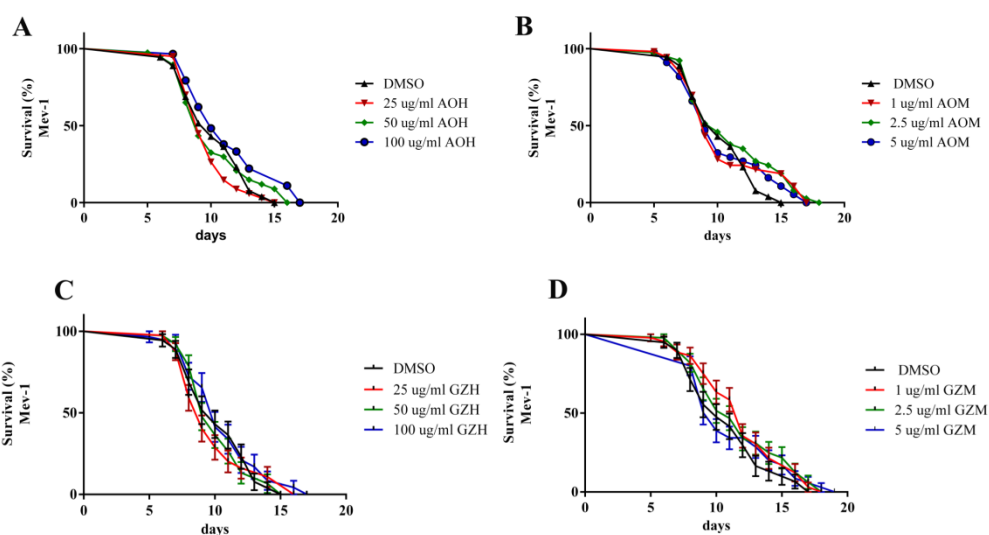


Figure 55. Effect of AO and GZ extracts on the lifespan of *mev-1* mutant worms

Survival curves of the worms at 20 °C on the plate treated with AOH (A), AOM (B), GZH (C) and GZM (D) at different concentrations. Survival plots were drawn by GraphPad Prism 6.0.

4.8 Neurite outgrowth properties and underlying mechanisms of AO and GZ extracts

4.8.1 Neurite outgrowth

To investigate the effect of the extracts on neurite outgrowth activity in Neuro-2a cells, the cells were maintained in a low-serum medium (DMEM supplemented with 1% FBS). The retinoic acid (RA) was used as a positive control. The Neuro-2a cells treated with 20-50 μM RA significantly increased neurite lengths and neurite bearing cells in a concentration-dependent manner ($p < 0.0001$) (Figure 56). Thus, the positive control concentration was chosen at 20 μM RA.

The Neuro-2a cells treated with 1 $\mu\text{g/mL}$ AOH extract significantly increased neurite lengths (23.36 μm) and neurite bearing cells (43.25%) when compared to the 1% FBS control (neurite length, 17.68 μm ; neurite bearing cells, 22.06%). The Neuro-2a cells treated with 10 $\mu\text{g/mL}$ AOM extract significantly increased neurite lengths (30.38 μm) and neurite bearing cells (54.06%) when compared to the 1% FBS control ($p < 0.0001$) (Figure 57). In addition, the Neuro-2a cells treated with 1 $\mu\text{g/mL}$ GZM extract significantly increased neurite lengths (30.91 μm) and neurite bearing cells (52.35%) when compared to the 1% FBS control ($p < 0.0001$) (Figure 58). The neurite outgrowth inducing effects were similar to those of 20 μM RA (neurite lengths: 25.59 μm and neurite bearing cells: 42.00%), which is a well-known inducer of neuronal differentiation [157]. RA is a differentiation-inducing molecule that inhibits cell proliferation. RA down regulated the expression of pro-proliferation transcription factors such as Notch signaling, *geminin*, and *zic1/2/3*, consequently induced neuronal differentiation [158]. To further confirm neurite outgrowth activities, GAP-43 expression, a marker of neurite outgrowth, was measured. The Neuro-2a cells treated with 1 $\mu\text{g/mL}$ AOH extract significantly increased GAP-43 expression (mRNA; 183% and protein; 42%) when compared to 1% FBS control ($p < 0.0001$). The Neuro-2a cells treated with 10 $\mu\text{g/mL}$ AOM extract significantly increased GAP-43 expression (mRNA; 197% and protein; 131%) when compared to 1% FBS control ($p < 0.0001$) (Figure 57). In addition, The Neuro-2a cells treated with 1 $\mu\text{g/mL}$ GZM extract significantly increased GAP-43 expression (mRNA; 273% and

protein; 192%) when compared to 1% FBS control ($p < 0.0001$) (Figure 58). Results suggest that AO extracts have an effect on neuriteogenesis in Neuro2a cells.

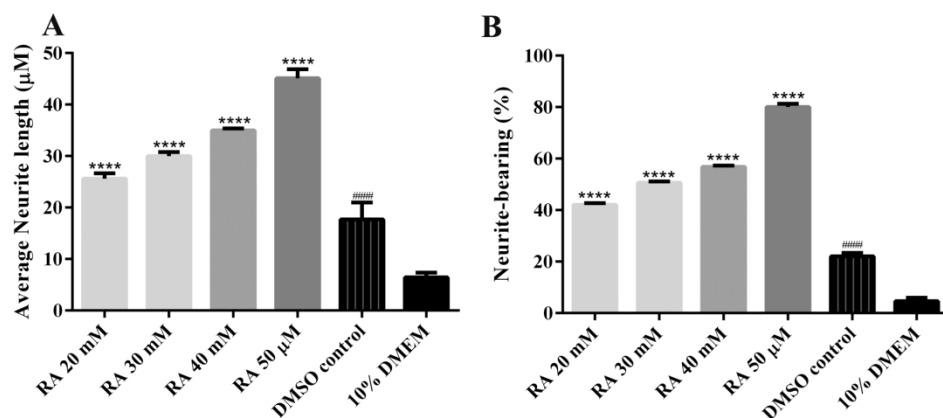


Figure 56. Effect of RA on neurite outgrowth.

RA treatment increased the average of neurite lengths (**A**) and the percentage of neurite-bearing cells (**B**) in Neuro-2a cells, in a dose dependent manner. All data were shown as the mean \pm SEM in at least three independent experiments. * $p < 0.05$, ** $p < 0.01$, *** $p < 0.001$ and **** $p < 0.0001$ compared to the 1% FBS control; ### $p < 0.001$ and #### $p < 0.0001$ compared to the 10% FBS control by one-way ANOVA following Bonferroni's method (post hoc).

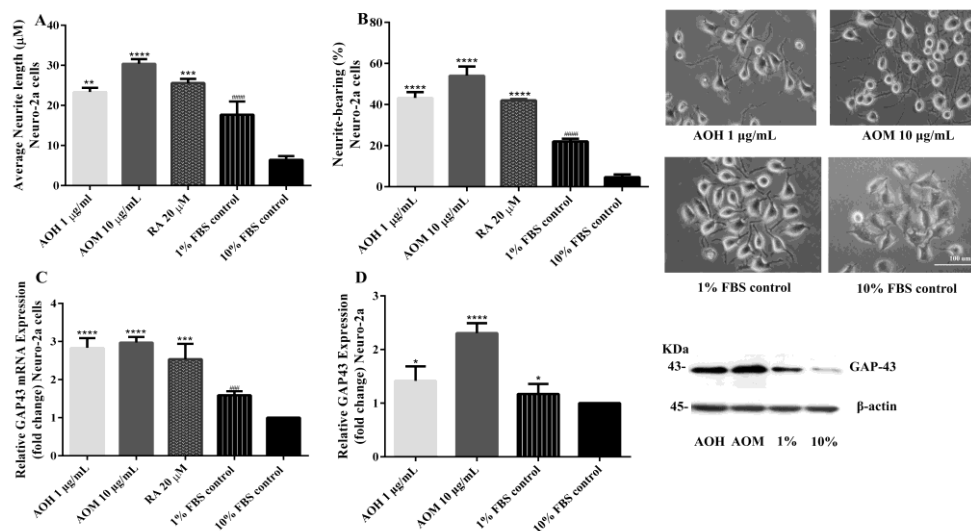


Figure 57. Effect of AO extracts on neurite outgrowth.

AO extract treatment increased the average of neurite lengths (A) and the percentage of neurite-bearing cells (B) in Neuro-2a cells. Cell morphology of Neuro-2a cells was observed under a microscope at 10×magnification. Neuro-2a cells in DMEM supplemented with 10% FBS showed a round shape without neurite extension, whereas Neuro-2a cells in DMEM supplemented with 1% FBS (serum-starved cells) appeared to increase neurite number and the length. Relative expression levels of mRNA (C) and protein (D) GAP-43 in Neuro-2a cells.

Whole-cell lysates were subjected to western blot analysis of the GAP43 level after AO extract treatment. β -actin was used as endogenous loading control for western blot assay and internal control for RT-PCR assay. All data were normalized to 10% FBS control level and shown as the mean \pm SEM in at least three independent experiments. $*p < 0.05$, $**p < 0.01$, $***p < 0.001$ and $****p < 0.0001$ compared to the 1% FBS control; $###p < 0.001$ and $####p < 0.0001$ compared to the 10% FBS control by one-way ANOVA following Bonferroni's method (post hoc).

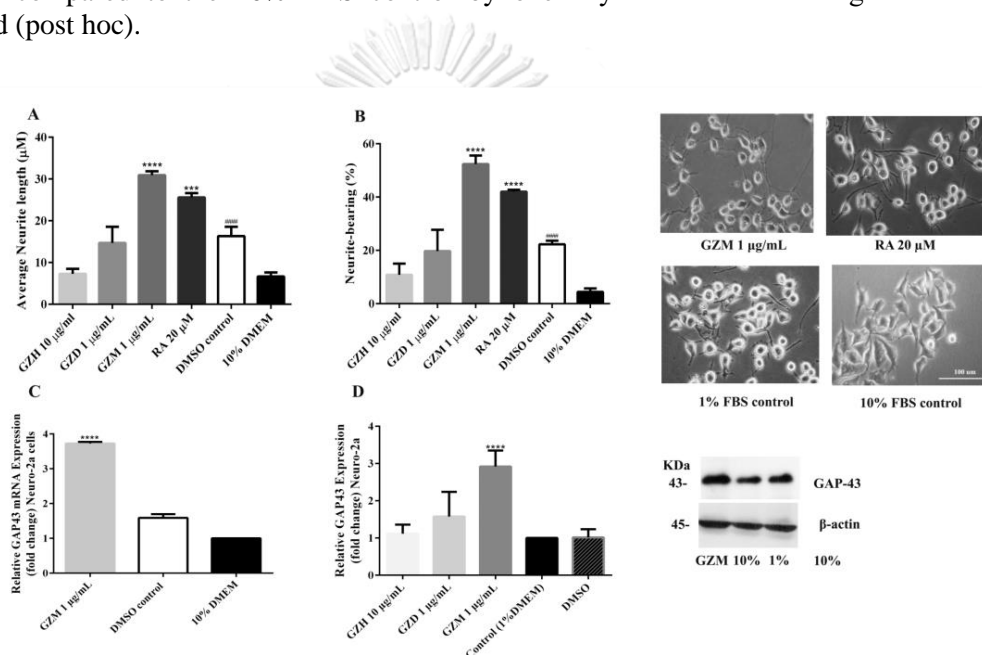


Figure 58. Effect of GZ extracts on neurite outgrowth.

GZ extract treatment increased the average of neurite lengths (A) and the percentage of neurite-bearing cells (B) in Neuro-2a cells. Cell morphology of Neuro-2a cells was observed under a microscope at 10×magnification. Relative expression levels of mRNA (C) and protein (D) GAP-43 in Neuro-2a cells.

Whole-cell lysates were subjected to western blot analysis of the GAP43 level after GZ extract treatment. β -actin was used as endogenous loading control for western blot assay and internal control for RT-PCR assay. All data were normalized to 10% FBS control level and shown as the mean \pm SEM in at least three independent experiments. $*p < 0.05$, $**p < 0.01$, $***p < 0.001$ and $****p < 0.0001$ compared to the 1% FBS control; $###p < 0.001$ and $####p < 0.0001$ compared to the 10% FBS control by one-way ANOVA following Bonferroni's method (post hoc).

4.8.2 Neurite outgrowth mechanisms (Teneurin 4)

To investigate whether Ten-4 expression is involved in the extracts-induced neurite growth in Neuro-2a cells, mRNA and protein expression levels of Ten-4 were examined. The Neuro-2a cells treated with 10 µg/mL AOM extract significantly increased expression of Ten-4 mRNA and protein levels by 447% and 109% when compared to the 10% FBS control ($p < 0.0001$). However, 1 µg/mL AOH was inactive (Figure 59). In addition, the Neuro-2a cells treated with 1 µg/mL GZM extract significantly increased expression of Ten-4 mRNA and protein levels by 335% and 186% when compared to the 10% FBS control ($p < 0.0001$) (Figure 60).

To confirm the role of Ten-4 in the methanol extracts-induced neurite outgrowth in Neuro-2a cells, Ten-4 siRNA (siTen-4) were used. Knockdown efficiency of siTen-4 was assessed by quantitative RT-PCR. The Neuro-2a cells treated with siTen-4 significantly decreased expression of Ten-4 mRNA expression by 62.23% compare to scrambled siRNA (si-control) ($p < 0.0001$) (Figure 18). After treated the cells with siScramble (siControl), the neurite length, neurite bearing cells and GAP-43 mRNA expression did not significantly different in the 1% FBS control (Figure 59-61). These data indicated that siRNA did not alter the normal systems of the cells. However, after treated the cells in 1% FBS with siTen-4, the neurite length, neurite bearing cells and GAP-43 mRNA expression significantly lower when compare with 1% FBS (without siTen4) (Figure 61). These results indicated that the Ten-4 siRNA knockdown influenced in neurite outgrowth in Neuro-2a cells. Thus, Teneurin 4 transmembrane protein may involve in neuritogenesis in Neuro-2a cells.

In normal condition (without siRNA), the Neuro-2a cells treated with 10 µg/mL AOM extract significantly increased neurite length neurite bearing cells, compare to 1% FBS control. However, when Ten-4 expression was knocked down by siTen-4, AOM failed to induce neurite length (18.09 µm) and neurite bearing cells (18.08 %) in Neuro-2a cells agreeing with GAP-43 expression (26% decreased) (Figure 59-60). In addition, when Ten-4 expression was knocked down by siTen-4, 1 µg/mL GZM extracts failed to induce neurite length (26.53 µm) and neurite bearing cells (35.80%) in Neuro-2a cells agreeing with GAP-43 expression (23% decreased) (Figure 59-60).

Taken together, the findings demonstrate that the methanol extracts promote neurite outgrowth in Neuro-2a cells mediated by the Teneurin-4 transmembrane protein.

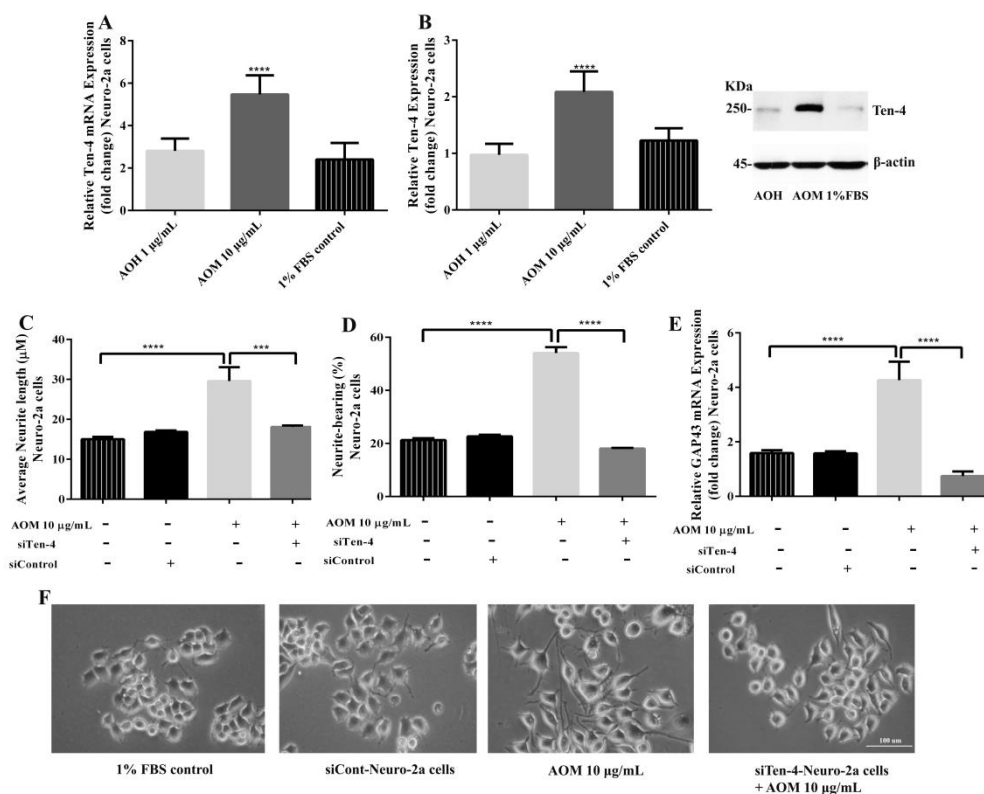


Figure 59. Effect of AO extracts on Ten-4-mediated neurite outgrowth.

AO methanol extract treatment increased expression level of Ten-4 mRNA (**A**) and protein (**B**). AO methanol extract failed to induced neurite length (**C**) and neurite-bearing cells (**D**) in siTen-4-Neuro-2a cells. Results were confirmed by GAP-43 mRNA expression (**E**). Cell morphology of Neuro-2a cells was observed under a microscope at 10× magnification (**F**).

Whole cell lysates were subjected to western blot analysis at the Ten-4 level after AO extract treatment. β-actin was used as endogenous loading control for western blot assay and internal control for RT-PCR assay. All data were normalized to 10% FBS control levels in siCont-Neuro-2a cells and shown as the mean ± SEM in at least three independent experiments. * $p < 0.05$, ** $p < 0.01$, *** $p < 0.001$ and **** $p < 0.0001$, compared to the 1% FBS control by one-way ANOVA following Bonferroni's method (post hoc).

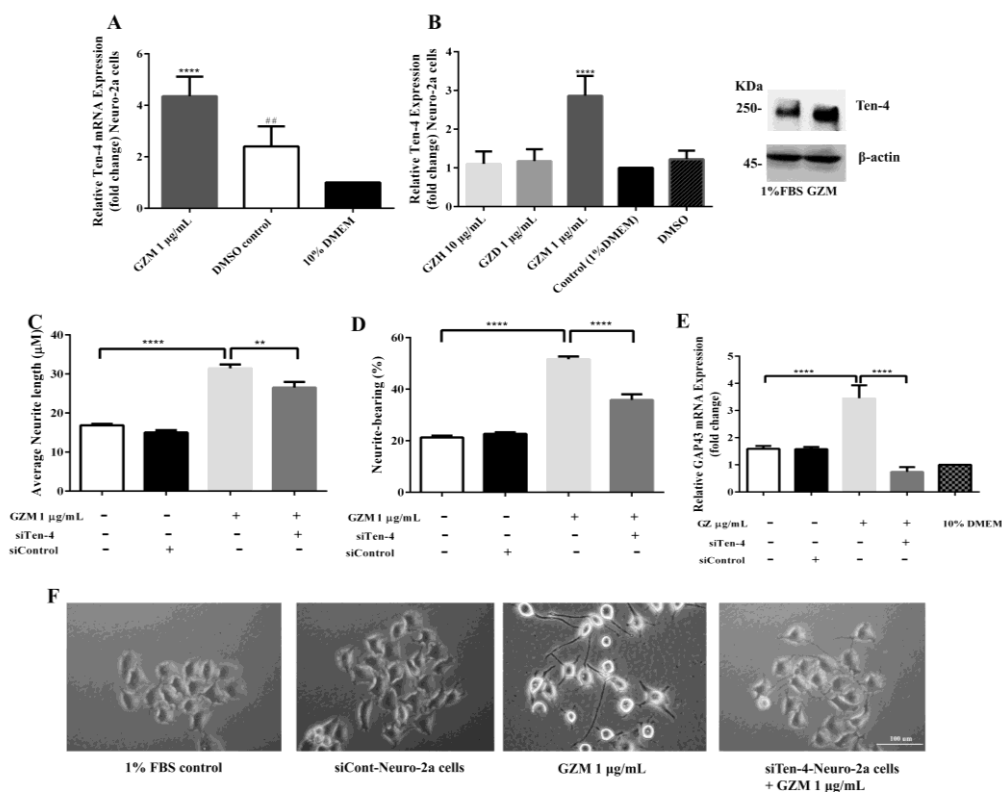


Figure 60. Effect of GZ extracts on Ten-4-mediated neurite outgrowth.

GZ methanol extract treatment increased expression level of Ten-4 mRNA (A) and protein (B). AO methanol extract failed to induce neurite length (C) and neurite-bearing cells (D) in siTen-4-Neuro-2a cells. Results were confirmed by GAP-43 mRNA expression (E). Cell morphology of Neuro-2a cells was observed under a microscope at 10× magnification (F).

Whole cell lysates were subjected to western blot analysis at the Ten-4 level after GZ extract treatment. β -actin was used as endogenous loading control for western blot assay and internal control for RT-PCR assay. All data were normalized to 10% FBS control levels in siCont-Neuro-2a cells and shown as the mean \pm SEM in at least three independent experiments. * $p < 0.05$, ** $p < 0.01$, *** $p < 0.001$ and **** $p < 0.0001$, compared to the 1% FBS control by one-way ANOVA following Bonferroni's method (post hoc).

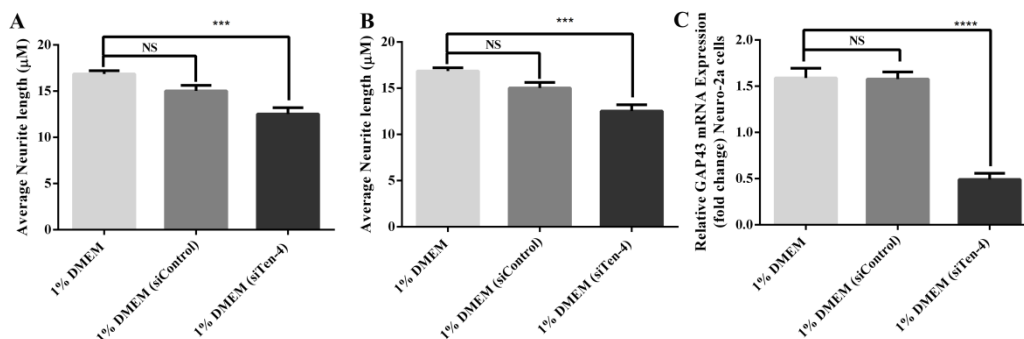


Figure 61. Effect of siTen-4-mediated neurite outgrowth.

Ten-4 siRNA knockdown influenced in neurite length (A) and neurite-bearing cells (B) neurite outgrowth in Neuro-2a cells. Results were confirmed by GAP-43 mRNA expression (C). β -actin was used as internal control for RT-PCR assay. All data were normalized to 10% FBS control and shown as the mean \pm SEM in at least three independent experiments. * p < 0.05, ** p < 0.01, *** p < 0.001 and **** p < 0.0001, compared to the 1% FBS control by one-way ANOVA following Bonferroni's method (post hoc).

CHAPTER V

DISCUSSION

Neurodegenerative diseases are brain pathologies which described progressive neuronal degeneration and neuronal cell death [42]. Neurodegeneration is an irreversible condition during aging which is the progressive loss of structure or function of neurons lead to neuronal death and cognitive abilities impairment in the functions of learning and memory [42, 93]. The most common of neurodegenerative diseases is Alzheimer's disease (AD) which is associated with mitochondrial dysfunction, neuro-inflammation, and oxidative stress [42]. Over the past decade, most of the research focused on oxidative stress mechanisms and its importance in neurodegenerative diseases [159]. Oxidative stress plays an essential role in neuronal cell damage and toxicity [85], which is a major factor in the progress of neurological disorders such as Alzheimer's disease (AD), and Parkinson's disease (PD) [160-162]. Glutamate, the main excitatory neurotransmitter in the brain, has been recognized as one initiating factor for several neurodegenerative disorders [9, 10]. High levels of glutamate activate structural degradation, ROS/RNS production, mitochondrial and DNA damage, which further lead to neurotoxicity and neuronal cell damage [9, 11]. Glutamate induced neuronal toxicity have been proposed in two pathways [80]. First, excitotoxicity, is mediated by over-stimulation of glutamate receptors resulting increased of extracellular Ca^{2+} influx [81]. Second, oxidative toxicity, is mediated by inhibition of cystine uptake, depletion of intracellular glutathione levels, induction reactive oxygen species (ROS) and NADPH oxidase-dependent extracellular hydrogen peroxide (H_2O_2) accumulation [82, 83]. In the central nervous system (CNS), H_2O_2 has caused lipid peroxidation, mitochondrial dysfunction, and DNA damage leading to neuronal dysfunction through the overproduction of intracellular ROS and malondialdehyde (MDA) [84]. H_2O_2 is one of the major ROSs associated with neurological damage induced by oxidative stress [85]. The excessive generation of reactive oxygen species (ROS) induced by glutamate and H_2O_2 leading to oxidative stress and neurotoxicity play a major role in a variety of neurodegenerative diseases, especially Alzheimer's disease (AD) [9, 12].

Neurogenesis describes the process of growth, survival, proliferation, differentiation and regeneration of neurons [4]. Impairment of neurogenesis affects neuronal differentiation and neuronal cell loss in various neurodegenerative disorders [4]. During neuronal differentiation, neurite outgrowth is an essential step for functional networks (connectome) of neurons. Regulation of neurite outgrowth can promote neuronal regeneration from nerve injury or neurological disorders which plays an important role in development of therapies for neurodegenerative diseases [5]. Millions of people around the world are currently affected by neurodegenerative diseases. As aging populations increase rapidly, the economic cost of neurodegenerative disease treatment is expected to grow rapidly as more people live longer [42]. Reduction of oxidative stress and induction of neuronal differentiation are the key parameters for neuroprotective effects. In particular, a number of natural medicinal plants have been studied in neuroprotective action against oxidative stress damage. The various phytochemicals found in edible plants have been reported for their therapeutic properties, to reduce the risk of neurological diseases and disorders induced by oxidative stress [42]. Plant-based medicine might provide an alternative treatment for neurodegenerative diseases [163]. An improvement of oxidative stress resistance and neuronal differentiation constitute key factors for neuroprotection. Thus, natural products from herbs or plant extracts with antioxidative and neuroprotective properties could provide an alternative approach to treat neurodegenerative diseases.

In the present study, we demonstrate apparent neuroprotective and neuritogenesis properties of the AO and GZ extracts in cultured neuronal (HT22 and Neuro-2a) cells as well as oxidative resistance properties and lifespan extending in *C. elegans* models. We reported the antioxidant properties of the extracts *In vitro*, in cell and *In vivo*. The AO and GZ methanol extracts exhibited powerful antioxidant activity *In vitro*. In accordance with the antioxidant activities, high phenolic and flavonoid contents were recorded from the methanol extracts. The AO hexane extract showed radical scavenging activity as determined by the ABTS assay but did not exhibit radical scavenging activity in DPPH assay. The ABTS assay can measure the scavenging activity of hydrophilic and hydrophobic substances. It is possible that

the scavenging activity of the AO hexane extract depends on some hydrophobic bioactive compounds in the AO hexane extract. The antioxidant properties may be due to the antioxidant bioactive compounds (flavonoid glycoside) which are found in AOM (gallic acid, catechin and quercetin) and GZM (gallic acid and catechin) leaf extracts. Flavonoids, polyphenolic substances in plants, contain structural diversity. The flavone skeleton in flavonoids contains two aromatic rings which are essential functions of antioxidants by deactivate reactive oxidants such as singlet molecular oxygen and ROS [164]. The antioxidant bioactive compounds (gallic acid, catechin and quercetin) of AO and GZ extracts may play an important role in antioxidant properties in this study. These results are consistent with previous researches that reported the antioxidant activities of *A. occidentale* leaf extracts [28, 38, 39] and the leaf extracts from *Glochidion* species [28, 165].

Oxidative stress is generated from glutamate and H₂O₂ induced-excessive ROS levels affect the neuronal cell survival. High levels of ROS activate neuronal structural degradation, e.g. protein, enzyme and nucleic acid, which further lead to neuron apoptosis, ageing or other neurological diseases [9, 11]. Excessive concentration of ROS can be scavenged by the antioxidant defense systems including enzymatic antioxidants (SODs, CAT, and GPx) and non-enzymatic antioxidants (GSH and NAD(P)H [166]) which are the antioxidant enzymes found in brain tissue for ROS detoxification [10]. The antioxidants which contain a potent action to interact with the ROS generated by glutamate/H₂O₂ or ROS detoxification are likely to prevent glutamate mediated neuronal cell death. In the present study, we found that the AO and GZ extracts exhibited neuroprotective effects against glutamate/H₂O₂-induced oxidative stress and toxicity in neuronal HT22 and Neuro-2a cells. Intracellular ROS level was significantly elevated in HT22 (approximately 1.7 fold) and Neuro-2a (approximately 1.9 fold) cells after exposure to glutamate, compared to the untreated control. Therefore, glutamate-induced cytotoxicity in neuronal (HT22 and Neuro-2a) cells was indeed associated with intracellular ROS increase. However, we found that the AO and GZ extracts significantly reduced the elevated levels of ROS in the same range as the quercetin positive control. These results suggest that the AO and GZ extracts protect against glutamate/H₂O₂-induced

cytotoxicity by suppressing intracellular ROS production. Moreover, we found that the treatment of the neuronal cells with the AO and GZ extracts markedly up-regulated the gene expressions of antioxidant enzymes, namely SOD, GPx and GSTs which are the ROS detoxification enzymes in brain tissue [10]. The neuroprotective effects of AO extracts may come from antioxidant bioactive compounds such as palmitic acid [167], α -linolenic acid [168], gallic acid [169], catechin [170], and quercetin [171] which have known neuroprotective properties in several studies.

Sirtuin 1 (SIRT1) is a class III histone deacetylases that plays an important role in cell physiological and biochemical processes, including aging, inflammation and neuroprotection [91]. SIRT1 regulates transcription factors including nuclear factor-E2-related factor 2 (Nrf2), which is a major regulator in antioxidant defenses [92]. Nrf2 translocates to the nucleus and activates the antioxidant response elements (AREs) in the promoter region of many antioxidant genes, including heme oxygenase (decycling) 1 (HMOX1), NAD(P)H:quinone oxidoreductase 1 (NQO1), glutamate cysteine ligase complex modifier subunit (GCLM), glutamate-cysteine ligase catalytic subunit (GCLC), and glutathione S-transferase pi 1 (GSTP1) [92, 93]. Neuroprotection role of Nrf2 against ROS generation is considered as a potential therapeutic target for neurodegenerative disorders such as Amyotrophic lateral sclerosis, Alzheimer's and Parkinson's disease [85]. Accumulating evidence suggest that SIRT1 and Nrf2 are involved in CNS redox balance of neurodegenerative disorders by promoting antioxidant responses [26, 27, 172]. In addition, enhancing SIRT1 and Nrf-2/HO-1 expression can protect neurons against oxidative injury in neuronal cells [27]. In the present study, we found that the AO and GZ methanol extracts promote antioxidant defense in Neuro-2a cells via the SIRT1-Nrf2 signaling pathway. Pretreatment with AOM, GZH and GZM extracts significantly increased the expressions of SIRT1 and Nrf2. Moreover, the AOM, GZH and GZM extracts also induced antioxidant-related target genes that are regulated by the SIRT1-Nrf2 signaling pathway including NQO1, GCLM, and EAAT3 in Neuro-2a cells. The recent studies demonstrated that phenolic antioxidants and aromatic compounds can activate ARE and induce the Nrf2/ARE signaling pathway [173], the AO and GZ methanol extracts contain phenolic (flavonoid glycoside) compounds including gallic

acid, catechin and quercetin. Thus the protective effects mediated by the SIRT1-Nrf2 signaling pathway may be due to the phenolic compounds in the AO and GZ methanol extracts. Taken together, the protective effect of the AO and GZ extracts against glutamate/H₂O₂-induced cytotoxicity was achieved not only by suppressing intracellular ROS production, but also through enhancing the expression of endogenous antioxidant enzymes in cultured neuronal (HT22 and Neuro-2a) cells. The present study demonstrated that the neuroprotective effects of the AO and GZ extracts mediated by the SIRT1-Nrf2 signaling pathway.

Neuritogenesis or neurite outgrowth is a process in the differentiation of neurons and plays a central role in neuronal development and formation of synapses [4]. The neurogenesis process impairment cause the neuronal cell loss and inability of neuronal differentiation, resulting forgetfulness, poor memory, anxiety, neuronal cell death and leading to various neurodegenerative diseases [4]. The induction of neuronal differentiation is one of the neuroprotective factors. In the present study, the AO and GZ extracts promoted neurite outgrowth in Neuro2a cells. These results agree with several recent studies regarding the neurodegeneration properties of α -linolenic acid [174], gallic acid [175], catechin [170] and quercetin [176, 177]. Teneurin-4 (Ten-4), a transmembrane protein, is highly expressed in the central nervous system and plays a role in neurogenesis. Ten-4 activate neurite outgrowth by activation of focal adhesion kinase (FAK) and Rho-family small GTPases, Cdc42 and Rac1 [178]. Moreover, Ten-4 expression regulated the formation of filopodia-like protrusion and neurite outgrowth of the Neuro-2a cells [8]. Recent study reported that herbal extract, *Mucuna pruriens*, increase neurite outgrowth dependent on Ten-4 expression [179]. In the present study, we found that the AO and GZ methanol extracts increased Ten-4 mRNA and protein levels in Neuro-2a cells. However, when Ten-4 expression was knocked down by siTen-4, The AO and GZ methanol extracts failed to induce neurite length and neurite bearing cells in Neuro-2a cells agreeing with GAP-43 expression. Taken together, the findings demonstrate that the AO and GZ methanol extracts promote neurite outgrowth in Neuro-2a cells mediated by the Teneurin-4 transmembrane protein.

The available evidences suggest that SIRT1 and Nrf2 are also involved in neuroprotection and neurogenesis [180, 181]. SIRT1 promotes nerve growth factor-induced neurite outgrowth by affects small GTPase cascades in the Ras GTPase family [181]. Previous results showed that the neuroprotective effects of the AO and GZ extracts mediated by the SIRT1-Nrf2 signaling pathway. It is possible that the neurogenesis effects of the AO and GZ methanol extract may be mediated by the SIRT1-Nrf2 signaling pathway. The evidence suggests that neurite outgrowth are inhibited by oxidative stress, involved in the neurotoxicity [182]. These data supported the hypothesis that neuroprotective and neuritogenesis properties of AO and GZ extracts may involve in the antioxidant activities. Nevertheless, further studies are needed to investigate the effects of the AO and GZ methanol extract on neurite outgrowth via the SIRT1-Nrf2 signaling pathway.

Long life and healthy aging depend on many fold interactions among biological and environmental factors. Aging is an inevitably natural process accompanied by accumulation of damaged macromolecules such as nucleic acids, lipids and proteins. Consequently, physiological characters changed such as increased oxidative stress and increased inflammation can negatively affect the quality of life [13]. Although the mechanisms of the aging process are not completely understood, increasing evidence suggests that aging is apparently associated with the bioactivity of reactive oxygen species (ROS). The protective effects of ROS are the strategy to delay aging and related degenerative diseases. Several lines of evidence previously reported that the reduction of ROS and low-grade inflammation can extend lifespan in a wide spectrum of model organisms [13, 14]. As people want to live longer and healthier, a healthy nutrition has been increasingly received much attention in recent years. Several studies reported a positive correlation between antioxidants in foods, drinks and longevity. A number of natural products have been reported to extend lifespan in *C. elegans*, such as a variety of antioxidant compounds [32, 33] including epigallocatechingallate [34], quercetin [35] or anthocyanins [36]. Therefore, natural products from food supplements and medicinal plants with antioxidant properties could be promising candidates for fighting against various aging-related diseases and promoting longevity.

The free-living soil nematode *C. elegans* has become a valuable model for studying genetic and pharmacological influences of ROS on health and longevity. *C. elegans* has a rapid reproduction rate, a short lifespan, and is easy to maintain [15]. Its genome has been completely sequenced, and various transgenic strains are available for experimental studies [16]. Importantly, *C. elegans* has conserved longevity and stress resistance genes that are homologous to human genes and thus can serve as a model for human aging processes [17]. Therefore, *C. elegans* has become a popular model organism to explore the potential anti-aging and stress resistance properties of natural compounds. To further extend our study, the oxidative stress resistance and anti-aging properties of the AO and GZ extracts were elucidated in *C. elegans* models. Natural compounds can represent novel anti-aging agents, and numerous studies have reported correlations between natural antioxidant compounds and anti-aging capacities [34, 35]. This study is the first report describing the anti-aging potential and oxidative stress resistance properties of the AO and GZ extracts observed in *C. elegans*.

In present study, we observed that the AO and GZ extracts can effectively protect *C. elegans* against severe oxidative stress and attenuate intracellular ROS levels at moderate concentrations [153, 154, 156]. In contrast, the higher concentrations of the AO extracts failed. It is possible that the AO extracts contain anacardic acid, which was reported to be toxic to melanoma cells, bacteria and insects at high doses [39, 183, 184]. We assumed that the plant extract might act as a pro-oxidant and need an optimal concentration to protect and decrease the ROS level in the worms [185]. HSPs represent a family of proteins involved in the sensor of oxidative stress function. In *C. elegans*, HSP-16.2 plays a key role in protecting against oxidative stress and ROS [186]. In present study, we observed that the AO and GZ extracts have a protective effect against oxidative stress because they reduce intracellular ROS accumulation and counteract the activity of juglone (observed via the reduction of HSP-16.2 expression) [153, 154, 156]. These abilities were similar to effects of the antioxidant agents such as EGCG [34] and anthocyanin-rich purple wheat extracts [187]. The insulin/IGF-1 signaling (IIS) pathway is one of the most well-known pathways studied in *C. elegans*, which is involved in the regulation of

nutrient level responses via the forkhead box O (FoxO) transcription factor and its downstream targets. The components of the IIS pathway are well-conserved, and are linked to longevity in *C. elegans* and humans as well [18]. In *C. elegans*, the FoxO transcription factor DAF-16 plays a role in metabolism, dauer formation, stress resistance and lifespan modulation [19, 20].

In addition, the transcriptional target genes of DAF-16, including superoxide dismutase-3 (SOD-3), catalase-1 (CTL-1), and small heat shock protein-16.2 (HSP-16.2), are key factors that contribute to mediating oxidative stress and heat shock stress response [21-23]. Under normal conditions, DAF-16/FoxO remains inactive in the cytosol until environmental conditions such as stress or certain ligands stimulate DAF-16/FoxO translocation from the cytoplasm to the nucleus, leading to the expression of various genes that contribute to stress response [21]. SOD-3 is an antioxidant enzyme that is activated by DAF-16; it mediates $O_2^{\bullet-}$ scavenging and balancing of ROS [36]. In present study, we observed that the AO and GZ extracts affected SOD-3 expression and stress resistance in *C. elegans* via the DAF-16/FoxO pathway [153, 154, 156]. These effects are similar to other polyphenols such as an anthocyanin-rich extract of purple wheat [188], an anthocyanin-rich extract of acai [36], and chlorophyll [189] which have also been shown to activate DAF-16/FoxO pathway in *C. elegans*.

The SKN-1/Nrf-2 signaling pathway, with the transcription factor SKN-1, is localized in the intestine. It is regulated and influenced by growth, nutrients, and metabolic signals in *C. elegans*. SKN-1 is also involved in acute stress response functions by regulating its downstream targets such as glutathione S-transferase 4 (GST-4), which is a phase II detoxification enzyme. Importantly, SKN-1 plays a central role in many regulatory pathways and interventions that extend lifespan in *C. elegans* [24]. A previous report suggests that both DAF-16 and SKN-1 promote stress resistance and, consequently, lifespan extension [25]. Glutathione (GSH), downstream targets of the SKN-1/Nrf-2 signaling pathway, protects against acute oxidative stress conditions [24]. In present study, we observed that the AO and GZ methanol extracts affected GST-4 expression and stress resistance in *C. elegans* via the SKN-1 signaling pathway [153, 154, 156]. The results are consistent with previous results about

neuroprotective effects of the AO and GZ extracts which involved in the SIRT1-Nrf2 signaling pathways in neuronal cells. Moreover, these effects are similar to some natural products including peptides from sesame and rose essential oils [190, 191]. Although the AO and GZ hexane extract did not affect SKN-1 nuclear localization, it induced GST-4 expression. It is possible that, GST-4 is activated by another transcription factor. These data were supported by Giel Detienne, showing that not only SKN-1 but also EOR-1, which is a transcription factor mediating the effects of the epidermal growth factor (EGF) pathway, can activate GST-4 [192].

C. elegans is a model widely used to analyze longevity and aging because of its rapid reproduction rate and a short lifespan [15]. In mammals, aging markers include muscle function decline, lipofuscin or aging pigment accumulation, and protein oxidative damage (carbonylation)[36, 193, 194]. In *C. elegans*, lipofuscin or autofluorescent pigment accumulation and pharyngeal pumping function are well known aging markers [193]. Importantly, the AO and GZ extracts could reduce the level of lipofuscin and improved the pharyngeal pumping rate in late adult worms [153, 154, 156], which had already been reported for EGCG [34, 195], anthocyanins [36], chlorophyll [189], caffeic acid, quercetin, and kaempferol [35, 150]. Aging can be influenced by dietary restriction (DR) [196]. We found that brood size and body length in wild-type worms (which would decrease under DR) were not affected by the AO and GZ extracts [153, 154, 156]. These data indicate that the effects of the AO and GZ extracts were not caused by DR. In addition, the AO and GZ extracts influenced longevity of the wild-type *C. elegans* under normal condition. In present study, we observed that the worms that were treated with 50 µg/mL AOH extract, 1 µg/mL AOM extract, 100 µg/mL GZH and 1.0 and 5 µg/mL GZM had a significantly longer mean lifespan than wild-type worms. However, the AO and GZ extracts failed to extend the mean lifespan of mev-1 mutant worms (TK22), which showed a shortened lifespan [153, 154, 156]. These effects were similar to those seen in some other natural products such as chlorophyll [189] and natural lignans from *Arctium lappa* [185], indicating that the lifespan extension effect is likely not based on the oxidative stress resistance and antioxidant effect alone. This result strongly suggests that endogenous signaling pathways other than a direct antioxidant mechanism are

involved. Stress resistance and lifespan extension are mostly dependent on the DAF-16/FoxO-dependent pathway [20]. The AO and GZ extracts can increase both DAF-16/FoxO and SKN-1 gene expression, which belong to the insulin/IGF-1 signaling (IIS) longevity pathway in *C. elegans*. The transcription factors DAF-16 and SKN-1 are part of the modulators for lifespan extension in *C. elegans*. Thus, the AO and GZ extracts may extend lifespan via the DAF-16 pathway. However, the underlying mechanism through which the AO and GZ extracts affect the lifespan extension of *C. elegans* needs further study.

To our knowledge, this study is the first report about the bioactive compounds (flavonoid glycoside) in the AO and GZ leaf extracts. Flavonoid rich plant extracts and quercetin can extend the lifespan, reduce lipofuscin accumulation and protect worms against oxidative stress by reducing internal oxidative stress and intracellular ROS in *C. elegans* [35, 150, 152]. These data support our result that the AO and GZ extracts modulate oxidative stress resistance and lifespan extension in *C. elegans*. Moreover, phytochemical analysis shows that the AO and GZ hexane extract contains palmitic acid, α -linolenic acid and β -caryophyllene [153, 154, 156]. Previous works have reported that α -linolenic acid can recover pharyngeal pumping and increase lifespan in *C. elegans* via the SKN-1 signaling pathway [197, 198], and β -caryophyllene can modulate the stress response by reducing intracellular free radical levels and influencing feeding behavior and pharyngeal pumping rate, as well as reducing intestinal lipofuscin levels and increasing the lifespan in *C. elegans* via SIR-2.1, SKN-1 and DAF-16 [199]. These findings suggest that the AO and GZ extracts enhance the oxidative stress resistance through the DAF-16/FoxO and SKN-1/Nrf2 signaling pathways. Since it is known that healthspan and lifespan effects are highly correlated [185], the AO and GZ extracts may mediate both effects via the DAF-16/FoxO and SKN-1/Nrf2 signaling pathways. However, further studies are needed to elucidate the underlying mechanisms of the AO and GZ extracts on the lifespan extension of *C. elegans*.

CHAPTER VI

CONCLUSION

6.1 Conclusion

In summary, this study is the first report about the phytochemical composition of *A. occidentale* and *G. zeylanicum* along with neuroprotective, neuritogenesis, antioxidant and anti-aging effects *In vitro* and *In vivo*. These findings demonstrate the neuroprotective effects against glutamate/H₂O₂-induced oxidative stress and toxicity of the AO and GZ extracts in neuronal cells. Extracts neuroprotection were mediated via inhibition of ROS accumulation, up-regulation of endogenous antioxidant enzymes, and the increase of the SIRT1-Nrf2 signaling pathway. The AO and GZ extracts promoted neurite outgrowth via the up-regulation of Ten-4 expression. Moreover, the AO and GZ extracts demonstrated oxidative stress resistant properties via DAF-16/FOXO and SKN-1/Nrf-2 signaling pathway. The extracts at moderate concentrations can increase the survival rate of nematodes under oxidative stress, possibly attenuating intracellular ROS level and inducing stress response genes, such as SOD-3 and GST-4. The AO and GZ extracts exhibited anti-aging effects by pharyngeal pumping improvement and autofluorescent pigment attenuation. The AO and GZ extracts also can increase the mean lifespan of wild-type *C. elegans* under normal conditions. Since oxidative stress plays a role in many diseases and contributes to aging, the AO and GZ leaf extracts may lead to production of a new supplement drug against oxidative stress and aging in the near future. However, further studies and *In vivo* tests with more complex model organisms are required to elucidate the mechanisms to support the therapeutic potential of the plant extracts for alternative treatment age-related neurodegenerative disorders or as an anti-aging agent.

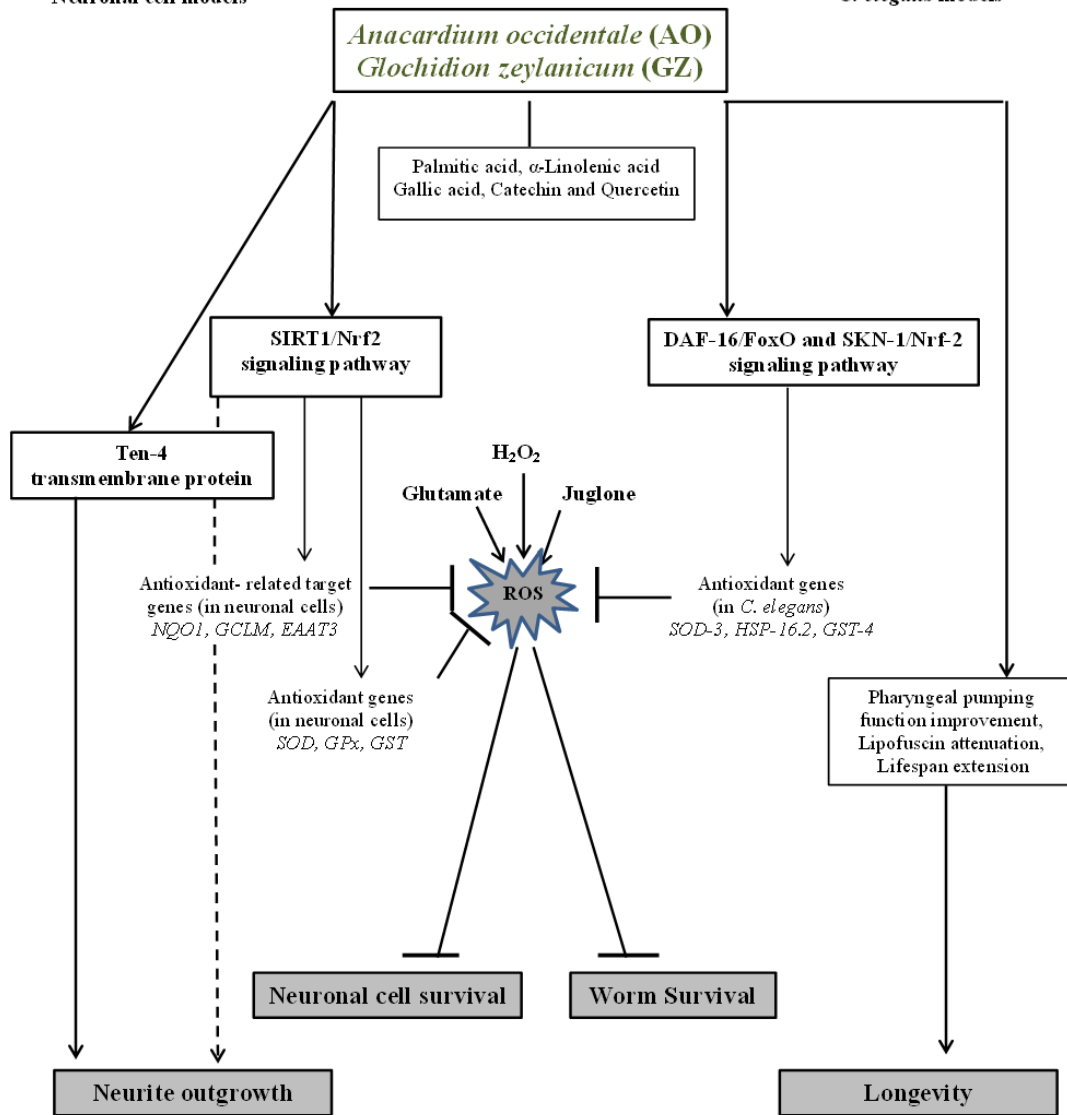


Figure 62. Effects and underlying mechanisms of *Anacardium occidentale* and *Glochidion zeylanicum* leaf extracts on neuroprotective, neuritogenesis, oxidative stress resistance and anti-aging properties *in vitro* and *in vivo* models.

6.2 Benefits of the study

The present study proposed the Thai plants AO and GZ, as promising natural products for neuroprotective, neurite outgrowth promoting, anti-oxidative stress anti-aging agents that further support the alternative treatment of age-related neurodegenerative diseases. This finding may help to increase the commercial value of Thai plants, as well as to support the new natural product for recovering the aging and neurodegenerative disorders in the near future.

6.3 Limitations of the study

The HT-22 cell line which was sensitive with glutamate toxicity and used as *In vitro* model of neurodegeneration in the present study is limited to only some neurodegenerative diseases such as AD. The gene expression assay in *C. elegans* models, which were determined by a GFP reporter is limited to identify the quantitative gene expression, RT-PCR and Western blott analysis are required to identify the specificity and accuracy of gene and protein expressions. Moreover, the TK22 worm that highly sensitive with the environment, is limited to identify the lifespan assay under Mev-1 mutants induced-oxidative stress and short lifespan.

REFERENCES



จุฬาลงกรณ์มหาวิทยาลัย
CHULALONGKORN UNIVERSITY

1. Nussbaum, R.L. and C.E. Ellis *Alzheimer's Disease and Parkinson's Disease*. New England Journal of Medicine, 2003. **348**(14): p. 1356-1364.
2. Ferri, C.P., et al., *Global prevalence of dementia: a Delphi consensus study*. Lancet, 2005. **366**(9503): p. 2112-2117.
3. Xu, T.-H., et al., *Alzheimer's disease-associated mutations increase amyloid precursor protein resistance to γ -secretase cleavage and the $A\beta_{42}/A\beta_{40}$ ratio*. Cell Discovery, 2016. **2**: p. 16026.
4. Lam, C.T., et al., *Jujube-containing herbal decoctions induce neuronal differentiation and the expression of anti-oxidant enzymes in cultured PC12 cells*. J Ethnopharmacol, 2016. **188**: p. 275-83.
5. Bonaterra, G.A., et al., *Neurotrophic, Cytoprotective, and Anti-inflammatory Effects of St. John's Wort Extract on Differentiated Mouse Hippocampal HT-22 Neurons*. Frontiers in pharmacology, 2018. **8**: p. 955-955.
6. Erturk, A., et al., *Disorganized microtubules underlie the formation of retraction bulbs and the failure of axonal regeneration*. J Neurosci, 2007. **27**(34): p. 9169-80.
7. Lehmann, M., et al., *Inactivation of Rho signaling pathway promotes CNS axon regeneration*. J Neurosci, 1999. **19**(17): p. 7537-47.
8. Suzuki, N., et al., *Teneurin-4 promotes cellular protrusion formation and neurite outgrowth through focal adhesion kinase signaling*. Faseb j, 2014. **28**(3): p. 1386-97.
9. Jin, M.L., et al., *The neuroprotective effects of cordycepin inhibit glutamate-induced oxidative and ER stress-associated apoptosis in hippocampal HT22 cells*. Neurotoxicology, 2014. **41**: p. 102-11.
10. Sukprasansap, M., P. Chanvorachote, and T. Tencomnao, *Cleistocalyx nervosum var. paniala berry fruit protects neurotoxicity against endoplasmic reticulum stress-induced apoptosis*. Food Chem Toxicol, 2017. **103**: p. 279-288.
11. Hirata, Y., et al., *Novel oxindole derivatives prevent oxidative stress-induced cell death in mouse hippocampal HT22 cells*. Neuropharmacology, 2018. **135**: p. 242-252.
12. Mittal, M., et al., *Reactive oxygen species in inflammation and tissue injury*. Antioxid Redox Signal, 2014. **20**(7): p. 1126-67.
13. Si, H. and D. Liu, *Dietary antiaging phytochemicals and mechanisms associated with prolonged survival*. J Nutr Biochem, 2014. **25**(6): p. 581-91.
14. Robert, L. and J. Labat-Robert, *Stress in biology and medicine, role in aging*. Pathologie Biologie, 2015. **63**(4): p. 230-234.
15. Lee, E.B., et al., *Lifespan Extending and Stress Resistant Properties of Vitexin from Vigna angularis in Caenorhabditis elegans*. Biomol Ther (Seoul), 2015. **23**(6): p. 582-9.
16. Chondrogianni, N., et al., *Proteasome activation: An innovative promising approach for delaying aging and retarding age-related diseases*. Ageing Res Rev, 2015. **23**(Pt A): p. 37-55.
17. Feng, S., et al., *Thermal stress resistance and aging effects of Panax notoginseng polysaccharides on Caenorhabditis elegans*. Int J Biol Macromol, 2015. **81**: p. 188-94.

18. Braeckman, B.P., K. Houthoofd, and J.R. Vanfleteren, *Insulin-like signaling, metabolism, stress resistance and aging in Caenorhabditis elegans*. Mech Ageing Dev, 2001. **122**(7): p. 673-93.
19. Jensen, V.L., M. Gallo, and D.L. Riddle, *Targets of DAF-16 involved in Caenorhabditis elegans adult longevity and dauer formation*. Exp Gerontol, 2006. **41**(10): p. 922-7.
20. Daitoku, H. and A. Fukamizu, *FOXO transcription factors in the regulatory networks of longevity*. J Biochem, 2007. **141**(6): p. 769-74.
21. Murphy, C.T., et al., *Genes that act downstream of DAF-16 to influence the lifespan of Caenorhabditis elegans*. Nature, 2003. **424**(6946): p. 277-83.
22. Lee, S.S., et al., *DAF-16 target genes that control C. elegans life-span and metabolism*. Science, 2003. **300**(5619): p. 644-7.
23. McElwee, J., K. Bubb, and J.H. Thomas, *Transcriptional outputs of the Caenorhabditis elegans forkhead protein DAF-16*. Aging Cell, 2003. **2**(2): p. 111-21.
24. Blackwell, T.K., et al., *SKN-1/Nrf, stress responses, and aging in Caenorhabditis elegans*. Free Radic Biol Med, 2015. **88**(Pt B): p. 290-301.
25. Tullet, J.M.A., et al., *The SKN-1/Nrf2 transcription factor can protect against oxidative stress and increase lifespan in C. elegans by distinct mechanisms*. Aging Cell, 2017. **16**(5): p. 1191-1194.
26. Lim, J.L., et al., *Antioxidative defense mechanisms controlled by Nrf2: state-of-the-art and clinical perspectives in neurodegenerative diseases*. Arch Toxicol, 2014. **88**(10): p. 1773-86.
27. Gao, X.Y., et al., *Gartanin Protects Neurons against Glutamate-Induced Cell Death in HT22 Cells: Independence of Nrf-2 but Involvement of HO-1 and AMPK*. Neurochem Res, 2016. **41**(9): p. 2267-77.
28. Kongkachuichai, R., et al., *Nutrients value and antioxidant content of indigenous vegetables from Southern Thailand*. Food Chem, 2015. **173**: p. 838-46.
29. Thang, T.D., et al., *Chemical constituents of the leaves of Glochidion obliquum and their bioactivity*. Archives of Pharmacal Research, 2011. **34**(3): p. 383-389.
30. Krishnaiah, D., R. Sarbatly, and R. Nithyanandam, *A review of the antioxidant potential of medicinal plant species*. Food and Bioproducts Processing, 2011. **89**(3): p. 217-233.
31. Tanaka, R., et al., *Potential anti-tumor promoting activity of lupane-type triterpenoids from the stem bark of Glochidion zeylanicum and Phyllanthus flexuosus*. Planta Med, 2004. **70**(12): p. 1234-6.
32. Melov, S., et al., *Extension of life-span with superoxide dismutase/catalase mimetics*. Science, 2000. **289**(5484): p. 1567-9.
33. Harrington, L.A. and C.B. Harley, *Effect of vitamin E on lifespan and reproduction in Caenorhabditis elegans*. Mech Ageing Dev, 1988. **43**(1): p. 71-8.
34. Abbas, S. and M. Wink, *Epigallocatechin gallate from green tea (Camellia sinensis) increases lifespan and stress resistance in Caenorhabditis elegans*. Planta Med, 2009. **75**(3): p. 216-21.

35. Kampkotter, A., et al., *Increase of stress resistance and lifespan of Caenorhabditis elegans by quercetin*. Comp Biochem Physiol B Biochem Mol Biol, 2008. **149**(2): p. 314-23.
36. Peixoto, H., et al., *An Anthocyanin-Rich Extract of Acai (Euterpe precatoria Mart.) Increases Stress Resistance and Retards Aging-Related Markers in Caenorhabditis elegans*. J Agric Food Chem, 2016. **64**(6): p. 1283-90.
37. Moosavi, F., et al., *Modulation of neurotrophic signaling pathways by polyphenols*. Drug Des Devel Ther, 2016. **10**: p. 23-42.
38. Baptista, A., et al., *Antioxidant and Antimicrobial Activities of Crude Extracts and Fractions of Cashew (Anacardium occidentale L.), Cajui (Anacardium microcarpum), and Pequi (Caryocar brasiliense C.): A Systematic Review*. Oxid Med Cell Longev, 2018. **2018**: p. 3753562.
39. Souza, N.C., et al., *Antioxidant and Anti-Inflammatory Properties of Anacardium occidentale Leaf Extract*. Evid Based Complement Alternat Med, 2017. **2017**: p. 2787308.
40. Park, S.J., et al., *Emodin induces neurite outgrowth through PI3K/Akt/GSK-3beta-mediated signaling pathways in Neuro2a cells*. Neurosci Lett, 2015. **588**: p. 101-7.
41. Link, P., et al., *Carlina acaulis Exhibits Antioxidant Activity and Counteracts Abeta Toxicity in Caenorhabditis elegans*. Molecules, 2016. **21**(7).
42. Perez-Hernandez, J., et al., *A Potential Alternative against Neurodegenerative Diseases: Phytodrugs*. Oxid Med Cell Longev, 2016. **2016**: p. 8378613.
43. de Magalhaes, J.P., *How ageing processes influence cancer*. Nat Rev Cancer, 2013. **13**(5): p. 357-65.
44. Manayi, A., et al., *Methods for the discovery of new anti-aging products--targeted approaches*. Expert Opin Drug Discov, 2014. **9**(4): p. 383-405.
45. Dato, S., et al., *The impact of nutrients on the aging rate: A complex interaction of demographic, environmental and genetic factors*. Mech Ageing Dev, 2016. **154**: p. 49-61.
46. Chen, W., et al., *Ameliorative effect of aspalathin from rooibos (Aspalathus linearis) on acute oxidative stress in Caenorhabditis elegans*. Phytomedicine, 2013. **20**(3-4): p. 380-6.
47. Corral-Debrinski, M., et al., *Mitochondrial DNA deletions in human brain: regional variability and increase with advanced age*. Nat Genet, 1992. **2**(4): p. 324-9.
48. Harman, D., *Aging: a theory based on free radical and radiation chemistry*. J Gerontol, 1956. **11**(3): p. 298-300.
49. Dillon, L.M., et al., *Increased mitochondrial biogenesis in muscle improves aging phenotypes in the mtDNA mutator mouse*. Hum Mol Genet, 2012. **21**(10): p. 2288-97.
50. Longo, V.D., et al., *Interventions to Slow Aging in Humans: Are We Ready?* Aging Cell, 2015. **14**(4): p. 497-510.
51. Fontana, L., L. Partridge, and V.D. Longo, *Extending healthy life span--from yeast to humans*. Science, 2010. **328**(5976): p. 321-6.
52. Failla, M.L., *Trace elements and host defense: recent advances and continuing challenges*. J Nutr, 2003. **133**(5 Suppl 1): p. 1443s-7s.

53. Santoro, A., et al., *Combating inflammaging through a Mediterranean whole diet approach: the NU-AGE project's conceptual framework and design*. Mech Ageing Dev, 2014. **136-137**: p. 3-13.
54. Darnton-Hill, I., C. Nishida, and W.P. James, *A life course approach to diet, nutrition and the prevention of chronic diseases*. Public Health Nutr, 2004. **7(1a)**: p. 101-21.
55. Darmon, N. and A. Drewnowski, *Does social class predict diet quality?* Am J Clin Nutr, 2008. **87(5)**: p. 1107-17.
56. Tahirovic, S. and F. Bradke, *Neuronal Polarity*. Cold Spring Harbor Perspectives in Biology, 2009. **1(3)**: p. a001644.
57. Cotta-Grand, N., et al., *Melanin-concentrating hormone induces neurite outgrowth in human neuroblastoma SH-SY5Y cells through p53 and MAPKinase signaling pathways*. Peptides, 2009. **30(11)**: p. 2014-24.
58. Lestanova, Z., et al., *Oxytocin Increases Neurite Length and Expression of Cytoskeletal Proteins Associated with Neuronal Growth*. J Mol Neurosci, 2016. **59(2)**: p. 184-92.
59. Krug, A.K., et al., *Evaluation of a human neurite growth assay as specific screen for developmental neurotoxicants*. Arch Toxicol, 2013. **87(12)**: p. 2215-31.
60. Hyman, C., et al., *BDNF is a neurotrophic factor for dopaminergic neurons of the substantia nigra*. Nature, 1991. **350(6315)**: p. 230-2.
61. Hetman, M. and A. Gozdz, *Role of extracellular signal regulated kinases 1 and 2 in neuronal survival*. Eur J Biochem, 2004. **271(11)**: p. 2050-5.
62. Riccio, A., et al., *An NGF-TrkA-Mediated Retrograde Signal to Transcription Factor CREB in Sympathetic Neurons*. Science, 1997. **277(5329)**: p. 1097.
63. Ginty, D.D. and R.A. Segal, *Retrograde neurotrophin signaling: Trk-ing along the axon*. Current Opinion in Neurobiology, 2002. **12(3)**: p. 268-274.
64. Moustafa, K., et al., *MAPK cascades and major abiotic stresses*. Plant Cell Rep, 2014. **33(8)**: p. 1217-25.
65. Komis, G., et al., *Microtubules and mitogen-activated protein kinase signalling*. Curr Opin Plant Biol, 2011. **14(6)**: p. 650-7.
66. Read, D.E. and A.M. Gorman, *Involvement of Akt in neurite outgrowth*. Cellular and Molecular Life Sciences, 2009. **66(18)**: p. 2975-2984.
67. Chai, L., et al., *Scutellarin and caffeic acid ester fraction, active components of Dengzhanxixin injection, upregulate neurotrophins synthesis and release in hypoxia/reoxygenation rat astrocytes*. J Ethnopharmacol, 2013. **150(1)**: p. 100-7.
68. Lonze, B.E. and D.D. Ginty, *Function and regulation of CREB family transcription factors in the nervous system*. Neuron, 2002. **35(4)**: p. 605-23.
69. Heiser, J.H., et al., *TRPC6 channel-mediated neurite outgrowth in PC12 cells and hippocampal neurons involves activation of RAS/MEK/ERK, PI3K, and CAMKIV signaling*. J Neurochem, 2013. **127(3)**: p. 303-13.
70. Fujita, Y., A. Sato, and T. Yamashita, *Brimonidine promotes axon growth after optic nerve injury through Erk phosphorylation*. Cell Death Dis, 2013. **4**: p. e763.

71. Zhou, C., et al., *BIG1, a brefeldin A-inhibited guanine nucleotide-exchange protein regulates neurite development via PI3K-AKT and ERK signaling pathways*. Neuroscience, 2013. **254**: p. 361-8.
72. Zhao, J., et al., *Botanical drug puerarin coordinates with nerve growth factor in the regulation of neuronal survival and neuritogenesis via activating ERK1/2 and PI3K/Akt signaling pathways in the neurite extension process*. CNS Neurosci Ther, 2015. **21**(1): p. 61-70.
73. Tang, G., et al., *A natural diarylheptanoid promotes neuronal differentiation via activating ERK and PI3K-Akt dependent pathways*. Neuroscience, 2015. **303**: p. 389-401.
74. Nishizuka, Y., *Protein kinase C and lipid signaling for sustained cellular responses*. Faseb j, 1995. **9**(7): p. 484-96.
75. Izumi, Y., et al., *An atypical PKC directly associates and colocalizes at the epithelial tight junction with ASIP, a mammalian homologue of Caenorhabditis elegans polarity protein PAR-3*. J Cell Biol, 1998. **143**(1): p. 95-106.
76. Shi, S.H., L.Y. Jan, and Y.N. Jan, *Hippocampal neuronal polarity specified by spatially localized mPar3/mPar6 and PI 3-kinase activity*. Cell, 2003. **112**(1): p. 63-75.
77. Nishimura, T., et al., *PAR-6-PAR-3 mediates Cdc42-induced Rac activation through the Rac GEFs STEF/Tiam1*. Nat Cell Biol, 2005. **7**(3): p. 270-7.
78. Shi, S.H., et al., *APC and GSK-3beta are involved in mPar3 targeting to the nascent axon and establishment of neuronal polarity*. Curr Biol, 2004. **14**(22): p. 2025-32.
79. Zhang, J., et al., *The impact of next-generation sequencing on genomics*. J Genet Genomics, 2011. **38**(3): p. 95-109.
80. Lau, A. and M. Tymianski, *Glutamate receptors, neurotoxicity and neurodegeneration*. Pflugers Arch, 2010. **460**(2): p. 525-42.
81. Mehta, A., et al., *Excitotoxicity: bridge to various triggers in neurodegenerative disorders*. Eur J Pharmacol, 2013. **698**(1-3): p. 6-18.
82. Ha, J.S., H.M. Lim, and S.S. Park, *Extracellular hydrogen peroxide contributes to oxidative glutamate toxicity*. Brain Res, 2010. **1359**: p. 291-7.
83. Sadeghnia, H.R., et al., *Berberine protects against glutamate-induced oxidative stress and apoptosis in PC12 and N2a cells*. Iran J Basic Med Sci, 2017. **20**(5): p. 594-603.
84. Byun, E.B., et al., *Neuroprotective effect of Capsicum annuum var. abbreviatum against hydrogen peroxide-induced oxidative stress in HT22 hippocampus cells*. Biosci Biotechnol Biochem, 2018. **82**(12): p. 2149-2157.
85. Byun, E.B., et al., *Neuroprotective effect of polysaccharide separated from Perilla frutescens Britton var. acuta Kudo against H2O2-induced oxidative stress in HT22 hippocampus cells*. Biosci Biotechnol Biochem, 2018. **82**(8): p. 1344-1358.
86. Popoli, M., et al., *The stressed synapse: the impact of stress and glucocorticoids on glutamate transmission*. Nature reviews. Neuroscience, 2011. **13**(1): p. 22-37.

87. Kritis, A.A., et al., *Researching glutamate - induced cytotoxicity in different cell lines: a comparative/collective analysis/study*. Front Cell Neurosci, 2015. **9**: p. 91.
88. Kim, G.H., et al., *The Role of Oxidative Stress in Neurodegenerative Diseases*. Experimental neurobiology, 2015. **24**(4): p. 325-340.
89. Pohl, F. and P. Kong Thoo Lin, *The Potential Use of Plant Natural Products and Plant Extracts with Antioxidant Properties for the Prevention/Treatment of Neurodegenerative Diseases: In Vitro, In Vivo and Clinical Trials*. Molecules, 2018. **23**(12).
90. Liu, Z., et al., *Oxidative Stress in Neurodegenerative Diseases: From Molecular Mechanisms to Clinical Applications*. Oxidative medicine and cellular longevity, 2017. **2017**: p. 2525967-2525967.
91. Xue, F., et al., *Nrf2/antioxidant defense pathway is involved in the neuroprotective effects of Sirt1 against focal cerebral ischemia in rats after hyperbaric oxygen preconditioning*. Behav Brain Res, 2016. **309**: p. 1-8.
92. Ye, J., et al., *Arbutin attenuates LPS-induced lung injury via Sirt1/ Nrf2/ NF-kappaBp65 pathway*. Pulm Pharmacol Ther, 2019. **54**: p. 53-59.
93. Prasansuklab, A., et al., *Ethanol extract of Streblus asper leaves protects against glutamate-induced toxicity in HT22 hippocampal neuronal cells and extends lifespan of Caenorhabditis elegans*. BMC Complement Altern Med, 2017. **17**(1): p. 551.
94. Yang, Z., et al., *Chrysin attenuates carrageenan-induced pleurisy and lung injury via activation of SIRT1/NRF2 pathway in rats*. Eur J Pharmacol, 2018. **836**: p. 83-88.
95. Han, B., et al., *Dietary melatonin attenuates chromium-induced lung injury via activating the Sirt1/Pgc-1alpha/Nrf2 pathway*. Food Funct, 2019. **10**(9): p. 5555-5565.
96. Wu, P.Y., et al., *Functional decreases in P2X7 receptors are associated with retinoic acid-induced neuronal differentiation of Neuro-2a neuroblastoma cells*. Cell Signal, 2009. **21**(6): p. 881-91.
97. Olsen, A., M.C. Vantipalli, and G.J. Lithgow, *Using Caenorhabditis elegans as a model for aging and age-related diseases*. Ann N Y Acad Sci, 2006. **1067**: p. 120-8.
98. Kenyon, C., *The first long-lived mutants: discovery of the insulin/IGF-1 pathway for ageing*. Philos Trans R Soc Lond B Biol Sci, 2011. **366**(1561): p. 9-16.
99. Tullet, J.M., *DAF-16 target identification in C. elegans: past, present and future*. Biogerontology, 2015. **16**(2): p. 221-34.
100. Brenner, S., *The genetics of Caenorhabditis elegans*. Genetics, 1974. **77**(1): p. 71-94.
101. Herndon, L.A., et al., *Stochastic and genetic factors influence tissue-specific decline in ageing C. elegans*. Nature, 2002. **419**(6909): p. 808-14.
102. Adachi, H., Y. Fujiwara, and N. Ishii, *Effects of oxygen on protein carbonyl and aging in Caenorhabditis elegans mutants with long (age-1) and short (mev-1) life spans*. J Gerontol A Biol Sci Med Sci, 1998. **53**(4): p. B240-4.

103. Nakamura, A., et al., *Vitellogenin-6 is a major carbonylated protein in aged nematode, Caenorhabditis elegans*. *Biochem Biophys Res Commun*, 1999. **264**(2): p. 580-3.
104. Yasuda, K., et al., *Protein carbonyl accumulation in aging dauer formation-defective (daf) mutants of Caenorhabditis elegans*. *J Gerontol A Biol Sci Med Sci*, 1999. **54**(2): p. B47-51; discussion B52-3.
105. Tatar, M., A. Bartke, and A. Antebi, *The endocrine regulation of aging by insulin-like signals*. *Science*, 2003. **299**(5611): p. 1346-51.
106. Landis, J.N. and C.T. Murphy, *Integration of diverse inputs in the regulation of C. elegans DAF-16/FOXO*. *Developmental dynamics : an official publication of the American Association of Anatomists*, 2010. **239**(5): p. 10.1002/dvdy.22244.
107. Vowels, J.J. and J.H. Thomas, *Genetic analysis of chemosensory control of dauer formation in Caenorhabditis elegans*. *Genetics*, 1992. **130**(1): p. 105-23.
108. Gottlieb, S. and G. Ruvkun, *daf-2, daf-16 and daf-23: genetically interacting genes controlling Dauer formation in Caenorhabditis elegans*. *Genetics*, 1994. **137**(1): p. 107-20.
109. Hertweck, M., C. Gobel, and R. Baumeister, *C. elegans SGK-1 is the critical component in the Akt/PKB kinase complex to control stress response and life span*. *Dev Cell*, 2004. **6**(4): p. 577-88.
110. Paradis, S., et al., *A PDK1 homolog is necessary and sufficient to transduce AGE-1 PI3 kinase signals that regulate diapause in Caenorhabditis elegans*. *Genes Dev*, 1999. **13**(11): p. 1438-52.
111. Paradis, S. and G. Ruvkun, *Caenorhabditis elegans Akt/PKB transduces insulin receptor-like signals from AGE-1 PI3 kinase to the DAF-16 transcription factor*. *Genes Dev*, 1998. **12**(16): p. 2488-98.
112. Ogg, S., et al., *The Fork head transcription factor DAF-16 transduces insulin-like metabolic and longevity signals in C. elegans*. *Nature*, 1997. **389**(6654): p. 994-9.
113. Lin, K., et al., *daf-16: An HNF-3/forkhead family member that can function to double the life-span of Caenorhabditis elegans*. *Science*, 1997. **278**(5341): p. 1319-22.
114. Ogg, S. and G. Ruvkun, *The C. elegans PTEN homolog, DAF-18, acts in the insulin receptor-like metabolic signaling pathway*. *Mol Cell*, 1998. **2**(6): p. 887-93.
115. Padmanabhan, S., et al., *A PP2A regulatory subunit regulates C. elegans insulin/IGF-1 signaling by modulating AKT-1 phosphorylation*. *Cell*, 2009. **136**(5): p. 939-51.
116. Clancy, D.J., et al., *Extension of life-span by loss of CHICO, a Drosophila insulin receptor substrate protein*. *Science*, 2001. **292**(5514): p. 104-6.
117. Tatar, M., et al., *A mutant Drosophila insulin receptor homolog that extends life-span and impairs neuroendocrine function*. *Science*, 2001. **292**(5514): p. 107-10.
118. Blüher, M., B.B. Kahn, and C.R. Kahn, *Extended longevity in mice lacking the insulin receptor in adipose tissue*. *Science*, 2003. **299**(5606): p. 572-4.
119. Holzenberger, M., et al., *IGF-1 receptor regulates lifespan and resistance to oxidative stress in mice*. *Nature*, 2003. **421**(6919): p. 182-7.

120. Suh, Y., et al., *Functionally significant insulin-like growth factor I receptor mutations in centenarians*. Proc Natl Acad Sci U S A, 2008. **105**(9): p. 3438-42.
121. Willcox, B.J., et al., *FOXO3A genotype is strongly associated with human longevity*. Proc Natl Acad Sci U S A, 2008. **105**(37): p. 13987-92.
122. Murphy, C.T. and P.J. Hu, *Insulin/insulin-like growth factor signaling in C. elegans*. WormBook, 2013: p. 1-43.
123. Gaglia, M.M., et al., *Genes that act downstream of sensory neurons to influence longevity, dauer formation, and pathogen responses in Caenorhabditis elegans*. PLoS Genet, 2012. **8**(12): p. e1003133.
124. Halaschek-Wiener, J., et al., *Analysis of long-lived C. elegans daf-2 mutants using serial analysis of gene expression*. Genome Res, 2005. **15**(5): p. 603-15.
125. Mallo, G.V., et al., *Inducible antibacterial defense system in C. elegans*. Curr Biol, 2002. **12**(14): p. 1209-14.
126. Flachsbart, F., et al., *Association of FOXO3A variation with human longevity confirmed in German centenarians*. Proc Natl Acad Sci U S A, 2009. **106**(8): p. 2700-5.
127. Giannakou, M.E., et al., *Long-lived Drosophila with overexpressed dFOXO in adult fat body*. Science, 2004. **305**(5682): p. 361.
128. Landis, J.N. and C.T. Murphy, *Integration of diverse inputs in the regulation of Caenorhabditis elegans DAF-16/FOXO*. Developmental dynamics : an official publication of the American Association of Anatomists, 2010. **239**(5): p. 1405-1412.
129. An, J.H. and T.K. Blackwell, *SKN-1 links C. elegans mesendodermal specification to a conserved oxidative stress response*. Genes Dev, 2003. **17**(15): p. 1882-93.
130. Oliveira, R.P., et al., *Condition-adapted stress and longevity gene regulation by Caenorhabditis elegans SKN-1/Nrf*. Aging Cell, 2009. **8**(5): p. 524-41.
131. Tullet, J.M., et al., *Direct inhibition of the longevity-promoting factor SKN-1 by insulin-like signaling in C. elegans*. Cell, 2008. **132**(6): p. 1025-38.
132. Ewald, C.Y., et al., *Dauer-independent insulin/IGF-1-signalling implicates collagen remodelling in longevity*. Nature, 2015. **519**(7541): p. 97-101.
133. Przybysz, A.J., et al., *Increased age reduces DAF-16 and SKN-1 signaling and the hormetic response of Caenorhabditis elegans to the xenobiotic juglone*. Mech Ageing Dev, 2009. **130**(6): p. 357-69.
134. Rahman, M.M., et al., *Declining signal dependence of Nrf2-MafS-regulated gene expression correlates with aging phenotypes*. Aging Cell, 2013. **12**(4): p. 554-62.
135. Moreno-Arriola, E., et al., *Caenorhabditis elegans: A useful model for studying metabolic disorders in which oxidative stress is a contributing factor*. Oxid Med Cell Longev, 2014. **2014**: p. 705253.
136. Valdivia-Correa, B., et al., *Herbal Medicine in Mexico: A Cause of Hepatotoxicity. A Critical Review*. International Journal of Molecular Sciences, 2016. **17**(2): p. 235.
137. Vilar, S.M., et al., *Assessment of Phenolic Compounds and Anti-Inflammatory Activity of Ethyl Acetate Phase of Anacardium occidentale L. Bark*. Molecules, 2016. **21**(8).

138. Fagbohun, T.R. and K.T. Odufuwa, *Hypoglycemic effect of methanolic extract of Anacardium occidentale leaves in alloxan-induced diabetic rats*. Niger J Physiol Sci, 2010. **25**(1): p. 87-90.
139. Lingaraju, S.M., K. Keshavaiah, and B.P. Salimath, *Inhibition of in vivo angiogenesis by Anacardium occidentale L. involves repression of the cytokine VEGF gene expression*. Drug Discov Ther, 2008. **2**(4): p. 234-44.
140. Barbosa-Filho, V.M., et al., *Phytochemicals and modulatory effects of Anacardium microcarpum (cajui) on antibiotic drugs used in clinical infections*. Drug Des Devel Ther, 2015. **9**: p. 5965-72.
141. Royo, V.A., et al., *Anatomy, Histochemistry, and Antifungal Activity of Anacardium humile (Anacardiaceae) Leaf*. Microsc Microanal, 2015. **21**(6): p. 1549-1561.
142. Yoo, K.M., et al., *Relative antioxidant and cytoprotective activities of common herbs*. Food Chemistry, 2008. **106**(3): p. 929-936.
143. Xu, S.L., et al., *Isorhamnetin, A Flavonol Aglycone from Ginkgo biloba L., Induces Neuronal Differentiation of Cultured PC12 Cells: Potentiating the Effect of Nerve Growth Factor*. Evid Based Complement Alternat Med, 2012. **2012**: p. 278273.
144. Amara, F., et al., *Neuroprotection by Cocktails of Dietary Antioxidants under Conditions of Nerve Growth Factor Deprivation*. Oxid Med Cell Longev, 2015. **2015**: p. 217258.
145. Wang, L.-Y., X. Li, and Y.-Z. Han, *Neuroprotection by epigallo catechin gallate against bupivacaine anesthesia induced toxicity involves modulation of PI3/Akt/PTEN signalling in N2a and SH-SY5Y cells*. International journal of clinical and experimental medicine, 2015. **8**(9): p. 15065-15075.
146. Harikumar, K.B. and B.B. Aggarwal, *Resveratrol: a multitargeted agent for age-associated chronic diseases*. Cell Cycle, 2008. **7**(8): p. 1020-35.
147. Witte, A.V., et al., *Effects of resveratrol on memory performance, hippocampal functional connectivity, and glucose metabolism in healthy older adults*. J Neurosci, 2014. **34**(23): p. 7862-70.
148. Ding, A.J., et al., *Current Perspective in the Discovery of Anti-aging Agents from Natural Products*. Nat Prod Bioprospect, 2017. **7**(5): p. 335-404.
149. Pietsch, K., et al., *Quercetin mediated lifespan extension in Caenorhabditis elegans is modulated by age-1, daf-2, sek-1 and unc-43*. Biogerontology, 2009. **10**(5): p. 565-78.
150. Pietsch, K., et al., *Hormetins, antioxidants and prooxidants: defining quercetin-, caffeic acid- and rosmarinic acid-mediated life extension in C. elegans*. Biogerontology, 2011. **12**(4): p. 329-47.
151. Cheng, S.C., et al., *Antioxidant activity and delayed aging effects of hot water extract from Chamaecyparis obtusa var. formosana leaves*. J Agric Food Chem, 2014. **62**(18): p. 4159-65.
152. Kampkotter, A., et al., *Investigations of protective effects of the flavonoids quercetin and rutin on stress resistance in the model organism Caenorhabditis elegans*. Toxicology, 2007. **234**(1-2): p. 113-23.
153. Duangjan, C., et al., *Lifespan Extending and Oxidative Stress Resistance Properties of a Leaf Extracts from Anacardium occidentale L. in Caenorhabditis elegans*. Oxid Med Cell Longev, 2019. **2019**: p. 9012396.

154. Duangjan, C., et al., *Data on the effects of Glochidion zeylanicum leaf extracts in Caenorhabditis elegans*. Data Brief, 2019. **26**: p. 104461.
155. Eik, L.F., et al., *Lignosus rhinocerus (Cooke) Ryvarde: A Medicinal Mushroom That Stimulates Neurite Outgrowth in PC-12 Cells*. Evid Based Complement Alternat Med, 2012. **2012**: p. 320308.
156. Duangjan, C., et al., *Glochidion zeylanicum leaf extracts exhibit lifespan extending and oxidative stress resistance properties in Caenorhabditis elegans via DAF-16/FoxO and SKN-1/Nrf-2 signaling pathways*. Phytomedicine, 2019. **64**: p. 153061.
157. Kumar, M. and A. Katyal, *Data on retinoic acid and reduced serum concentration induced differentiation of Neuro-2a neuroblastoma cells*. Data Brief, 2018. **21**: p. 2435-2440.
158. Janesick, A., S.C. Wu, and B. Blumberg, *Retinoic acid signaling and neuronal differentiation*. Cellular and Molecular Life Sciences, 2015. **72**(8): p. 1559-1576.
159. Sajjad, N., et al., *Artemisia amygdalina Upregulates Nrf2 and Protects Neurons Against Oxidative Stress in Alzheimer Disease*. Cell Mol Neurobiol, 2019. **39**(3): p. 387-399.
160. Arduino, D.M., et al., *Endoplasmic reticulum and mitochondria interplay mediates apoptotic cell death: relevance to Parkinson's disease*. Neurochem Int, 2009. **55**(5): p. 341-8.
161. Lindholm, D., H. Wootz, and L. Korhonen, *ER stress and neurodegenerative diseases*. Cell Death Differ, 2006. **13**(3): p. 385-92.
162. Stanciu, M. and D.B. DeFranco, *Prolonged nuclear retention of activated extracellular signal-regulated protein kinase promotes cell death generated by oxidative toxicity or proteasome inhibition in a neuronal cell line*. J Biol Chem, 2002. **277**(6): p. 4010-7.
163. Essa, M.M., et al., *Neuroprotective effect of natural products against Alzheimer's disease*. Neurochem Res, 2012. **37**(9): p. 1829-42.
164. Han, R.-M., J.-P. Zhang, and L.H. Skibsted, *Reaction dynamics of flavonoids and carotenoids as antioxidants*. Molecules (Basel, Switzerland), 2012. **17**(2): p. 2140-2160.
165. Anantachoke, N., et al., *Polyphenolic compounds and antioxidant activities of the leaves of Glochidion hypoleucum*. Nat Prod Commun, 2015. **10**(3): p. 479-82.
166. Zhang, R., et al., *Nrf2-a Promising Therapeutic Target for Defending Against Oxidative Stress in Stroke*. Mol Neurobiol, 2017. **54**(8): p. 6006-6017.
167. Ghareghani, M., et al., *Safflower Seed Oil, Containing Oleic Acid and Palmitic Acid, Enhances the Stemness of Cultured Embryonic Neural Stem Cells through Notch1 and Induces Neuronal Differentiation*. Front Neurosci, 2017. **11**: p. 446.
168. Lee, A.Y., et al., *Protective effects of perilla oil and alpha linolenic acid on SH-SY5Y neuronal cell death induced by hydrogen peroxide*. Nutr Res Pract, 2018. **12**(2): p. 93-100.
169. S, M., P. T, and D. Goli, *Effect of wedelolactone and gallic acid on quinolinic acid-induced neurotoxicity and impaired motor function: significance to sporadic amyotrophic lateral sclerosis*. Neurotoxicology, 2018. **68**: p. 1-12.

170. Herges, K., et al., *Neuroprotective effect of combination therapy of glatiramer acetate and epigallocatechin-3-gallate in neuroinflammation*. PLoS One, 2011. **6**(10): p. e25456.
171. Park, D.J., et al., *Quercetin alleviates the injury-induced decrease of protein phosphatase 2A subunit B in cerebral ischemic animal model and glutamate-exposed HT22 cells*. J Vet Med Sci, 2019.
172. Lin-Holderer, J., et al., *Fumaric acid esters promote neuronal survival upon ischemic stress through activation of the Nrf2 but not HIF-1 signaling pathway*. Neuropharmacology, 2016. **105**: p. 228-240.
173. Jung, K.A. and M.K. Kwak, *The Nrf2 system as a potential target for the development of indirect antioxidants*. Molecules, 2010. **15**(10): p. 7266-91.
174. Walczewska, A., et al., *[The role of docosahexaenoic acid in neuronal function]*. Postepy Hig Med Dosw (Online), 2011. **65**: p. 314-27.
175. Siddiqui, S., et al., *Gallic and vanillic acid suppress inflammation and promote myelination in an in vitro mouse model of neurodegeneration*. Mol Biol Rep, 2019. **46**(1): p. 997-1011.
176. Katebi, S., et al., *Superparamagnetic iron oxide nanoparticles combined with NGF and quercetin promote neuronal branching morphogenesis of PC12 cells*. Int J Nanomedicine, 2019. **14**: p. 2157-2169.
177. Chan, G.K.L., et al., *Quercetin Potentiates the NGF-Induced Effects in Cultured PC 12 Cells: Identification by HerboChips Showing a Binding with NGF*. Evid Based Complement Alternat Med, 2018. **2018**: p. 1502457.
178. Ming-Ming, C., et al., *Quercetin promotes neurite growth through enhancing intracellular cAMP level and GAP-43 expression*. Chinese journal of natural medicines, 2015. **13**(9): p. 667-672.
179. Wansawat, S., et al., *Mucuna pruriens Seed Extract Promotes Neurite Outgrowth via TEN-4 Dependent and Independent Mechanisms in NEURO2A Cells*. Sains Malaysiana, 2018. **47**: p. 3009-3015.
180. Liang, Y., et al., *Astragaloside IV and ferulic acid synergistically promote neurite outgrowth through Nrf2 activation*. Mech Ageing Dev, 2019. **180**: p. 70-81.
181. Sugino, T., et al., *Protein deacetylase SIRT1 in the cytoplasm promotes nerve growth factor-induced neurite outgrowth in PC12 cells*. FEBS Lett, 2010. **584**(13): p. 2821-6.
182. He, W., et al., *Sonic hedgehog promotes neurite outgrowth of cortical neurons under oxidative stress: Involving of mitochondria and energy metabolism*. Exp Cell Res, 2017. **350**(1): p. 83-90.
183. Kubo, I., et al., *Multifunctional cytotoxic agents from Anacardium occidentale*. Phytother Res, 2011. **25**(1): p. 38-45.
184. Castillo-Juarez, I., et al., *Anti-Helicobacter pylori activity of anacardic acids from Amphipterygium adstringens*. J Ethnopharmacol, 2007. **114**(1): p. 72-7.
185. Su, S. and M. Wink, *Natural lignans from Arctium lappa as antiaging agents in Caenorhabditis elegans*. Phytochemistry, 2015. **117**: p. 340-350.
186. Rea, S.L., et al., *A stress-sensitive reporter predicts longevity in isogenic populations of Caenorhabditis elegans*. Nat Genet, 2005. **37**(8): p. 894-8.

187. Chen, W., et al., *Anthocyanin-rich purple wheat prolongs the life span of Caenorhabditis elegans probably by activating the DAF-16/FOXO transcription factor*. J Agric Food Chem, 2013. **61**(12): p. 3047-53.
188. Shi, Y.C., et al., *Monascus-fermented dioscorea enhances oxidative stress resistance via DAF-16/FOXO in Caenorhabditis elegans*. PLoS One, 2012. **7**(6): p. e39515.
189. Wang, E. and M. Wink, *Chlorophyll enhances oxidative stress tolerance in Caenorhabditis elegans and extends its lifespan*. PeerJ, 2016. **4**: p. e1879.
190. Wang, Z., et al., *Peptides from sesame cake extend healthspan of Caenorhabditis elegans via upregulation of skn-1 and inhibition of intracellular ROS levels*. Exp Gerontol, 2016. **82**: p. 139-49.
191. Zhu, S., et al., *Rose Essential Oil Delayed Alzheimer's Disease-Like Symptoms by SKN-1 Pathway in C. elegans*. 2017. **65**(40): p. 8855-8865.
192. Detienne, G., et al., *SKN-1-independent transcriptional activation of glutathione S-transferase 4 (GST-4) by EGF signaling*. Worm, 2016. **5**(4): p. e1230585.
193. Chow, D.K., et al., *Sarcopenia in the Caenorhabditis elegans pharynx correlates with muscle contraction rate over lifespan*. Exp Gerontol, 2006. **41**(3): p. 252-60.
194. Kuzmic, M., et al., *Interplay between ionizing radiation effects and aging in C. elegans*. Free Radic Biol Med, 2019. **134**: p. 657-665.
195. Brown, M.K., J.L. Evans, and Y. Luo, *Beneficial effects of natural antioxidants EGCG and alpha-lipoic acid on life span and age-dependent behavioral declines in Caenorhabditis elegans*. Pharmacol Biochem Behav, 2006. **85**(3): p. 620-8.
196. Shpigel, N., et al., *Dietary restriction and gonadal signaling differentially regulate post-development quality control functions in Caenorhabditis elegans*. Aging Cell, 2019: p. e12891.
197. Shashikumar, S., et al., *Alpha-linolenic acid suppresses dopaminergic neurodegeneration induced by 6-OHDA in C. elegans*. Physiol Behav, 2015. **151**: p. 563-9.
198. Qi, W., et al., *The omega-3 fatty acid alpha-linolenic acid extends Caenorhabditis elegans lifespan via NHR-49/PPARalpha and oxidation to oxylipins*. 2017. **16**(5): p. 1125-1135.
199. Pant, A., et al., *Beta-caryophyllene modulates expression of stress response genes and mediates longevity in Caenorhabditis elegans*. Exp Gerontol, 2014. **57**: p. 81-95.

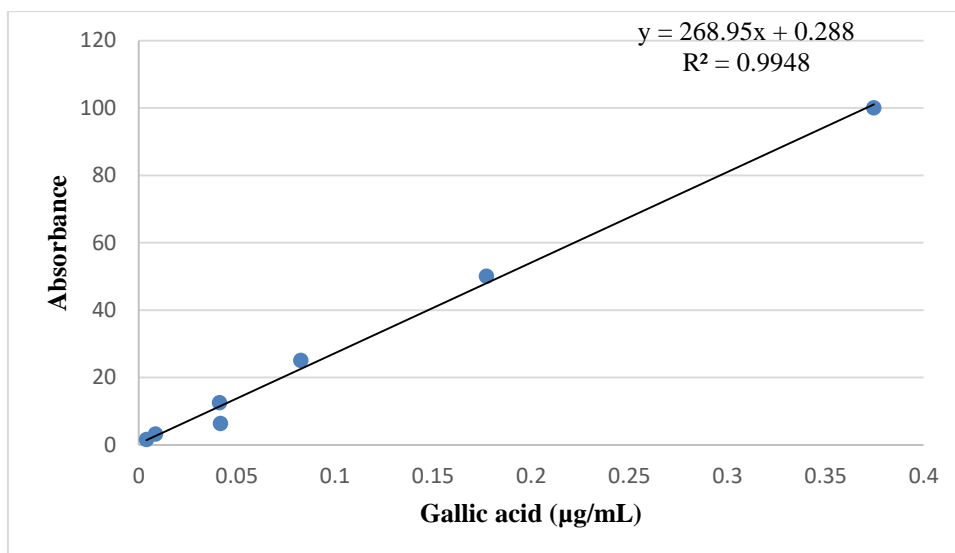
APPENDIX

1. Plant extraction

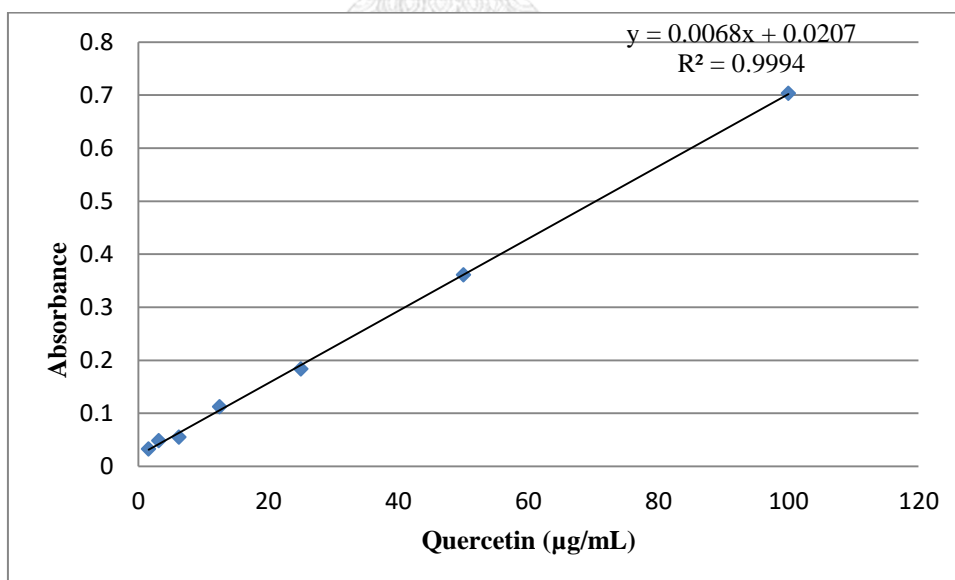


2. Standard calibration curve of antioxidant capacity assay

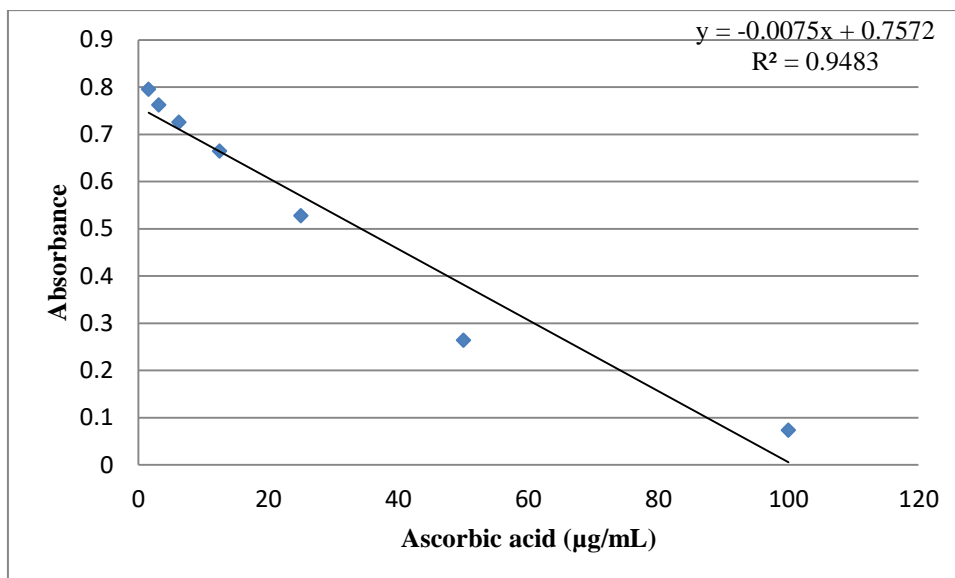
2.1 Total phenolic content



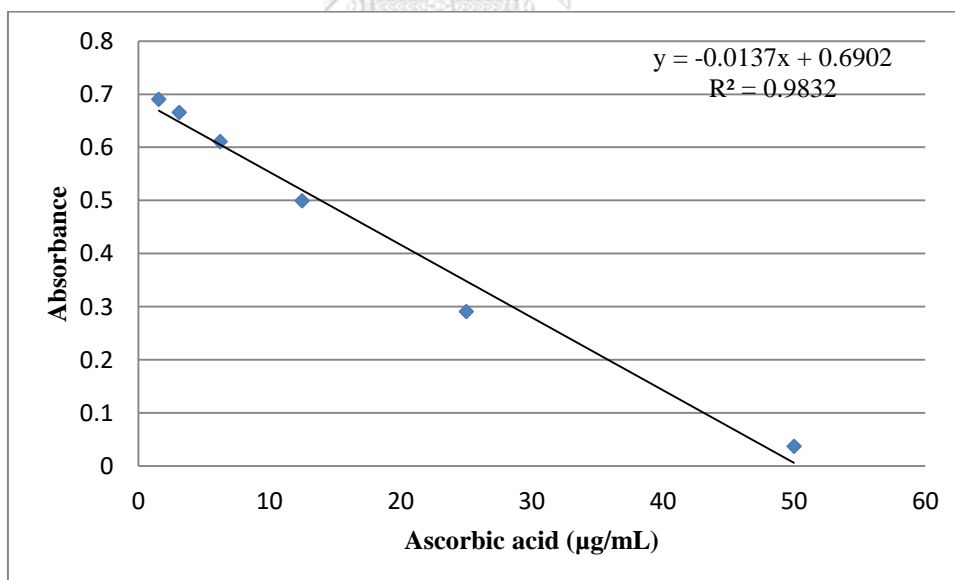
2.2 Total flavonoid content



2.3 DPPH assay

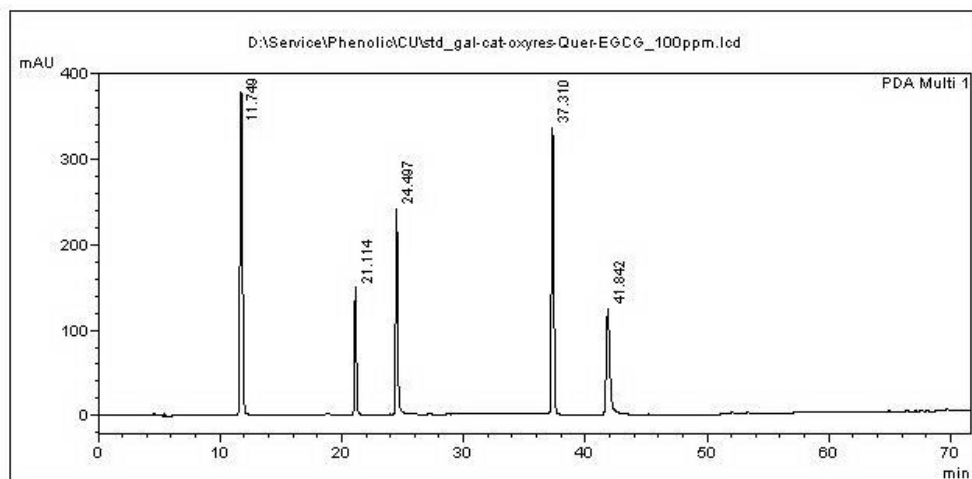


2.4 ABTS assay

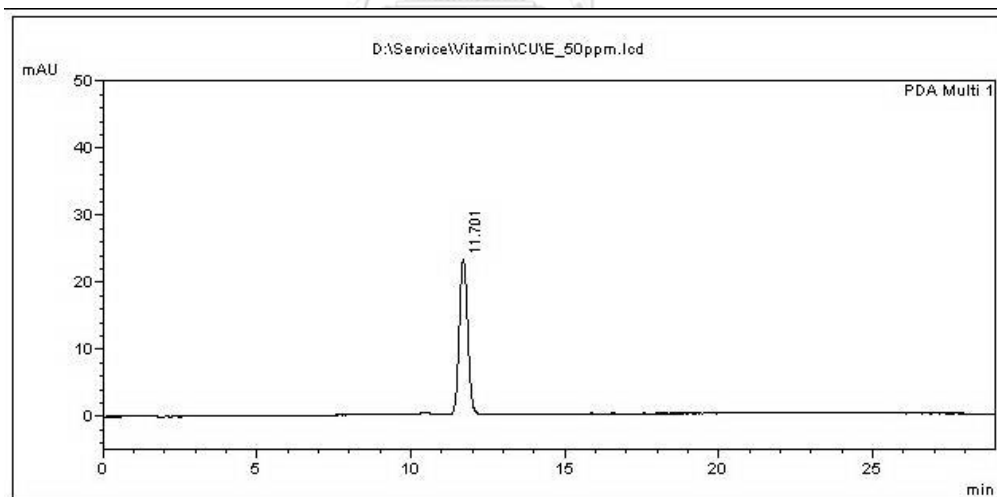


3. Standard calibration curve of HPLC analysis

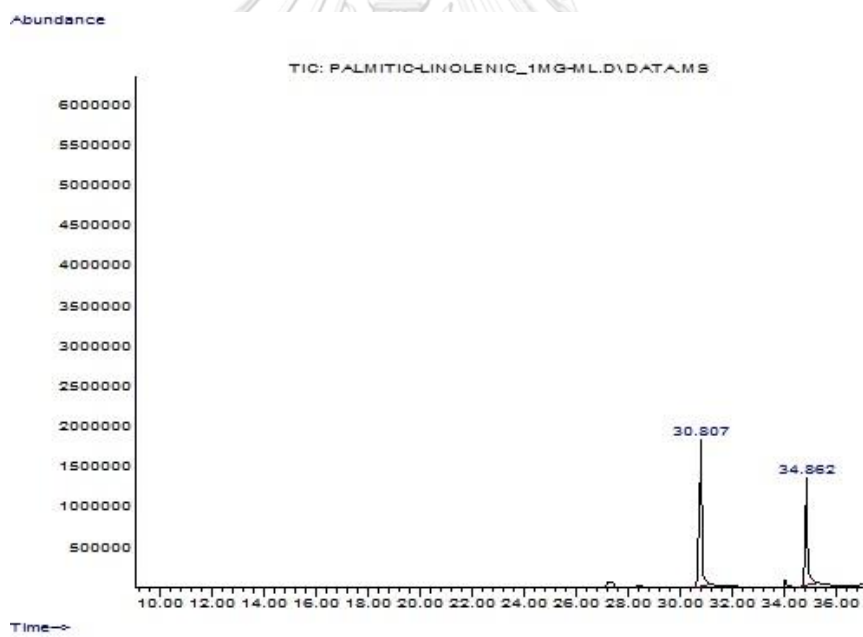
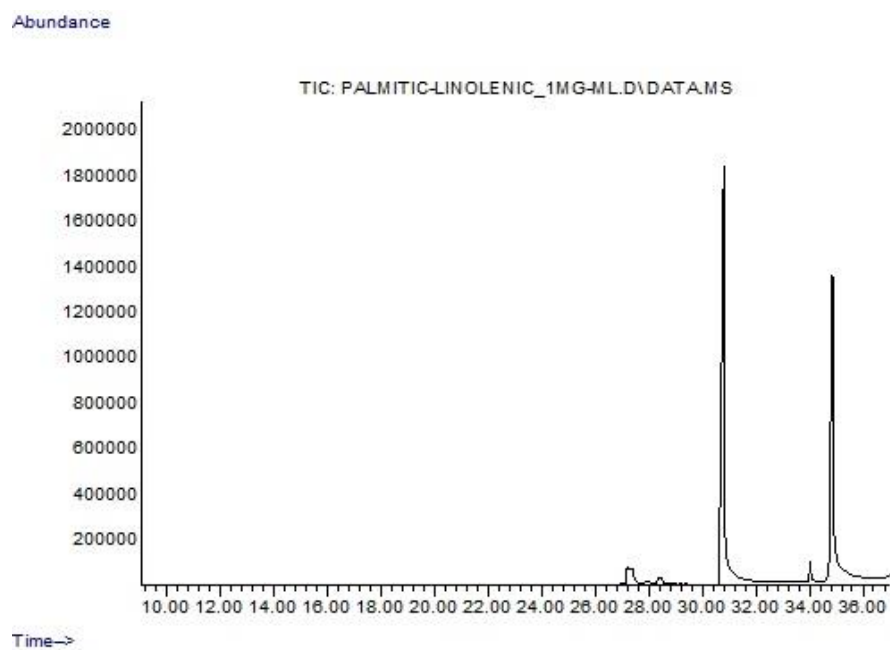
3.1 Standard phenolic data graph from HPLC analysis



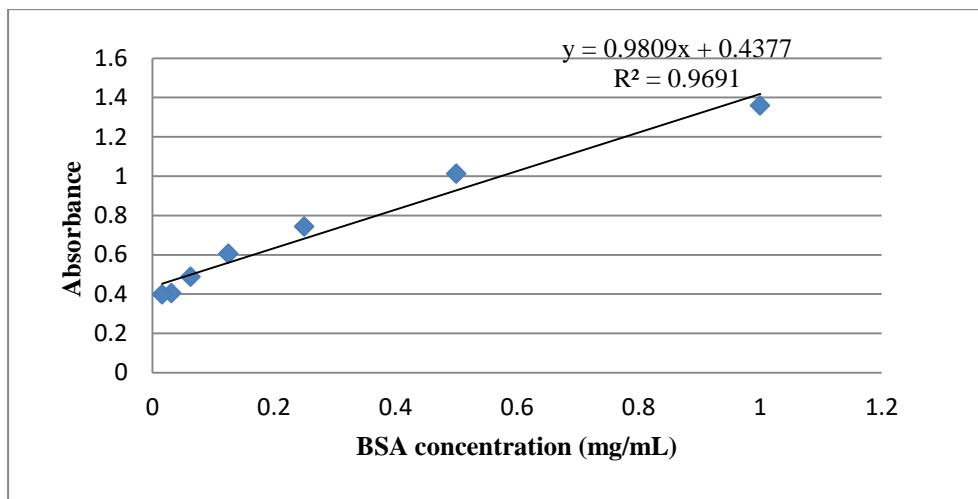
3.2 Standard tocopherol data graph from HPLC analysis



3.3 Standard palmitic and linolenic data graph from HPLC analysis



4. Standard calibration curve of Bradford assay





จุฬาลงกรณ์มหาวิทยาลัย
CHULALONGKORN UNIVERSITY

VITA

NAME CHATRAWEE DUANGJAN

DATE OF BIRTH 12 September 1992

PLACE OF BIRTH Suphanburi

INSTITUTIONS ATTENDED Program in Clinical Biochemistry and Molecular Medicine, Department of Clinical Chemistry, Faculty of Allied Health Sciences, Chulalongkorn University, Bangkok 10330, Thailand

HOME ADDRESS 153 Moo.2 WATDAOW BANGPLAMA SUPHANBURI 72150

PUBLICATION

1. Chatrawee Duangjan, Panthakarn Rangsinth, Xiaojie Gu, Michael Wink and Tewin Tencomnao: "Lifespan extending and oxidative stress resistance properties of a leaf extracts from *Anacardium occidentale* L. in *Caenorhabditis elegans*", *Oxidative Medicine and Cellular Longevity*, vol. 2019, Article ID 9012396, 16 pages, 2019, doi.org/10.1155/2019/9012396.
2. Chatrawee Duangjan, Panthakarn Rangsinth, Xiaojie Gu, Shaoxiong Zhang, Michael Wink and Tewin Tencomnao: "Glochidion zeylanicum leaf extracts exhibit lifespan extending and oxidative stress resistance properties in *Caenorhabditis elegans* via DAF-16/FoxO and SKN-1/Nrf-2 signaling pathways", *Phytomedicine*, 2019, doi: 10.1016/j.phymed.2019.153061.
3. Chatrawee Duangjan, Panthakarn Rangsinth, Xiaojie Gu, Shaoxiong Zhang, Michael Wink and Tewin Tencomnao: "Data on the effects of *Glochidion zeylanicum* leaf extracts in *Caenorhabditis elegans*", *Data Brief*, 2019 doi: 10.1016/j.dib.2019.104461.
4. Panthakarn Rangsinth, Anchalee Prasansuklab, Chatrawee Duangjan, Xiaojie Gu, Krai Meemon, Michael Wink and Tewin Tencomnao: "Leaf extract of *Caesalpinia mimosoides* enhances oxidative stress resistance and prolongs lifespan in *Caenorhabditis elegans*.", *BMC Complementary and Alternative Medicine*, 2019, 19, 164, doi:10.1186/s12906-019-2578-5.

AWARD RECEIVED

2014- 2019: Full scholarship by the 72nd Birthday Anniversary of His Majesty the King's University Fund for Doctoral Scholarship, Chulalongkorn University

2015: Inter-university Exchange Program toward Medical and Dental Networking in

Southeast Asia, Student exchanges at Tokyo Medical and Dental University

2016: Full scholarship by the 90th Anniversary Chulalongkorn University Fund,
Chulalongkorn University

2017: Full scholarship by the Overseas Research Experience Scholarship for Graduate
Students, Chulalongkorn University

2018: Short term research fellowship in Institute of Pharmacy and Molecular
Biotechnology, Heidelberg University, Germany.

2018: Full scholarship by the Overseas Academic Presentation Scholarship for Graduate
Students, Chulalongkorn University

November, 2018 : Best oral presenter award for INBIOSIS GRADUATED
SYMPOSIUM 2018, University Kebangsaan Malaysia

